Proteinase-activated Receptor 4 and Cell Apoptosis

Ai-Yen Chin

BSc (Hons) Hull

UNIVERSITY OF Hull

A dissertation submitted to the University of Hull
for the degree of Doctor of Philosophy

September 2013

In memory of my beloved Dad

Chin Pau Kong

1958 – 2000

For everyone in my family...
especially my mum and Yong

Declaration

This dissertation is the result of my own work and includes nothing that is the outcome of work done in collaboration except where specifically indicated in the text.

This dissertation is also not substantially the same as any that I have submitted for a degree or diploma or other qualification at any other University.

Ai-Yen Chin
September 2013

Acknowledgements

I would like to thank my supervisors Dr Simon Hart and Prof Sunil Bhandari for giving me the opportunity to work on this project. I really appreciate their support, patient guidance and advice over the past three years. I am grateful to Prof Alyn Morice for his advice and helpful suggestions on many aspects of the work.

Many thanks to Dr Laura Sadofsky, who is always ready to help and is very friendly to share all sorts of valuable experience. I also want to thank Chris Crow who never refuses to provide assistance in the lab.

In addition, I would like to thank everyone in the Division of Cardiovascular & Respiratory Studies at Castle Hill Hospital for help with various things over the past three years. Very importantly, many thanks to the Renal and Respiratory Medicine Joint Funding for supporting my PhD studies.

Lastly, I like to express my utmost gratitude to my family and Yong for their love and ceaseless encouragement and support at all times.

Proteinase-activated Receptor 4 and Cell Apoptosis

Ai-Yen Chin

In response to injury, the collagen-producing cells fibroblasts and myofibroblasts play an important role in promoting extracellular matrix deposition and release of inflammatory mediators in order to repair the damaged tissue. However, persistence and over-activity of these cells is associated with excessive collagen deposition and hence development of fibrosis, a pathological scarring process that leads to destruction of organ architecture and impairment of organ function. Removal of fibroblasts and myofibroblasts during fibrogenesis by apoptosis is therefore required for the normal resolution of tissue repair responses.

Proteinase-activated protein 4 (PAR_4) belongs to a subfamily of multifunctional G protein-coupled receptors which are activated by the proteolytic unmasking of a tethered peptide ligand that resides within their N-terminus. In addition to its well-studied role in platelet function, PAR_4, like the other PAR family members, is thought to be involved in pro-inflammatory responses and fibroproliferative processes. However, the role of PAR_4 in these processes remains largely unknown.

The hypothesis of this thesis is that during injury, PAR_4 expression is upregulated and this somehow contributes to apoptosis. To test this, the expression of PAR_4 was examined in two types of fibroblasts, cultured from human lung and renal explants. Results indicate that PAR_4 is not expressed in these cultured fibroblasts. Surprisingly, contradictory to a previous observation, exposure of lung fibroblasts to lipopolysaccharide did not consistently induce PAR_4 expression. As an alternative to the use of PAR_4-expressing fibroblasts, a stable PAR_4-expressing human cell line (HEK-PAR_4) was generated. Using these cells in an *in vitro* signalling assay, PAR_4 was found to confer responsiveness to PAR_4 activating peptide but not to a serine protease cathepsin G, which was previously shown to activate PAR_4 in platelets. Interestingly, the observation that cathepsin G-treated cells elicit a reduced signalling response to the stimulatory action of PAR_4 activating peptide suggests that cathepsin G might cleave PAR_4 at the ECL2 domain and cause PAR_4 to be unresponsive to the PAR_4 AP.

Next, serine proteases cathepsin G and trypsin were demonstrated as apoptosis inducers for human lung and renal fibroblasts. They induced pronounced morphologic changes in the fibroblasts (which do not express PAR_4). In HEK-PAR_4 cells, cathepsin G induced similar apoptotic level in comparison to empty vector control. Together, these findings suggest that cathepsin G can trigger apoptosis independently of PAR_4. On the other hand, PAR_4 activating peptide triggered higher percentage of apoptosis in HEK-PAR_4 cells compared to empty vector control, suggesting that apoptosis is mediated by PAR_4 signalling in this case.

Epithelium has a role in modulating a variety of inflammatory processes through the production and release of inflammatory cytokines. Apoptosis of damaged epithelium during inflammation has been reported to promote fibroblast growth and collagen deposition. In the last part of this thesis, media derived from confluent epithelial cell cultures were demonstrated to induce proliferation of lung and renal fibroblasts in a concentration dependent manner. This observation preliminarily supports the idea that epithelial cell injury may promote the proliferation of fibroblasts via the secretion of multiple cytokines.

In conclusion, this thesis demonstrates that apoptosis can be induced, first, by cathepsin G and trypsin in human primary bronchial fibroblasts and human primary renal fibroblasts independently of PAR_4, and second, by activation of PAR_4 in a non-fibroblastic PAR_4-expressing cell line.

Contents

List of Figures

List of Tables

Chapter 1

Introduction

1.1 Fibrogenesis

Repair of damaged tissues is an essential biological process that allows the ordered replacement of dead or damaged cells after injury, allowing tissue architecture to restore and regain normal organ function. Fibrogenesis is a mechanism of wound healing and repair. Generally, it can be classified into three phases: (1) induction, (2) inflammation and matrix synthesis, and, (3) resolution (Kuncio *et al.*, 1991).

1.1.1 Induction

The induction of conditions necessary for the establishment of active fibrogenesis and matrix remodelling represents the first phase of fibrogenesis. Injury caused by autoimmune or allergic reactions, environmental particulates, infection or mechanical damage often results in the disruption of normal tissue architecture, initiating a healing response. Acute damage to endothelial cells leads to the release of inflammatory mediators and initiation of a clotting cascade. Stimulation of the clotting cascade results in the cleavage of fibrinogen by thrombin to form a fibrin plug, which together with fibronectin, hold damaged tissues together and

provide a provisional matrix for the recruitment of inflammatory cells, fibroblasts and other resident cells (Mutsaers *et al.*, 1997; Chambers *et al.*, 2003). During induction phase, platelets aggregate and produce large amounts of platelet-derived growth factor (PDGF), which is a potent chemoattractant for fibroblasts, and transforming growth factor-β (TGF-β), a strong stimulant to fibroblast proliferation (Seppä *et al.*, 1982; Postlethwaite *et al.*, 1987; Kuncio *et al.*, 1991). Furthermore, activated fibroblasts themselves secrete TGF-β and collagenases, hence enhancing their growth and motility (Kuncio *et al.*, 1991).

1.1.2 Inflammation and Matrix Synthesis

Inflammatory cells propagate at the injury sites through the secretion of chemokines, cytokines and growth factors. Neutrophils are the first cells recruited, followed by the macrophages that infiltrate damaged tissue and secrete fibrogenic cytokines. Among many cytokines, interleukin (IL)-4, IL-13 and TGF-β are highly significant and exhibit pro-fibrotic activities by recruitment, activation and proliferation of macrophages, fibroblasts and myofibroblasts (Clark, 1989; Kuncio *et al.*, 1991). Macrophages are vital for normal healing. The healing process is impaired if their infiltration is prevented. They are a source of chemoattractants and growth factors, including PDGF, TGF-β and tumour necrosis factor-α (TNF-α). They act in concert with neutrophils to phagocytose debris and invading pathogenic microorganisms. TGF-β1 secreted by macrophages then causes the fibroblasts to differentiate into myofibroblasts and initiate the production of matrix proteins, predominantly types I and III collagen, which increase the tensile strength of the wound (Mutsaers *et al.*, 1997). Type III collagen is often deposited initially in higher ratios, but as fibrogenesis proceeds, type III collagen decreases relative to type I (Jimenez *et al.*, 1984; Dean *et al.*, 1988; Kuncio *et al.*, 1991). An imbalance in the production of stimulatory chemokines and growth factors can result in excess secretion of pro-fibrotic

cytokines and over-activation of myofibroblasts, leading to fibrosis (see **Section 1.2**) (Erjefält *et al.*, 1996; Elovic *et al.*, 1998; Gauldie, 2002; Piguet, 2003).

1.1.3 Resolution

The third phase, the resolution phase of wound healing, consists of an orchestrated cellular reorganisation guided by a fibrin-rich scaffold formation, wound contraction, closure and re-epithelialisation (Wilson and Wynn, 2009). Myofibroblasts migrate along the extracellular matrix (ECM) network and repair the wound. They also form stress fibres and α-smooth muscle actin (α-SMA) which confer high contractile activity within myofibroblasts. TGF-β also induces a contractile response, regulating the orientation of collagen fibres. (Mirastschijski *et al.*, 2004; Hinz, 2006; Farahani and Kloth, 2008). The attachment of myofibroblasts to the ECM at specialised sites called the fibronexus pulls the wound together, reducing the size of the lesion during the contraction phase. The degree of ECM laid down and the quantity of activated myofibroblasts determine the amount of collagen deposition (Singer, 1982; Thannickal and Horowitz, 2006). The rapid synthesis and degradation of connective tissue proteins is known as remodelling. The degradation of wound collagen and other matrix proteins are controlled by a variety of collagenases and the other metalloproteinases from granulocytes, macrophages, epidermal cells and fibroblasts. Imbalance of collagen synthesis and degradation will cause scar formation (Mutsaers *et al.*, 1997). The resolution of inflammation through the removal of inflammatory cells and activated myofibroblasts by apoptosis and phagocytic pathways often leaves minimal damage and restores normal tissue architecture. However, delayed removal of myofibroblasts and the resistance of cells to apoptosis signals potentially cause fibrotic diseases (see **Section 1.2**) (Thannickal and Horowitz, 2006; Fattman, 2008). A tightly

regulated repair response following tissue injury is therefore critical.

1.2 Fibrosis

Fibrosis is the deregulation of fibrogenesis and continued exposure to chronic injury. Fibrosis is a pathological feature of most chronic inflammatory diseases. It is characterised by interstitial hypercellularity, matrix accumulation and atrophy of epithelial structures that lead to loss of normal function and organ failure. In spite of having distinct aetiological and clinical manifestations, most chronic fibrotic disorders have in common a persistent irritant that sustains the production of growth factors, proteolytic enzymes, angiogenic factors and fibrogenic cytokines, which stimulate the deposition of connective tissue elements that progressively remodel and destroy normal tissue architecture (Wynn, 2008).

Epithelium damage has an important role at the onset of fibrosis. During injury, damaged epithelial cells become activated and cytokines, growth factors and chemoattractants are secreted to activate and recruit macrophages to the injury sites (Kisseleva and Brenner, 2008). Macrophages then secrete TGF-β1 which promotes fibroblasts activation and proliferation (Kisseleva and Brenner, 2006). Activated fibroblasts and myofibroblasts will produce high amounts of TGF-β1 and extracellular reactive oxygen species (ROS) (**Section 1.2.1.2**) which facilitate apoptosis of damaged epithelial cells (Waghray *et al.*, 2005). Similar responses to injury have been described for pulmonary epithelium and kidney epithelium (Zeisberg *et al.*, 2001; Thannickal and Horowitz, 2006). See **Chapter 6** for further details.

1.2.1 Aetiological Factors in Fibrosis

1.2.1.1 TGF-β1

TGF-β1 is not expressed constitutively and is strongly upregulated during injury and inflammation. Macrophages are the major source of TGF-β1 in fibrosing organs (Bataller and Brenner, 2005). Overexpression of TGF-β1 in transgenic mice caused fibrosis in multiple organs, indicating that TGF-β1 is a major pro-fibrogenic cytokine (Bataller and Brenner, 2005). Another fibrogenic factor, connective tissue growth factor (CTGF), is a downstream mediator of TGF-β1 responses and it acts as a chaperone that augments TGF-β1 signalling. CTGF binds to TGF-β1 and increases its affinity to the TGF-β1 receptor, causing a sustained, enhanced response (Leask and Abraham, 2004). It regulates cellular apoptosis, fibroblast proliferation, angiogenesis and deposition of ECM. These mechanisms of CTGF signalling have been documented in fibrogenesis in lungs, liver, kidneys and skin (Perbal, 2004).

TGF-β is normally secreted as an inactive complex that is bound to a latency-associated peptide (LAP), a protein that prevents the binding of TGF-β1 with its receptors (Budinger *et al.*, 2006). Once activated, TGF-β binds to its cell membrane type I and type II serine/threonine kinase receptors (**Figure 1.1**). This triggers the phosphorylation and activation of both Smad2 and Smad3. Phosphorylated Smad2/3 bind to Smad4 and translocate into the nucleus where they control the transcription of TGF-β-responsive genes (Meng *et al.*, 2013). Zhao *et al.* (2002) has demonstrated that fibroblasts from Smad3 knockout mice did not synthesize collagen in response to TGF-β1 and the mice were resistant to bleomycin-induced pulmonary fibrosis. In fibrosis, a multitude of mechanisms lead to a hyperactive TGF-β/Smad signalling and thus enhance post-translational activation of TGF-β protein (Meng *et al.*, 2013).

TGF-β is involved in many fundamental biological processes such as cell proliferation, cell migration, cell differentiation, ECM deposition and immune responses. TGF-β disrupts the balance between ECM synthesis and degradation, including an increase in the synthesis of matrix components and a parallel decrease in the matrix proteolytic activity (Brenmoehl *et al.*, 2009). An increase in the expression of TGF-β1 has been demonstrated in fibrotic tissues and regions of increased ECM deposition.

TGF-β is present in normal human bronchoalveolar lavage fluid. High levels of TGF-β1 were found in the lungs in animal models of pulmonary fibrosis. Transient overexpression of TGF-β1 in rat lung using adenovirus resulted in prolonged and severe pulmonary fibrosis (Sime *et al.*, 1997). Bleomycin-induced lung fibrosis was blocked in mice lacking the TGF-β1-dependent Smad3 signalling pathway (Bonniaud *et al.*, 2004; Budinger *et al.*, 2006). TGF-β is also present at the sites of ECM deposition in patients with cryptogenic fibrosing alveolitis. Furthermore, alveolar macrophages and epithelial cells from patients with pulmonary fibrosis highly express TGF-β1 (Xu *et al.*, 2003). In renal fibrosis, TGF-β can stimulate interstitial fibroblasts, mesangial cells and tubular epithelial cells to undergo myofibroblastic activation or transition, leading to the formation of matrix producing fibrogenic cells. In contrast, the inhibition of TGF-β suppresses renal fibrotic lesions and prevents progressive loss of kidney functions (Liu *et al.*, 2006).

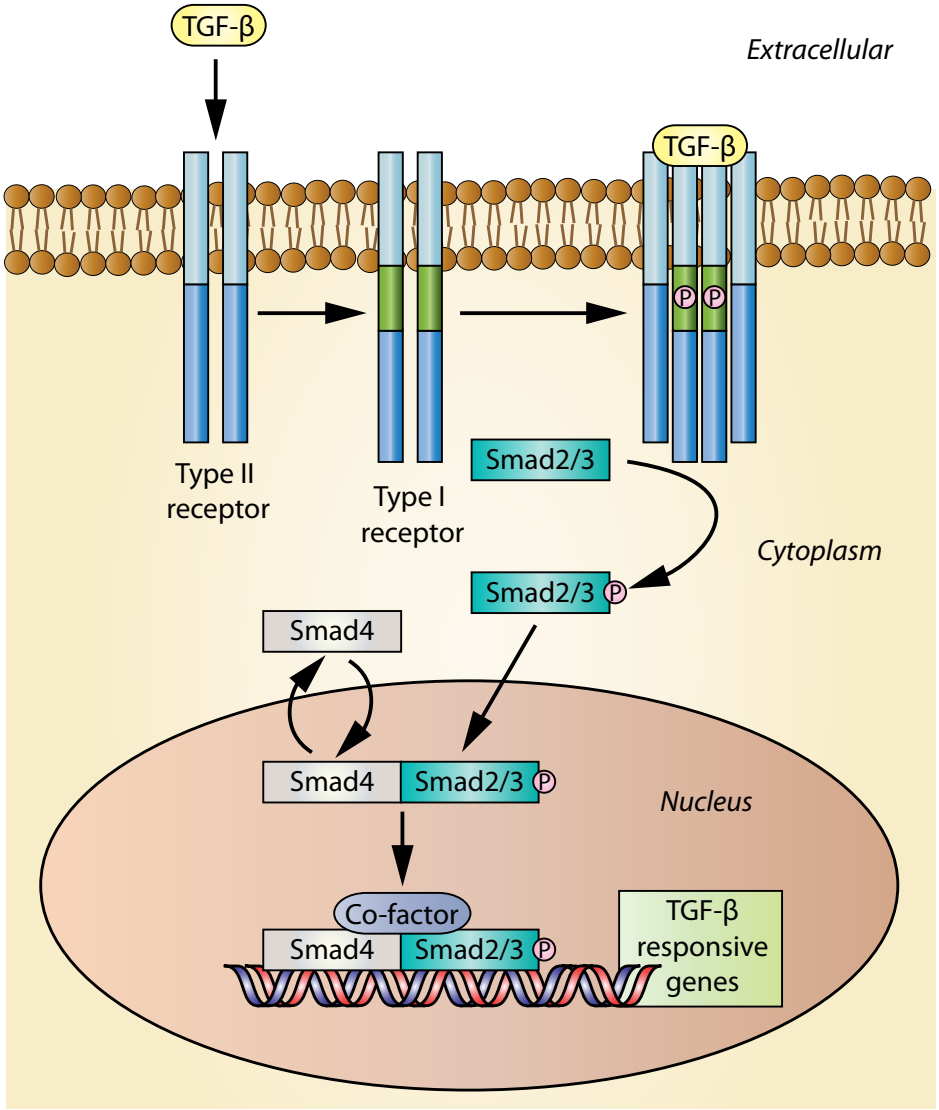

Figure 1.1: TGF-β/Smad signalling Pathway. Binding of TGF-β to the type II receptor results in phosphorylation and activation of the type I receptor. The activated type I receptor then phosphorylates Smad2/3 that promote dimer or trimer formation with Smad4, followed by nuclear translocation. Smad complexes together with their co-factor modulate transcription of TGF-β target genes. Adapted from Meng *et al.*, 2013.

1.2.1.2 ROS

Oxidative stress caused by an increase in ROS is closely related with fibrosis. Neutrophils, eosinophils, alveolar macrophages and alveolar epithelial cells contribute to ROS production in the lung (Piotrowski and Marczak, 2000). Anti-oxidant compounds such as N-acetylcysteine has been demonstrated to protect against the tissue damage and pulmonary fibrosis induced by bleomycin (an oxygen-sensitive anti-cancer drug known to cause pulmonary fibrosis as a side effect) (Serrano-Mollar *et al.*, 2003). In addition, Manoury and colleages showed that NADPH oxidase-deficient p47phox-null mice were resistant against the development of bleomycin-induced lung fibrosis, indicating that NADPH oxidase-derived ROS production contributes to the development of pulmonary fibrosis (Manoury *et al.*, 2005). In the kidney, ROS is a key factor in glomerulosclerosis and tubulointerstitial fibrosis. Renal ROS can be produced by fibroblasts, endothelial cells, vascular smooth muscle cells, mesangial cells, tubular cells and podocytes (Gill and Wilcox, 2006). Anti-oxidants are effective in inhibiting several models of fibrosis, however, none of these has been effective in clinical trials (Kisseleva and Brenner, 2008).

1.2.1.3 Resident Fibroblasts

Resident fibroblasts and myofibroblasts are the major collagen-producing cells in organs including the lungs, kidneys, liver and skin. Depending on the ECM deposition, fibroblasts remain quiescence or differentiate into myofibroblasts. Fibroblasts proliferate and differentiate into myofibroblasts in response to the changes in the mechanical stress of the ECM (Hinz, 2007). In fibrotic lung, the majority of myofibroblasts arise from the resident fibroblasts such as peribronchiolar and perivascular adventitial fibroblasts. These resident fibroblasts upregulate α-SMA, vimentin and collagen in response to fibrogenic stimuli (Phan, 2002; Hinz, 2007). In

fibrotic kidney, myofibroblasts arise from cortical fibroblasts. Cortical fibroblasts are quiescent cells with a low turnover rate under normal condition. However, they proliferate and produce excess matrix proteins in response to injury (Zeisberg *et al.*, 2000; Qi *et al.*, 2006).

In addition, there are several other resident cell types which also contribute to fibrosis. Fibrocytes, pericytes and vascular smooth muscle cells are the additional sources of myofibroblasts in lung and kidney fibrosis (Zhang *et al.*, 1994; Desmoulière *et al.*, 2003). Furthermore, epithelial cells have been identified as crucial precursors of fibroblasts, via epithelial-mesenchymal transition (EMT). EMT normally occurs physiologically during embryonic development. However, there is evidence which support EMT during fibrosis in lungs and kidneys (Okada *et al.*, 1997; Abe *et al.*, 2001) (See **Section 1.3.1.1 & 1.3.2.3**).

1.2.1.4 Fibrocytes

Fibrocytes are circulating connective tissue progenitor cells which are implicated in fibrosis in the skin, kidneys, lungs and liver. Fibrocytes originate from bone marrow. They account for 20% of cells in the lungs of animal models with lung injury (Epperly *et al.*, 2003). They have dual characteristics of lymphoid cells and fibroblasts. Fibrocytes express CD34, CD45 and collagen I but negative for α-SMA. In response to injury, fibrocytes migrate in the blood to the injured organ. The number of infiltrating fibrocytes correlates with the intensity of fibrosis (Bucala *et al.*, 1994). They are not only involved in the collagen deposition, they also secrete growth factors and cytokines that promote ECM deposition in the area of fibrosis. They can also differentiate into myofibroblasts (Quan *et al.*, 2006).

1.3 Clinical Models of Fibrosis

1.3.1 Pulmonary Fibrosis

Pulmonary fibrosis is the abnormal formation of fibre-like scar tissue in the alveoli and interstitium of the lungs, resulting in the thickening of the tissues and an irreversible loss of the tissues' ability to transfer oxygen into the bloodstream (Chapman, 1999). There are a number of conditions and risk factors associated with the disease, including smoking, occupational hazards, and viral and bacterial infections (Jakab, 1990; Meliconi *et al.*, 1996; Baumgartner *et al.*, 1997, 2000). In some patients, chronic pulmonary fibrosis develops without an identifiable cause, a condition called idiopathic pulmonary fibrosis (IPF) (Pardo *et al.*, 2005). It is characterised by alveolar epithelial cell (AEC) injury, fibroblast proliferation and excessive ECM deposition in the lung parenchyma. The accumulation of fibroblasts and myofibroblasts specifically between the vascular endothelium and alveolar epithelium disrupts the architecture of the lung (Qunn *et al.*, 2002). The main feature of IPF is the presence of fibroblastic/myofibroblastic foci (areas of active fibrogenesis, which are widely dispersed throughout the lung parenchyma) (Ramos *et al.*, 2001; Pardo *et al.*, 2005). If the disease progresses, the lung tissues eventually thicken and become stiff, leading to breathlessness. Misdiagnosis is common as the origin and development of the disease are not completely understood (Selman *et al.*, 2001; Pardo *et al.*, 2005).

IPF accounts for ∼55% of lung diseases classified as idiopathic interstitial pneumonia. IPF is uncommon in people aged under 50 years (Meltzer and Noble, 2008). Disease prevalence of IPF in the UK is approximately 15,000 and it has been estimated that approximately 5,000 new cases are diagnosed every year (Navaratnam *et al.*, 2011). The prognosis for individuals with IPF is poor, with a 5-year survival rate which is worse than several types of cancer (du Bois, 2012).

1.3.1.1 Cellular Mechanism of Pulmonary Fibrosis

It has been suggested that IPF involves abnormal wound healing in response to aberrant alveolar epithelial injury. Epithelial cell death is a prominent feature of fibrotic lung diseases. Continuous mechanical stretch of alveolar epithelium by forced ventilation results in pulmonary injury and fibrosis. AECs are in the alveolus to respond to injurious events by both proliferating to replace alveolar type I cell loss and by transdifferentiating into fibroblast/myofibroblast to promote repair (Kim *et al.*, 2006). The excessive formation of active fibroblasts/myofibroblasts leads to the exaggerated accumulation of ECM which causes irreversible destruction of lung parenchyma (Selman *et al.*, 2001; Thannickal *et al.*, 2004). The severity of fibrosis is inversely related to the efficiency of alveolar epithelial repair. A dysfunctional epithelial repair with a delay in appropriate re-epithelialisation could lead to fibrosis. Increased damage of the pulmonary epithelial cells leads to an increase in cytokine release, causing fibroblast activation and differentiation which is implicated in the pathogenesis of IPF (Plataki *et al.*, 2005). By preventing apoptosis of epithelial cells using an anti-Fas ligand (FasL) antibody, Kuwano and colleagues (1999a) were able to prevent the development of fibrosis in animal models of bleomycin-induced lung fibrosis.

EMT has been implicated in the pathogenesis of pulmonary fibrosis, AECs are the source of EMT in injured lungs. Biopsies from fibrotic human lungs showed epithelial cells with mesenchymal features, suggesting the possibility of EMT during fibrogenesis (Tanjore *et al.*, 2009). Alveolar epithelium consists of two types of epithelial cells, elongated alveolar type I cells which are responsible for gas exchange, and, cuboidal alveolar type II cells which synthesise and secrete surfactant (Yano *et al.*, 1997). Alveolar type II cells are the pulmonary multipotent progenitors which are capable

of self proliferating and differentiating into alveolar type I cells and fibroblasts during injury. During fibrosis, both alveolar cell types change morphology and gene expression patterns, downregulate of pulmonary epithelium markers and upregulate fibroblast specific markers (Willis *et al.*, 2006).

Furthermore, TGF-β1 derived from epithelial cells is implicated in both AEC apoptosis and EMT. Kim *et al.* (2006) demonstrated that the treatment of AEC on matrigel with exogenous TGF-β1 leads to AEC apoptosis whereas AECs on fibronectin undergo EMT through activation of endogenous TGF-β1. These results indicate that an initiating stimulus leads to AEC apoptosis and enhanced alveolar permeability, then later AECs within a fibrin-rich provisional matrix undergo EMT and contribute to fibrosis (Kim *et al.*, 2006).

The origin of lung fibroblasts during pulmonary fibrosis is believed to be derived from proliferation of resident lung interstitial fibroblasts, differentiation of fibrocytes or EMT. Resident fibroblasts within the lung likely make a major contribution to the population of myofibroblasts which are recruited and mobilised during fibrosis. Prior animal studies have demonstrated that *in situ* proliferation contributes to the lung fibroblast population (Zhang *et al.*, 1994). A few studies have suggested that lung fibroblast development during injury responses may also be derived from bone marrow progenitor cells (fibrocytes) that contribute to the fibrogenic process (Hashimoto *et al.*, 2004; Phillips *et al.*, 2004; Kim *et al.*, 2006). Furthermore, Kim *et al.* (2006) demonstrated AECs (particularly type II AECs) as the progenitors for fibroblasts *in vivo* and the provisional ECM as a key regulator of epithelial transdifferentiation during fibrogenesis. Tanjore *et al.* (2009) showed that 30% of the fibroblasts in fibrotic lung were derived from lung epithelium via EMT in the bleomycin-induced lung fibrosis model.

Lung myofibroblasts may derived from resident fibroblasts, fibrocytes and the lung epithelium (Hinz, 2007). Based on the studies that myofibroblasts arise *de novo* and on the kinetics of the induction of α-SMA expression, the perivascular and peribronchiolar adventitial fibroblasts are suggested as precursors (Zhang *et al.*, 1994). Circulating fibrocytes have been reported to migrate to tissue injury sites and differentiate into myofibroblast (Abe *et al.*, 2001). Furthermore, both EMT and EndoMT have been suggested as intrapulmonary precursors. The persistence of the myofibroblasts is thought to be of significant in the propagation of fibrosis with evolution to terminal end stage fibrotic lung disease.

1.3.1.2 Treatment

The pharmacological treatment that is currently available for IPF is clearly inadequate and drugs to treat lung scarring are still in the experimental phase (Selman *et al.*, 2001; Morrisey, 2003). Corticosteroids have been used as a mainstay of the other forms of pulmonary fibrosis. However, no studies have demonstrated a consistent benefit of corticosteroid monotherapy in the treatment of IPF (Munson *et al.*, 2010). IPF patients receiving medication for gastroesophageal reflux have longer survival compared to those not on treatment (Lee *et al.*, 2011). Pirfenidone, an anti-fibrotic agent with anti-inflammatory and anti-oxidant properties through TNF-α and TNF-β pathways, has been assessed in patients with IPF in four Phase III trials (Azuma *et al.*, 2005; Taniguchi *et al.*, 2010; Noble *et al.*, 2011). The meta-analysis of change in lung function shows a great consistency of treatment effect of pirfenidone in all four studies. Fewer overall deaths and significantly fewer on-treatment deaths related to IPF occurred in the pirfenidone group than in the placebo group. In all of the studies, pirfenidone was tolerated well. Commonly reported adverse events included gastrointestinal symptoms, photosensitivity, and dizziness.

1.3.2 Renal Fibrosis

The loss of renal function during kidney disease may occur rapidly and reversibly, as in the case of acute kidney injury (AKI); whereas in chronic kidney disease (CKD), the renal function declines slowly with no prominent symptoms in early stages of disease. It has been reported that patients who survived from AKI had significant risk for the development of progressive CKD and end-stage renal disease. Both AKI and CKD may progress to end-stage renal disease in which renal replacement therapy is required (Lim *et al.*, 2012). The annual incidence of end-stage renal disease generated from AKI survivors may account for quarter of the increase in end-stage renal disease incidence (Prunotto *et al.*, 2012).

Renal fibrosis is the final manifestation of chronic kidney disease which is characterised by tubulointerstitial fibrosis and glomerulosclerosis with excessive deposition and accumulation of ECM components in the renal interstitial and tubulointerstitial cells, including collagen types I, III and IV, fibronectin, laminin and proteolycans (Eddy, 2000; Schieppati and Remuzzi, 2005). In the early response to kidney injury, there is an expanding population of interstitial cells and deposition of collagen (Lin *et al.*, 2008; Humphreys *et al.*, 2010). These cells are embedded in the basement membrane of peritubular capillaries (Humphreys *et al.*, 2010; Chang *et al.*, 2012). Interstitial fibroblasts, tubular epithelial cells and mesangial cells are the key fibrogenic cells in the injured kidney (Eddy, 2000). Tubulointerstitial inflammation is believed to play a central role in the development and progression of renal fibrosis. Interstitial inflammation is associated with ROS and increased angiotensin II activity, with their combined effects leading to disruption in glomerulotubular continuity, development of hypoxia, and impairment of protective auto-regulation of glomerular blood flow resulting in glomerulosclerosis. Close correlations of

the extent of fibrosis and the decrease of organ function have been shown in the kidney (Ruiz-Ortega *et al.*, 2006).

1.3.2.1 Glomerulosclerosis

Glomerulosclerosis is the progressive sclerosis and fibrosis of the glomeruli, leading to loss of the filtration surface area and hence renal dysfunction. This process occurs in the glomeruli which are affected by immune, hypertensive or metabolic injuries (Brady, 1994; Savage, 1994). Glomerular endothelial cells are the key effector cells in the inflammatory processes within the glomerulus. Endothelial injury causes the loss of anti-coagulant properties, resulting in the adhesion of platelets and their aggregation within the glomerular capillaries (Johnson, 1991). The surface expression of cell adhesion molecules (CAMs) changes in injured endothelial cells and this facilitates the infiltration of monocytes and macrophages in the glomeruli (Brady, 1994; Savage, 1994). Indeed, the release of chemokines by injured or activated endothelial cells may further attract inflammatory cells to the glomeruli and lead to their activation (Stahl, 1995; Wenzel and Abboud, 1995). The interactions between glomerular endothelial cells with circulating leukocytes and platelets may initiate glomerulosclerosis. Changes in the glomerular endothelium may also activate the underlying mesangial cells. Mesangial cells are able to synthesis and release pro-inflammatory cytokines and chemokines as well as fibrogenic growth factors such as PDGF (Abboud, 1993). Furthermore, mesangial cells acquire an α-SMA positive myofibroblast phenotype in response to TGF-β released during injury. They have also been demonstrated to be capable of synthesizing collagens type I and III and degrade ECM by the release of matrix metalloproteinases (el Nahas *et al.*, 1997). An imbalance between excessive synthesis and decreased breakdown of the glomerular ECM will lead to glomerulosclerosis.

1.3.2.2 Renal Tubulointerstitial Fibrosis

Renal tubulointerstitial fibrosis is a common pathway in progressive renal impairment and the proximal tubular epithelial cells play a vital role in this process. The tubulointerstitial space is composed of tubules and surrounding interstitium. Renal tubulointerstitial fibrosis is characterised by increased proliferation of fibroblasts and accumulation of matrix proteins in the renal interstitium (Eddy, 1996; Nangaku, 2004). Chronic inflammation generally precedes the development of fibrosis and inflammatory cytokines are important mediators of fibrogenesis. The severity of tubulointerstitial inflammation and fibrosis has been considered as a vital determinant of progressive renal injury and long-term prognoses for both human and experimental glomerulonephritis (Kondo *et al.*, 2001). The area of active interstitial fibrosis predominantly exhibits a peritubular (rather than a perivascular) distribution (Koesters *et al.*, 2010). Moreover, in proteinuric nephropathies with progressive injury of the glomerular filtering barrier, abnormal uptake of ultrafilted proteins by proximal tubular cells induces release of TGF-β1, hence promoting interstitial fibrogenesis (Abbate *et al.*, 2002). Patients with tubulointerstitial fibrosis have a poor prognosis and the condition often progresses to end-stage renal failure. End-stage renal failure is characterised by inflammation, scarring of glomeruli (glomerulosclerosis), scarring of the tubules and the interstitial cells (tubulointerstitial fibrosis), and tubular atrophy, which together result in loss of nephrons (Strutz, 1995).

1.3.2.3 Cellular Mechanism of Renal Fibrosis

Fibroblasts are not particularly abundant in normal kidneys when compared with lungs, lymphoid nodes, and spleens (Marković-Lipkovski, 2002). During renal fibrogenesis, about 36% of new fibroblasts come from local EMT, about 14−15% from the bone marrow-derived circulating mesenchymal cells (fibrocytes), and the rest

from other resident cell types proliferation (Iwano *et al.*, 2002). Hence, EMT is a major contributor to the pathogenesis of renal fibrosis. Tubular epithelial cells can acquire a mesenchymal phenotype leading to a substantial increase in the number of myofibroblast during fibrosis (Zeisberg and Kalluri, 2004). EMT during kidney fibrosis correlates with the expression of fibroblast specific protein-1 (FSP-1). FSP-1 identifies tubular epithelial cells undergoing transition in damaged nephrons and the number of fibroblasts. These FSP-1-positive epithelial cells traverse through damaged tubular basement membrane and accumulate in the interstitium of the kidney where they lose their epithelial markers and gain a fibroblast phenotype (Okada *et al.*, 1996; Iwano *et al.*, 2002).

Fibroblasts are the resident interstitial cells of the kidneys which mainly cause renal tubulointerstitial fibrosis. In tubulointerstitial fibrosis, fibroblasts proliferate, migrate and synthesis growth factors and matrix proteins, contributing to the development of renal tubulointerstitial fibrosis. The tubules and peritubular capillaries ultimately disappear, the fibroblasts transform into myofibroblasts and increase in number and the mononuclear cells infiltrate into the interstitium, resulting in the formation of the interstitial scar (Marković-Lipkovski, 2002).

It appears that the loss of the normal, homeostatic microenvironmental is the main cause of myofibroblast differentiation in fibrosis. The cross talk between epithelial cells and fibroblasts is crucial for the maintenance of the local homeostatic microenvironment (Hinz *et al.*, 2012). Several progenitors have been proposed in addition to local fibroblasts, including circulating fibrocytes, local pericytes and resident epithelial cells, through EMT (Zeisberg and Kalluri, 2004; Lin *et al.*, 2008). The number of infiltrated fibrocytes correlates with the intensity of interstitial fibrosis in patients with glomerulonephritis (Okon *et al.*, 2003).

Pericytes are the major source of precursors of scar-producing myofibroblasts during kidney fibrosis. They are mesenchyme-derived perivascular cells aligned with the peritubular capillaries of the interstitium (Allt and Lawrenson, 2001). Unlike fibroblasts, they have important functions in regulating microvascular stability, angiogenesis, capillary permeability, capillary flow and capillary basement membrane synthesis (Allt and Lawrenson, 2001). Pericytes are found within the glomerular and tubulointerstitial compartments (Smith *et al.*, 2012). Pericytes detach from the interstitial capillary within hours of the induction of renal injury (Lin *et al.*, 2008). Using a mouse model that expresses enhanced green fluorescent protein (EGFP) under the regulation of collagen 1α1 promoter, Lin *et al.* (2008) demonstrated that activation of pericytes and peritubular fibroblasts contributed significantly to interstitial myofibroblast population in experimental renal fibrosis.

Although endothelial cells produce PDGF and TGF-β in fibrosing kidneys, injured epithelial cells are the major source of these cytokines, and the TGF-β activator integrin αvβ6 is restricted to kidney epithelium (Ma *et al.*, 2003; Chen *et al.*, 2011b). In normal and diseased kidneys, the TGF-β receptor is widely expressed in the kidney epithelium and pericytes, whereas the synthesis of ligand TGF-β is most upregulated in injured tubular epithelium (Wu *et al.*, 2013). TGF-β has been identified as an important cytokine during loss of epithelial cells known as tubular atrophy (Miyajima *et al.*, 2000; Ma *et al.*, 2003; Sato *et al.*, 2003). Increased TGF-β expression by epithelium is accompanied by the activation of intracellular signalling pathways and downstream effectors in the epithelium itself (Sato *et al.*, 2003). Blocking TGF-β and its downstream effectors can attenuate kidney injury and fibrosis (Sato *et al.*, 2003). Koesters *et al.* (2010) have shown that overexpression of TGF-β1 in renal tubules in a transgenic mouse model induced peritubular fibrosis of local degeneration of nephrons. They demonstrated that the initial response of

tubular cell-derived TGF-β1 consisted of robust peritubular cell proliferation and collagen deposition. Then, nephrons became degenerated with tubular dedifferentiation and proceeded to a total decomposition of tubular cells by autophagy. The fibrosis seen in between intact tubules and in areas of tubular decomposition were resulted from myofibroblasts that were derived from local fibroblasts. Ultimately, the remnants of tubular basement membrane collapsed and embedded into a dense collagenous fibrous tissue (Koesters *et al.*, 2010).

Macrophage infiltration is often associated with the degree of renal fibrosis. Macrophages infiltrating the kidneys produce various pro-inflammatory cytokines including TNF-α, IL-1β and metalloproteinases (Dowdy *et al.*, 2005). Depletion of macrophages during fibrogenesis reduces fibrosis, suggesting that macrophages also contribute in some way to fibrosis (Ricardo *et al.*, 2008). On the other hand, macrophages that take up apoptotic cells exhibit anti-inflammatory properties and may contribute to the resolution of inflammation (Kluth, 2007). Thus, macrophages likely play multiple, and often opposing, roles in kidney disease and repair.

1.3.2.4 Treatment

The treatments for chronic kidney disease has greatly improved following the introduction of drugs targeting the renin-angiotensin system, allowing proteinuria reduction and better control of blood pressure (Onuigbo, 2011). Angiotensin-converting enzyme inhibitors and angiotensin II receptor type I blockers are the first line drugs in combating renal fibrosis (Boor *et al.*, 2007). High dosage (Adamczak *et al.*, 2003) or combination (Wolf and Ritz, 2005) of these both drugs show potential in experimental studies to halt progression of renal fibrosis in the early stages. In addition, renin inhibitors are potential drugs for the treatment of renal fibrosis in

rats, however, its clinical effects on human remain to be determined (Pilz *et al.*, 2005).

Kidney injury is always associated with the release of growth factors such as TGF-β by inflammatory cells which can provoke EMT. Recombinant human bone morphogenic protein (BMP)-7 is the endogenous antagonist of TGF-β-induced EMT in the kidney and elsewhere (Zeisberg *et al.*, 2003). Mice with renal fibrosis that have been systemically treated using the cytokine BMP-7 showing reversal of EMT and repair of damaged tubular structures with repopulation of healthy tubular epithelial cells. A significant decrease in the number of EMT-derived and bone marrowed-derived fibroblasts was observed (Morrissey *et al.*, 2002; Zeisberg *et al.*, 2003). Interestingly, in non-uraemic type I diabetic patients who received pancreas transplantation, a reduction in interstitial collagen deposition and atrophic tubules was observed after 10 years of transplantation, indicating remodelling of renal lesions (Fioretto *et al.*, 2006).

Due to the complexity and variability of organ fibrosis, it is difficult to establish an anti-fibrotic therapy for clinical application. Thus, effective therapies to prevent or to reverse existing fibrotic lesions are not yet available for any organ. However, some strategies have been proposed, such as modulation of inflammation, pharmacological prevention of ECM deposition and inhibition of pro-fibrotic growth factors (Wynn and Ramalingam, 2012).

1.4 Proteinase-activated Receptors

Proteinase-activated receptors (PARs) have been implicated in a number of diseases including cancer and inflammation of the cardiovascular, respiratory, gastrointestinal, musculoskeletal and nervous systems. PAR activation induces the upregulation of pro-inflammatory mediators and adhesion molecules, vasodilation and enhanced vascular permeability, suggesting the involvement of PARs in inflammation and tissue repair (Cocks and Moffatt, 2000; Vergnolle *et al.*, 2001). Studies of PAR-deficient mice have provided unique insights into the strategies for drug development. Thus, PARs have become attractive targets for the development of therapeutic drugs.

PARs are a group of G protein-coupled receptors (GPCRs) that possess a unique mechanism of activation. Unlike the other GPCRs that have agonist-receptor systems, PAR activation is dependent on the specific cleavage of the extracellular N-terminus by proteinases such as thrombin, trypsin and cathepsin G (CG). Proteolytic unmasking of the N-terminal tail of the PARs reveals a tethered ligand sequence which interacts with the extracellular loop 2 (ECL2) of the PARs to trigger a sequence of events (Vu *et al.*, 1991a; Hollenberg and Compton, 2002) (**Figure 1.2**). Synthetic peptides that mimic the final five to seven amino acids of the tethered ligand sequence can also specifically activate PARs, providing useful pharmacological tools to understand the physiology of these receptors. To date, four members of the PARs family have been identified: PAR_1, PAR_2, PAR_3 and PAR_4. They have been shown to be differentially expressed in humans and mice and between tissues (Ortiz-Stern *et al.*, 2012). Several endogenous proteinases are able to activate the members of the PARs family. For instance, thrombin activates of PAR_1, PAR_3 and PAR_4; trypsin activates PAR_2, PAR_4 and to a lesser extent PAR_1; CG activates PAR_4; mast cell tryptase can activate PAR_2 (Vergnolle *et al.*, 2001)(**Table 1.1**).

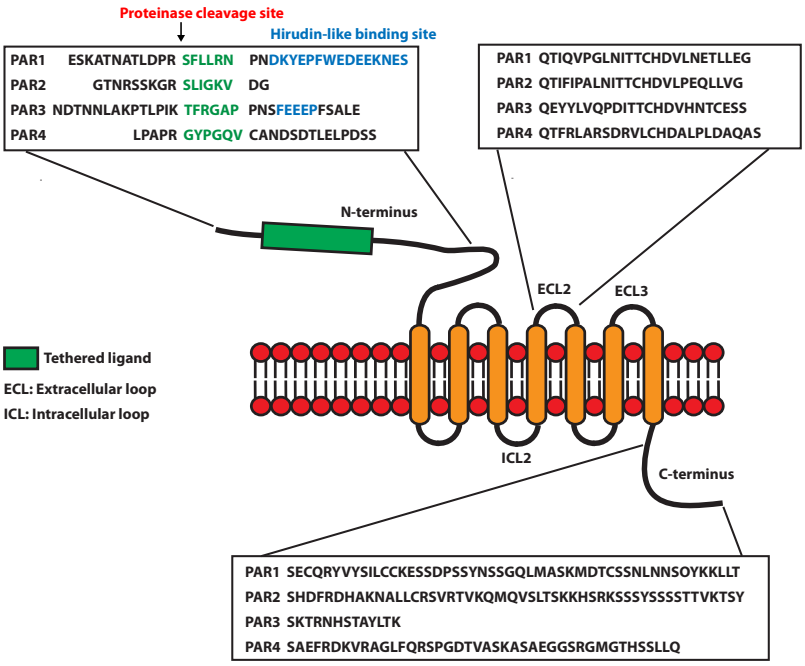

Figure 1.2: Structure of PAR and Their Activation. The proteinase cleaves PARs at a specific cleavage site and unmasks a tethered ligand which then interacts with the ECL2 to initiate signalling. The amino acid sequences of the tethered ligand, the ECL2 and the intracellular C-terminus of human PARs are presented in the boxes. Hirudin-like binding domain sequences for PAR_1 and PAR_3 are printed in blue (Adapted from STEINHOFF *et al.*, 2005).

Table 1.1: A Summary of PARs and Their Activating Proteases.

	PAR_1	PAR_2	PAR_3	PAR_4
Amino acid composition	425 aa	395 aa	374 aa	385 aa
Cleavage site	$LDPR^{41}\downarrow S^{42}FLLRN$	$SKGR^{34}\downarrow S^{35}LIGKV$	$LPIK^{38}\downarrow T^{39}FRGAP$	$PAPR^{47}\downarrow G^{48}YPGQV$
Tethered ligand sequence	SFLLRN	SLIGKV	TFRGAP	GFPGQV
Selective agonist peptide	TFLLRN-NH_2	SLIGKV-NH_2	None known	GYPGQV-NH_2
				AYPGQV-NH_2
Activatory protease	Thrombin	Trypsin	Thrombin	CG
	Trypsin	Tryptase		Thrombin
				Trypsin
Inhibitory protease	CG	Elastase	CG	None known
	Proteinase 3	Chymase	Elastase	
	Elastase	CG		
	Chymase			
Phenotype of knockout	Partial embryonic lethality,	No embryonic lethality	No embryonic lethality	No embryonic lethality
	Normal haemostasis	Impaired leukocyte migration	Impaired platelet activation	Loss of platelet activation

1.4.1 Discovery and Gene Structure

1.4.1.1 PAR_1

PAR_1 was the first member of the PAR family to be cloned and the first receptor for which this unique mechanism of activation was described (Vu *et al.*, 1991a). The interest in PAR_1 was initially driven by research on the receptor responsible for thrombin-induced activation of platelets (Vergnolle *et al.*, 2004). The observation that thrombin can mediate responses in cells which were distinct from its role in the blood clotting cascade led to the discovery of PAR_1 (Weksler *et al.*, 1978; Bar-Shavit *et al.*, 1983a,b; Babich *et al.*, 1990). PAR_1 was cloned in the same year by two laboratories using the strategy of expressing RNA from thrombin-responsive cells of humans and hamsters in oocytes of Xenopus (Rasmussen *et al.*, 1991; Vu *et al.*, 1991a). Sequencing of the cDNA revealed that it encodes a protein of 425 amino acid residues with a poly-adenines (poly-A) tail (Vu *et al.*, 1991a). The receptor contains eight hydrophobic domains, an N-terminal signal sequence and the seven transmembrane spanning characteristic of GPCRs (Vu *et al.*, 1991a). A potential cleavage site for thrombin ($LDPR^{41}\downarrow S^{42}FLLRN$, where $\downarrow$ is the cleavage site) has been identified within the N-terminal region of PAR_1 (Ossovskaya and Bunnett, 2004).

1.4.1.2 PAR_2

PAR_2 was found by screening a mouse genomic library with an oligonucleotide probe based on the bovine substance K receptor. A clone encoding a protein of 395 amino acid residues with a poly-A tail was identified (Nystedt *et al.*, 1994, 1995). The proteinase cleavage sites for the murine and human PAR_2 are identical ($SKGR^{34}\downarrow S^{35}LIGKV$) but the proteolytically revealed tethered ligand is not conserved (SLIGKV in humans and SLIGRL in mice) (Nystedt *et al.*, 1994; Ossovskaya and

Bunnett, 2004). Sequence comparison of murine and human PAR_1 with murine PAR_2 showed ∼30% homology. PAR_2 exhibits the hallmark of PAR_1 in terms of the tethered-ligand mechanism for its activation by trypsin (Nystedt *et al.*, 1994; Ossovskaya and Bunnett, 2004).

1.4.1.3 PAR_3

The discovery of PAR_2 and the absence of PAR_1 in murine platelets prompted a continued search for more thrombin receptors, resulting in the discovery of PAR_3 (Connolly *et al.*, 1996). Connolly and colleagues (1996) provided evidence for the presence of the second thrombin receptor from their observations that platelets derived from PAR_1 deficient mice still responded to thrombin. Subsequently, Ishihara *et al.* (1997) used degenerate primers to conserved domains of PAR_1 and PAR_2 to screen RNA from rat platelets and then employed the sequence obtained to identify human PAR_3. Human PAR_3 gene encodes a protein of 374 residues and shows ∼28% sequence homology to human PAR_1 and PAR_2. Like PAR_1 and PAR_2, PAR_3 is a typical GPCR with a thrombin cleavage site within the extracellular N-terminal region at $LPIK^{38}\downarrow T^{39}FRGAP$.

1.4.1.4 PAR_4

The identification of PAR-like sequences by searching expressed sequence tag databases using the coding region of PAR_2 lead to the discovery of murine PAR_4 (Ishii *et al.*, 1994; Kahn *et al.*, 1998). Human PAR_4 was then discovered by searching the DNA sequence databases with amino acid sequences derived from PAR_1, PAR_2 and PAR_3 (Xu *et al.*, 1998). The cDNA sequence of human PAR_4 encodes a protein of 385 residues, with a potential cleavage site for thrombin and trypsin within the extracellular N-terminal region at $PAPR^{47}\downarrow G^{48}YPGQV$ (Kahn *et al.*, 1998; Xu *et al.*, 1998). PAR_4 alignment to the other PAR family members showed ∼30%

sequence homology, with some differences in the N- and C-terminal domains (Xu *et al.*, 1998).

1.4.2 Mechanisms of PAR Activation

Unlike the typical GPCRs in which the cellular activation events are initiated by the small hydrophilic molecules that bind reversibly to the receptors' extracellular and transmembrane domains to elicit cellular responses, PARs have a unique mechanism of activation (Wettschureck and Offermanns, 2005). Initially established for PAR_1, this activation mechanism appears as a general paradigm for the PAR family members (Vu *et al.*, 1991a). PARs are activated by an unusual irreversible proteolytic mechanism in which the protease binds to and cleave a specific site within the receptors' N-terminal domain. This reveals a tethered ligand that binds intramolecularly to the body of the receptor to initiate transmembrane signalling (Steinhoff *et al.*, 2005). This tethered ligand mechanism has become the hallmark characteristic of the PAR family. Synthetic peptide which mimics the tethered ligand can also activate the receptor (Nystedt *et al.*, 1994).

1.4.2.1 PAR_1 Activation

The structural and functional determinants for proteolytically activated receptor have been investigated in detail in the case of the thrombin receptor and its activating peptides (Vu *et al.*, 1991a). The extracellular N-terminal domain of human PAR_1 contains a sequence of charged, hirudin-like residues ($D^{51}KYEPF^{56}$) that is distal to the thrombin cleavage site. The anion binding site on thrombin will bind to this hirudin-like domain, which serves to temporarily concentrate thrombin at the surface of the receptor (Ossovskaya and Bunnett, 2004). The importance of the hirudin-like domain is determined by the finding that its deletion markedly

diminishes the ability of thrombin to activate PAR_1 while its presence allows the full recovery of the activity (Vu *et al.*, 1991a; Bouton *et al.*, 1995). Thrombin cleaves PAR_1 at $LDPR^{41}\downarrow S^{42}FLLRN$ to expose the tethered ligand SFLLRN, which binds and activates the cleaved receptor, resulting in signal transduction (Vu *et al.*, 1991a; Ossovskaya and Bunnett, 2004). Vu *et al.* (1991b) demonstrated the importance of the cleavage recognition sequences by replacing LDPR with DDDK, the recognition site for the protease enterokinase, resulting in abolished thrombin responses and making the receptor susceptible to enterokinase activation.

In addition, blocking the cleavage site by antibodies or mutation of the cleavage site prevents the thrombin cleavage and signalling. The interaction between the ECL2 and the tethered ligand is crucial for signalling and proper receptor function. Hence, the ECL2 is a critical determinant of the specificity of the PARs, making important contributions to the receptor structure and function, and is not simply a passive link between the transmembrane domains (Gerszten *et al.*, 1994; Lerner *et al.*, 1996).

A synthetic peptide that mimics the tethered ligand domain ($S^{42}FLLRNPNDKYEPF$) can directly activate intact PAR_1 without the specific cleavage of the extracellular N-terminal domain by thrombin. Peptides as short as six residues, ($S^{42}FLLRN$) are also fully active (Vu *et al.*, 1991a) (**Figure 1.3**).

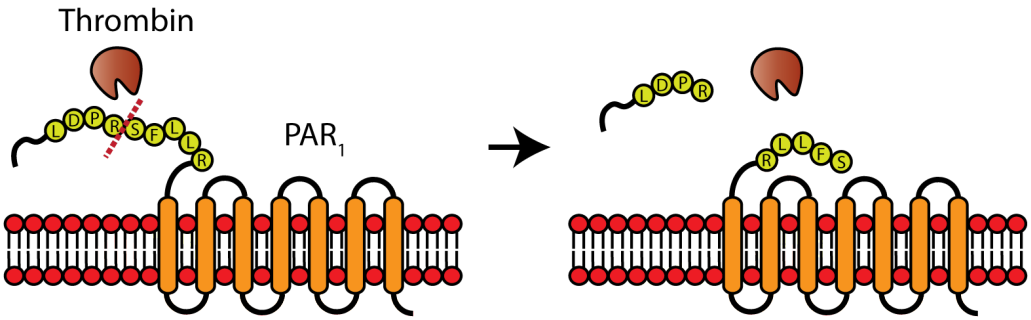

Figure 1.3: PAR_1 Activation. Thrombin cleaves human PAR_1 at its N-terminus, exposing the tethered ligand SFLLRN.

1.4.2.2 PAR_2 Activation

Trypsin cleaves PAR_2 at $SKGR^{34}\downarrow S^{35}LIGKV$ to reveal the N-terminal tethered ligand SLIGKV in humans (Nystedt *et al.*, 1994). Mutation or substitution of the domain in the trypsin cleavage site prevents the activation of PAR_2. Analysis of proteinase cleavage of peptide sequences corresponding to the human PAR_2 N-terminus revealed the $Arg^{34}\downarrow Ser^{35}$ bond as the site for trypsin cleavage and tryptase (Molino *et al.*, 1997). Similar to PAR_1, synthetic peptide corresponding to the tethered ligand domain (SLIGKV) can activate PAR_2 without the requirement of receptor cleavage (Nystedt *et al.*, 1995; Böhm *et al.*, 1996)(**Figure 1.4**).

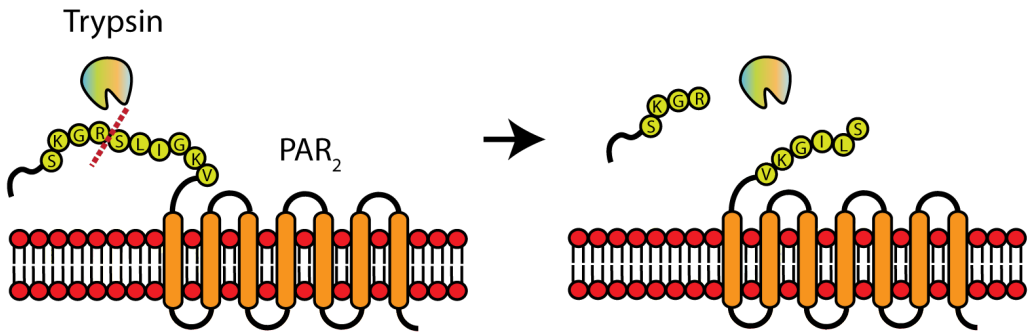

Figure 1.4: PAR_2 Activation. Trypsin cleaves human PAR_2, exposing the ligand sequence SLIGKV.

1.4.2.3 PAR_3 Activation

Similar observations indicate that thrombin cleaves PAR_3 at $LPIK^{38}\downarrow T^{39}FRGAP$ to reveal a new N-terminus (TFRGAP) that may interact with the receptor as a tethered ligand and mutation of the cleavage site would prevent the activation (Ishihara *et al.*, 1997). Synthetic peptides corresponding to this putative tethered ligand can activate PAR_1 and PAR_2 (Hansen *et al.*, 2004; Kaufmann *et al.*, 2005) but not PAR_3 (Ishihara *et al.*, 1997). The reason for this discrepancy is unknown. Another unexpected and unexplained observation is that murine PAR_3 does not appear to signal itself via its thrombin-revealed sequence. Rather, it appears to function as a co-receptor for PAR_4, perhaps allowing thrombin localisation through binding to its hirudin-like sequence and facilitating signalling at low thrombin concentration (Nakanishi-Matsui *et al.*, 2000) (**Figure 1.5**). PAR_3 contains a hirudin-like site (FEEFP) that is distal to the thrombin cleavage site, which interacts with thrombin (Ishihara *et al.*, 1997).

1.4.2.4 PAR_4 Activation

Thrombin, CG and trypsin can cleave PAR_4 at $PAPR^{47}\downarrow G^{48}YPGQV$ to reveal the tethered ligand and a peptide corresponding to the proteolytically revealed tethered ligand domain, GYPGQV, can directly activate PAR_4. Mutation of the cleavage site prevents activation by thrombin, CG and trypsin, but not by the synthetic peptide. This observation showed the importance of proteolytic cleavage for receptor activation (Kahn *et al.*, 1998; Xu *et al.*, 1998). In contrast to the other thrombin receptors, PAR_4 lacks a hirudin-like binding site for thrombin. Thus, PAR_4 is a low affinity receptor for thrombin while PAR_1 and PAR_3 are high affinity thrombin receptors (Kahn *et al.*, 1998; Xu *et al.*, 1998) (**Figure 1.5**).

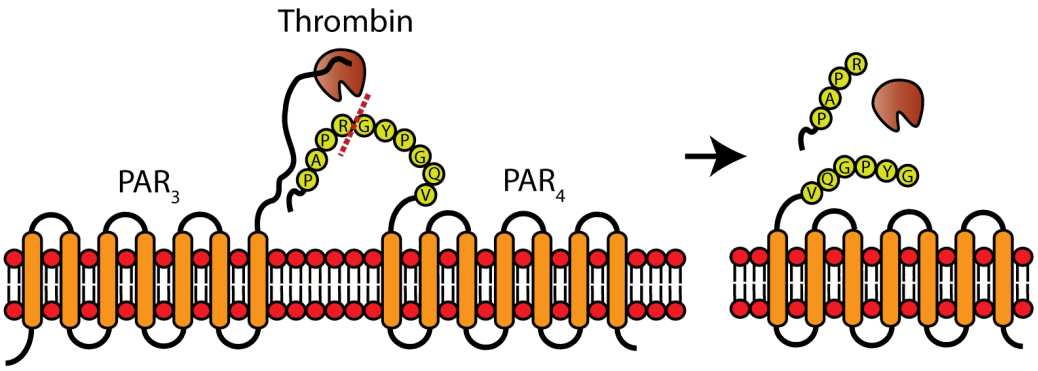

Figure 1.5: PAR_4 Activation. PAR_3 acts as a cofactor for PAR_4 cleavage by thrombin, exposing the tethered ligand GYPGQV in the human PAR_4 N-terminus.

1.4.3 Activation of Multiple signalling Cascades by PARs

Mammalian G-proteins are trimeric proteins made up of α, β and γ subunits. To date, there are four classes of Gα subunits: G_s, G_i, $G_{q/11}$ and $G_{12/13}$. The functional consequences of their activation are believed to be mediated by their α subunit (Wettschureck and Offermanns, 2005). G_s α subunits activate adenyl cyclase whereas G_i α subunits inhibit adenyl cyclase, all α-subunits of the $G_{q/11}$ class activate phospholipase C-β (PLCβ) and $G_{12/13}$ α subunits regulate cell processes via the guanine triphosphate (GTP)ase-activating proteins and guanine nucleotide exchange factors (Cabrera-Vera *et al.*, 2003).

1.4.3.1 PAR_1 signalling

PAR_1 interacts with several Gα subunits, in particular G_i, $G_{q/11}$ and $G_{12/13}$, which accounts for the pleiotropic action of its ligands (Macfarlane *et al.*, 2001). The major pathway of coupling is through $G_{q/11}$ subunits. $G_{q/11}$ subunits play a major role in coupling since thrombin signalling in fibroblasts and platelets that express PAR_1 is attenuated by the microinjection of $G_{q/11}$ α subunits antibodies (Baffy *et al.*, 1994). $G_{q/11}$ subunits activate PLCβ, leading to the generation of inositol 1,4,5-triphosphate (InsP3) which mobilises intracellular Ca^{2+} and diacylglycerol (DAG) and then activates protein kinase C (PKC). Fee *et al.* (1994) showed that thrombin-stimulated InsP3 generation and Ca^{2+} mobilisation were blunted in mutant fibroblasts that expressed low levels of PLCβ but normal levels of other phospholipases.

PAR_1 coupling with $G_{12/13}$ subunits was revealed through studies on thrombin stimulated platelets and astrocytoma cells (Offermanns *et al.*, 1994; Aragay *et al.*, 1995) where thrombin stimulates the incorporation of

a GTP analog into $G_{12/13}$ subunits in platelets, and thrombin-stimulated DNA synthesis is blocked by microinjection of antibodies to $G_{12/13}$ subunits in the astrocytoma cells. PAR_1 also couples to G_i subunits, which inhibit adenyl cyclase and suppress the formation of cyclic adenosine monophosphate (cAMP) (Hung *et al.*, 1992). Furthermore, PAR_1 activates multiple signalling pathways downstream of coupling to G-proteins, including the activation of phosphatidylinositol 3 (PI3) (Malarkey *et al.*, 1995), extracellular signal-regulated kinase/mitogen-activated protein kinase (ERK/MAPK) pathway (Vouret-Craviari *et al.*, 1993), and the Src family tyrosine kinases (Sabri *et al.*, 2000).

1.4.3.2 PAR_2 signalling

Less is known about the signalling mechanism for PAR_2. Activators of PAR_2 stimulate generation of InsP3 and mobilisation of Ca^{2+} in PAR_2 transfected cell lines, indicating, but not confirming that PAR_2 coupling and signalling via $G_{q/11}$ subunits and possibly G_i subunits (Macfarlane *et al.*, 2001).

In enterocytes and transfected epithelial cells, the activation of PAR_2 stimulates release of arachidonic acid and rapid generation of prostaglandins E_2 (PGE_2) and $F_{1\alpha}$, indicating activation of phospholipase A2 and cyclooxygenase-1 (Kong *et al.*, 1997; Ossovskaya and Bunnett, 2004). PAR_2 activation on smooth muscle and neuronal cells has been shown to activate PLC (Berger *et al.*, 2001b) and PKC (Okamoto *et al.*, 2001a), respectively.

The agonists of PAR_2 strongly activate the MAPK cascade in rat aortic smooth muscle cells (Belham *et al.*, 1996) and jun amino-terminal kinase (JNK1/2) and p38 MAPK in human keratinocytes (Kanke *et al.*, 2001). Macfarlane *et al.* (2005) reported that intracellular calcium mobilisation

in keratinocytes is a vital determinant of PAR_2 nuclear factor-kappaB (NFkB) signalling. Also, PAR_2 activation of ERK1/2 has been studied in a variety of cells including cardiomyocytes (Sabri *et al.*, 2000) and smooth muscle cells (Belham *et al.*, 1996).

PAR_2 was also shown to mediate Factor Xa that activates ERK1/2 in coronary artery smooth muscle cells (Koo *et al.*, 2002). Vouret-Craviari *et al.* (2003) showed that endothelial PAR_2 activation induced activation of small molecule G-protein, Rho-A, Rac and p21 activated kinase (PAK).

1.4.3.3 PAR_4 signalling

PAR_3-mediated signalling events are pretty much unclear and it has not been shown to signal through G-proteins (Hansen *et al.*, 2004; Arora *et al.*, 2007). PAR_4 was shown to couple to G_q and $G_{12/13}$ but not G_i in mice lung fibroblast (Faruqi *et al.*, 2000). PAR_4 signalling has been reported to activate MAPK signalling in vascular smooth muscle cells (Bretschneider *et al.*, 2001), mice cardiomyocytes (Sabri *et al.*, 2003b), and human lung endothelial cells (Fujiwara *et al.*, 2005).

1.4.4 Termination of PAR signalling

Due to the unique irreversible mechanism of PAR activation, tethered ligand remains bound to the receptor while PARs are activated, the activation state of the PARs therefore would be expected to elicit continuous signalling. However, PAR-mediated responses appear to be transient in nature with rapid desensitisation and receptor internalisation that tightly regulate PAR signalling (Macfarlane *et al.*, 2001; Hollenberg and Compton, 2002). Studies have shown that sequences within intracellular receptor domains and C-terminal tail regulate the

receptor desensitisation and internalisation. The mechanism of desensitisation varies between different PARs, probably due to structural differences, especially in the intracellular loop 3 and C terminus (Macfarlane *et al.*, 2001; Hollenberg and Compton, 2002; Ossovskaya and Bunnett, 2004). Receptor desensitisation and internalisation mechanisms have been well studied for PAR_1 and PAR_2 but little is known for PAR_3 and PAR_4 (Ossovskaya and Bunnett, 2004).

1.4.4.1 Disarming and Amputation of Tethered Ligand by Proteases

Many proteases can disable PAR activation by removing/ destroying the tethered ligand or by cleaving the binding domain in ECL2, resulting in the generation of receptors which are unresponsive to activating proteases (Ossovskaya and Bunnett, 2004).

Neutrophil, CG, elastase and proteinase 3 can abolish thrombin signalling by cleaving the activation site of PAR_1, whereas chymase (an abundant mast cell proteinase) has been shown to render keratinocytes unresponsive to thrombin, indicating that it can inactivate PAR_1 (Molino *et al.*, 1995; Renesto *et al.*, 1997; Schechter *et al.*, 1998). CG and elastase inactivate trypsin signalling by removing the N-terminal epitopes of PAR_2 but PAR_2 is still able to respond to the PAR_2 agonist peptide (Dulon *et al.*, 2003).

Surprisingly, some proteinases can cleave PARs both at their activation and disabling sites and the net result depends on the efficiency of cleavage at different sites (Ossovskaya and Bunnett, 2004). For example, CG can activate PAR_1 at the activation site Arg^{41}-Ser^{42}, but the major cleavage site is at Phe^{55}-Trp^{56}, which removes the tethered ligand and thus disables the receptor (Molino *et al.*, 1995; Ossovskaya and Bunnett, 2004). In

the case of tryptase, it can cleave PAR_2 at Lys^{41}-Val^{42} site which inactivates the receptor, but the activating cleavage is more important since tryptase activates PAR_2 (Molino *et al.*, 1997; Ossovskaya and Bunnett, 2004).

In human platelets, CG disables PAR_1 but activates PAR_4, whereas in murine platelets, CG disables PAR_3 and abolishes its co-receptor function for PAR_4, thus preventing platelet responses to thrombin (Cumashi *et al.*, 2001).

1.4.4.2 Desensitisation and Internalisation

Ligand occupation of the GPCR induces the translocation of the members of G protein receptor kinase (GRK) family from the cytosol to the activated receptor at the cell surface. GRKs are serine-threonine kinases that phosphorylate activated GPCRs, usually within the C-terminal domain or intracellular loop 3. Phosphorylation then triggers the membrane translocation of arrestins, which interact with GRK-phosphorylated GPCRs to disrupt the interaction between GPCRs and G proteins, thus terminate the signal (Ossovskaya and Bunnett, 2004).

The expression levels of receptors at the cell surface are determined by the balance between removal by internalisation and replenishment by recycling or mobilisation of intracellular pools (Ossovskaya and Bunnett, 2004). PAR_1 and PAR_2 are rapidly internalised after activation and directed to lysosomes for degradation (Hoxie *et al.*, 1993). However, approximately 25% of the receptors are recycled back to the cell surface in order to maintain the amount of receptors at the cell surface and in the intracellular pool (Hoxie *et al.*, 1993).

PAR_1 activation leads to rapid phosphorylation at its C-terminal by several GRKs including GRK3 and GRK5. It was thought that PAR_1

signalling is desensitised by its interaction with β-arrestin 1. However, this interaction with β-arrestin 1 was found to have an important role in the receptor phosphorylation state but not essential for internalisation and downregulation of the receptor (Wolfe *et al.*, 2007). Instead, the internalisation and targeting of phosphorylated PAR_1 to degradation pathway involves deubiquitylation of the receptor, which leads to the clathrin and dynamin-dependent processes (Paing *et al.*, 2006; Chen *et al.*, 2011a).

Activated PAR_2 is rapidly phosphorylated on a stretch of serine and threonine residues at the C-terminal domain, a process which is important for the recruitment of β-arrestins to the receptor. In contrast to PAR_1, the interaction between PAR_2 and β-arrestin is crucial for the desensitisation of signalling, receptor internalisation and targeting to lysosomes (DeFea *et al.*, 2000; Seatter *et al.*, 2004). The PAR_2-β-arrestin complex is targeted to early endosomes, and then to lysosomes in a process that involves deubiquitylation of the receptor (Déry *et al.*, 1999; DeFea *et al.*, 2000; Hasdemir *et al.*, 2009). The mechanism of lysosomal degradation of PARs is still unclear.

The mechanisms regulating the trafficking of PAR_3 and PAR_4 remain largely unknown. PAR_4 desensitisation has been shown to be slower than PAR_1 as PAR_4 is not rapidly phosphorylated in the C-terminal domain, possibly due to a lack of sites for GRK phosphorylation in the C-terminal domain (Shapiro *et al.*, 2000) (**Figure 1.6**).

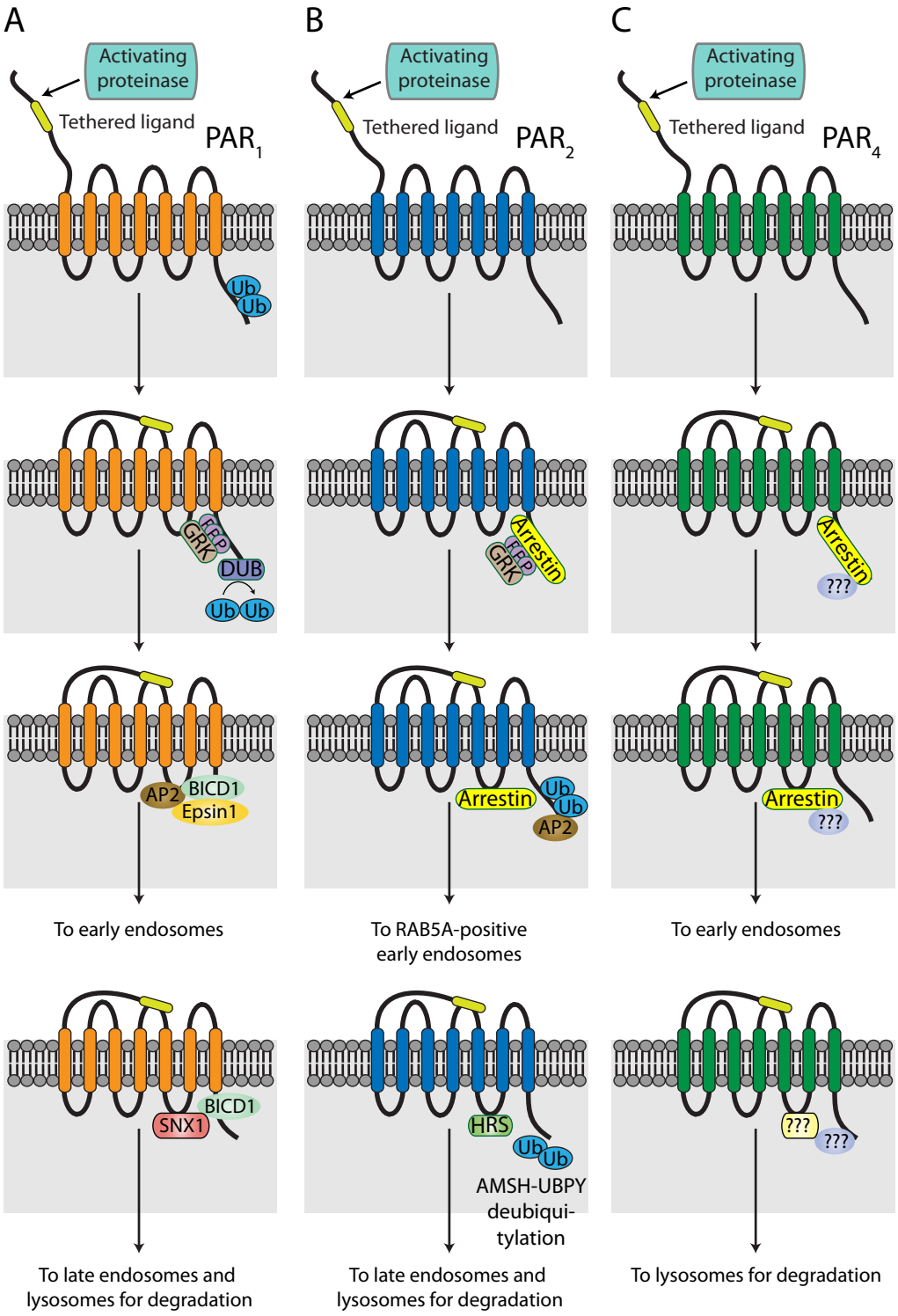
A
Activating proteinase
Tethered ligand
PAR1
Ub
Ub
GRK
FFP
DUB
Ub
Ub
AP2
BICD1
Epsin1
To early endosomes
BICD1
SNX1
To late endosomes and lysosomes for degradation
B
Activating proteinase
Tethered ligand
PAR2
GRK
FFP
Arrestin
Arrestin
Ub
Ub
AP2
To RAB5A-positive early endosomes
HRS
Ub
Ub
AMSH-UBPY deubiqui-tylation
To late endosomes and lysosomes for degradation
C
Activating proteinase
Tethered ligand
PAR4
Arrestin
???
Arrestin
???
To early endosomes
???
???
To lysosomes for degradation

Figure 1.6: Intracellular Trafficking of Activated PARs. PAR activation is irreversible and activated receptors are targeted to the lysosomes for degradation. (A) Following activation, PAR_1 is rapidly phosphorylated at its C-terminal by several GRKs including GRK3 and GRK5. The internalisation and degradation of activated PAR_1 involves deubiquitylation of the receptor which leads to its interaction with the clathrin adaptor protein AP2 and epsin 1. C-terminal of PAR_1 is important for specifying lysosomal targeting. Sorting nexin 1 (SNX1) (a membrane-associated lysosomal sorting protein) and bicaudal D homolog 1 (BICD1) are vital for the translocation of PAR_1 from plasma membrane to lysosomes for degradation. (B) In contrast to PAR_1, the interaction between PAR_2 and β-arrestin is crucial for the desensitisation of signalling, receptor internalisation and targeting to lysosomes. The PAR_2-arrestin complex is targeted to RAB5A-positive early endosomes then to lysosomes that involve the deubiquitylation of PAR_2. (C) The mechanism regulating PAR_3 and PAR_4 remain largely unknown. Due to the low level of PAR_4 C-terminal phosphorylation, PAR_4 desensitisation is slower than PAR_1. Adapted from Ramachandran *et al.*, 2012.

The internalisation of both PAR_1 and PAR_2 is mediated by a clathrin-mediated mechanism. Their internalisation requires GTPase dynamics that mediates the detachment of clathrin-coated pits (Böhm *et al.*, 1996; Déry *et al.*, 1999; Trejo *et al.*, 2000). β-arrestins play an important role in endocytosis of many GPCRs by serving as adaptor proteins that link GRK-phosphorylated receptors to clathrin (Ossovskaya and Bunnett, 2004) (**Figure 1.7**).

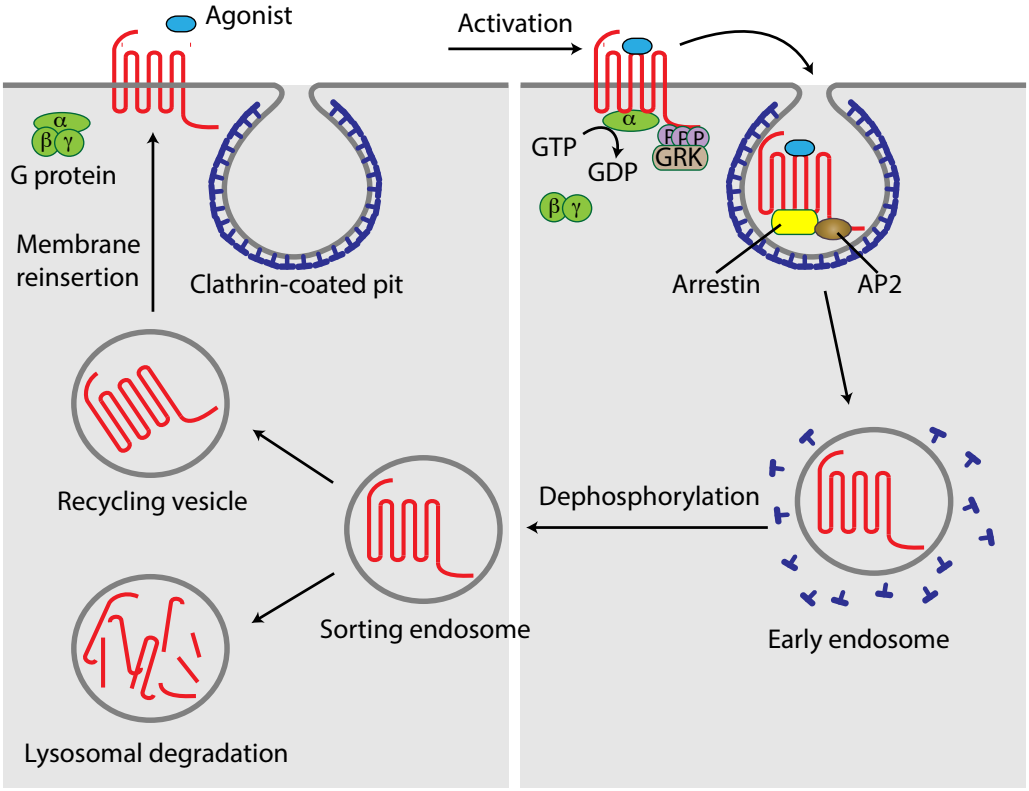

Figure 1.7: Mechanisms that Regulate PAR Desensitisation and Internalisation. Once activated, PARs are rapidly phosphorylated and form a complex with β-arrestin. The PAR-arrestin complex is then endocytosed via clathrin-coated pits and targeted to early endosome. The GTPase dynamics mediates detachment of clathrin-coated pits. Then, PARs are dephosphorylated by protein phosphatases. Finally, PARs are either reinserted into the membrane or targeted to lysosomes for degradation. Adapted from RAMACHANDRAN *et al.*, 2012.

1.4.5 PARs in Physiology and Pathophysiology

PARs are expressed in various tissues and cells throughout mammalian body. The specificities of their involvement in various processes remain to be verified. The PAR-mediated events are complicated as the signalling depends on the availability of the activating or disabling proteases, protease inhibitors and co-factors or anchoring proteins (Ossovskaya and Bunnett, 2004; Steinhoff *et al.*, 2005). In addition, the lack of specific PAR antagonists and the difficulties in extrapolating data obtained from animal models to human diseases make it difficult to determine the precise roles of PARs in human body (Ossovskaya and Bunnett, 2004).

Genetically modified animals have been used to study the role of PARs *in vivo*. Approximately 50% of PAR_1-knockout mice die before birth (Connolly *et al.*, 1996). Embryonic lethality was not associated with the deletion of PAR_2, PAR_3 or PAR_4, suggesting a specific role for PAR_1 in development (Major *et al.*, 2003). PAR_1-knockout mice were hemostatically normal, indicating that deletion of PAR_1 has no effect on thrombin-induced platelet activation (Darrow *et al.*, 1996). Decrease in the leukocytes rolling and delayed onset of inflammation were observed in PAR_2-deficient mice, suggesting the involvement of PAR_2 in inflammation Lindner *et al.* (2000). PAR_3-deficient mice demonstrated a marked reduction in response to thrombin, demonstrating that PAR_3 is a thrombin receptor on murine platelets and contributes to thrombin-induced platelet activation in mice. However, persistent thrombin responses suggest the presence of another thrombin receptor in mice (Kahn *et al.*, 1998; Ishihara *et al.*, 1998). PAR_4-deficient mice are completely insensitive to thrombin, indicating the importance of PAR_4 in mouse platelet (Sambrano *et al.*, 2001).

1.4.5.1 Respiratory System

The human respiratory tract expresses all four PAR members that distribute differently in the airway structures (**Table 1.2**).

Table 1.2: PAR Expression on Different Cell Types in Lung.

PAR	Cell Types	References
PAR_1	Fibroblasts,	Trejo *et al.* (1996); Chambers *et al.* (1998)
	epithelial cells,	Asokananthan *et al.* (2002)
	endothelial cells,	D'Andrea *et al.* (1998); Kataoka *et al.* (2003)
	smooth muscle cells	Lan *et al.* (2000); Walker *et al.* (2005)
PAR_2	Fibroblasts,	Akers *et al.* (2000); Matsushima *et al.* (2006)
	epithelial cells,	Knight *et al.* (2001); Asokananthan *et al.* (2002)
	smooth muscle cells	D'Andrea *et al.* (1998); Schmidlin *et al.* (2001)
PAR_3	Fibroblasts,	Ramachandran *et al.* (2006)
	epithelial cells,	Shimizu *et al.* (2000); Asokananthan *et al.* (2002)
	endothelial cells	Kataoka *et al.* (2003)
PAR_4	Fibroblasts,	Ramachandran *et al.* (2007)
	epithelial cells,	Shimizu *et al.* (2000); Asokananthan *et al.* (2002)
	endothelial cells,	Kataoka *et al.* (2003)
	smooth muscle cells	Lan *et al.* (2000)

PAR_1 and PAR_2 are important in the inflammatory and fibroproliferative processes. PAR_1-knockout mice are partially protected from bleomycin-induced lung fibrosis (Howell *et al.*, 2005). Similarly, PAR_2-null mice develop considerably less inflammation in the airway than the mice which overexpress PAR_2 (Schmidlin *et al.*, 2002). An *in vitro* study showed that PAR_1 and PAR_2 can induce proliferation of lung fibroblasts (Howell *et al.*, 2005). Their expression are upregulated during the development of pulmonary diseases. Increased protein levels of PAR_1 was detected by immunohistochemistry in lung tissues of patients with pulmonary fibrosis (Howell *et al.*, 2005; Blanc-Brude *et al.*, 2005) and in early stage of pulmonary fibrosis associated with scleroderma (Bogatkevich *et al.*, 2005).

PAR_1 expression decreases in fibroblasts following prostaglandin E_2 (PGE_2) exposure (Sokolova *et al.*, 2005). An increased expression of PAR_2 was detected in the bronchial epithelium of asthmatic patients (Knight *et al.*, 2001). PAR_2 expression is also elevated following exposure to a variety of inflammatory stimuli, including smoke, respiratory viruses, bacterial products and allergens (Ostrowska *et al.*, 2007). PAR_4 expression on bronchial fibroblasts was reported to be induced following exposure to inflammatory stimuli, such as lipopolysaccharide (LPS) and TNF-α (Ramachandran *et al.*, 2007).

PAR activation may also promote the inflammatory processes in the respiratory tract, inducing the release of pro-inflammatory cytokines and mediators in cell cultures relevant to airway diseases. PAR_1 and PAR_2 activations enhance the expressions of matrix metalloproteinase-9 and granulocyte-macrophage colony-stimulating factor (GM-CSF), which are the important mediators of inflammation. PAR_1 is also involved in the inflammatory cell recruitment in response to bleomycin injury, collagen accumulation and expressions of pro-fibrotic factors such as CTGF and TGF-β1 (Howell *et al.*, 2005). PAR_2 activation induces the release of IL-6, IL-8 and PGE_2 in primary human bronchial epithelial cells (Asokananthan *et al.*, 2002; Kawabata *et al.*, 2004; Kawabata and Kawao, 2005). PAR_4-mediated signalling has been suggested to contribute to a pro-inflammatory reaction, in which it plays a critical pro-inflammatory role in neutrophil rolling and adherence. Neutrophilic responses were diminished as a result of PAR_4 inhibition (Vergnolle *et al.*, 2002; Slofstra *et al.*, 2007).

PAR agonists can induce the rapid and sustained formation and release of prostanoids from a wide variety of cell and tissue types. For example, PAR_1 AP causes PGE_2 release from human bronchial epithelial cells

(Asokananthan *et al.*, 2002) and human lung fibroblasts (Sokolova *et al.*, 2005). Human cultured bronchial airway epithelial cells release PGE_2 following exposure to PAR_2 AP (Asokananthan *et al.*, 2002). PGE_2 promotes inflammatory processes in most organ systems, but produces predominantly anti-inflammatory effects in the lung. It appears to have a role in limiting the inflammatory response and tissue repair processes (Vancheri *et al.*, 2004). Trypsin induces PGE_2 release from airway smooth muscle cells independently of PAR_2, suggesting that PAR_4 which is also a trypsin receptor may induce PGE_2 release from airway smooth muscle (Chambers *et al.*, 2003). PAR_4 AP can also induce PGE_2 release from the cultured bronchial epithelial cells (Asokananthan *et al.*, 2002). These findings indicate that PAR-mediated PGE_2 production within the airway may inhibit fibrosis through a number of mechanisms.

Infiltration of immune cells has been shown to be inhibited in PAR_2 deficient mice, where allergic inflammation of the airway and neuroinflammation occurred (Noorbakhsh *et al.*, 2006). In pancreatitis, PAR_2 is activated by leaked trypsin, which mediates both pro-inflammatory and anti-inflammatory responses (Komatsu *et al.*, 2012). Involvement of PAR_2 in regulating airway tone has a dual role: protective bronchodilatory response and detrimental bronchoconstriction. The activation of PAR_2 causes relaxation in the main bronchi and trachea but produces contractile responses from the isolated smaller intrapulmonary bronchi. These findings suggest that PAR_2 might be protective in the larger airways but detrimental in the smaller bronchioles as it increases airway resistance by contraction (Ricciardolo *et al.*, 2000; Kawabata and Kawao, 2005).

PAR_4 may also play a pro-fibrotic role. The concentrations of thrombin and/or CG in bronchio-alveolar lavage fluid in patients with IPF or pulmonary fibrosis are much higher than those in healthy controls. Thus, thrombin and/or CG receptors such as PAR_1 and/or PAR_4 are responsible

for the pathogenesis of lung fibrosis (Hernández-Rodríguez *et al.*, 1995; Kimura *et al.*, 2005). Stimulation of PAR_4 in alveolar epithelial cells induced an increase in α-SMA expression and a decrease in epithelial cell marker E-cadherin, suggesting that PAR_4 stimulation induces EMT in these cells (Ando *et al.*, 2007b).

In contrast, PAR_4 may suppress pulmonary fibrosis by countering PAR_1-stimulated proliferation of fibroblasts (Ramachandran *et al.*, 2007). Exposure of human primary bronchial fibroblasts to pro-inflammatory stimuli induced expression of functional PAR_4 on the fibroblasts. In these TNF-α stimulated fibroblasts, thrombin no longer induced proliferation, and a PAR_4 AP caused a reduction in fibroblast cell number (Ramachandran *et al.*, 2007). Furthermore, induction of PAR_4 expression enables signalling of CG, which usually silences PAR_1 and PAR_2, to evoke a calcium signalling responses (Ramachandran *et al.*, 2007).

PAR_4 agonists can stimulate the release of IL-6, IL-8 and PGE_2 with an increase in cytoplasmic Ca^{2+} concentration in human respiratory epithelial cell lines (Asokananthan *et al.*, 2002). PAR_4 stimulation causes mobilisation of Ca^{2+} from intracellular stores in the initial peak response (phospholipase Cβ-dependent mobilisation of Ca^{2+}) and enhances Ca^{2+} entry through the store depletion-operated Ca^{2+} pathway in the delayed phase in mouse lung AECs (Ando *et al.*, 2007a).

PAR_4 can be activated by CG at sites of vascular injury. PAR_4 is the CG receptor on human platelets and the activation of PAR_4 by CG is crucial for neutrophil-dependent platelet activation (Sambrano *et al.*, 2000). PAR_4 is also involved in the late phase of platelet aggregation in which it sustains the aggregation in response to thrombin when PAR_1 becomes rapidly inactivated (Kahn *et al.*, 1998; Macfarlane *et al.*, 2001).

1.4.5.2 Renal System

The kidney expresses PAR_1, PAR_2 and PAR_4, particularly PAR_2 (Rasmussen *et al.*, 1991; Nystedt *et al.*, 1995; Hollenberg, 2003). PAR_4 mRNA has been identified from both renal cortex and medulla and expression has been reported in podocytes and from human tubular epithelial cells at low levels. The role of PAR_4 in kidney has not been studied in detail (Gui *et al.*, 2003; Harris *et al.*, 2009)(**Table 1.3**).

Table 1.3: PAR Expression on Different Cell Types in Kidney.

PAR	Cell Types	References
PAR_1	human glomerular epithelial cells, human glomerular mesangial cells, podocytes, glomerular endothelial cells, ubterstitial peritubular cells	Rondeau *et al.* (2001), Sakai *et al.* (2009)
PAR_2	epithelial cells, mesangial cells, blood vessel walls, infiltrating renal inflammatory cells, collecting duct cells	D'Andrea *et al.* (2001), Tanaka *et al.* (2005), Xiong *et al.* (2005), Bertog *et al.* (1999) Grandaliano *et al.* (2003)
PAR_4	tubular epithelial cells, podocytes	Gui *et al.* (2003) Harris *et al.* (2009)

Both PAR_1 and PAR_2 have functional roles in renal pathophysiology. PAR_1 is involved in renal inflammation. The treatment of PAR_1-knockout mice with PAR_1-AP protects them from renal injury, while PAR_1-AP caused glomerulonephritis in the wild-type control (Cunningham *et al.*, 2000). The contribution of PAR_2 to renal inflammation has been studied using knockout mice that highlight the importance of PAR_2 in the development of inflammation. Both Su *et al.* (2005) and Chignard and Pidard (2006) have demonstrated that PAR_2-knockout mice had substantially less inflammation compared to the wild type mice. Elevated expression levels of PAR_2 mRNA and protein have been shown in the proximal tubular cells, infiltrating interstitial mononuclear cells and glomerular epithelial cells in patients with IgA nephropathy. The PAR_2 mRNA levels correlate directly with the extent of fibrosis (Grandaliano *et al.*, 2003).

PAR_1 activation causes vasoconstriction of the afferent arteriole whereas PAR_2 activation causes vasodilation mainly via the release of nitric oxide in the kidney (Muramatsu *et al.*, 1992; Saifeddine *et al.*, 2001). Thrombin or PAR_1 agonist peptide TFLLR-amide caused a marked reduction in renal perfusion flow (Gui *et al.*, 2003), whereas activation of PAR_2 causing vasodilation of the afferent arteriole, resulted in an increase in perfusion flow in the kidney (Hollenberg *et al.*, 2003). These findings suggest that there is an increase in the glomerular filtration rate with PAR_2 activation and a decrease in the glomerular filtration rate with PAR_1 activation (Gui *et al.*, 2003). These effects may be of particular importance in the setting of renal diseases where the tissues may be exposed to serine proteinases (Hollenberg *et al.*, 2003).

As proximal tubular cells appear to be the predominant site of PAR_2 expression in the kidney, PAR_2 agonists have been proposed to regulate fluid and electrolyte secretion in the kidneys. Bertog *et al.* (1999) has

shown that PAR_2 can regulate chloride secretion in murine tubular cells. Tryptase and factor Xa were shown to stimulate proliferation of renal fibroblasts and mesangial cells, respectively (Kondo *et al.*, 2001; Tanaka *et al.*, 2005), suggesting a role for PAR_2 in renal fibrosis. PAR_2 induced cell proliferation is suggested to be mediated via EGF-receptor and downstream MAPK signalling (Chignard and Pidard, 2006).

1.5 Apoptosis

Apoptosis is a fundamental physiological event in the normal development and homeostatic processes to maintain a balance between cell proliferation and cell death. It is form of programmed cell death that requires the activation of specific enzymes and signalling pathways, offering potential for pharmacological manipulation. It results in the dismantling of the entire cell within the context of membrane-enclosed vesicles that can be recognised and engulfed by phagocytes. Hence, it prevents the release of intracellular components from dying cells and the activation of innate immune responses. Apoptosis is critical for the maintenance of postnatal adult tissue homeostasis as it eliminates the damaged or infected resident cells, inflammatory cells and mesenchymal cells that are involved in wound healing. Orchestrated death and removal of these cells is necessary for the restoration of normal cellular homeostasis and the maintenance of the tissue architecture and organ function (Saraste and Pulkki, 2000; Liu *et al.*, 2002; Thannickal and Horowitz, 2006).

Failure to clear unwanted cells by apoptosis will prolong inflammation due to the release of their toxic contents. Excessive apoptosis causes extensive cell loss, leading to the failure of clearing the apoptotic cell debris and eventually the amplification of inflammation and the possibility of forming scar tissue (Hagimoto *et al.*, 1997a; Matute-Bello *et al.*,

2001). Enhanced apoptosis of epithelial cells, fibroblasts and myofibroblasts occurs in fibrosis (Polunovsky *et al.*, 1993; Kapetanaki *et al.*, 2013).

Apoptosis can be triggered by external stimuli, such as soluble cell death ligands, which are released during inflammatory responses or intrinsic stimuli due to an alteration of the cellular function and metabolism (Tang *et al.*, 2008). It is characterised by a selection of morphological features, such as loss of plasma membrane asymmetry and attachment, cell shrinkage, chromatin condensation and chromosomal DNA fragmentation (Liu *et al.*, 2002). These morphological changes are a consequence of characteristic molecular and biochemical events occurring in an apoptotic cell. During early apoptosis, the cell rounds up, loses contact with its neighbouring cells and shrinks. Then, the chromatin in the nucleus condenses and aggregates into dense compact masses, the plasma membrane blebs or buds, and finally the cell is fragmented into compact membrane-enclosed structures called the apoptotic bodies which contain cytosol, condensed chromatin and organelles. The apoptotic bodies are engulfed by macrophages and thus are removed from the tissue without causing an inflammatory response (Saraste and Pulkki, 2000).

Apoptosis is different from the necrotic mode of cell death. Necrosis is an accidental, unplanned death occurring in response to sudden and severe cell injury due to hypoxia, toxins, extreme temperaturess or attack by complement and lytic viruses (Savill, 1994). The plasma membrane is damaged and becomes abnormally permeable, resulting in a loss of membrane integrity, swelling and rupture of the cells. The cellular contents are released uncontrolled into the cellular environment, which causes damage to the surrounding cells and provokes tissue injury and inflammation (Savill, 1994).

Caspases are a family of cysteine proteases which play an important role in the execution of apoptosis (Alikhani *et al.*, 2004). Caspases are synthesized as inactive zymogens in the cell, which are known as pro-caspases and are activated by proteolytic cleavage into a heterodimer consisting of a large (20 kDa) and a small (10 kDa) subunits. A heterotetramer consisting of two small and two large subunits then forms an active caspase with two active sites (Thornberry *et al.*, 1997; Budihardjo *et al.*, 1999; Alikhani *et al.*, 2004). The pro-apoptotic caspases can be divided into a group of initiator caspases including pro-caspase-2, -8, -9 and -10, and a group of executioner caspases including pro-casapase-3, -6, and -7. The initiator caspases are recruited to and activated at the death-inducing signalling complexes in response to either the ligation of the cell surface death receptors (extrinsic pathway) or the signals originating from inside the cell (intrinsic pathways) (Earnshaw *et al.*, 1999; Plataki *et al.*, 2005).

The caspase cascade can be activated by an extrinsic or intrinsic pathway. Caspase-8 activation is part of the cytoplasmic (extrinsic) pathway of apoptosis while caspase-9 activation is usually associated with the mitochondrial (intrinsic) pathway of apoptosis (Green, 2000). The extrinsic or death receptor pathway involves the activation of death receptors present in the cell membrane such as Fas and TNF-receptor 1. These receptors contain cysteine-rich extracellular subdomains that allow them to recognize their ligands specifically and an intracellular death domain that is crucial for the transduction of the apoptotic signal. Binding of the death ligand to its receptor leads to the activation of an adaptor protein called the activated death domain and the subsequent activation of pro-caspase-8 or -10. Activated caspase-8 then directly activates the effectors caspases, caspase-3 and caspase-7, which execute the apoptotic cell death programme (Goltsev *et al.*, 1997; Irmler *et al.*, 1997).

The intrinsic pathway is initiated by the intracellular stress signals such as DNA damage and oxidative stress that will activate the BH3-only (pro apoptotic), member of the B cell lymphoma-2 (Bcl-2) family proteins, translocate from the cytosol to the mitochondrion. There they induce the release of cytochrome c from the mitochondrial intermembrane space to the cytosol. Cytochrome c then binds to the apoptotic protease-activating factor 1 (Apaf-1), which undergoes an adenosine 5'-triphosphate (ATP)-dependent conformational change and forms the multimeric complex known as the apoptosome. The apoptosome will activate the initiator caspase, caspase-9, which will subsequently activate caspase-3 and caspase-7 and execute apoptosis (Zou *et al.*, 1997; Srinivasula *et al.*, 1998; Thannickal and Horowitz, 2006) (**Figure 1.8**).

Accumulating evidence supports the importance of apoptosis as a potential pathogenic mechanism in fibrosis. Components of the Fas-Fas ligand (Fas-FasL) immunological pathway have been detected in patients with IPF (Kuwano *et al.*, 1999b). The Fas-FasL pathway is an important apoptosis-signalling pathway. Fas antigen is a cell surface protein that mediates apoptosis. It is expressed in various cells and tissues including kidney, lung, liver and heart. FasL is a cell surface molecule that belongs to TNF (Suda *et al.*, 1993). It is expressed predominantly in the activated T-lymphocytes and in the organs including small intestines, kidney, testis and lung (Suda *et al.*, 1993). Removal of fibroblasts and myofibroblasts by programmed cell death is required for the normal resolution of tissue repair responses. Resistance of these cells to apoptosis may result in a chronic inflammation or fibrosis (Kisseleva and Brenner, 2008).

AEC apoptosis with subsequent fibrosis is well documented in the bleomycin-induced fibrosis model of IPF (Hagimoto *et al.*, 1997b,c). Lee *et al.* (2004) showed that activation of Fas pro-apoptosis pathway together with TGF-β overexpression causes apoptosis in AEC which is essential for

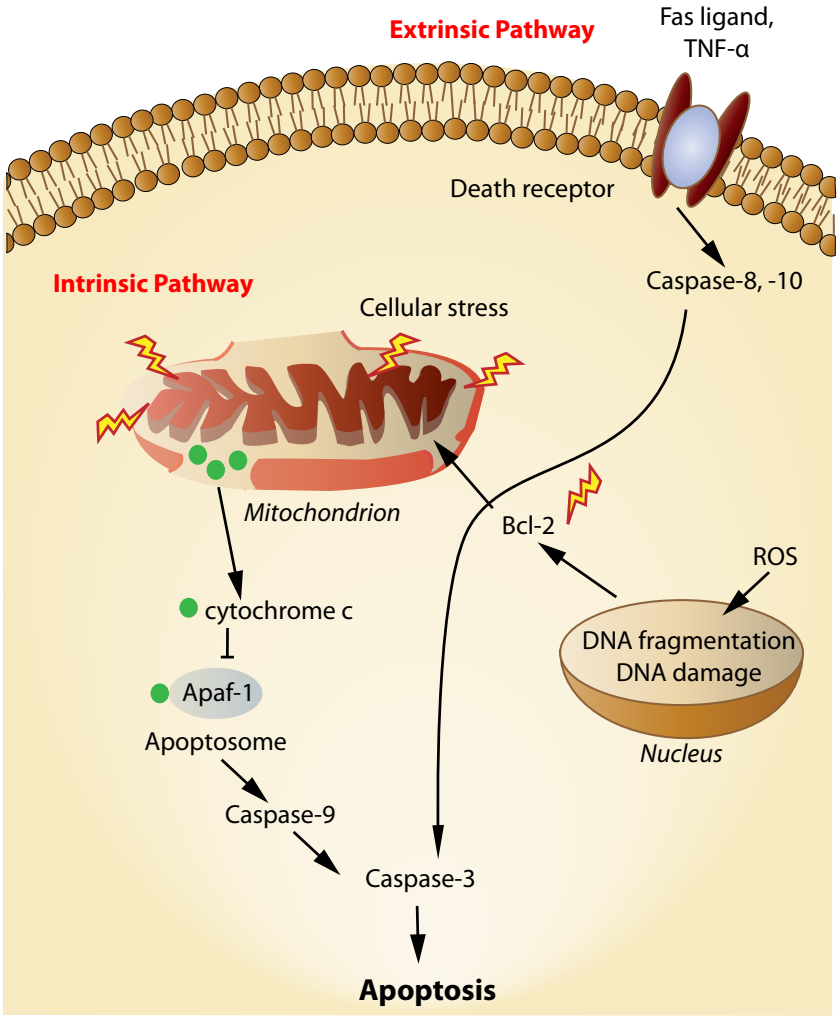

Figure 1.8: Representative of Major Intrinsic and Extrinsic Pathways of Apoptosis. In extrinsic pathway, binding of death ligand to the death receptor mediates the activation of initiator caspase-8. Activated caspase-8 initiates the effector caspase and leads to apoptosis. In intrinsic pathway, intracellular stress and DNA damage induce the release of cytochrome c from the mitochondrian and contribute to the formation of apoptosome. The apoptosome activates caspase-9 which is another initiator caspase and execute the apoptosis. Adapted from Havasi and Borkan, 2011.

the induction of pulmonary fibrosis in mice. Furthermore, ROS generated by mitochondria has been linked to increased cellular oxidative stress and apoptosis of AECs. It has been shown by the early induction of ROS-dependent AEC apoptosis in murine model of bleomycin-induced pulmonary fibrosis (Wallach-Dayan *et al.*, 2006). Exaggerated apoptosis of epithelial cells causes deranged tissue homeostasis and contributes to fibrosis (Humphreys *et al.*, 2010; Koesters *et al.*, 2010).

CG and elastase are highly present in the active phase of inflammation. Owens (1995) demonstrated that CG and elastase are expressed on the cell surface of polymorphonuclear leukocytes neutrophil (PMN). They can be upregulated by pro-inflammatory mediators. Apoptotic PMN accumulated in lung as a result of the interference of CG and elastase with phagocytosis of apoptotic cells by alveolar macrophages, leading to the retention of apoptotic cells in the lungs. Failure of PMN removal may contribute to chronic inflammatory diseases (Vandivier *et al.*, 2002; Guzik *et al.*, 2007).

Apoptosis occurs in both human and animal kidneys during acute kidney injury. Apoptosis can be detected in the kidneys after ischaemia, toxin exposure, inflammation and sepsis. Recent studies have indicated that injured tubular epithelial cells either undergo apoptosis or remain in a state of G2/M arrest with characteristic phenotypic changes, including flattened morphology and loss of polarity. Moreover, exaggerated apoptosis of epithelial cells also causes deranged tissue homeostasis and contributes to fibrosis (Humphreys *et al.*, 2010; Koesters *et al.*, 2010). Proximal tubule epithelial cells are highly susceptible to apoptosis. Apoptosis of parenchymal cells is one of the major factors which contributing to the loss of renal function during the progression of kidney disease. Counterbalancing the loss of epithelial cells is the activation of proliferative pathways in an attempt to recreate tubules within the kidney (Havasi and Borkan, 2011).

1.6 Thesis Hypothesis

The main hypothesis of this thesis is that PAR_4 is expressed in both lung and renal fibroblasts, and PAR_4 activating peptide and cathepsin G can induce apoptosis in fibroblasts via PAR_4-dependent and independent mechanisms.

1.7 Aims

1. To study the expression of PARs in lung and renal fibroblasts (Chapter 3).
2. To study whether TGF-β1 can differentiate fibroblast into myofibroblast (Chapter 3).
3. To generate a stable PAR_4-expressing transgenic cell line using HEK293 cells (termed HEK-PAR_4 cells) (Chapter 4).
4. To determine if cathepsin G and PAR_4 activating peptide can trigger apoptosis in fibroblasts and HEK-PAR_4 cells (Chapter 5).
5. To examine the effect of media derived from confluent epithelial cell cultures on fibroblast proliferation and differentiation (Chapter 6).

Chapter 2

General Materials and Methods

2.1 Materials and Reagents

Dulbecco's Modified Eagles Medium (DMEM), sodium pyruvate, antibiotic/antimycotic (penicillin G sodium, streptomycin sulphate and amphotericin B), foetal bovine serum (FBS), trypsin EDTA, Roswell Park Memorial Institute (RMPI) medium, G418, Opti-MEM media and Lipofectamine were purchased from Gibco (Paisley, UK). dNTPs, random primers, Cy3 goat anti-mouse IgG, and CyQUANT cell proliferation assay kit were obtained from Invitrogen (Paisley, UK). Fibroblast growth medium and TGF-β1 were purchased from Promocell (Heidelberg, Germany). Anti-prolyl 4-hydroxylase, rabbit polyclonal anti-α SMA and polyclonal anti-collagen I were purchased from Abcam (Cambridge, UK). NucleoSpin RNA II Kit was obtained from Macherey-Nagel (Duren, Germany). Primers were purchased from MWG Eurofins (Ebersberg, Germany). Taq DNA polymerase and restriction enzymes (Xho1 and HindIII) were obtained from New England Biolabs (Hitchin, UK). Qiagen miniprep Kit was obtained from Qiagen (Crawley, UK). Fermentas RT kit was purchased from Fermentas (Opelstrasse, St. Leon-Rot, Germany). PAR antibodies, anti-α-tubulin and goat anti-mouse IgG HRP were purchased from Santa Cruz Biotechnology, Germany). Cathepsin G was purchased from EPC

(Missouri, USA). Fluo-3 acetoxymethyl ester (Fluo-3 AM) was purchased from Cambridge Biolabs and later Invitrogen (Cambridge, UK). Both human and rat PAR_4 APs were purchased from Peptides International (Kentucky, USA). The enhanced chemilumescence (ECL) western blotting detection reagents and donkey anti-rabbit HRP were obtained from GE Healthcare (Amersham, Buckinghamshire, UK). Glycerol/PBS solution AF1 was purchased from Citiflour (London, UK). XL1-Blue supercompetent cells was obtained from Strategene Europe (Amsterdam, Netherland). Coomassie Brilliant Blue was purchased from Bio-Rad Laboratories Ltd (Hertford, UK) FITC-conjugated Annexin V was purchased from IQ product (DL Groningen, Netherlands). Caspase-3 and cleaved caspase-3 antibodies were purchased from Cell Signalling Technology (Hertford, UK). All other chemcicals and reagents were purchased from Sigma-Aldrich (Poole, Dorset, UK) unless otherwise stated.

2.2 Cell Culture

Human primary bronchial fibroblast (HPBF) and human primary renal fibroblast (HPRF) cultures were established from bronchial and renal tissue explants, respectively. Renal tissue explants were obtained under informed written consent from patient undergoing nephrectomy. Ethics approval was obtained from the Hull and East Riding Local Research Ethics Committee (12/SC/0474) for lung specimen, Hull and East Yorkshire Hospitals NHS Trust (Hull , UK), with approval of the local ethics committee (Elsy no CHH 341) for kidney specimen.

Cell cultures were established using methods based on previously published papers (Akers *et al.*, 2000; Ramachandran *et al.*, 2007). Briefly, explants were dissected into pieces ≤ 1 mm^3, placed into individual wells of a 24-well culture plate with 500 μl of DMEM containing in v/v

10% FBS, 1% sodium pyruvate, and 1% antibiotic/antimycotic (penicillin G sodium, streptomycin sulphate and amphotericin B) and then incubated at 37℃ in a humidified atmosphere of air containing 5% CO_2. The medium was changed at least twice a week. After 3 weeks, confluent fibroblasts were seen growing out from the explants. The cells were then harvested by trypsinization and transferred to 25 cm^2 flasks with 5 ml of fresh fibroblast growth medium. These cells were cultured for further a 1 or 2 weeks until confluent islands of cells were observed. Then, the cultures were passaged with a split ratio of 1:3 into 75 cm^2 flasks in 10 ml fresh fibroblast growth medium. The purity of the fibroblast culture was confirmed by staining with anti-vimentin and anti-prolyl 4-hydroxylase antibodies and by observing the typical spindle shape and characteristic swirls formation when confluent. See **Section 2.7**.

HEK293 cells were routinely maintained in DMEM complete growth medium containing in v/v 10% FBS, 1% sodium pyruvate, and 1% antibiotic/antimycotic (penicillin G sodium, streptomycin sulphate and amphotericin B). Cells were harvested by washing with 5 ml of phosphate buffered saline (PBS) and dissociating the cells from the flask using fresh 5 ml of PBS. The cultures were passaged with a split ratio 1:5 into 75 cm^2 flasks approximately every 2 days with 10 ml fresh growth medium.

2.3 Quiescing of HPBF and HPRF

Prior to certain experiments, cells were cultured in a serum free media consisting of fibroblast growth media supplemented with antibiotic/antimycotic only. This was to arrest cell division and to elucidate the specific effects of single agonist without interference from FBS components.

2.4 mRNA Extraction

Cells were cultured in 25 cm^2 flasks with 5 ml of complete growth medium. Total RNA was prepared using the NucleoSpin RNA II Kit as per manufacturer's instructions. Using the NucleoSpin RNA methods, cells are lysed by incubation in a solution containing large amounts of chaotropic ions which will immediately inactivate ribonuclease (RNase) and create appropriate binding conditions which favour absorption of RNA to the silica membrane. Contaminating DNA which is also bound to the silica membrane is then removed by a recombinant DNase (rDNase) solution. Simple washing steps with two different buffers remove salts, metabolites and macromolecular cellular components. Finally, pure RNA is eluted under low ionic strength condition with diethylpyrocarbonate (DEPC) water. The mRNA was quantified with a GeneQuant spectrophotometer (Amersham, UK).

2.5 Reverse Transcription (RT)

cDNA was synthesized using the Fermentas RT kit. The reagents used were summarised in (**Table 2.1**).

Table 2.1: Reagents Used in a RT Reaction.

Reagent	Volume (Final Volume = 20 μl)	Final Concentration
5× RT Buffer	4 μl	1×
dNTPs (10 mM)	1 μl	0.5 mM
Random Primers (3 μg/μl)	0.2 μl	30 ng/μl
RNase Inhibitor (40 U/μl)	0.5 μl	20 U
Reverse Transcriptase (200 U/μl)	1 μl	200 U
mRNA	Variable	2 μg
DEPC water	Added to 20 μl	-

Briefly, the reaction was cycled at 25℃ for 10 min for random primer annealing, 50℃ for 30 min to allow reverse transcription, 85℃ for 5 min to inactivate reverse transcriptase, followed by a final hold at 4℃. The reaction was carried out in TC-3000 Personal 25-well Thermal Cycler (Bibby Scientific, UK).

2.6 Polymerase Chain Reaction (PCR)

PCRs were performed for 35 cycles. Denaturation at 94℃ for 30 sec, primer annealing at 59℃ for 30 sec and elongation at 72℃ for 30 sec. The reagents used are summarised in **Table 2.2**. All reactions included an initial denaturation at 94℃ for 2 min and final extension at 72℃ for 10 min. PCR was carried out in TC-3000 Personal 25-well Thermal Cycler (Bibby Scientific, UK).

Table 2.2: A Typical PCR Reaction to Amplify PARs.

Reagent	Volume (Final Volume = 50 μl)	Final Concentration
10× PCR Buffer	5 μl	1×
dNTPs (10 mM)	1 μl	0.5 mM
Forward Primer (20 pM)	1 μl	0.4 pM
Reverse Primer (20 pM)	1 μl	0.4 pM
Taq Polymerase (250 U)	0.25 μl	1.25 U
cDNA	Variable	2 μg
DEPC Water	Added to 50 μl	-

All experiments included a control where the cDNA was omitted from the reaction mixture as well as a mock reverse transcription containing all the RT-PCR reagents, except the reverse transcriptase (no RT control).

The PCR product was separated on a 1.3% agarose gel, stained with ethidium bromide (0.75 μg/ml) and visualised under ultraviolet light. Images were obtained using an Epichemi system (consisting of a Epichemi dark room, high resolution deeply cooled scientific grade digital CCD and 3UV transilluminator) coupled to a Labworks 4.0 image acquisition and analysis software (UVP Laboratory Products, Cambridge, UK).

2.7 Immunocytochemical Staining

HPBFs or HPRFs were seeded on cover slips and grown in 6-well plates with 2 ml of fibroblast complete growth medium. Once confluent, cells were washed with PBS, fixed with 4% paraformalaldehyde for 20 min, and washed 3 times with PBS. The cells were then permeabilised using 0.1% Triton X-100 in PBS for 15 min at room temperature. After 3 further washes with PBS, the cells were incubated with blocking solution (1% BSA in PBS) for 20 min and washed 3 times with PBS. Then, the cells were incubated with primary antibody. The irrelevant isotype matched antibody was used as a negative control. After washing 3 times with PBS, the cells were incubated with biotinylated antibody at 1:100 at room temperature for 40 min. Again, the cells were washed 3 times with PBS and incubated with streptavidin conjugated peroxidise enzyme at 1:100 for another 40 min at room temperature. After 3 washes with PBS, the cells were incubated with 200 μl of 3,3'-diaminobenzinetetrahydrochloride (DAB) for 5 min. The cells were then washed 3 times with distilled water and mounted with glycerol based gelatine. Finally, slides were visualised under a light microscope (Nikon) and images were taken with a Nikon Coolpix 930 digital camera at 10$\times$ magnification.

2.8 Immunofluorescent Staining for α-SMA

After 24 h treatment with TGF-β1 (10 ng/ml), fibroblasts were washed with PBS, fixed with 4% paraformalaldehyde for 20 min, and then washed 3 times with PBS. The cells were then permeabilised using 0.1% Triton X-100 in PBS for 15 min at room temperature. After 3 washes with PBS, the cells were incubated with blocking solution (1% BSA in PBS) for 20 min and washed 3 times with PBS. Then, the cells were incubated with 50 μl of monoclonal anti-actin, α-smooth muscle clone 1A4 (5 μg/ml) for 40 min at room temperature. As a negative control, the irrelevant isotype matched antibody IgG2a (5 μg/ml) was used in place of the primary antibody. After a further 3 washes with PBS, the cells were incubated with 50 μl of Cy3 goat anti-mouse (1:200) for 40 min at room temperature in dark. The cells were then washed 3 times with PBS, followed by mounting on a slide using the glycerol/PBS solution, AF1, and sealing with nail polish. Slides were visualized under a fluorescent microscope (Nikon) with FITC or Cy3 filter.

2.9 Intracellular Calcium Mobilisation Assay

Calcium signalling assays were performed using the methods described by Compton *et al.* (2001). Cells at 70-85% confluence in 75 cm^2 flasks were washed and harvested with PBS (without calcium or magnesium). Cells were pelleted and resuspended in 500 μl of normal culture medium containing 0.25 mM sulphinpyrazone and 7 μM of Fluo-3 acetoxymethyl ester (Fluo-3 AM) in DMSO. The cells were then incubated at room temperature for 25 min whilst gently shaking, allowing the fluorescent probe to be taken up by the cells. The cells were washed by adding 4.5 ml of PBS and centrifuged to remove the excess Fluo-3 AM, then resuspended in 300 μl of calcium assay buffer (CAB) (150 mM sodium chloride, 250 μM sulphinpyrazone, 3 mM potassium chloride, 10 mM glucose, 20 mM HEPES and 280 nM calcium chloride, pH 7.4). 100 μl of cell suspension was then

added to the calcium assay cuvette containing 1.9 ml of CAB and a magnetic flea to keep the cells suspended. Increases in intracellular calcium levels were measured at room temperature using a fluorospectrometer (Photo Technology International), set to measure the Fluo-3 AM with excitation at 480 nm and emission at 530 nm. The increase in fluorescence measured at 530nm were expressed as a percentage of the maximum fluorescence signal after the addition of 2 μM calcium ionophore.

2.10 Generation of Whole Cell Lysate

Cells were passaged into 25 cm^2 culture flasks and allowed to reach over 85% confluence. Cells were then harvested, pelleted by centrifugation at 500 $\times$ g for 5 min and lysed by adding 500 μl Laemilli's sample buffer (containing 2% SDS, 10% glycerol, 50 mM Tris-HCl (pH 6.8), 5 mM EDTA, 0.008% bromophenol blue and 0.5% β-mercaptoethanol). The cell lysates were then transferred into a 1.5 ml eppendorf tube. Cell lysates were heated to 100℃ on a heat block for 10 min and centrifuged at 13,200 $\times$ g for 10 min at 4℃.

2.11 SDS Polyacrylamide Gel Electrophoresis (SDS-PAGE)

Gel forming apparatus was constructed as per the manufacturer's instructions. A 12.5% SDS-PAGE gel was made according to **Table 2.3** and adding N,N,N′,N′-tetramethylethylenediamine (TEMED) last, quickly mixed before adding to gel former, 5ml per gel. Propan-2-ol was pipette onto the top of the gel to get rid of bubbles and ensure a flat surface. The gel was then left to set for 30-60 min at room temperature. Once the gel is set, propan-2-ol was poured off and the gel surface was washed with dH_2O

for two times and dried. Then, the stacking gel was made according to **Table 2.4** and adding TEMED last, quickly mixed and added to the gel former filling it to the top. A 12 sample comb was then inserted into the gel and the gel was left to set for another 30 min at room temperature.

Table 2.3: 12.5% SDS-PAGE Gel.

12.5% SDS-PAGE Gel (Final Volume = 8 ml)		
Reagents	Volume	Concentration
Acrylamide/Bis-acrylamide, 30% solution	3.33 ml	12.5%
1.5 M Tris pH 8.8	2 ml	375 mM
10% SDS	80 μl	0.1%
10% Ammonia Persulphate (APS)	80 μl	0.1%
Deionised Water	2.5 ml	-
TEMED	8 μl	-

Table 2.4: 6% Stacking Gel.

6% Stacking Gel (Final Volume = 5 ml)		
Reagents	Volume	Concentration
Acrylamide/Bis-acrylamide, 30% solution	2.6 ml	6%
0.5 M Tris pH 6.8	1.25 ml	78 mM
10% SDS	50 μl	0.1%
10% Ammonia Persulphate (APS)	50 μl	0.1%
Deionised Water	2.6 ml	-
TEMED	5 μl	-

Proteins were separated in 12.5% SDS-PAGE gel and the gel was run in a vertical gel electrophoresis unit in electrode buffer consisting of 25 mM Tris base, 190 mM glycine and 0.1% SDS, pH 8.3. The gel former was placed into the gel tank and enough electrode buffer was poured into the internal gel former reservoir until the buffer was levelled with the top of the gels and the remaining buffer was poured into gel tank up to the max fill mark, ensuring that the bottom of the gels were submerged in the buffer.

10 μl of Precision Plus Protein^{TM} Dual colour standards (BIO-RAD) was used as size markers on the gels. 20 μl of the samples were loaded into sample wells alongside 10 μl of protein standard. Electrophoresis was carried out at 100 V for approximately 2 h or until the blue dye had run to the bottom of the gel.

2.12 Western Blotting

The proteins on the gel were electrotransferred to a nitrocellulose membrane using the Invitrogen i-blot dry blotting system as per the manufacturer's instructions. The membrane was then blocked with 5% w/v non-fat powdered milk in PBS containing 0.1% Tween 20 (PBS-Tween) at room temperature for 1 h to block the non-specific binding. The non-fat milk solution was then removed and the membrane washed 4 $\times$ 10 min with PBS-Tween. The membrane was then incubated with primary antibody (in PBS-tween containing 5% non-fat milk) at 4°C overnight on a rocker. Following 4 washes with PBS-Tween for 10 min, the membrane was then incubated with HRP conjugated secondary antibody (in PBS-Tween containing 5% non-fat milk) at room temperature for 1 h. The secondary antibody was then removed by 4 washes with PBS-Tween.

Protein bands on the membrane were visualised by enhanced chemiluminescence (ECL) according to manufacturer's instructions. Briefly, ECL reagent A and B were mixed together in equal volumes and applied to the protein binding surface and incubated at room temperature for 1 minute. Excess reagent was then removed and the membrane photographed using a UVP Laboratory Products Epichem II Darkroom setup to measure chemiluminescence. Bands were visualised using Lab Works Image Acquisition and Analysis software (UVP Laboratory Products, Cambridge, UK). Pictures were taken every 5 min for 20 min. Finally, bands were

quantified using ImageJ software.

2.13 Statistical Analysis

Statistical analyses were carried out using IBM SPSS 19. All data were expressed as mean ± SEM. Paired t test was used to compare values between two groups. Differences between control and experimental groups were performed using a one-way ANOVA for repeated measures, followed by Dunnett's post hoc test for multiple comparisons. A value of $p < 0.05$ was considered as significant.

Chapter 3

Characterisation and Detection of PAR Expression in Primary Human Fibroblasts and Myofibroblast Differentiation

3.1 Introduction

Fibroblasts are ubiquitous mesenchymal cells that display a spindle-shaped elongated cellular phenotype with elliptical nuclei. They have a thin cytoplasm with abundant granular materials and electron microscopy reveals a well-developed rough endoplasmic reticulum and a golgi apparatus (Lemley and Kriz, 1991; Camelliti *et al.*, 2005). They are widely distributed in the stroma of many tissues of most vertebrate organisms. Fibroblasts are involved in the maintenance of tissue structure and the assembly of ECM by producing factors including growth factors, cytokine and matrix metalloproteinases which are necessary to maintain a balance between the synthesis and the degradation of connective tissue components (Camelliti *et al.*, 2005).

Fibroblasts play central roles in tissue homeostasis and repair. Lung fibroblasts, renal mesangial cells and renal fibroblasts express little to no α-SMA in their resting state (Elger *et al.*, 1993; Barnes and Gorin, 2011). During fibrogenesis, fibroblasts become activated, migrate into the damaged tissue and contribute to the inflammatory responses by secreting cytokines and chemokines that drive the recruitment of leukocytes (Ramachandran *et al.*, 2006). Fibroblasts then differentiate into contractile and highly synthetic myofibroblasts that are involved in promoting wound closure, ECM deposition and tissue remodeling (Hinz *et al.*, 2007). Fibroblasts are present in the adventitia of vascular structures and airways in the normal adult lung. In adult kidney, fibroblasts can be found in the renal cortex and medulla (Camelliti *et al.*, 2005; Qi *et al.*, 2006; Phan, 2008).

The activation and differentiation of fibroblasts into myofibroblasts were first described by Gabbiani *et al.* (1971). Myofibroblast differentiation and persistence are mainly dependent on the mechanical resistance of the ECM together with the action of pro-fibrotic TGF-β1 (Hinz *et al.*, 2007). During wound healing or progressive fibrotic events after injury, activated fibroblasts highly express α-SMA along with the extracellular mesenchymal matrix proteins, collagen types I and III, and cellular fibronectin upon activation by TGF-β, PDGF, or TNF-α (Jarnagin *et al.*, 1994; Schnaper and Kopp, 2003). The differentiation of the myofibroblasts from fibroblasts involves the formation of proto-myofibroblasts (Desmoulière *et al.*, 2005). The proto-myofibroblast phenotype is characterised by the increased expression of fibronectin (Hinz *et al.*, 2007; Hinz, 2007) and specifically the expression of the alternately spliced ectodysplasin-A (ED-A) isoform, which is not expressed by fibroblasts. Proto-myofibroblasts do not express α-SMA and thus are distinct from myofibroblasts, suggesting that proto-myofibroblast is an intermediate in the process of myofibroblastic differentiation (Hinz, 2007) (**Figure 3.1**).

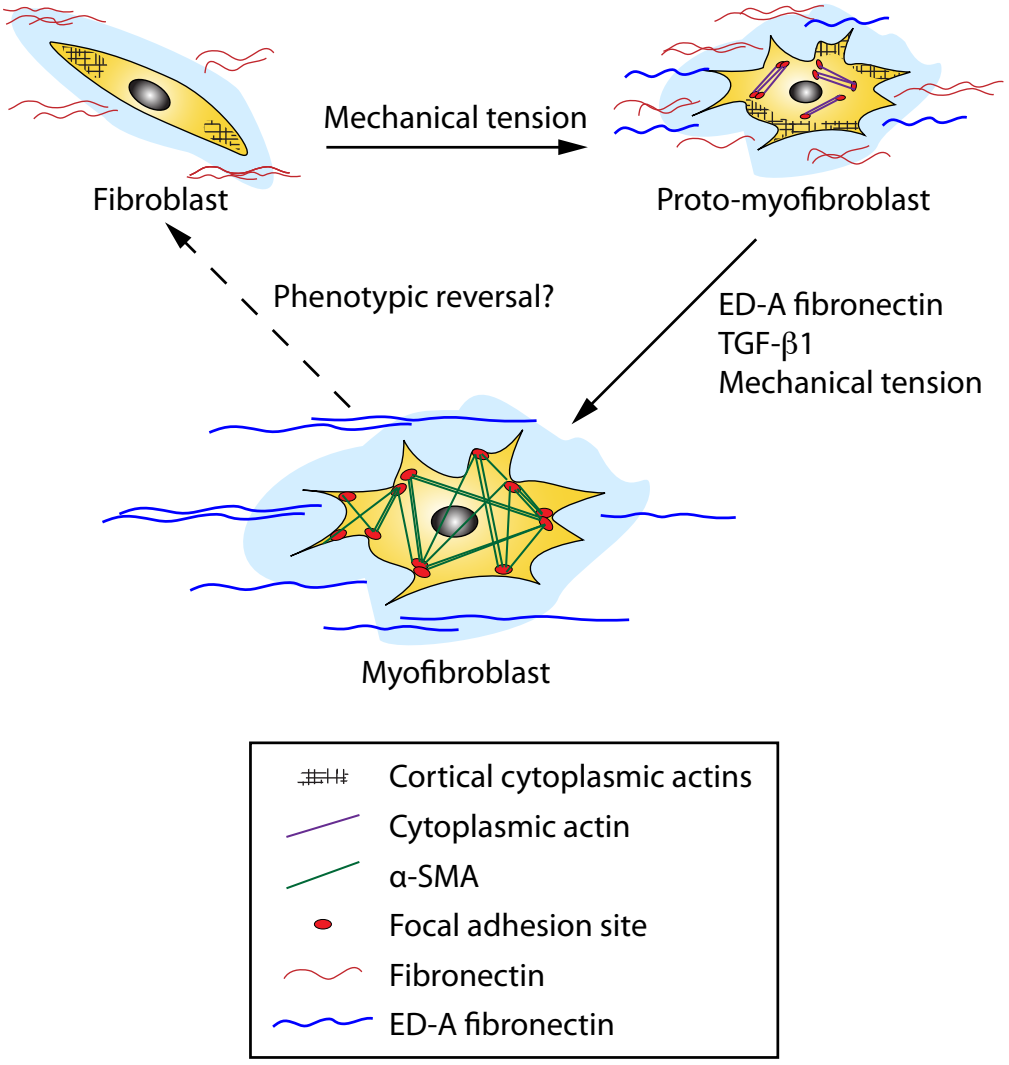

Figure 3.1: Myofibroblast Differentiation. Under mechanical stress, fibroblasts will differentiate into proto-myofibroblasts. Proto-myofibroblasts are characterised by the presence of stress fibres containing filamentous actins, and synthesis of ED-A fibronectin. In the presence of prolonged mechanical tension, TGF-β1 and ED-A fibronectin, further differentiation occurs. Proto-myofibroblasts differentiate into myofibroblasts that are characterised by the expression of α-SMA. Adapted from Tomasek *et al.*, 2002.

Myofibroblasts display cytoplasmic stress fibres (actin microfilaments) and are connected to each other by adherens and gap junctions. They are also in contact with the ECM by focal contact (fibronexus), a transmembrane complex made up of intracellular contractile microfilaments and the ECM protein fibronectin (Powell *et al.*, 1999). They are present in many tissues in the body and play an important role in tissue remodelling after inflammation or injury. They are responsible for the synthesis and accumulation of the interstitial ECM components such as collagen types I and III as well as fibronectin during wound healing and at the sites of scarring and fibrosis (Gabbiani *et al.*, 1971). Myofibroblasts can produce cytokines and are capable of augmenting or down-regulating the inflammatory response. Myofibroblasts regress and disappear by apoptosis on wound epithelialisation. When myofibroblast activities become excessive and persists, beneficial tissue repair turns into the detrimental tissue deformities characteristic of organ fibrosis (Hinz, 2007).

Depending on the type of tissue to be remodelled, myofibroblast precursor cells are recruited from different sources, resident fibroblasts seem to be the most common among these (Hinz *et al.*, 2007). Other myofibroblast progenitors are fibrocytes, pericytes, EMT or endothelial-mesenchymal transition (EndoMT) (**Figure 3.2**). Hence, damaged organs seem to recruit myofibroblast precursors from several sources to satisfy the temporarily high demand of cells with tissue remodeling activity. (Hao *et al.*, 2006; he Li *et al.*, 2009). In normal wound healing, the contractile activity of myofibroblasts is terminated when the tissue is repaired, α-SMA expression decreases and myofibroblasts disappear by apoptosis. In pathological wound healing, myofibroblast activity persists, leading to tissue deformation, which is particularly evident in hypertrophic scars developing after injury. Besides, Waghray *et al.* (2005) has demonstrated that myofibroblast secretion of H_2O_2 plays a role in alveolar epithelial apoptosis and retardation of epithelial regeneration.

Thus, myofibroblasts are important in promoting ECM deposition, release of inflammatory mediators and epithelial injury, all of which are considered as key factors in the cycle of injury and fibrosis. Myofibroblasts have been demonstrated to be involved in fibrosis of the lung (Hashimoto *et al.*, 2004), kidney (Direkze *et al.*, 2003) and liver (Forbes *et al.*, 2004).

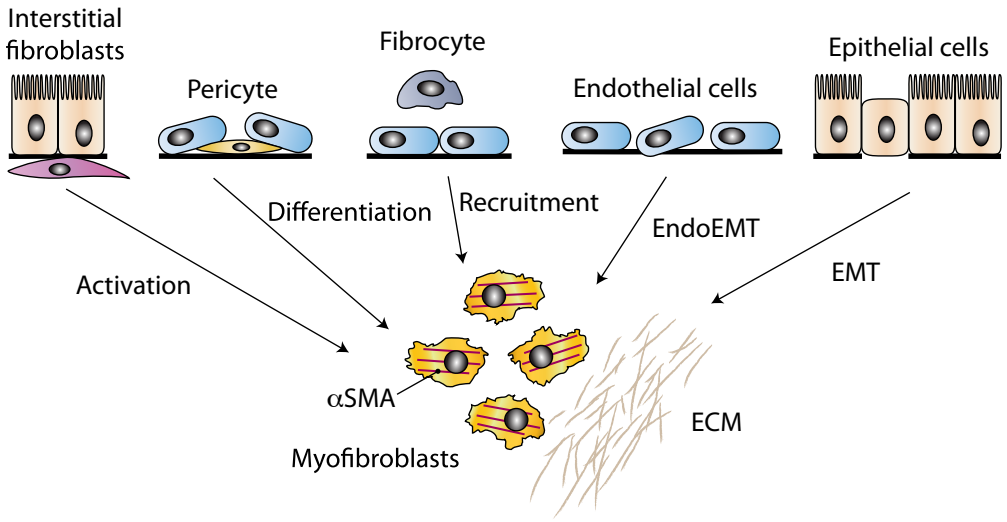

Figure 3.2: Multiple Origins of Myofibroblasts. Myofibroblasts can be derived from phenotypic activation from interstitial fibroblasts, differentiation from pericytes, recruitment from circulating fibrocytes, EndoEMT and EMT. Adapted from Liu, 2011.

TGF-β, PDGF and basic fibroblast growth factor-2 (bFGF-2) are the three main growth factors that have been shown to be associated with myofibroblast differentiation (Floege *et al.*, 1992). Among these cytokines, TGF-β is well recognised as a pluripotent cytokine that drives organ fibrosis. It is a strong inductor of fibroblast differentiation to myofibroblasts by inducing expression of α-SMA. Increased expression of TGF-β and its downstream Smad signalling have been demonstrated in a variety of animal models and human diseases associated with fibrosis

(Abbate *et al.*, 2002; Gabbiani, 2003; Desmoulière *et al.*, 2003). Recently, Wu *et al.* (2013) has demonstrated that TGF-β1 released from the injured kidney tubular epithelial cells stimulated pro-fibrotic cytokine production that promoted the proliferation and transition of pericytes to myofibroblasts. Pro-fibrotic cytokine production was reversed by TGF-β receptor 1 kinase inhibitor SB431542 in TGF-β1-treated tubular epithelial cells, showing the importance role of TGF-β1 and tubular epithelial cells in kidney fibrosis. Besides, TGF-β1 upregulates expression of fibronectin and its integrin receptors was observed in lung fibroblasts which is linked to the induction of myofibroblast differentiation (Thannickal *et al.*, 2003). Conversely, α- and γ-interferon (IFN) decrease the expression of α-SMA in myofibroblasts by either transdifferentiating them back to the fibroblast state or by down-regulating the amount of α-SMA in the cell (Powell, 2000).

3.1.1 Distribution of PARs

The widespread tissue distribution of PARs strongly implies their potential roles in a variety of biological processes (**Tables 3.1** and **Table 3.2**). However, the specificities of these remain to be fully elucidated. PARs are self-activated by a tethered ligand that becomes exposed after extracellular N-terminal cleavage by proteinase. PAR activation depends on the concentration of the active enzyme and agonist in the extracellular fluid and the existence of uncleaved PARs at the surface of the target cells where they can be activated by proteolysis and coupled to signalling pathways (Déry *et al.*, 1998).

Table 3.1: PAR Distribution.

PAR	Tissues	References
PAR_1	Lung airway, platelets, kidney, nervous system, immune system, cardiomyocytes	Chambers *et al.* (2000); Vu *et al.* (1991a) Cunningham *et al.* (2000) Conant *et al.* (2002) Roche *et al.* (2003); Sabri *et al.* (2002)
PAR_2	Lung airway, kidney, cardiovascular system, platelets, nervous system	Akers *et al.* (2000); Bertog *et al.* (1999) Koo *et al.* (2002); Storck *et al.* (1996) Lourbakos *et al.* (2001) Okamoto *et al.* (2001b)
PAR_3	Lung airway, platelets, immune system	Ramachandran *et al.* (2006) Ishihara *et al.* (1997) Bar-Shavit *et al.* (2002)
PAR_4	Lung airway, platelets, endothelium	Asokananthan *et al.* (2002) Sambrano *et al.* (2000) Hamilton *et al.* (2001); Sabri *et al.* (2003a)

3.2 Aims

This chapter aims to:

1. Establish human primary bronchial and renal fibroblast cultures from bronchial sections and renal tissue explants, respectively.
2. Study the fibroblastic phenotype of the cultured cells through staining with fibroblast specific markers.
3. Examine the expressions of PARs in these cultured cells.
4. Differentiate fibroblasts into myofibroblasts by treatment with TGF-β1.
5. Characterise the myofibroblasts through staining with α-SMA and Western blotting.

Table 3.2: PARs on Fibroblasts in Different Tissues.

PAR	Cell Types	References
PAR_1	Human bronchial fibroblast,	Ramachandran *et al.* (2006)
	gingival fibroblast, cardiac fibroblast,	Hou *et al.* (1998)
	synovial fibroblasts,	Sabri *et al.* (2002)
	human kidney glomerular mesangial cells,	Hirano *et al.* (2002)
	rat kidney glomerular epithelial,	Choudhury *et al.* (1996)
	rat kidney mesangial cells.	Laping *et al.* (1997)
PAR_2	Human bronchial fibroblast,	Ramachandran *et al.* (2006)
	mouse kidney cortical duct cells	Akers *et al.* (2000)
	rat kidney afferent arteriole	Bertog *et al.* (1999)
		Trottier *et al.* (2002)
PAR_3	Human bronchial fibroblast	Ramachandran *et al.* (2006)
PAR_4	Human bronchial fibroblast	Asokananthan *et al.* (2002)

3.3 Methods

3.3.1 Cell Culture

HPBFs and HPRFs were cultured as described in **Section 2.2**. Fibroblasts between passages 2 and 5 at 80-95% confluence were used for all of the experiments described in this Chapter.

3.3.2 Immunocytochemical Staining

HPBFs and HPRFs were stained as described in **Section 2.7**.

To stain for fibroblastic markers, anti-prolyl 4-hydroxylase (5 μg/ml) or monoclonal anti-vimentin (0.25 mg/ml) antibodies were used. The isotype matched IgG1 (for prolyl 4-hydroxylase staining) or mouse ascitic fluid IgM (for vimentin staining) was used as a negative control. The secondary antibody, biotinylated goat anti-mouse antibody was used at 1:100 dilution. The PAR antibodies were used according to **Table 3.3**.

Table 3.3: Immunocytochemical Staining for PARs Expression.

PAR	Primary Antibody	Isotype antibody	Secondary antibody
PAR_1	PAR_1 (10 μg/ml)	IgG1 (10 μg/ml)	biotinylated goat anti-mouse antibody (1:100)
PAR_2	PAR_2 (10 μg/ml)	IgG2a (10 μg/ml)	biotinylated goat anti-mouse antibody (1:100)
PAR_3	PAR_3 (10 μg/ml)	Rabbit IgG (10 μg/ml)	biotinylated goat anti-rabbit antibody (1:100)
PAR_4	PAR_4 (10 μg/ml)	Goat IgG (10 μg/ml)	biotinlylated rabbit anti-goat antibody (1:100)

3.3.3 PAR_4 Induction Assay

Cells were placed into 25 cm^2 flasks and allowed to grow to 70-80% confluence. The cells were then quiesced in serum free media for 24 h (see **Section 2.3**) before treatment with LPS (100 ng/ml) for 24 h as described in Ramachandran *et al.* (2007).

3.3.4 RT-PCR Detection of PARs

Fibroblasts were cultured in 25 cm^2 flasks with 5 ml of fibroblast growth medium. Total RNA was extracted and reverse transcription of HPBF and HPRF mRNA were carried out as described in **Sections 2.4** and **2.5**. 2 μg of cDNA product was subsequently used in the PCR reaction in the final volume of 50 μl in TC-3000 Personal 25-well Thermal Cycler (Bibby Scientific, UK) as described in (see **Section 2.6**).

Primers were ordered according to the published sequences in Ramachandran *et al.* (2006), except that PAR_4 was designed using Primer-BLAST. All primers were synthesized by MWG Eurofins. The sequences of oligonucleotides used to amplify PARs and β-actin are summarised in **Table 3.4**. The PCR products were analysed as described in **Section 2.6**.

Table 3.4: PCR Primer Sequences for PAR and β-actin.

Target	Primer Sequence	Product Size
PAR_1	5'-CACGGATCCTATTTTTCCGGCAGTGATTGG-3'	450 bp
	3'-CACGAATTCTCAAATGATAGACACATAACAGACCCT-5'	
PAR_2	5'-TGAAGATTGCCTATCACATAC-3'	550 bp
	3'-GGCTCTTAATCAGAAAATAATGCA-5	
PAR_3	5'-TCCCCTTTTCTGCCTTGGAAG-3'	500 bp
	3'-AAACTGTTGCCCACACCAGTCCAC-5'	
PAR_4	5'-TCACCTGCCTGGCGCTGTTG-3'	340 bp
	3'-CGTTGGAAGAGCCCTGCCCG-5'	
β-actin	5'-CGTGGGCCGCCCTAGGCACCA-3'	242 bp
	3'-TTGGCCTTAGGGTTCAGGGGG-5'	

3.3.5 Intracellular Calcium Mobilisation Assay

Calcium signalling assay was performed as described in **Section 2.9**. Agonists used were: PAR_1 AP (TFLLRN), 100 μM; PAR_2 AP (SLIGKV), 100 μM; and PAR_4 AP (AYPGQV), 100 μM. As the peptides were reconstituted in 4-(2-hydroxyethyl)-1-piperazineethanesulfonic acid (HEPES), this was used as a negative control.

3.3.6 TGF-β1 Treatment for Immunofluorescent Staining of α-SMA

HPBFs and HPRFs were seeded on coverslips and grown in 6-well plates with 2 ml of fibroblast complete growth media. Once reaching the desired confluency (80%), cells were treated with TGF-β1 (10 ng/ml) for 24 h before proceeding for staining as described in **Section 2.8**.

3.3.7 Preparation of Whole Cell Lysates

HPBFs or HPRFs were passaged into 25 cm^2 culture flasks and allowed to reach over 70% confluence. Once reaching the desired confluency, cells were treated with TGF-β1 (10 ng/ml) for 24 h. Cells were then harvested by centrifugation at 500 $\times$ g for 5 min and lysed by adding 500 μl Laemilli's sample buffer as described in **Section 2.10**.

3.3.8 SDS-PAGE and Western Blotting

Protein samples were separated on a 12.5% SDS-PAGE gel before transferring to a nitrocellulose membrane using the i-blot system (Invitrogen, UK) as described in **Sections 2.11** and **2.12**. The membrane was then blocked with 5% milk solution, incubated with primary and secondary antibodies as described in **Section 2.12**. Finally, the blot was visualised using the ECL detection system as describe in **Section 2.12** .

For PAR blots, primary antibodies were: mouse anti-human PAR_1 (1:200), mouse anti-human PAR_2 (1:200), rabbit anti-human PAR_3 (1:200) and rabbit anti-human PAR_4 (1:200); secondary antibody was: donkey anti-mouse HRP (PAR_1 and PAR_2) and donkey anti-rabbit HRP (PAR_3 and PAR_4).

For collagen type I and α-SMA blots, primary antibodies were: rabbit polyclonal anti-α-SMA (1:100) and rabbit polyclonal anti-collagen type I (1:5000); secondary antibody was: donkey anti-rabbit HRP (1:5000).

For α-tubulin loading control, mouse monoclonal IgG1 anti-α-tubulin (1:1000) was used as the primary antibody and goat anti-mouse IgG HRP (1:2000) was used as secondary antibody.

3.4 Results

3.4.1 HPBFs and HPRFs stain positively for Fibroblast Specific Markers

To study the fibroblastic phenotypes of the cultured cells, immunocytochemical stainings using the fibroblast specific markers anti-prolyl 4-hydroxylase and anti-vimentin antibodies were performed. Both HPBFs and HPRFs cultures showed no detectable staining with the negative control antibodies (**Figure 3.3A & B**; and **Figure 3.4A & B**). HPBFs and HPRFs were positively stained by the anti-prolyl 4-hydroxylase and anti-vimentin antibodies (**Figure 3.3C & D**; and **Figure 3.4C & D**), showing the characteristic fibroblastic phenotypes.

3.4.2 PARs detected by RT-PCRs in HPBFs and HPRFs

RT-PCRs were performed to investigate PAR expression in fibroblasts. RT-PCR of cDNAs derived from confluent HPBFs indicated mRNA expressions for PAR_1, PAR_2 and PAR_3 but not PAR_4 (**Figure 3.5A**). The intensities of the bands for PAR_1 and PAR_3 were higher than that for PAR_2. Prior to certain experiments, fibroblasts were cultured in a serum free media consisting of fibroblast growth media supplemented with antibiotic/antimycotic only. Thus, RT-PCR on cDNAs isolated from HPBFs that had been placed in serum free media for 24 h was performed to investigate whether PAR expression was altered when quiesced compared to fibroblasts grown in full growth media. There was no detectable difference in the PAR mRNA expression profile for quiescent HPBFs (**Figure 3.5B**) compared to that for HPBFs in full growth media (**Figure 3.5A**). In PAR_4 induction experiments, HPBFs were treated with LPS (100 ng/ml) for 24 h before mRNA extraction. mRNA expression for PAR_4 was not consistent.

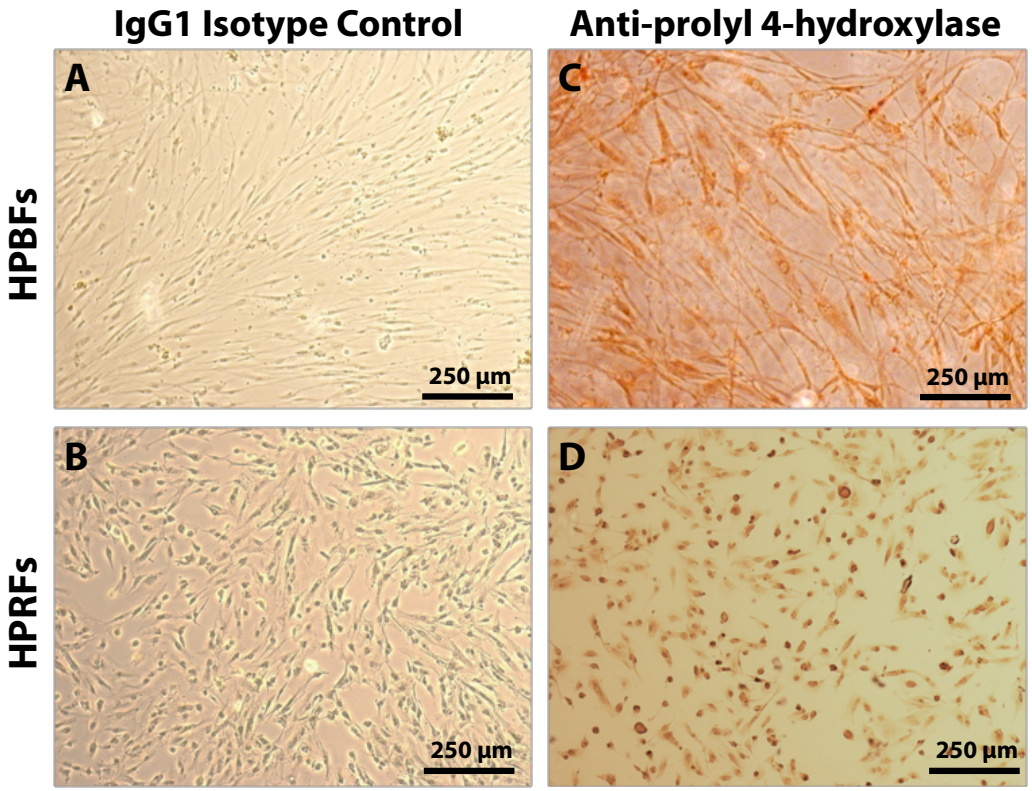

Figure 3.3: HPBFs and HPRFs were Positively Stained for Prolyl 4-hydroxylase. HPBFs and HPRFs were seeded on cover slips and grown in 6-well plates with 2 ml of fibroblast complete growth medium. Once confluent, cells were fixed with 4% paraformalaldehyde, permeabilised with 0.1% Triton X-100 and blocked with 1% BSA/PBS. Cells were then incubated with the relevant isotype controls (A & B) or anti-prolyl 4-hydroxylase antibody (C & D). A secondary antibody conjugated to biotin was used to detect primary antibody. Streptavidin and DAB development were used to detect secondary antibody binding. Positive staining is indicated by the development of a brown colour. Results are representative of five independent experiments.

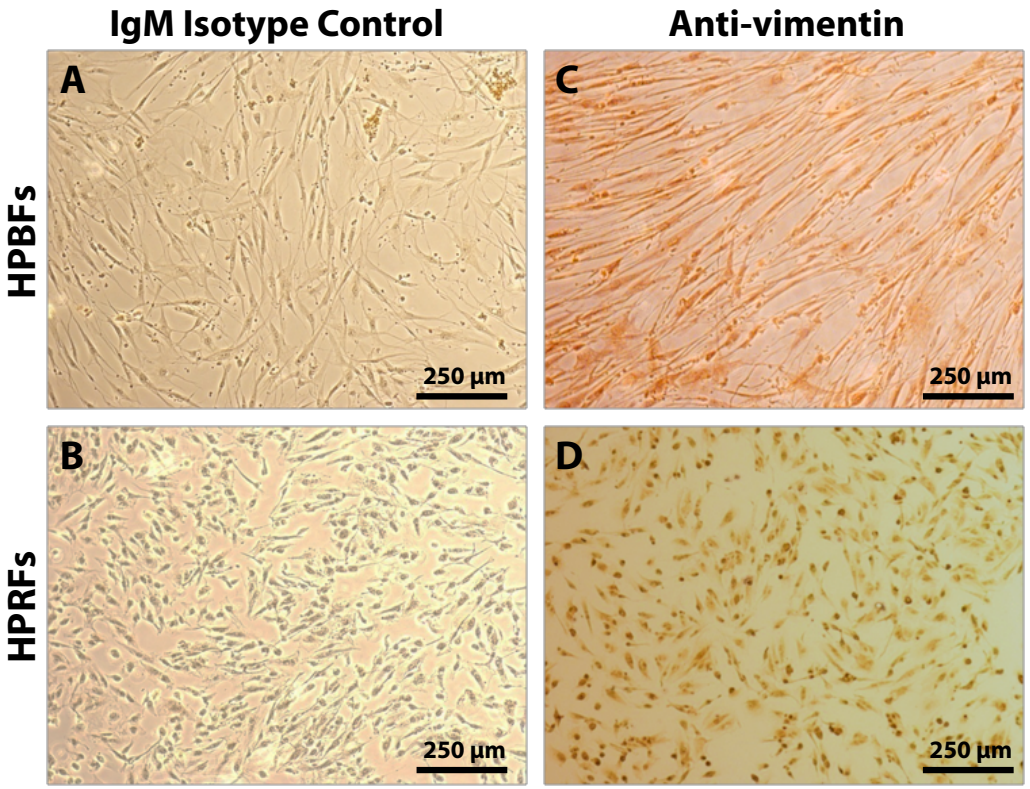

Figure 3.4: HPBFs and HPRFs were Positively Stained for Vimentin. HPBFs and HPRFs were seeded on cover slips and grown in 6-well plates with 2 ml of fibroblast complete growth medium. Once confluent, cells were fixed with 4% paraformalaldehyde, permeabilised with 0.1% Triton X-100 and blocked with 1% BSA/PBS. Cells were then incubated with the relevant isotype controls (A & B) or anti-vimentin antibody (C & D). A secondary antibody conjugated to biotin was used to detect primary antibody. Streptavidin and DAB development were used to detect secondary antibody binding. Positive staining is indicated by the development of a brown colour. Results are representative of five independent experiments.

Over ten independent experiments, the PAR_4 band was observed only in three experiments (for example, **Figure 3.5C**), but not in the remaining seven experiments. No band was observed in the negative controls where reverse transcriptase (RT) enzyme or no template control reactions (NTC) where cDNA was omitted. See **Section 2.6** .

To ensure the PAR_4 primers were functional, LN CAP cells (androgen-sensitive human prostate adenocarcinoma cells derived from a left supraclavicular lymph node metastasis) were used as a positive control. LN CAP cells are known to express PAR_1, PAR_2 and PAR_4. RT-PCR of cDNAs derived from confluent LN CAP cells showed mRNA expressions for PAR_1, PAR_2 and PAR_4 but not PAR_3 (**Figure 3.6**), indicating that the PAR_4 primers were functional.

For HPRFs, RT-PCR of cDNAs derived from cell cultures showed mRNA expressions of PAR_1 and PAR_2 but not PAR_3 and PAR_4 (**Figure 3.7A**). In addition, RT-PCR of cDNAs isolated from HPRFs that had been placed in serum free media for 24 h was carried out. The mRNA expression profiles for quiescent HPRFs and HPRFs grown in full growth media were comparable (**Figures 3.7A & 3.7B**). In PAR_4 induction experiments, no mRNA expression for PAR_4 was detected (**Figure 3.7C**), indicating that renal fibroblasts do not express PAR_4 after LPS stimulation.

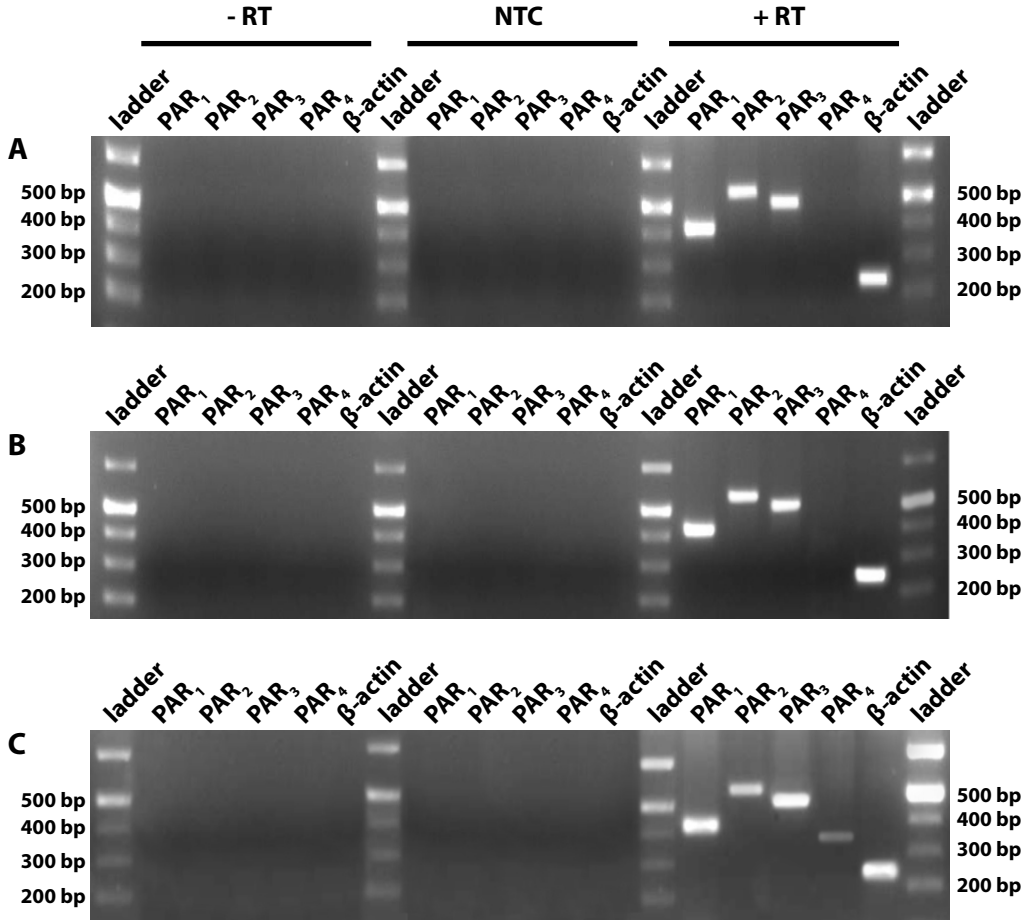

Figure 3.5: RT-PCR Detection of PAR mRNA in HPBFs. HPBFs were cultured in (A) Complete growth media; (B) Serum free media for 24 h; (C) LPS (100 ng/ml) under serum free condition. RNAs were extracted and reverse transcribed. PCR was carried out for 35 cycles using primers specific to PAR_1, PAR_2, PAR_3 or PAR_4. β-actin primers were included as a positive control. No template controls (NTC) and no reverse transcriptase (-RT) samples were included. Expected band sizes: PAR_1 (450 bp), PAR_2 (550 bp), PAR_3 (500 bp), PAR_4 (340 bp) and β-actin (242 bp). Results are representative of ten independent experiments performed with HPBFs cultured from ten different tissue samples.

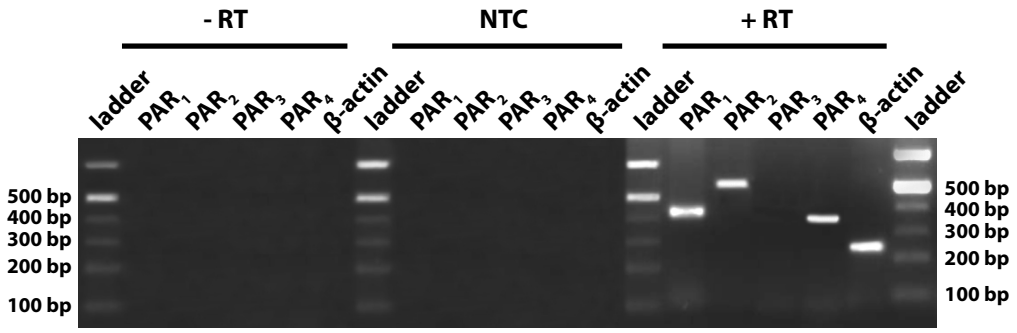

Figure 3.6: RT-PCR Detection of PAR_4 mRNA in LN-CAP cells. RNAs were extracted and reverse transcribed by RT-PCR (35 cycles) using primers specific to PAR_1, PAR_2, PAR_3 or PAR_4. β-actin primers were included as a positive control. No template controls (NTC) and no reverse transcriptase (-RT) samples were included as negative controls. Expected band sizes: PAR_1 (450 bp), PAR_2 (550 bp), PAR_3 (500 bp), PAR_4 (340 bp) and β-actin (242 bp). Results are representative of three independent experiments.

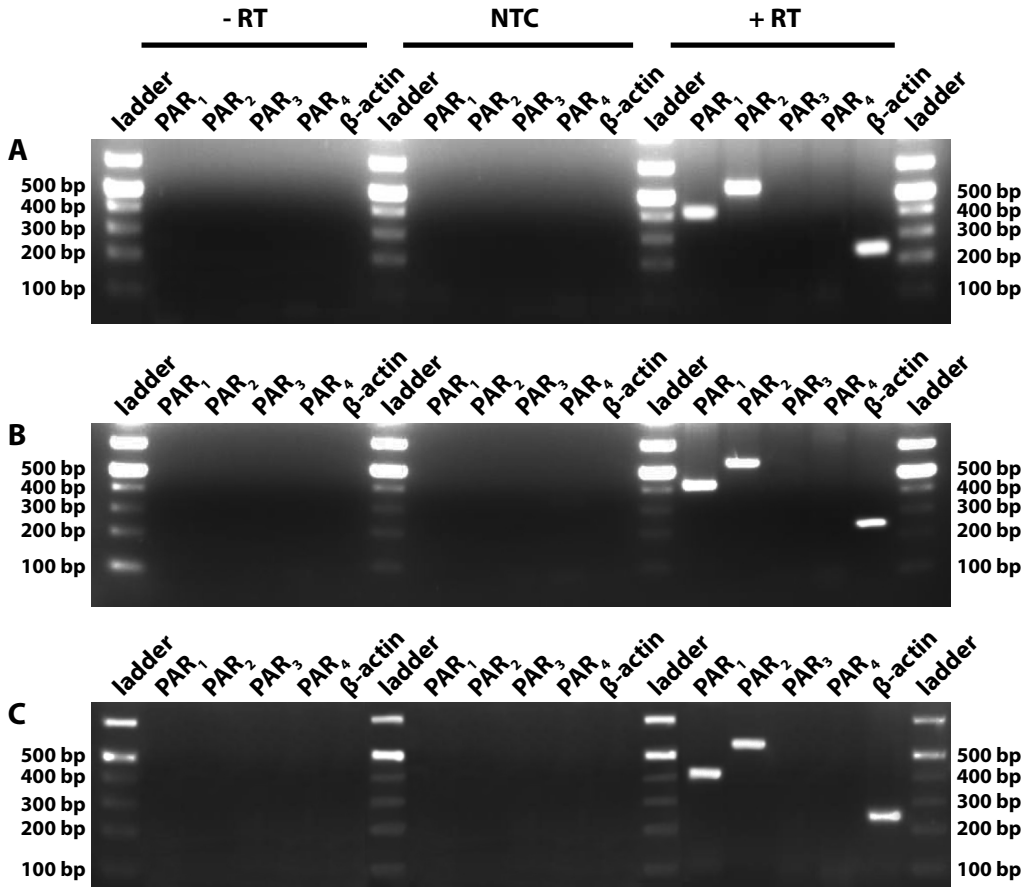

Figure 3.7: RT-PCR Detection of PAR mRNA in HPRFs. HPRFs were cultured in (A) Complete growth media; (B) Serum free media for 24 h; (C) LPS (100 ng/ml) under serum free condition. RNAs were extracted and reverse transcribed. PCR was carried out for 35 cycles using primers specific to PAR_1, PAR_2, PAR_3 and PAR_4. β-actin primers were included as a positive control. No template controls (NTC) and no reverse transcriptase (-RT) samples were included. Expected band sizes: PAR_1 (450 bp), PAR_2 (550 bp), PAR_3 (500 bp), PAR_4 (340 bp) and β-actin (242 bp). Results are representative of ten independent experiments performed with HPBFs cultured from ten different tissue samples.

3.4.3 Detection of PARs on HPBFs and HPRFs by Calcium Assay

Western blottin analysis failed to detect expression of PAR proteins despite including lysates of cells which have been previously shown to express PARs (**Figure 3.8**). Therefore, an intracellular calcium mobilisation assay was performed to confirm the presence of active PARs in HPBFs and HPRFs. However, PAR_3 expression could not be investigated using this assay because there is no available known PAR_3 AP. Both PAR_1 AP and PAR_2 AP caused elevations in intracellular calcium levels in both HPBFs (**Figure 3.9B & 3.9C**) and HPRFs (**Figure 3.9G & 3.9H**), indicating that PAR_1 and PAR_2 are expressed and functional in these cells. For PAR_4, only HPBFs treated with LPS for 24 h showed an increase in the calcium level (**Figure 3.9E & 3.9J**). HEPES was used as a negative control and no calcium increase was observed (**Figure 3.9A & 3.9F**). These results are consistent with the findings by RT-PCRs (**Figures 3.5** & **3.7**).

3.4.4 Immunocytochemical Staining of PARs in HPBFs and HPRFs

As PAR_3 could not be studied using a calcium mobilisation assay, immunocytochemical staining using DAB was performed. HPBFs were positively stained by PAR_1, PAR_2 and PAR_3 antibodies. LPS-treated HPBFs were also positively stained by the PAR_4 antibody (**Figures 3.10**). Consistent with the RT-PCR results, HPRFs were only positively stained by PAR_1 and PAR_2 antibodies (**Figures 3.11**).

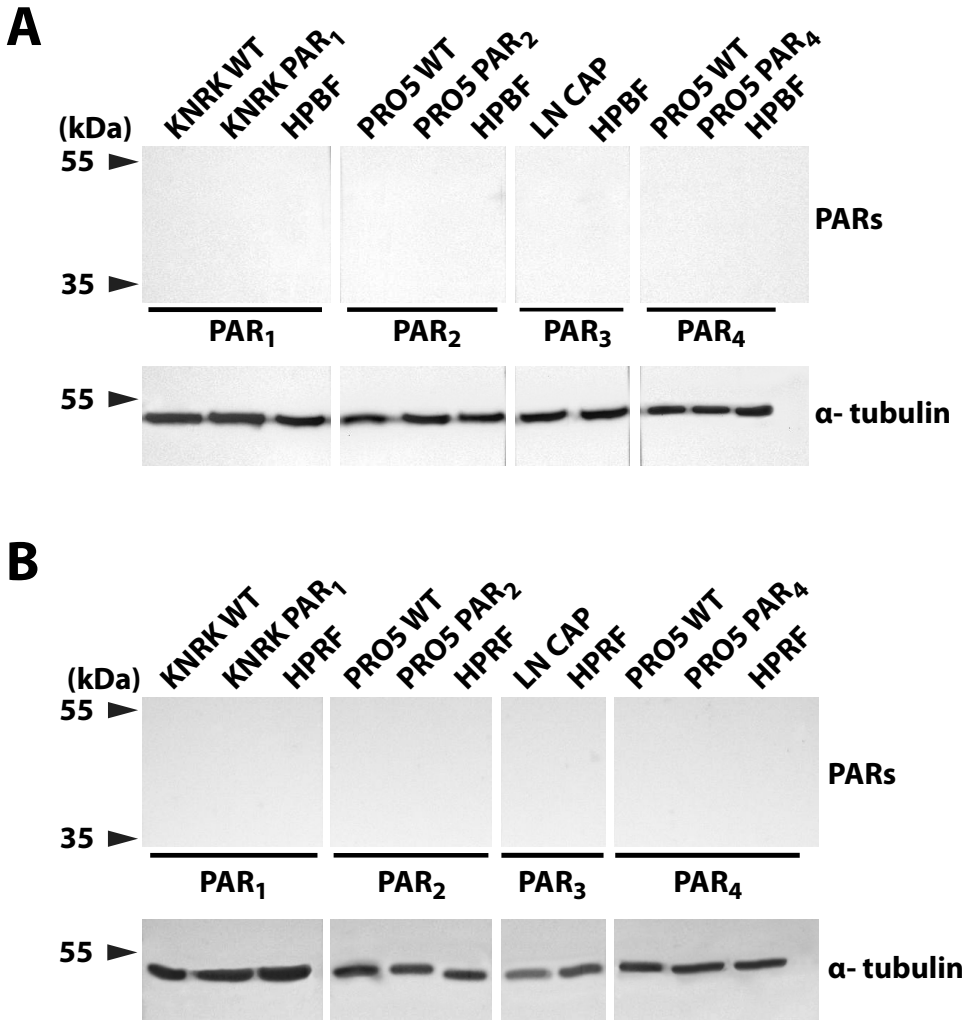

Figure 3.8: Western Blot Detection of PAR Expression. (A) HPBFs and (B) HPRFs were analysed for the expression of PARs. Various cell lines expressing different PARs (along with the corresponding WT cells which do not express PARs as negative controls) were included as controls. Cell lysates were obtained and then subjected to SDS-PAGE followed by immunoblotting with antibodies against PAR_1 (ATAP2), PAR_2 (SAM11), PAR_3 (H-103) and PAR_4 (C-20). α-tubulin was used as a loading control. 20 μg of protein was loaded to each lane. Expected band sizes: PAR1 ~47 kDa, PAR2 ~44 kDa, PAR3 ~43 kDa, PAR4 ~38 kDa and α-tubulin ~52 kDa. Results are representatives of two independent experiments.

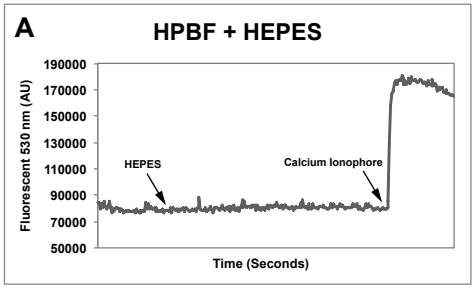
A
HPBF + HEPES
Fluorescent 530 nm (AU)
190000
170000
150000
130000
110000
90000
70000
50000
HEPES
Calcium Ionophore
Time (Seconds)

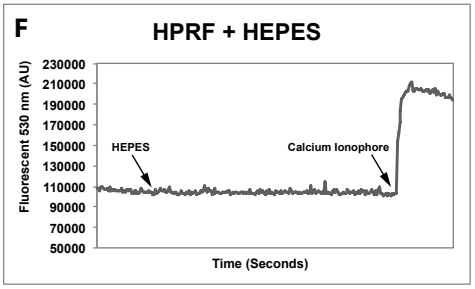
F
HPRF + HEPES
Fluorescent 530 nm (AU)
230000
210000
190000
170000
150000
130000
110000
90000
70000
50000
HEPES
Calcium Ionophore
Time (Seconds)

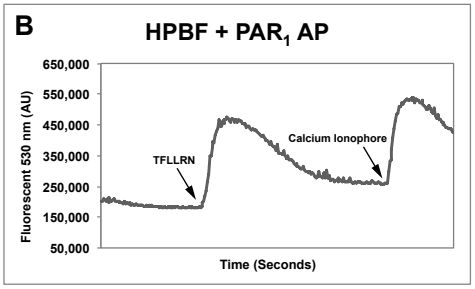
B
HPBF + PAR1 AP
Fluorescent 530 nm (AU)
650,000
550,000
450,000
350,000
250,000
150,000
50,000
TFLLRN
Calcium Ionophore
Time (Seconds)

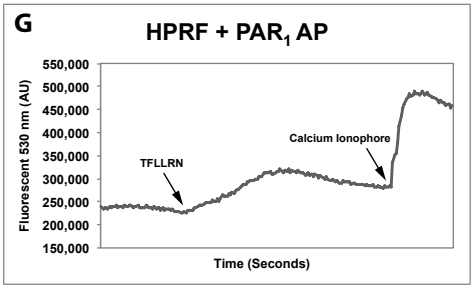
G
HPRF + PAR1 AP
Fluorescent 530 nm (AU)
550,000
500,000
450,000
400,000
350,000
300,000
250,000
200,000
150,000
TFLLRN
Calcium Ionophore
Time (Seconds)

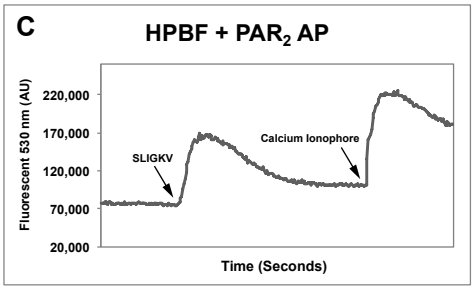
C
HPBF + PAR2 AP
Fluorescent 530 nm (AU)
220,000
170,000
120,000
70,000
20,000
SLIGKV
Calcium Ionophore
Time (Seconds)

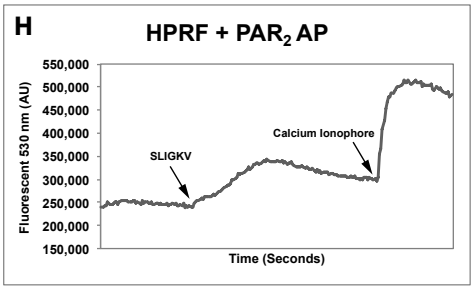
H
HPRF + PAR2 AP
Fluorescent 530 nm (AU)
550,000
500,000
450,000
400,000
350,000
300,000
250,000
200,000
150,000
SLIGKV
Calcium Ionophore
Time (Seconds)

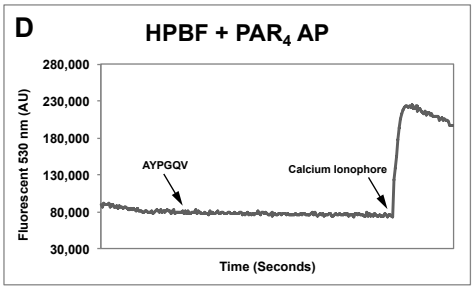
D
HPBF + PAR4 AP
Fluorescent 530 nm (AU)
280,000
230,000
180,000
130,000
80,000
30,000
AYPGQV
Calcium Ionophore
Time (Seconds)

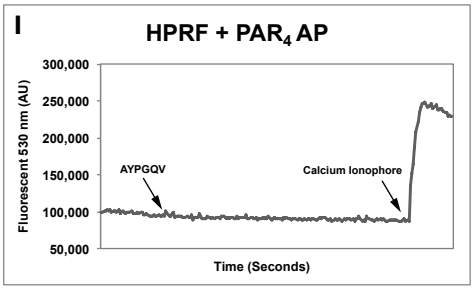
I
HPRF + PAR4 AP
Fluorescent 530 nm (AU)
300,000
250,000
200,000
150,000
100,000
50,000
AYPGQV
Calcium Ionophore
Time (Seconds)

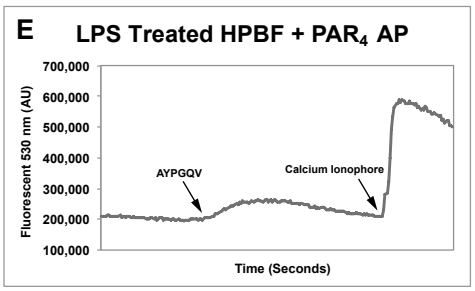
E
LPS Treated HPBF + PAR4 AP
Fluorescent 530 nm (AU)
700,000
600,000
500,000
400,000
300,000
200,000
100,000
AYPGQV
Calcium Ionophore
Time (Seconds)

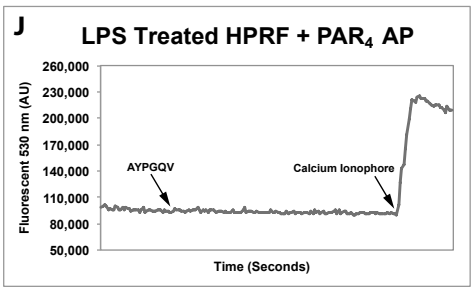
J
LPS Treated HPRF + PAR4 AP
Fluorescent 530 nm (AU)
260,000
230,000
200,000
170,000
140,000
110,000
80,000
50,000
AYPGQV
Calcium Ionophore
Time (Seconds)

Figure 3.9: Calcium Responses to PAR Agonists in HPBFs and HPRFs. Cells at 70-85% confluence in 75 cm^2 flasks were harvested and incubated with Fluo-3 AM at room temperature for 25 min. Cells were then washed and resuspended in calcium assay buffer. Functional PAR activities were assessed by treating (A−E) HPBFs or (F−J) HPRFs with (A & F) HEPES as negative control, (B & G) PAR_1 AP (TFLLRN, 100 μM), (C & H) PAR_2 (SLIGKV, 100 μM), (D & I) PAR_4 (AYPGQV, 100 μM), and, (E & J) PAR_4 (AYPGQV, 100 μM). In E and J, the cells were pre-treated with LPS before the calcium assay. An increase in fluorescence (E530) monitored by fluorescence spectrophotometer is indicative of calcium mobilisation. Arrows indicate the time when test agonists were added. These results represent data from three independent experiments.

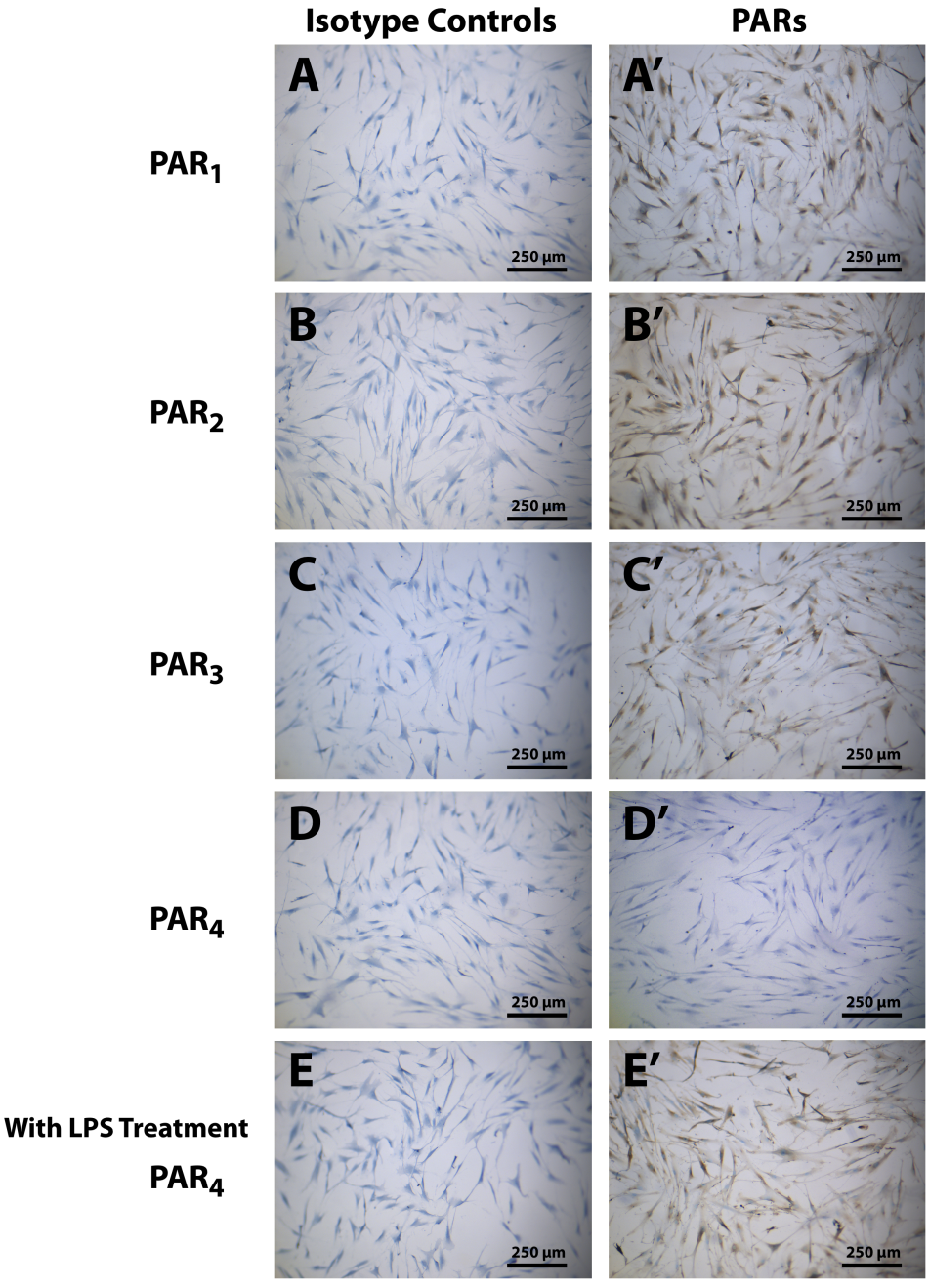
Isotype Controls
PARs
A
A′
PAR1
250 µm
B
B′
PAR2
250 µm
C
C′
PAR3
250 µm
D
D′
PAR4
250 µm
E
E′
With LPS Treatment
PAR4
250 µm

Figure 3.10: Immunocytochemical Staining of PARs in HPBFs. HPBFs were seeded on cover slips and grown in 6-well plates with 2 ml of fibroblast complete growth medium. For PAR_4 induction, quiescent HPBFs were treated with LPS (100 ng/ml) for 24 h. After blocking with 1% BSA/PBS, HPBFs were stained with primary antibodies: (A) Mouse IgG1, (A') PAR_1 (ATAP2), (B) Mouse IgG2a, (B') PAR_2 (SAM11), (C) Rabbit IgG, (C') PAR_3 (H-103), (D) Goat IgG, (D') PAR_4 (C-20), (E) Goat IgG, and, (E') PAR_4 (C-20). A secondary antibody conjugated to biotin was used to detect primary antibody. Streptavidin and DAB development were used to detect secondary antibody binding. Positive staining is indicated by the development of a brown colour. All samples were also counterstained with haematoxylin. Left panels (A−E) are the isotype controls for corresponding anti-PAR antibodies. E and E' represent HPBFs treated with LPS. These pictures represent results from three independent experiments.

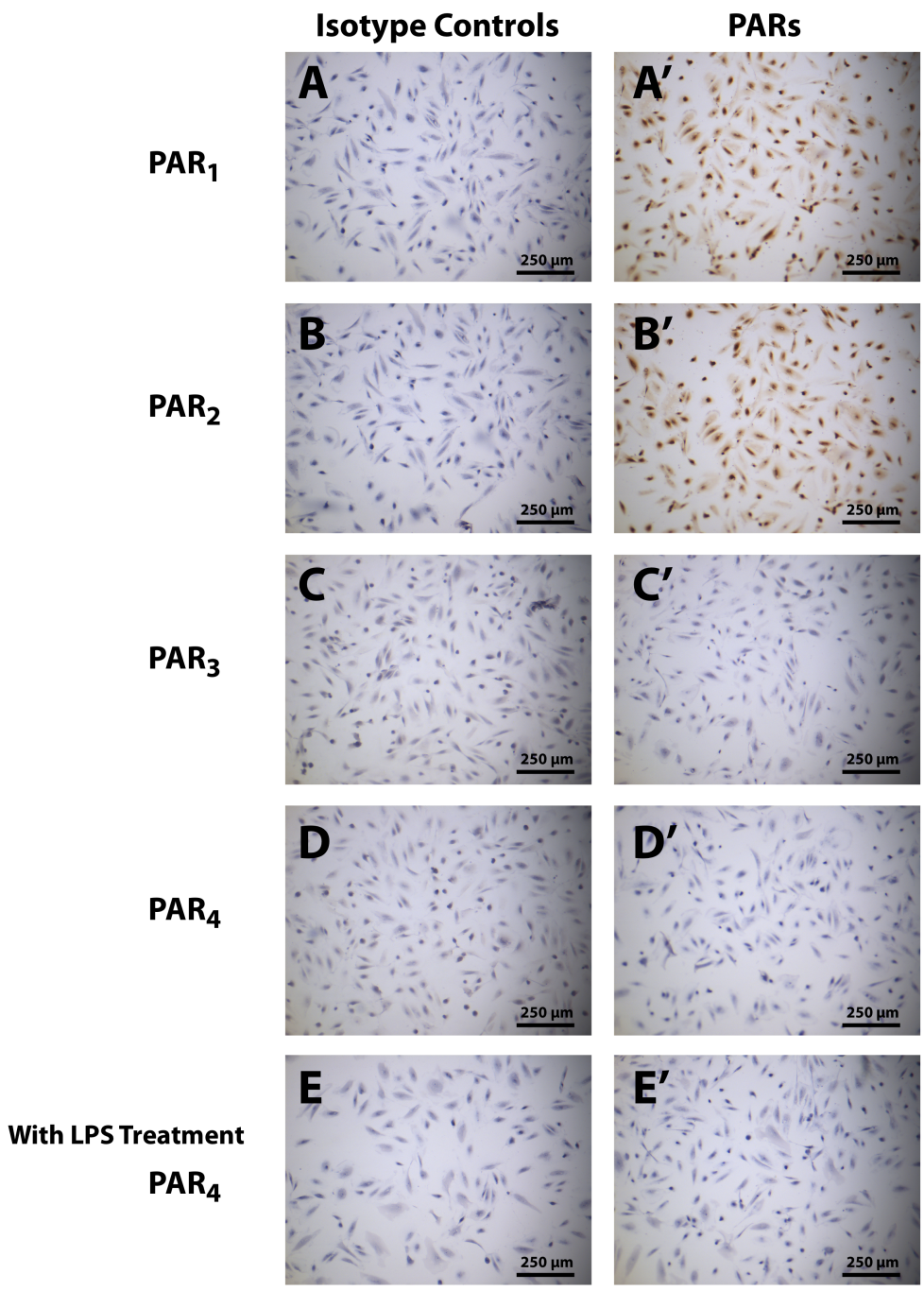
Isotype Controls
PARs
PAR1
PAR2
PAR3
PAR4
With LPS Treatment
PAR4
A
A′
B
B′
C
C′
D
D′
E
E′
250 µm

Figure 3.11: Immunocytochemical Staining of PARs in HPRFs. HPRFs were seeded on cover slips and grown in 6-well plates with 2 ml of fibroblast complete growth medium. For PAR_4 induction, quiescent HPBFs were treated with LPS (100 ng/ml) for 24 h. HPRFs were stained with primary antibodies: (A) Mouse IgG1, (A') PAR_1 (ATAP2), (B) Mouse IgG2a, (B') PAR_2 (SAM11), (C) Rabbit IgG, (C') PAR_3 (H-103), (D) Goat IgG, (D') PAR_4 (C-20), (E) Goat IgG, and, (E') PAR_4 (C-20). A secondary antibody conjugated to biotin was used to detect primary antibody. Streptavidin and DAB development were used to detect secondary antibody binding. Positive staining is indicated by the development of a brown colour. All samples were also counterstained with haematoxylin. Left panels (A−E) are the isotype controls for corresponding anti-PAR antibodies. E and E' represent HPBFs treated with LPS. These pictures represent results from three independent experiments.

3.4.5 Immunofluorescent Characterisation of Human Lung and Renal Myofibroblasts

TGF-β is the most potent inducer of α-SMA expression and fibroblast to myofibroblast differentiation, Therefore, TGF-β1 was used to stimulate differential expression of α-SMA in HPBFs and HPRFs. Various concentrations of TGF-β1 were used in order to determine the optimal concentration for the induction of α-SMA expression (See **Appendix**). The effect of TGF-β1 (10 ng/ml) addition to the culture medium was examined on the phenotypic transformation of fibroblasts to myofibroblasts. Immunofluorescent staining with anti-α-SMA antibody showed increases in the levels of α-SMA in TGF-β1-treated HPBFs and HPRFs in comparison to the untreated controls (**Figure 3.12**).

3.4.6 TGF-β1 induces Collagen Type I and α-SMA expressions in lung and renal fibroblasts

In order to confirm the results above, Western blot analysis was performed using collagen type I and α-SMA antibodies. Untreated fibroblasts or fibroblasts treated with 10 ng/ml TGF-β1 were used. TGF-β1-treated fibroblasts exhibited higher levels of collagen type I and α-SMA expression than untreated fibroblasts (**Figure 3.13**). Thus, this data further supports the finding that both lung and renal fibroblasts upregulate α-SMA and collagen type I in response to the stimulation of exogenously added TGF-β1.

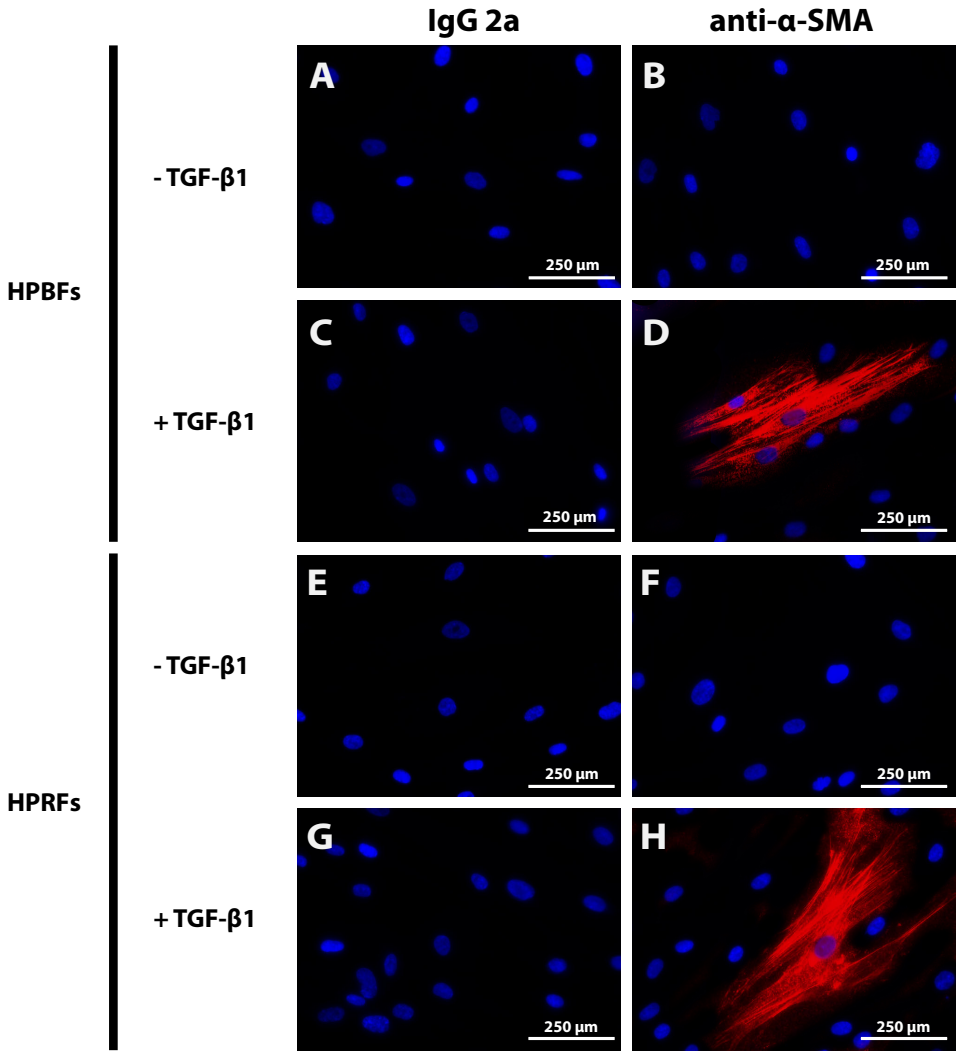

Figure 3.12: α-SMA expression increases in HPBFs and HPRFs after TGF-β1 treatment. HPBFs and HPRFs were seeded on cover slips and grown in 6-well plates with 2 ml of fibroblast complete growth medium. For α-SMA expression induction, quiescent HPBFs and HPRFs were treated with TGF-β1 (10 ng/ml) for 24 h. Cells were then fixed, permeabilised and blocked with 1% BSA/PBS. Untreated HPBFs (A & B) and HPRFs (E & F) were stained with (A & E) mouse IgG2a negative control antibody or (B & F) mouse anti-α-SMA antibody. Similarly, TGF-β1-treated HPBFs (C & D) and HPRFs (G & H) were stained with (C & G) mouse IgG2a negative control antibody (D & H) or mouse anti-α-SMA antibody. All samples were also stained for nuclei (blue) using DAPI. Red depicts α-SMA. These images represent results from three independent experiments.

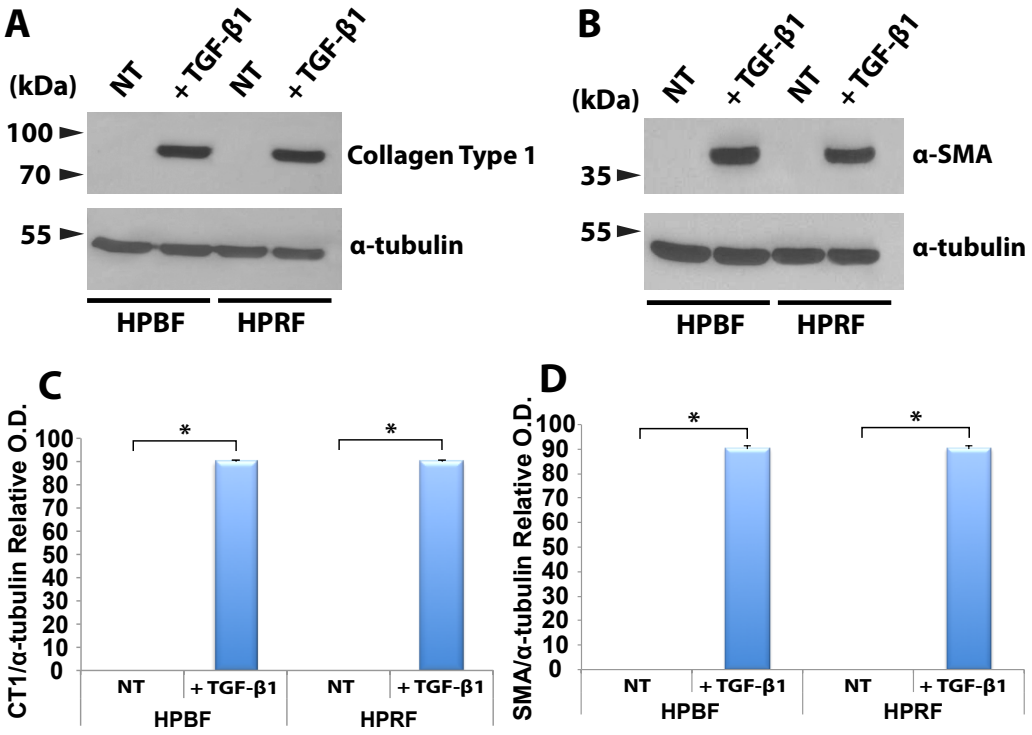

Figure 3.13: Collagen Type I and α-SMA are detected by Western blotting in TGF-β1-treated HPBFs and HPRFs. Amounts of collagen type I (A & C) and α-SMA (B & D) in HPBFs and HPRFs, either untreated or treated with TGF-β1, were analysed using Western blotting. Quiescent HPBFs and HPRFs were stimulated with TGF-β1 (10 ng/ml) under serum free conditions for 24 h. Cell lysates were obtained and then subjected to SDS-PAGE followed by immunoblotting with antibodies against collagen type 1, α-SMA and α-tubulin. α-tubulin was used as a loading control. Expected band sizes: collagen type I ($\sim$90 kDa), α-SMA ($\sim$42 kDa) and α-tubulin ($\sim$52 kDa). (C & D) Results were quantitated and summarised in a bar chart, where optical densities were normalised to α-tubulin loading controls. Results are expressed as mean $\pm$ SEM of three independent experiments. * indicates $p < 0.05$ compared with untreated samples in paired t-test.

3.5 Discussion

The purity of confluent cultures of fibroblasts grown from finely dissected pieces of tissue in fibroblast growth media were assessed by their morphological appearance and immunocytochemical staining for the fibroblast specific markers: prolyl 4-hydroxylase and vimentin. Prolyl 4-hydroxylase is a critical enzyme for collagen formation. It is a putative marker of collagen producing cells and also a cytoplasmic marker of human fibroblasts (Smith *et al.*, 1998). Vimentin is a member of the intermediate filament family of proteins. It is responsible for maintaining cell integrity and exists as a dynamic structure in fibroblasts (Clarke and Allan, 2002). Although anti-vimentin antibody can react with the abundant intermediate filaments of fibroblasts, this antibody also labels the other cells types such as the vascular endothelial cells and the neurons that contain intermediate filaments. Given the morphology differences between these cell types, anti-vimentin is a suitable tool for reliable identification of fibroblasts (Camelliti *et al.*, 2005). In this study, along with the morphological appearance, both HPBFs and HPRFs were positively stained for prolyl 4-hydroxylase and vimentin, confirming the fibroblastic nature of these cells.

Ramachandran *et al.* (2006) have demonstrated that HPBFs express mRNA for PAR_1, PAR_2 and PAR_3, but not PAR_4. The RT-PCR results presented above are consistent with this previously published data. This observation was reproducible in different tissue samples. In contrast, the PAR expression profile in HPRFs is different from the one in HPBFs. The findings described herein demonstrate that only PAR_1 and PAR_2 were expressed in HPRFs. To date, there is no evidence that PAR_3 and PAR_4 are expressed in human renal fibroblasts. Interestingly, RT-PCR data in this study inconsistently showed that LPS induced PAR_4 expression in HPBFs. This is somewhat inconsistent with the previous findings that LPS reproducibly induced expression of functional PAR_4 in HPBFs under the

same experimental conditions (Ramachandran *et al.*, 2007). This difference might be due to several factors such as age, gender and smoking habit of the donors or underlying disease process. Besides, LPS treatment failed to induce PAR_4 expression in HPRFs, suggesting that there is no PAR_4 expression in human renal fibroblasts.

Reliable Western blot results could not be obtained using the anti-PAR antibodies available for this thesis in three different independent experiments (**Figure 3.8**). In contrast, Bae and Rezaie (2008); Strande and Phillips (2009); Banfi *et al.* (2011); Zhang *et al.* (2012) demonstrated positive Western blot results using the same PAR antibodies. This might be because different cell types were used in this thesis. Besides, the failure of the Western blotting for detecting PARs here might be due to insufficient amount of the proteins loaded (20 μg total protein was used in this study). Also, ithe antibody may only effectively recognise PAR_4 protein in its native form. All of these could potentially cause the negative Western blot results. Hence, calcium assay and immunocytochemical staining using DAB were used to further confirm the PAR expressions in HPBFs and HPRFs. Following initial experiments, it was decided to use haemotoxylin to facilitate the visualisation of cells stained with isotype controls.

Fibroblasts and myofibroblasts are often quiescent in nature. However, these cells become activated after injury. IPF and renal fibrosis strongly correlate with a substantial increase in the presence of activated fibroblasts in lung and kidney, respectively (Powell, 2000). During wound healing, epithelial cells and myofibroblasts initially form a new basement membrane replacing the damaged membrane. Then, the epithelial stem cells undergo mitosis, proliferate and migrate along the newly formed basement membrane in response to various growth factors secreted by myofibroblasts. In order to limit the surface area of the damaged tissue, myofibroblasts are

connected to each other in a syncytium as they contain α-SMA and smooth muscle myosin isoforms. The ability of the myofibroblasts to contract the tissue mainly depends on the changes in the cellular cytoskeleton (the formation of stress fibres), the formation of the Rho-regulated focal contacts (fibronexus), and the integrin expression that allows attachment of the myofibroblasts to the ECM (Powell, 2000). A few studies also suggested that the α-SMA expression is involved in the regulation of signal transduction and gene expression, including the ECM components, where α-SMA is found in abundance in areas of high ECM expression (Leivonen *et al.*, 2002; Chaqour *et al.*, 2006; Wang *et al.*, 2006). The number of myofibroblasts gradually decreases as the healing process of active fibrosis progresses to completion or termination. Persistence of the activated cells is associated with excessive collagen deposition and fibrosis (Ramos *et al.*, 2006). Thus, a better understanding of the processes inducing the transformation of fibroblasts to myofibroblasts and the alterations of the biology of fibroblasts associated with this transformation are of great interest for drug discoveries.

Myofibroblasts are distinguishable from fibroblasts based on the expression and organisation of α-SMA (Zhang *et al.*, 1994). The most widely used molecular marker for myofibroblast in research and clinical diagnostics is the *de novo* expression of α-SMA. Both HPBFs and HPRFs express little to no collagen type I and α-SMA in their resting state. However, upon activation *in vitro* or during disease, they highly express α-SMA along with extracellular mesenchymal matrix proteins collagen types I and III, and cellular fibronectin, which are the main features of myofibroblasts (Barnes and Gorin, 2011). Immunofluorescent staining results described in this chapter demonstrated that TGF-β1-treated fibroblasts were stained positively for α-SMA. α-SMA-positive stress fibers appeared parallel to the long axis of the cells. These observations indicate that the cells have differentiated into myofibroblasts and are consisted with

the study demonstrated by Serpero *et al.* (2006). This is further supported by Western blotting, which showed significant levels of collagen type I and α-SMA in TGF-β1-treated fibroblasts but not in the untreated samples. In this study, collagen type I antibody was not used for the immunofluorescent staining because there might be cross reactivity with other forms of collagen in fibroblasts.

In conclusion, PAR_1, PAR_2 and PAR_3 are present in the human lung fibroblasts and only PAR_1 and PAR_2 are present in the human renal fibroblasts without LPS stimulation. The differences of PAR family expression in fibroblasts may be due to the different origins of the fibroblasts used. LPS was shown to induce PAR_4 expression in HPBFs but this was inconsistent. LPS did not induce PAR_4 in HPRFs. TGF-β1 potently stimulates the production of collagen type I and α-SMA in both HPBFs and HPRFs. The levels of collagen type I and α-SMA for TGF-β1 treated fibroblasts were significantly higher than that for untreated fibroblasts, suggesting that they differentiated into myofibroblasts. These results confirmed the ability of TGF-β1 to stimulate α-SMA expression, consistent with its ability to promote myofibroblast differentiation.

Chapter 4

Generation of PAR_4-expressing Cell Line

4.1 Introduction

PAR_4 has a number of physiological roles. Kahn *et al.* (1998) first demonstrated that PAR_4 is an important thrombin receptor for the aggregation of both human and mouse platelets. Subsequently, Sambrano *et al.* (2001) demonstrated that mice lacking the PAR_4 gene showed an increased bleeding time, indicating the importance of PAR_4 signalling in coagulation events *in vivo*. PAR_4 is also present in endothelial cells and leukocytes (Vergnolle *et al.*, 2002).

With the exception of PAR_3, PARs can be activated by PAR APs. PAR APs are synthetic peptides having sequences designed based on the revealed tethered ligands that can activate the receptor. They mimic the PAR-mediated action of proteinases in a variety of tissues. These observations facilitate the study of the physiological and pharmacological properties of the PARs by investigating the potential consequences of activating PARs in bioassay systems *in vitro* and in *in vivo*. The synthetic PAR_4 AP (AYPGQV-NH_2) was designed based on the human PAR_4 tethered ligand sequence (Hollenberg and Compton, 2002).

PAR_4 AP is able to induce *in vivo* leukocyte rolling and adhesion to the endothelium in rat mesenteric venules, as monitored by intravital microscopy (Vergnolle *et al.*, 2002). The mechanisms by which PAR_4 recruits leukocytes to the inflammatory site via the endothelium is unknown, but PAR_4 has been detected by immunohistochemistry at the surface of neutrophils, endothelial cells and smooth muscle cells of the aorta in rats (Vergnolle *et al.*, 2002). These findings suggest that the pro-inflammatory effects of the PAR_4 agonists are mediated through PAR_4 activation on endothelial cells and/or leukocytes (Vergnolle *et al.*, 2002; Kataoka *et al.*, 2003). Hollenberg *et al.* (2004) and Houle *et al.* (2005) further demonstrated that PAR_4 plays a critical role in inflammatory responses. Activation of PAR_4 generates two hallmarks of the inflammatory response: oedema and granulocyte infiltration. PAR_4 AP caused oedema in rats (Hollenberg *et al.*, 2004) and increased the recruitment of granulocytes to the site of inflammation in the mouse paws (Houle *et al.*, 2005). All of these observations strongly support a possible involvement of PAR_4 in inflammation.

PAR_4 is not expressed endogenously in human renal fibroblasts. To study the signaling pathway of PAR_4, a stable PAR_4-expressing cell line is generated in this chapter using HEK293 cells. HEK293 cells are a transformed cell line derived from human embryonic kidney cells with sheared adenovirus DNA. The exact origin of HEK293 cell is unknown and embryonic kidney cells may differentiate into a variety of cell types present in the body. They are polygonal in shape and exhibit epithelial morphology. They are semi-adherent cell line, they do not adhere well to culture plate and can easily detach. Because they are experimentally transformed, they are easy to culture and transfect and are commonly used as a model for examining a transfected receptor (Thomas and Smart, 2005). HEK293 cells endogenously expressed PAR_1 and PAR_2 (Grishina *et al.*, 2005).

4.2 Aim

The aim of this chapter is to establish a stable PAR_4-expressing cell line using HEK293 cells.

4.3 Methods

4.3.1 Propagation of PAR_4-containing Plasmid

The plasmid containing pro-opiomelanocortin-AU1-$hPAR_4$ (POMC-AU1-$hPAR_4$) with the C-terminus tagged with a hemagglutinin 11(HA.11) epitope in pcDNA3.1 vector (**Figure 4.1**) was provided by Dr S. J. Compton and Dr Y. P. Xiao. The expected structure of this PAR_4 construct is depicted in **Figure 4.2**.

The bacterial transformation was carried out as per standard transformation protocol provided by Stratagene, UK. For each transformation, a 5 ml falcon tube was pre-chilled on ice before adding 50 μl of XL1-Blue supercompetent *E. coli*. The cells were incubated on ice for 10 min with 0.5% β-mercaptoethanol, swirling at regular intervals. 1 μl of vector DNA was added to the β-mercaptoethanol treated *E. coli*, swirled and incubated on ice for 30 min. The cells were then heat shocked at 42℃ for 45 sec before placing back onto ice for further 2 min. 500 μl of LB broth (pre-heated to 42℃) was then added and the cells were incubated at 37℃ with shaking at 200 rpm for 60 min. After that, 4.5 ml of LB broth containing 5 μl of 1 mg/ml ampicillin (100 μg/ml final concentration in 5 ml) was added to 500 μl of transformation reaction mixture and incubated at 37℃ overnight.

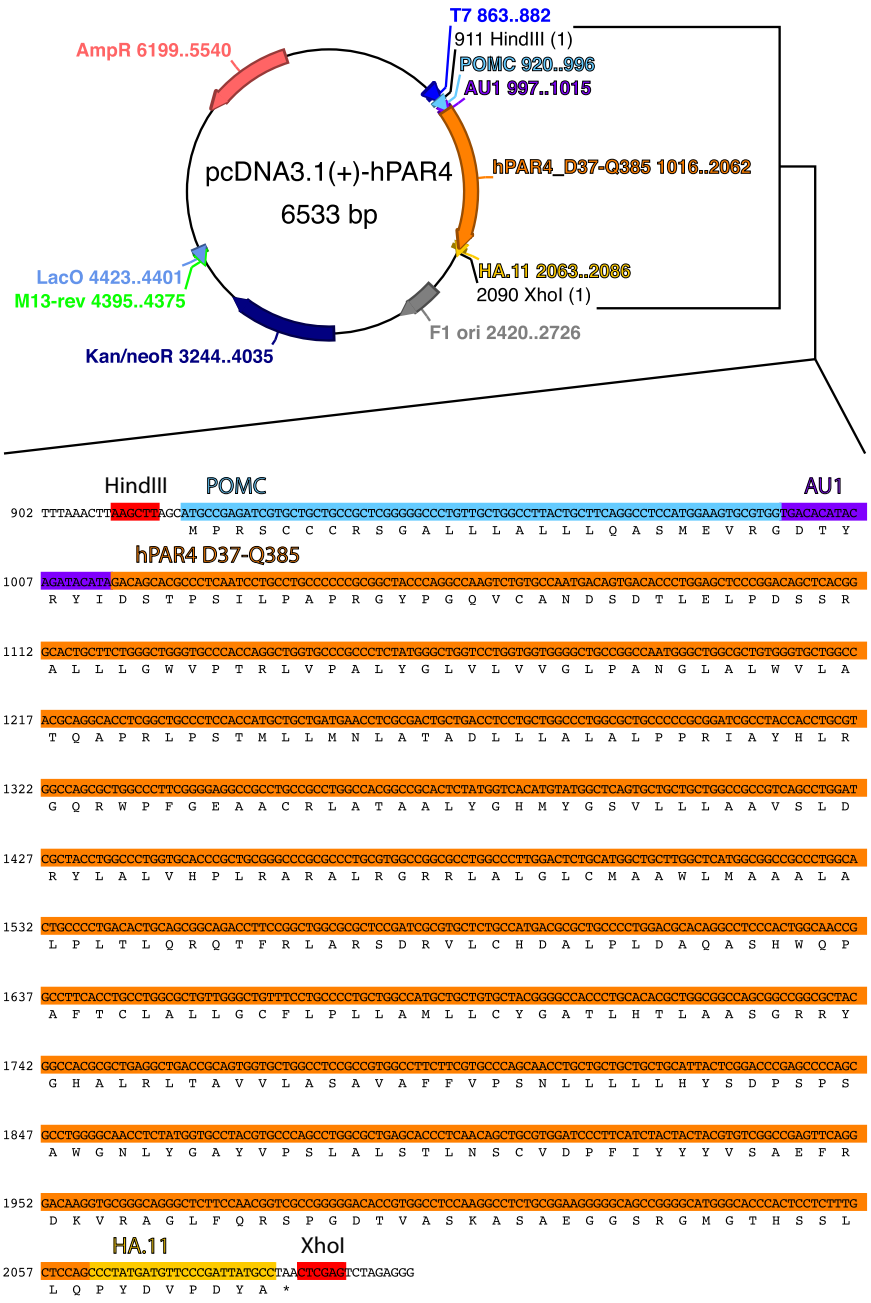

Figure 4.1: PAR_4 Sequence Map.

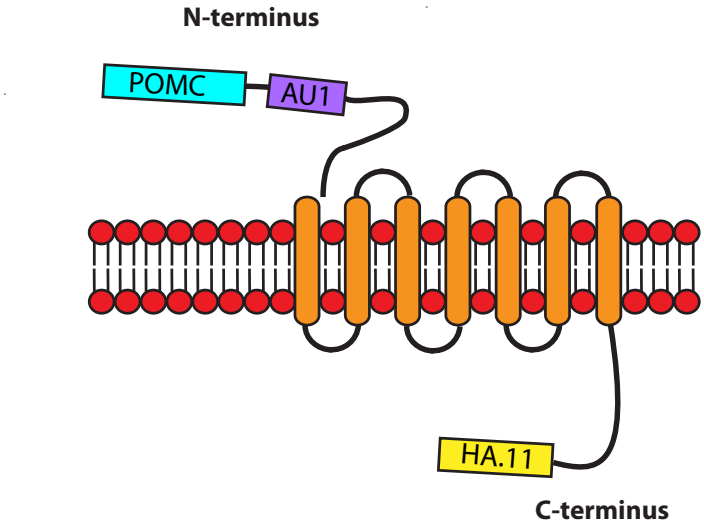

Figure 4.2: Schematic Structure of POMC-AU1-hPAR4-HA.11. The POMC signal peptide and AU1 are fused to the N-terminus and the HA.11 is fused to the C-terminus of hPAR4. The POMC signal peptide enables efficient expression of PAR4 whereas the AU1 and HA.11 epitope tags facilitate isolation and detection of the receptor.

Plasmid DNA was extracted from the overnight cultures using a Qiagen Miniprep Kit as per manufacturer's instructions. To check if the purified plasmid contained the insert sequence, a restriction digest reaction was performed by incubating the reagents according to **Table 4.1** at 37℃ for 1 h. Then, the sample was run on a 1.3% agarose gel alongside 1 kb Plus DNA Ladder. The DNA concentration was then determined using a Genequent spectrophotometer and an aliquot of the sample was sent to MWG Biotech for sequencing using T7 primers to further verify the insert.

Table 4.1: Reagent used in Restriction Digest Reaction.

Reagent	Volume	Final Concentration
10× NEB Buffer 2	2 μl	1×
BSA	2 μl	100 μg/ml
Xho1	0.5 μl	2000 U/μl
HindIII	0.5 μl	2000 U/μl
Plasmid DNA	5 μl	-
DEPC water	10 μl	-

4.3.2 Preparation of PAR_4-expressing Cell Lines

4.3.2.1 Cell Culture

HEK293 cells were routinely maintained in DMEM complete growth medium containing in v/v 10% FBS, 1% sodium pyruvate, and 1% antibiotic/antimycotic (penicillin G sodium, streptomycin sulphate and amphotericin B).

The cells were harvested by washing with 5 ml of PBS and dissociating the cells from the flask using fresh 5 ml of PBS. The cultures were passaged with a split ratio 1:5 into 75 cm^2 flasks every 2 days with 10 ml fresh growth medium. A549 (human adenocarcinomic alveolar basal epithelial) cells were cultured in RPMI 1640 medium containing in v/v 10% FBS, 1%

sodium pyruvate, and 1% antibiotic/antimycotic (penicillin G sodium, streptomycin sulphate and amphotericin B). The cultures were passaged with a split ratio 1:5 into 75 cm^2 flasks approximately every 2 days with 10 ml fresh growth medium.

4.3.2.2 Cell Transfection

The transfection was carried out by using the Lipofectamine method (Invitrogen, UK), according to the manufacturer's protocol.

Briefly, HEK293 cells at 50-70% confluence in 65 mm petri dishes were used. 4 ml of Opti-MEM medium was applied to the cells after the normal growth medium was aspirated. Then, two 5 ml Falcon polystyrene round bottom tubes (labelled '1' and '2') containing 1 ml of Opti-MEM medium were prepared. 5 μg of vector DNA was added into tube 1 and 20 μl of lipofectamine was added into tube 2. Both tubes were then incubated at room temperature for 15 min. The content of tube 2 was poured directly into tube 1 after the incubation, vortexed for 4 sec and incubated at room temperature for a further 15 min. Finally, the mixture was applied to the cells after 4ml of Opti-MEM medium had been aspirated off. After 24 h incubation at 37℃ 5% CO_2, the mixture medium was removed and 3 ml of fresh DMEM complete growth medium was added. The cells were then incubated for a further 24 h before being grown in DMEM complete growth medium containing G418 (1.4 g/l) for two weeks.

4.3.2.3 Single Cell Cloning

A single cell cloning procedure was carried out to obtain a cell line with optimum receptor expression. The transfected cells in 25 cm^2 flasks at 70-85% were counted using a haemocytometer and diluted using selective media to give a cell suspension with a final cell concentration of 5 cells per

ml. Cells were then pipetted into a 96-well plate with a volume of 200 μl per well. After approximately two weeks, colonies of cells became visible in the wells and only the wells containing single visible colony were selected and transferred to 25 cm^2 flasks containing 5 ml of selective media. These cells were then left growing to reach ∼70-80% confluence before intracellular calcium signalling measurements were performed to identify cells expressing functional receptor (See **Section 2.9**). PAR_4 AP was used as an agonist. Once a clone had been identified, this clone was taken through second and third rounds of single cell cloning to ensure that the final set of clones were derived from a single cell.

4.3.2.4 Storage of Frozen Cell Lines

The clone showing the highest increase in calcium following agonist activation as determined by calcium signalling experiments was selected as the expressing clone for all future analysis and passaged up into larger flasks before being frozen down in FBS with 10% dimethyl sulfoxide (DMSO) in liquid nitrogen for long-term storage.

4.3.3 RT-PCR Detection of PAR_4 in HEK-PAR_4 Cells

Cells were cultured in 25 cm^2 flasks with 5 ml of DMEM containing G418. Total RNA was prepared using the Nucleospin RNA II Kit and reverse transcription of empty vector control (with empty pcDNA3.1 vector) and HEK-PAR_4 mRNA were carried out as described in **Sections 2.4** and **2.5**. 2 μg of cDNA products were amplified by PCR in 50 μl final volume in TC-3000 Personal 25-well Thermal Cycler (Bibby Scientific, UK).

PCR detection of PAR_4 was carried out as described in **Section 2.6**. The sequences of oligonucleotides used in PCR to amplify PAR_4 and β-actin are summarised in **Table 3.4**. Reaction products were analysed as described in **Section 2.6**.

4.3.4 Preparation of Whole Cell Lysates

Cells were passaged into 25 cm^2 culture flasks and allowed to reach over 70% confluence. Cells were then harvested by centrifugation at 500 $\times$ g for 5 min and lysed by adding 500 μl Laemilli's sample buffer as described in **Section 2.10**.

4.3.5 SDS-PAGE and Western Blotting

Protein samples (20 μg) were separated on a 12.5% SDS-PAGE gel before transferring to a nitrocellulose membrane using the i-blot (Invitrogen, UK) as described in **Sections 2.11** and **2.12**. The membrane was then blocked with 5% milk solution, incubated with primary and secondary antibodies as described in **Section 2.12**.

Primary antibodies were: mouse HA.11 antibody (1 μg/ml); secondary antibody was: goat anti-mouse IgG HRP (1:2000). As a loading control, mouse monoclonal IgG1 anti-α-tubulin (1:1000) was used as the primary antibody and goat anti-mouse IgG HRP (1:2000) was used as secondary antibody. The blot was visualised using the ECL detection system as describe in **Section 2.12**.

4.3.6 Detection of PAR_4 Expression on HEK-PAR_4 Cells by Flow Cytometry

Empty vector control and HEK-PAR_4 cells were passaged into 6-well plate and allowed to reach over 85% confluence. Cells were then harvested by centrifugation at 400 $\times$ g for 3 min. They were resuspended in 50 μl of ice cold PBS and incubated with PAR_4 antibody (10 μg/ml) for 30 min on ice and washed 2 times with ice cold PBS. The cells were then incubated with anti-goat IgG FITC (1:100) for 30 min on ice, in the dark and washed 2 times with PBS before analysing on a Becton Dickinson flow cytometry. A minimum of 10,000 events per sample were measured. Multiparameter data analysis was performed with CellQuest software (Becton-Dickinson).

4.4 Results

4.4.1 Verification of PAR_4 Plasmid

A restriction digest reaction was performed to check if the purified PAR_4 plasmid contained the insert sequence. Double digestion with HindIII and XhoI yielded two fragments on a 1.3% agarose gel, representing the pcDNA3.1 backbone (5428 bp) and the POMC-AU1-hPAR_4-HA.11 (1167 bp) insert (**Figure 4.3**). The presence and accuracy of POMC-AU1-hPAR_4-HA.11 insert was further confirmed by sequencing (data not shown).

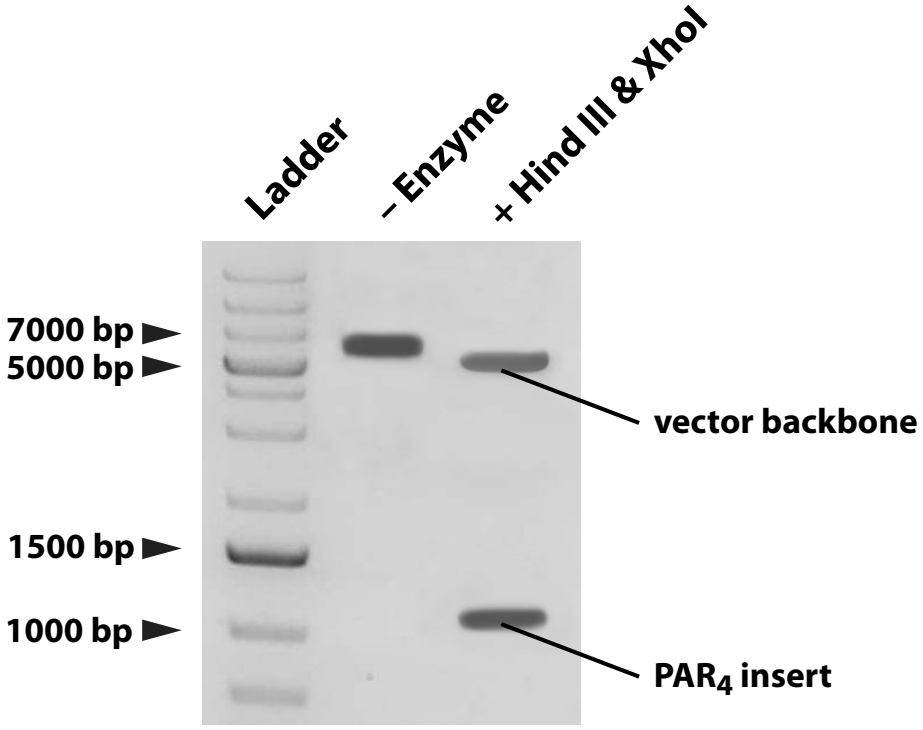

Figure 4.3: PAR_4 Plasmid Checked by Restriction Digest. pcDNA3.1-POMC-AU1-hPAR4-HA.11 plasmid was incubated with or without HindIII and XhoI. In the presence of these enzymes, the plasmid was cut into two fragments, where the higher band corresponds to the pcDNA3.1 backbone (5428 bp) and the lower band corresponds to the POMC-AU1-hPAR$_4$-HA.11 insert (1167 bp).

4.4.2 Detection of PAR_4 Expression in HEK-PAR_4 Cells

To determine if the PAR_4 transgene was successfully introduced into HEK293 cells and was expressed in these cells, RT-PCR and flow cytometry were carried out.

4.4.2.1 PAR_4 mRNA Detected by RT-PCR

Empty vector control cells and four different transfected HEK-PAR_4 clones grown from four independent colonies were examined. No band was observed in the negative controls when no RT enzyme was added or no template control reactions (NTC) where cDNA was omitted (**Figure 4.4A**). While no band was detected in the empty vector control, a PCR product of an expected size of 340 bp was amplified from all four HEK-PAR_4 clones, demonstrating the presence of PAR_4 mRNA in these transfected cells (**Figure 4.4B**). As a positive control, a 242 bp band corresponding to β-actin was detected in all samples when β-actin primers were used (**Figure 4.4B**, lane 2-6).

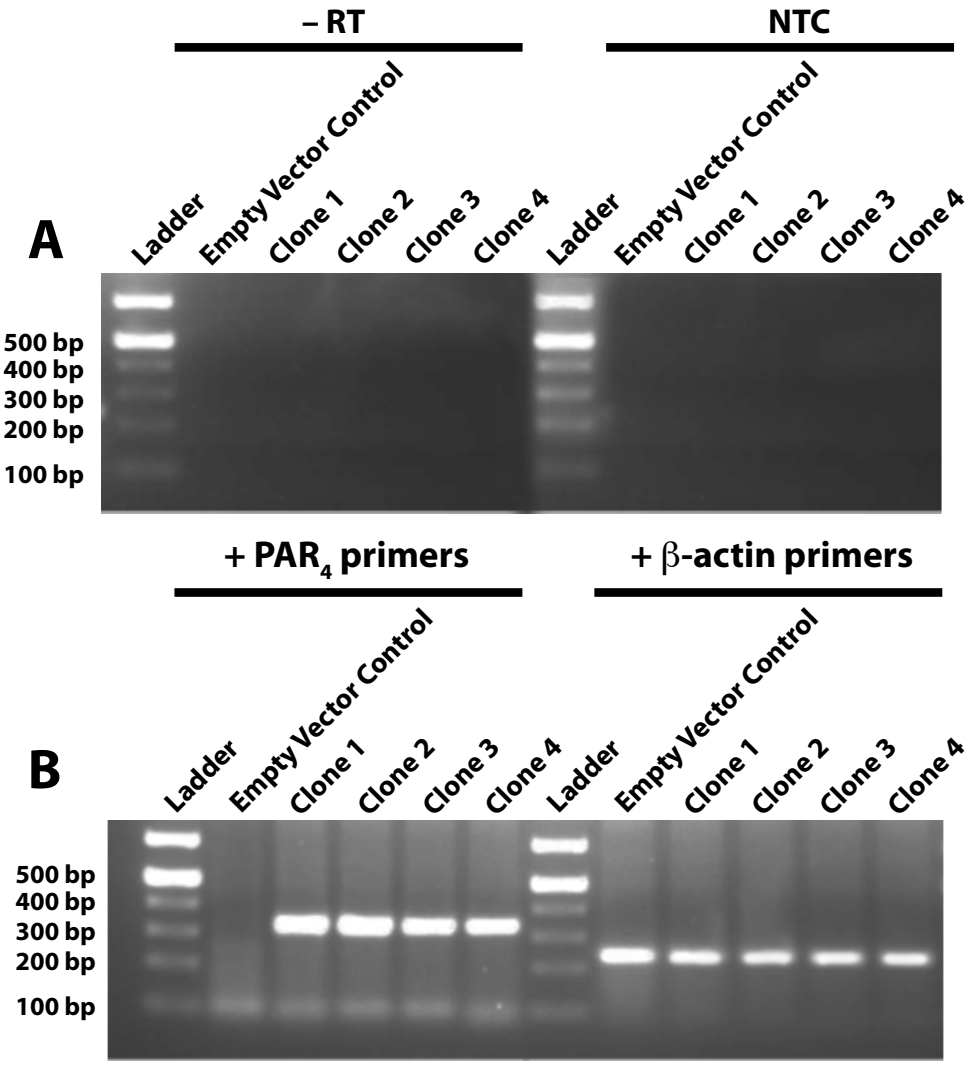

Figure 4.4: RT-PCR Detection of PAR_4 in HEK-PAR_4 Cells. Empty vector control or PAR_4-transfected (four clones) HEK cells were analysed by RT-PCRs. RNAs were extracted and reverse transcribed. PCRs were performed for 35 cycles using primers specific to PAR_4 or β-actin. β-actin primers were included as a positive control. No template controls (NTC) and no reverse transcriptase (-RT) samples were included with PAR_4 primers. These PCRs were done in parallel. Expected band sizes: PAR_4 (340 bp) and β-actin (242 bp). Results are representative of three independent experiments.

4.4.2.2 Detection of PAR_4 Protein by Western Blotting using HA.11 antibody

In chapter 3, it was shown that PAR_4 protein could not be determined by Western blotting using PAR_4 specific antibodies. As the PAR_4 transgene was tagged with HA.11, HA. 11 antibody was used to detect the presence of this transgene. **Figure 4.5** shows that PAR_4 protein was successfully expressed in the HEK- PAR_4 cells.

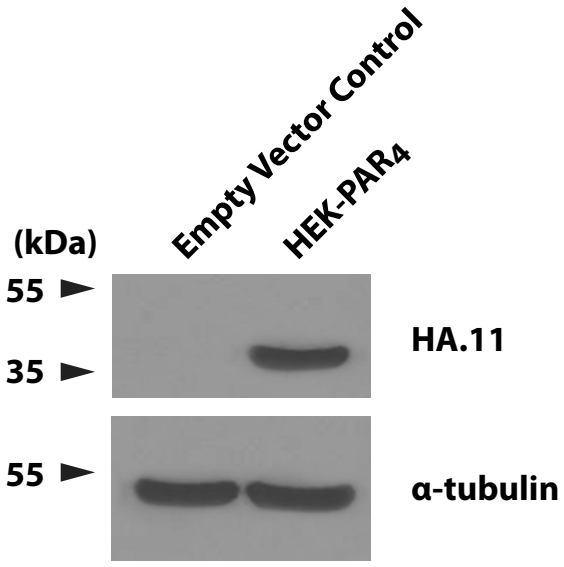

Figure 4.5: Detection of HA.11 tag of PAR_4 protein by Western blotting. Cells at 70-85% confluence in 25 cm^2 flasks were harvested and lysed. Cell lysates obtained were subjected to SDS-PAGE followed by immunoblotting with antibodies against HA.11 and α-tubulin. Expected band sizes: HA.11 ($\sim$38 kDa) and α-tubulin ($\sim$52 kDa). Results are representative of three independent experiments.

4.4.2.3 PAR_4 Protein Detected by Flow Cytometry

Flow cytometry analysis was also performed to determine the PAR_4 protein expression on HEK-PAR_4 cells. Flow cytometry data demonstrate that HEK-PAR_4 cells showed clear rightward shift in fluorescence when compared to empty vector control, indicating the surface expression of PAR_4 on HEK-PAR_4 cells (**Figure 4.6**).

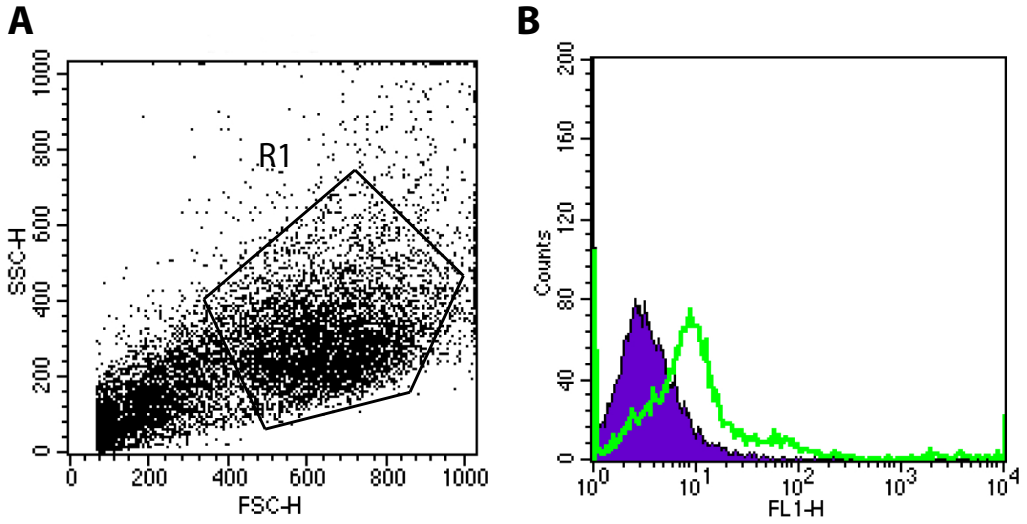

Figure 4.6: Detection of Cell Surface PAR_4 Expression on HEK-PAR_4 Cells by Flow Cytometry. Cells at 70-85% confluence in 6-well plate were harvested and incubated with anti-PAR_4 antibody. The cells were then incubated with anti-goat IgG FITC in the dark before analysing on a Becton Dickinson flow cytometry. (A) Cells were gated (R1) from the debris. (B) PAR_4 expression on gated HEK-PAR_4 cells (green line) was compared with the empty vector control cells (blue area). The histogram shows fluorescence intensity (x-axis) against number of events (y-axis). Data are representative of three independent experiments.

4.5 Discussion

PAR_4 activation is known to lead to pro-inflammatory effects. A greater understanding of PAR_4 activation and the its downstream signalling pathways could reveal novel targets for the treatment of inflammatory diseases as PAR_4 expression is upregulated during inflammation. In this chapter, stable cell line expressing functional PAR_4 (HEK-PAR_4 cells) was generated.

Results from RT-PCR (**Figure 4.4B**), Western blotting using HA.11 tag (**Figure 4.5**) and flow cytometry (**Figure 4.6**) all show that HEK293 cells have been successfully transfected with the PAR_4 transgene. Unfortunately, the anti-PAR_4 antibody (same PAR_4 antibody used in the flow cytometry experiment) was unable to produce reliable Western blotting results. One possible reason is that the antibody may only effectively recognise PAR_4 protein in its native form (e.g. in flow cytometry) but not in denatured condition (e.g. Western blotting).

In conclusion, a stable and functional PAR_4-expressing HEK293 cell line has been established, which is used in the functional studies of PAR_4 presented in the next chapters.

Chapter 5

PAR_4 Independent and Dependent Apoptosis Induction

5.1 Introduction

Apoptosis is thought to be involved in the development of fibrosis via three different mechanisms: (1) resistance to apoptosis of fibroblasts and myofibroblasts, (2) increased apoptosis of epithelial cells leading to inefficient re-epithelialisation, and (3) ineffective removal of apoptotic cells sustains a persistent inflammatory response (Drakopanagiotakis *et al.*, 2008). Fibroblasts and myofibroblasts are the primary matrix producing cells and excessive activation of these cells are considered to be the principal mediator of lung and renal fibrosis. The number of these cells closely correlates with the severity of fibrosis. Thus, fibroblast apoptosis is vital to the regression of scars and the restitution of healthy tissue during wound repair. Failure to eliminate excessive fibroblasts may contribute to severe fibrotic disease.

An increased amount of fibroblasts, myofibroblasts, resident glomerular cells and infiltrating leukocytes can be seen within the interstitium of scarred kidneys during the progression of clinical and experimental nephropathies. It has been proposed that efficient removal of these cells by

apoptosis is beneficial for the resolution of glomerulonephritis (Savill, 1994). Samples obtained from the alveolar surface of patients during lung repair contained peptides such as progesterone and glucocorticoids that can induce both fibroblast and endothelial cell death (Savill, 1994). Histological examination of lung tissue obtained from patients also revealed mesenchymal cell death within the airspace (Polunovsky *et al.*, 1993). These studies indicate a role for apoptosis in eliminating the excessive fibrotic tissue and allowing the restoration of normal alveolar and kidney anatomy.

Serine proteases are a class of proteases where serine is the key enzymatic residue that initiates the proteolytic cleavage of the target proteins (Kessenbrock *et al.*, 2011). Cathepsin G (CG), neutrophil elastase and proteinase 3 are the three main neutrophil serine proteases that are released during inflammation. These proteases are important for maintaining the balance between tissue protection and destruction during an inflammatory response (Pham, 2008). During inflammation, neutrophils infiltrate and release granules containing proteinases, cytokines, chemokines and other enzymes at the site of injury. They also secrete collagenase and have the potential to recruit more neutrophils to the inflammatory site (Gadek *et al.*, 1984). Recruitment and activation of neutrophils are fundamental processes in the pathogenesis of fibrosis. Neutrophils can modify the inflammatory response by modulating the production of pro-inflammatory cytokines and anti-inflammatory mediators. They are important regulators of the inflammatory processes and hence serve as the potential targets for new therapeutic approaches against inflammatory diseases.

CG and trypsin are known to regulate cell signalling by cleaving and activating PARs (Vesey *et al.*, 2007). CG is stored in the azurophil granules in an active form and is secreted in limited amounts following

chemotactic and phagocytic stimuli. It is involved in clearance of internalised pathogens, proteolytic modification of chemokines and cytokines, activation and shedding of cell surface receptors, and apoptosis (Pham, 2008). Shimoda *et al.* (2007) reported that CG was a major mediator of tissue injury in ischaemic kidney during reperfusion. Prolonged neutrophil-mediated inflammation in the kidneys led to tubular apoptosis and development of tissue fibrosis. Compared to wild type mice, CG-deficient mice showed reduced mortality in response to ischaemic reperfusion induced damage. CG also acts as a monocyte chemoattractant in joint inflammation of rheumatoid arthritis. Monocyte chemotactic activity was detected in synovial fluid of rheumatoid arthritis patients which contained high concentrations of CG. The chemotactic activity was partially decreased by the treatment with CG inhibitors such as α1-antichymotrypsin (ACT) and phenylmethylsulfonyl fluoride (PMSF) (Miyata *et al.*, 2007).

The blockade of inflammation using steroids and other drugs has been the main focus for fibrosis treatment. However, the clinical benefits of such treatment are limited despite excellent anti-inflammatory efficacy of the agents used (Munson *et al.*, 2010). Thus, treatments that directly target fibroblasts would be desirable as fibroblasts are the key effector cells in fibrosis that produce excessive ECM. Therapies that promote fibroblast apoptosis during the repair phase after injury may facilitate recovery by eliminating excessive fibrotic tissue. Therefore, potential therapeutic targets in fibrosis may involve the administration of inducers of fibroblast apoptosis or the promotion of their mediators, provided that this can be achieved in a cell type specific manner. As CG and PAR_4 expression levels are upregulated during inflammation, CG may be important in PAR_4-mediated inflammation.

5.2 Aims

In **Chapter 3**, the purity of fibroblast cultures was assessed morphologically and immunocytochemically by staining for the fibroblast markers, vimentin and prolyl-4-hydroxylase. PAR expression in these fibroblasts was determined, and results indicate that PAR_4 is not present in these fibroblasts. PAR_4 is thought to be involved in pro-inflammatory responses and fibroproliferative processes (Vergnolle *et al.*, 2002; Ando *et al.*, 2007b). Thus, as described in **Chapter 4**, a stable HEK-PAR_4 cell line was generated using HEK293 cells (human embryonic kidney cells) in order to study PAR_4. This chapter aims to investigate whether:

1. PAR_4 AP and CG can induce PAR_4 signalling in HEK-PAR_4 cells
2. CG and trypsin induce apoptosis
3. Activation of PAR_4 triggers apoptosis of HEK-PAR_4 cells.

5.3 Methods

5.3.1 Intracellular Calcium Mobilisation Assay

A calcium signalling assay was performed using the methods described in **Section 2.9**. Agonists used were: AYPGQV (100 μM), CG (300 nM) and antagonist PMSF (1 mM).

5.3.2 Staining of Enzyme Activity After PAGE

For enzyme activity staining, the SDS-PAGE was prepared as described in **Section 2.11**. CG (300 nM) was added to casein (5 mg/ml) and the mixture was incubated at 37°C for 24 h. To inhibit CG enzymatic activity, PMSF was added to CG for 30 min before CG was added to casein. CG was inactivated in each sample before loading on the gel by heating at

100℃ for 5 min.

After electrophoresis, gel was fixed in 50% ethanol containing 10% acetic acid for 30 min and washed with 50% methanol containing 10% acetic acid for another 30 min. Gel was then stained with 0.1% v/v Coomassie brilliant blue (CBB) in 20% methanol containing 10% acetic acid overnight. After that, gel was destained in 50% methanol containing 10% acetic acid. The solution was replenish several times until background of the gel was fully destained.

5.3.3 Acridine Orange Apoptosis Assay

HPBFs and HPRFs were cultured in 24-well plates with 500 μl of fibroblast growth medium and allowed to grow to 70-80% confluence before quiescing in serum free media for 24 h. Quiescent cells were then treated with different apoptosis inducers for a further 24 h. As a negative control (no treatment), PBS was used to treat the quiescent cells. To inhibit the enzyme activity of CG and trypsin, 1 mM PMSF was added to the CG and trypsin for 30 min before being added to the cells for 24 h.

Acridine orange (2.5 μg/ml) was added to the cells before visualising using a fluorescent microscope (Nikon) with a filter for green fluorescence (525 nm). Detection of apoptotic cells was performed on the basis of nuclear morphology and rounding up of cells that were losing adhesion. Cells with condensed chromotin, rounded morphology and fragmentated DNA were classified as apoptotic. Five microscopic fields at 60× magnification with approximately 800 cells were randomly selected, and the number of apoptotic cells was counted.

5.3.4 Annexin V Binding to Phosphatidylserine (PS) Flow Cytometry Assay

HEK-PAR_4 cells were passaged into 6-well plates and allowed to reach over 70-80% confluence before treating with different apoptosis inducers for a further 24 h. In the enzyme inhibition assay, 1 mM PMSF was added to CG and trypsin for 30 min before being added to the cells for 24 h.

Next, the cells were resuspended in 100 μl of calcium buffer (10.9 mM HEPES, 140 mM sodium chloride and 2.5 mM calcium chloride) and incubated with 10 μl of FITC-conjugated Annexin V for 20 min on ice, in the dark. 1 μl of propidium iodide (PI) (stock concentration: 1 mg/ml) was added before analysing on a Becton Dickinson flow cytometer. A minimum of 10,000 events per sample were measured. Multiparameter data analysis was performed with CellQuest software (Becton-Dickinson). Cells were analysed using a fluorescence intensity histogram.

5.3.5 Preparation of Whole Cell Lysates

HPBFs or HPRFs were passaged into 25 cm^2 culture flasks and allowed to reach over 70% confluence. Once reaching the desired confluency, cells were treated with different apoptosis inducers for 24 h. Cells were then harvested by centrifugation at 500 $\times$ g for 5 min and lysed by adding 500 μl Laemilli's sample buffer as described in **Section 2.10**.

5.3.6 SDS-PAGE and Western Blotting

Protein samples were separated on a 12.5% SDS-PAGE gel before transferring to a nitrocellulose membrane using i-blot (Invitrogen, UK) as described in **Sections 2.11** and **2.12**.

The membrane was blocked with 5% milk solution, and then incubated with primary and secondary antibodies as described in **Section 2.12**. Primary antibodies were: rabbit caspase-3 (1:500) and rabbit cleaved caspase-3 (1:500); secondary antibody: donkey anti-rabbit HRP (1:5000). As a loading control, mouse monoclonal IgG1 anti-α-tubulin (1:1000) was used as primary antibody and goat anti-mouse IgG HRP (1:2000) was used as secondary antibody. The blot was visualised using the ECL detection system.

5.4 Results

5.4.1 Functional Characterisation of HEK-PAR_4 Cells by CG

5.4.1.1 CG does not activate PAR_4

To determine whether the PAR_4 developed in these HEK-PAR_4 cells is functional, a calcium mobilisation assay was performed. Exposure of empty vector control to the PAR_4 AP (100 μM) showed no calcium response (**Figure 5.1A**). A robust increase in intracellular calcium (60 $\pm$ 4.5% of calcium ionophore) was detected in the HEK-PAR_4 cells in the presence of PAR_4 AP (100 μM) (**Figure 5.1B**). A549 cells that possess functional PAR_4 were used as a positive control and a calcium response (35 $\pm$ 2.4% of calcium ionophore) was detected when PAR_4 AP was added (**Figure 5.1C**).

To test whether CG activates PAR_4, a calcium mobilisation assay was performed. 300 nM CG failed to induce a calcium response as the intracellular calcium did not change during acute incubation with CG (**Figures 5.1E & 5.1**F). **Figure 5.2** shows the summary of the calcium mobilisation in empty vector control, HEK-PAR_4 and A549 cells in response to PAR_4 and CG.

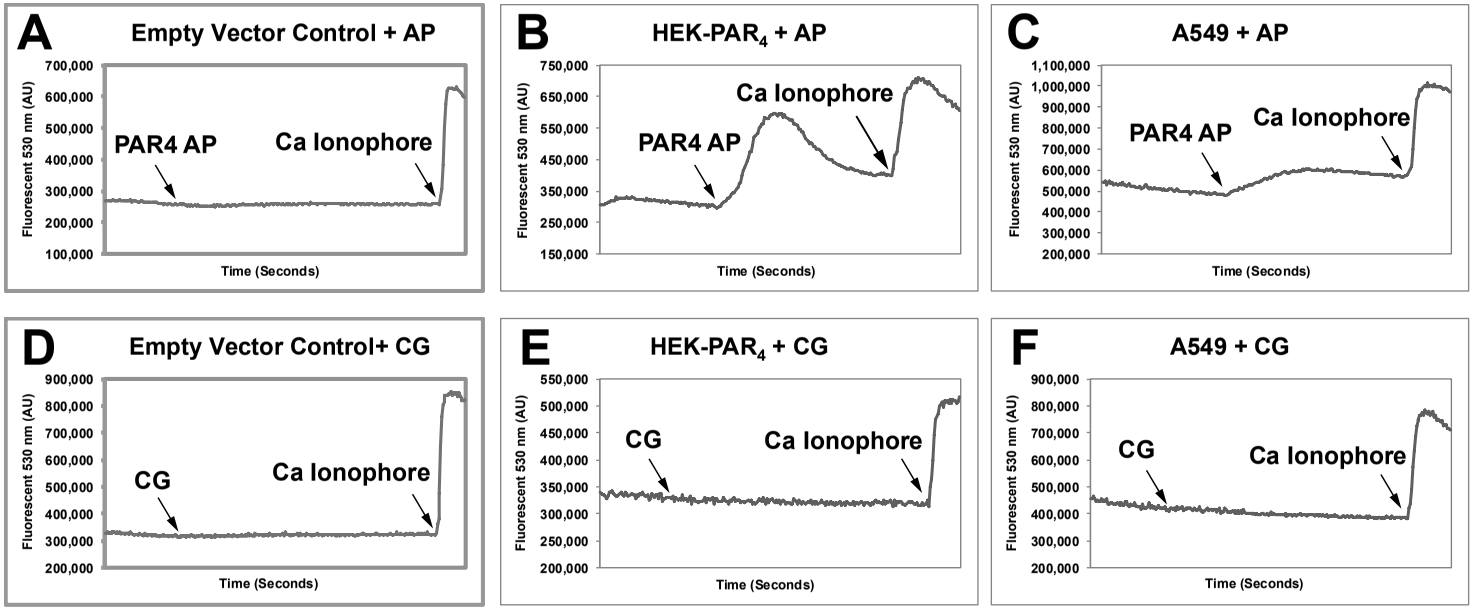
A
Empty Vector Control + AP
Fluorescent 530 nm (AU)
700,000
600,000
500,000
400,000
300,000
200,000
100,000
PAR4 AP
Ca Ionophore
Time (Seconds)
B
HEK-PAR4 + AP
Fluorescent 530 nm (AU)
750,000
650,000
550,000
450,000
350,000
250,000
150,000
PAR4 AP
Ca Ionophore
Time (Seconds)
C
A549 + AP
Fluorescent 530 nm (AU)
1,100,000
1,000,000
900,000
800,000
700,000
600,000
500,000
400,000
300,000
200,000
PAR4 AP
Ca Ionophore
Time (Seconds)
D
Empty Vector Control+ CG
Fluorescent 530 nm (AU)
900,000
800,000
700,000
600,000
500,000
400,000
300,000
200,000
CG
Ca Ionophore
Time (Seconds)
E
HEK-PAR4 + CG
Fluorescent 530 nm (AU)
550,000
500,000
450,000
400,000
350,000
300,000
250,000
200,000
CG
Ca Ionophore
Time (Seconds)
F
A549 + CG
Fluorescent 530 nm (AU)
900,000
800,000
700,000
600,000
500,000
400,000
300,000
200,000
CG
Ca Ionophore
Time (Seconds)

Figure 5.1: Calcium Signalling Assay for PAR_4 Cells in Response to PAR_4 AP or CG. Cells at 70-85% confluence in 75 cm^2 flasks were harvested and incubated with Fluo-3 AM at room temperature for 25 min. Cells were then washed and resuspended in calcium assay buffer. Empty vector control (A & D) or PAR_4-expressing HEK cells (B & E) and A549 cells (C & F) were assayed for calcium mobilisation in the presence of 100 μM PAR_4 AP (AYPGQV) (A−C) or 300 nM CG (D−E). An increase in fluorescence (E530) monitored by fluorescence spectrophotometry is indicative of calcium mobilisation. Arrows indicate the time when test agonists were added. Data shown are representative of five independent experiments.

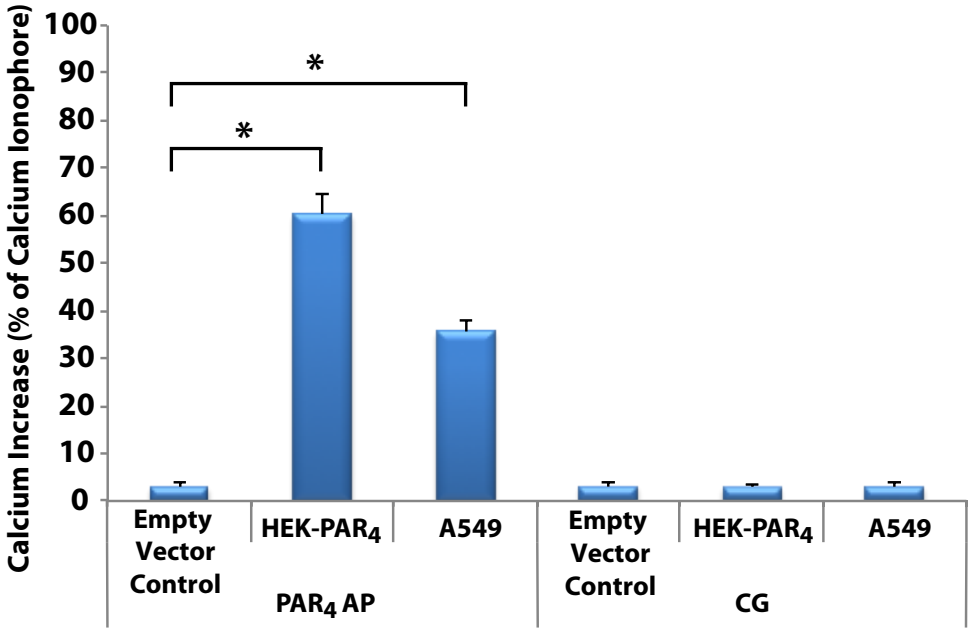

Figure 5.2: Summary of the Calcium Mobilisation for PAR_4 Cells in Response to PAR_4 AP or CG. The data in **Figure 5.1** were quantitated and summarised in a bar chart, where the calcium response was expressed as a percentage of the calcium ionophore mean response (maximum obtainable response). Results are expressed as mean ± SEM of five independent experiments. * indicates $p < 0.05$ compared with empty vector control in one way-ANOVA with Dunnett's post hoc test.

5.4.1.2 Examination of CG Enzyme Activity

As no calcium response was observed in the experiments above in the presence of CG, a possible reason might be that the CG used was inactive. To eliminate this possibility, the ability of CG to cleave casein (a known CG substrate, Considine *et al.* (2002)) was tested. As shown in **Figure 5.3**, casein can clearly be seen at ∼35 kDa. Following CG treatment, casein is degraded by CG and a cluster of bands at smaller molecular weights were detected. Importantly, this degradation of casein was prevented when CG was pre-incubated with its inhibitor PMSF. These results indicate that the CG used in this study was active, and thus the negative results described in **Section 5.4.1** are not due an inactive CG.

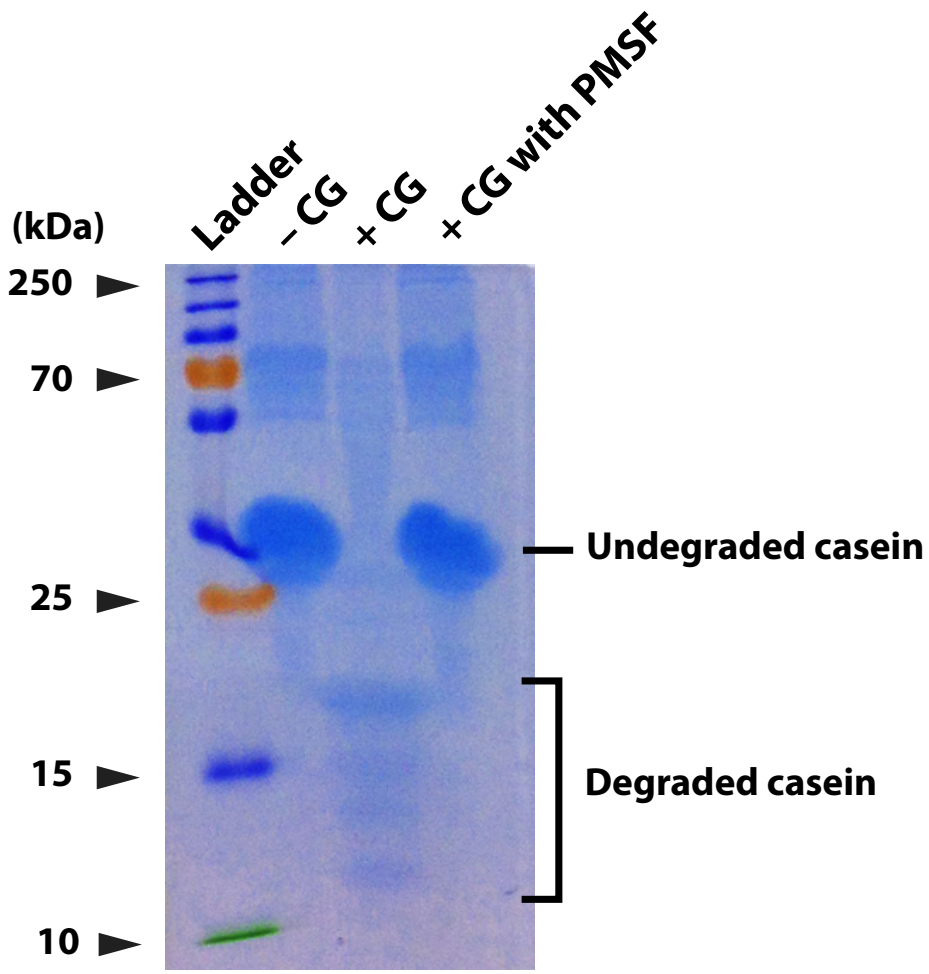

Figure 5.3: Confirmation that Cathepsin G is enzymatically active. Casein was incubated at 37℃ for 24 h without CG (A), with 300 nM CG (B), or, with 300nM CG pre-treated with PMSF (C). Samples were then subjected to SDS-PAGE. Gel was fixed and stained with 0.1% v/v CBB overnight to visualise the protein bands.

5.4.1.3 CG inhibits PAR_4

As CG did not activate PAR_4, the possibility that CG could inhibit PAR_4 was investigated. CG (300 nM) was added before PAR_4 AP. Compared to the reactions with PAR_4 AP alone without CG (**Figure 5.4B & 5.4C**), the amplitude of the response to PAR_4 AP was reduced after incubation with CG in HEK-PAR_4 (17 ± 3.3% of calcium ionophore) and A549 cells (15 ± 1.6% of calcium ionophore) (**Figures 5.4E, 5.4F & 5.4J**), indicating that CG could somehow inhibit PAR_4. In addition, PMSF (1 mM) was used to inhibit CG enzyme activity to test if the calcium could be increased. As expected, the magnitude of the calcium responses increased back to the levels observed when PAR_4 AP alone was added, HEK-PAR_4 (51 ± 5.2% of calcium ionophore) and A549 (38 ± 2.9% of calcium ionophore) (**Figures 5.4H & 5.4I**, compared to **Figure 5.4B & 5.4C**).

To investigate whether the reduced calcium response was due to the cleavage of PAR_4 AP by CG, PAR_4 AP and CG were mixed together and incubated for 30 min before performing the calcium assay. The results obtained (**Figure 5.7**) were similar to the observations when PAR_4 AP and CG were added sequentially (**Figures 5.5**), indicating that CG did not cleave PAR_4 AP.

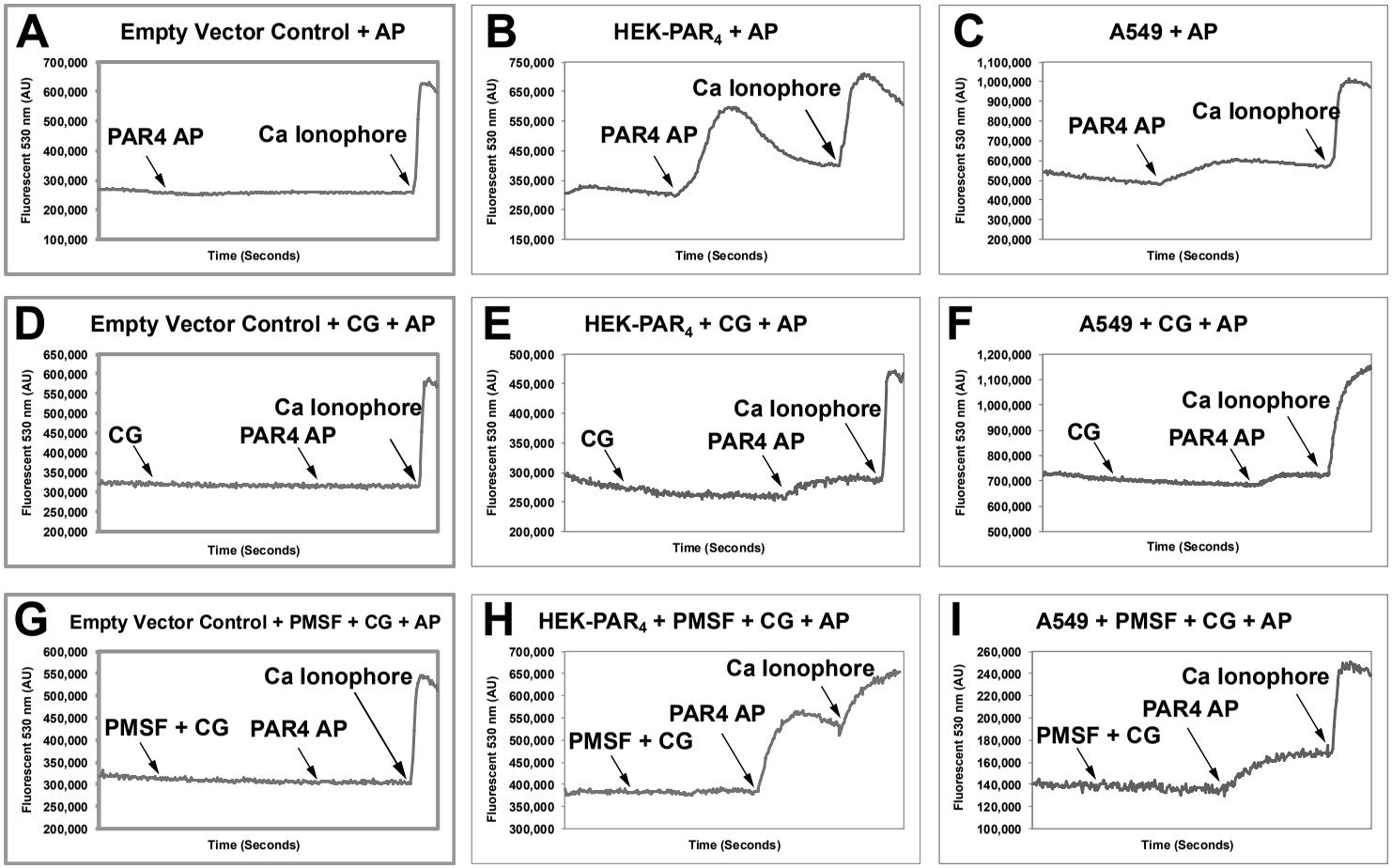
A
Empty Vector Control + AP
PAR4 AP
Ca Ionophore
B
HEK-PAR4 + AP
PAR4 AP
Ca Ionophore
C
A549 + AP
PAR4 AP
Ca Ionophore
D
Empty Vector Control + CG + AP
CG
PAR4 AP
Ca Ionophore
E
HEK-PAR4 + CG + AP
CG
PAR4 AP
Ca Ionophore
F
A549 + CG + AP
CG
PAR4 AP
Ca Ionophore
G
Empty Vector Control + PMSF + CG + AP
PMSF + CG
PAR4 AP
Ca Ionophore
H
HEK-PAR4 + PMSF + CG + AP
PMSF + CG
PAR4 AP
Ca Ionophore
I
A549 + PMSF + CG + AP
PMSF + CG
PAR4 AP
Ca Ionophore
Fluorescent 530 nm (AU)
Time (Seconds)

Figure 5.4: Calcium Signalling Assay for PAR_4 Cells in Response to Sequential Addition of PAR_4 AP and CG. Cells at 70-85% confluence in 75 cm^2 flasks were harvested and incubated with Fluo-3 AM at room temperature for 25 min. Cells were then washed and resuspended in calcium assay buffer. (A−F) Empty vector control or PAR_4-expressing HEK cells and A549 cells were assayed for calcium mobilisation after the addition of PAR_4 AP alone (A−C), 300 nM CG followed by 100 μM PAR_4 AP (AYPGQV) (D−F), or, 300 nM CG which had been pre-incubated with 1 mM PMSF, followed by 100 μM PAR_4 AP (AYPGQV) (G−I). An increase in fluorescence (E530) monitored by fluorescence spectrophotometry is indicative of calcium mobilisation. Arrows indicate the time when test agonists were added. Data shown are representative of five independent experiments.

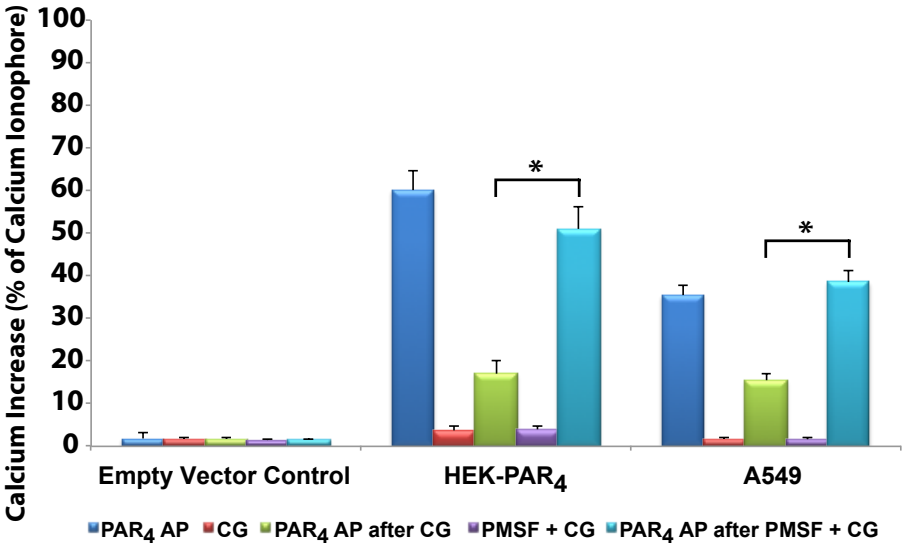

Figure 5.5: Summary of the Calcium Mobilisation for PAR_4 Cells in Response to Sequential Addition of PAR_4 AP and CG. The data in **Figure 5.4** were quantitated and summarised in a bar chart, where the calcium response was expressed as a percentage of the calcium ionophore mean response (maximum obtainable response). Results are expressed as mean ± SEM of five independent experiments. * indicates $p < 0.05$ comparison of calcium response by paired t-test.

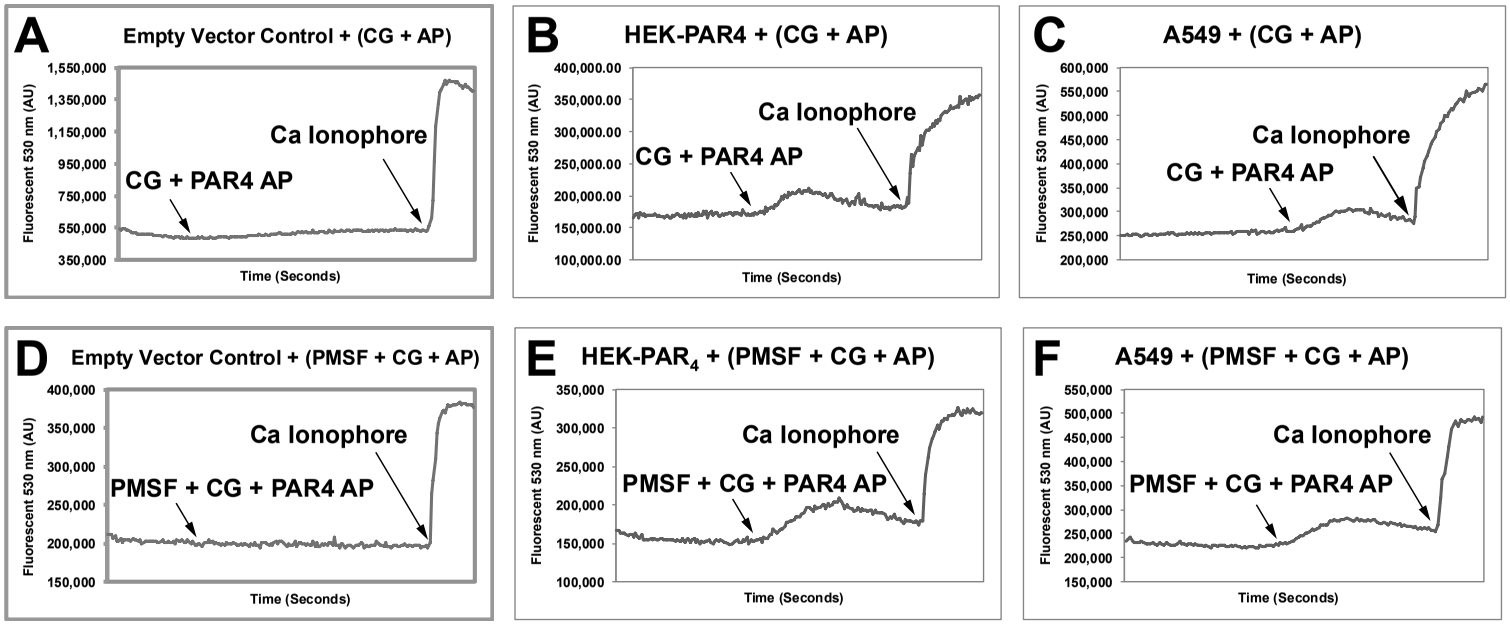
A
Empty Vector Control + (CG + AP)
Fluorescent 530 nm (AU)
1,550,000
1,350,000
1,150,000
950,000
750,000
550,000
350,000
CG + PAR4 AP
Ca Ionophore
Time (Seconds)
B
HEK-PAR4 + (CG + AP)
Fluorescent 530 nm (AU)
400,000.00
350,000.00
300,000.00
250,000.00
200,000.00
150,000.00
100,000.00
CG + PAR4 AP
Ca Ionophore
Time (Seconds)
C
A549 + (CG + AP)
Fluorescent 530 nm (AU)
600,000
550,000
500,000
450,000
400,000
350,000
300,000
250,000
200,000
CG + PAR4 AP
Ca Ionophore
Time (Seconds)
D
Empty Vector Control + (PMSF + CG + AP)
Fluorescent 530 nm (AU)
400,000
350,000
300,000
250,000
200,000
150,000
PMSF + CG + PAR4 AP
Ca Ionophore
Time (Seconds)
E
HEK-PAR4 + (PMSF + CG + AP)
Fluorescent 530 nm (AU)
350,000
300,000
250,000
200,000
150,000
100,000
PMSF + CG + PAR4 AP
Ca Ionophore
Time (Seconds)
F
A549 + (PMSF + CG + AP)
Fluorescent 530 nm (AU)
550,000
500,000
450,000
400,000
350,000
300,000
250,000
200,000
150,000
PMSF + CG + PAR4 AP
Ca Ionophore
Time (Seconds)

Figure 5.6: Calcium Signalling Assay for PAR_4 Cells in Response to Pre-mixed PAR_4 AP and CG. Cells at 70-85% confluence in 75 cm^2 flasks were harvested and incubated with Fluo-3 AM at room temperature for 25 min. Cells were then washed and resuspended in calcium assay buffer. Empty vector control (A & D) or PAR_4-expressing HEK cells (B & E) and A549 cells (C & F) were assayed for calcium mobilisation after the addition of a mixture of 300 nM CG and 100 μM PAR_4 AP (AYPGQV) (A−C), or, a mixture of 1 mM PMSF, 300 nM CG and 100 μM PAR_4 AP (AYPGQV) (D−F) . An increase in fluorescence (E530) monitored by fluorescence spectrophotometry is indicative of calcium mobilisation. Arrows indicate the time when test agonists were added. Data shown are representative of five independent experiments.

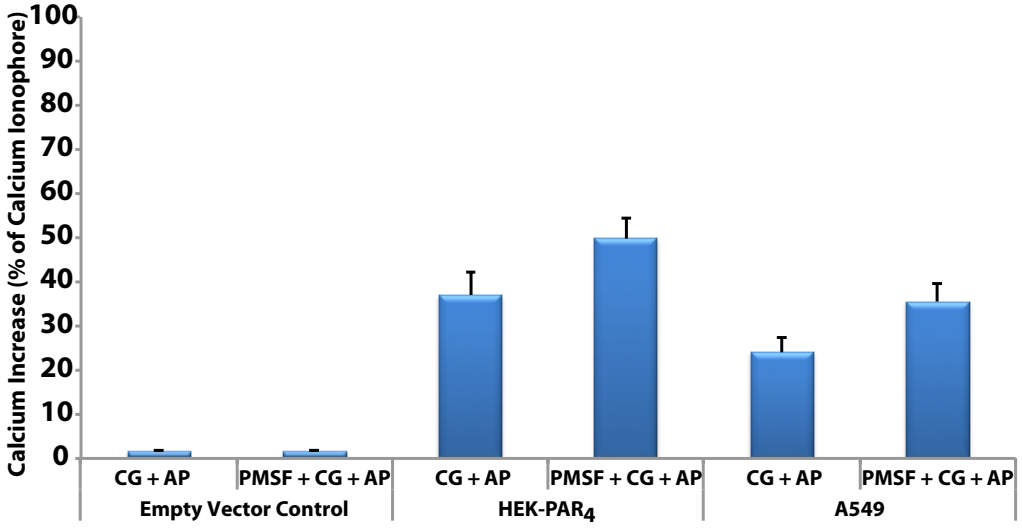

Figure 5.7: Summary of the Calcium Mobilisation for PAR_4 Cells in Response Pre-mixed PAR_4 AP and CG. The data in **Figure 5.6** were quantitated and summarised in a bar chart, where the calcium response was expressed as a percentage of the calcium ionophore mean response (maximum obtainable response). Results are expressed as mean ± SEM of five independent experiments. * indicates $p < 0.05$ compared with empty vector control in one way-ANOVA with Dunnett's post hoc test.

5.4.2 Apoptosis Induction in HPBFs and HPRFs

To test response to apoptosis apoptosis inducing agents, HPBFs and HPRFs were treated with hydrogen peroxide (H_2O_2) (1 mM) and staurosporine (1 μM) and then stained with acridine orange that will binds to DNA. Without treatment with these agents, HPBFs and HPRFs showed a flattened and spread appearance with bright green chromatin (**Figure 5.8A**). However, pronounced chromatin condensation were observed in > 90% of cells treated with H_2O_2 or staurosporine (**Figures 5.8A & 5.8B**).

Next, to determine whether CG and trypsin induced apoptosis in fibroblasts, HPBFs and HPRFs were treated with CG or trypsin for 24 h under serum free conditions. In the presence of CG, fibroblasts appeared as stellate shape and the cells lost cell-cell contacts (**Figure 5.9A**). CG induced apoptosis in both HPBFs and HPRFs in a concentration dependent fashion (**Figures 5.9B & 5.9C**). While 300 nM GC caused 22 ± 1.2% of HPBFs to become apoptotic and 42 ± 8.4% of HPRFs to become apoptotic, 600 nM CG induced 86 ± 1.5% and 85 ± 4.8% apoptosis in HPBFs and HPRFs, respectively (**Figures 5.9B & 5.9C**, blue bars). Pre-incubation of CG with 1 mM PMSF, a serine protease inhibitor, caused only minimal amounts of apoptotic cells (**Figures 5.9B & 5.9C**, red bars).

Treatment of HPBFs and HPRFs with trypsin also induced apoptosis in a dose-dependent manner (**Figure 5.10**). At 250 nM, trypsin induced a significant 73 ± 10% apoptosis in HPBFs and a significant 36 ± 7.4% apoptosis in HPRFs. When the concentration of trypsin was increased to 500 nM, 95 ± 2.7% and 66 ± 4.8% apoptotic cells were observed in HPBFs and HPRFs, respectively (**Figures 5.10B & 5.10C**, blue bars). This apoptosis-inducing activity of trypsin was significantly suppressed when it was pre-incubated with 1 mM PMSF before being added to the cells (**Figures 5.10B & 5.10C**, red bars).

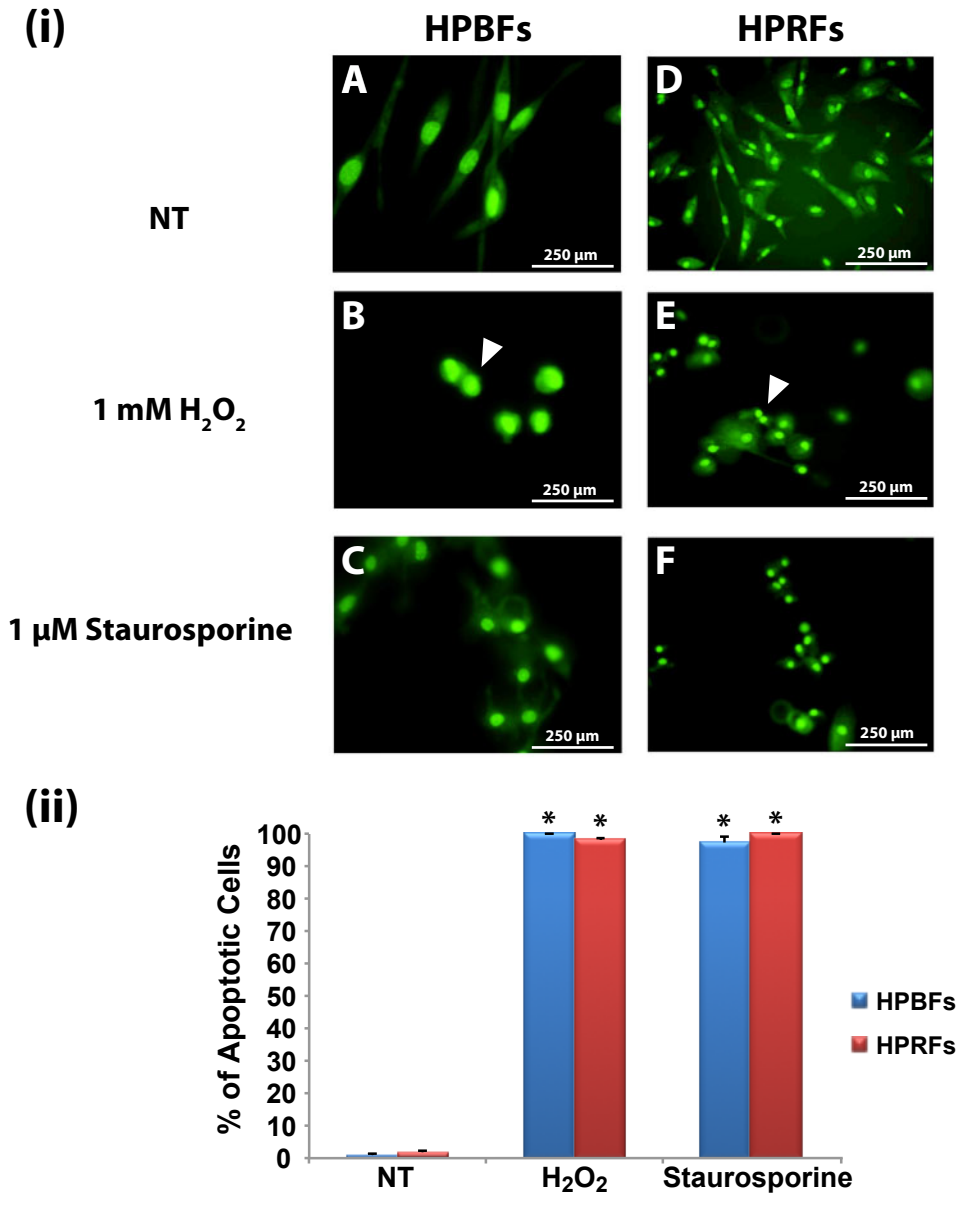
(i)
HPBFs
HPRFs
NT
1 mM H_2O_2
1 µM Staurosporine
A
B
C
D
E
F
250 µm
(ii)
% of Apoptotic Cells
100
90
80
70
60
50
40
30
20
10
0
NT
H_2O_2
Staurosporine
HPBFs
HPRFs

Figure 5.8: H_2O_2 and Staurosporine Induce Apoptosis in HPBFs and HPRFs. Cells at 70-85% confluence in 24-well plates were quiesced. Quiescent cells were then treated with different apoptosis inducers for 24 h. Then, acridine orange was added to the cells before visualising with fluorescent microscope. (i) HPBFs: (A) No treatment (NT); (B) H_2O_2 and (C) Staurosporine. HPRFs: (D) NT; (E) H_2O_2 and (F) Staurosporine. White arrowheads indicate apoptosis fibroblasts. Data shown are representative of six independent experiments. (ii) Apoptotic cells were quantified. Error bars represent mean ± SEM of six independent experiments. * indicates $p < 0.05$ compared to NT in one way ANOVA with Dunnett's post hoc test.

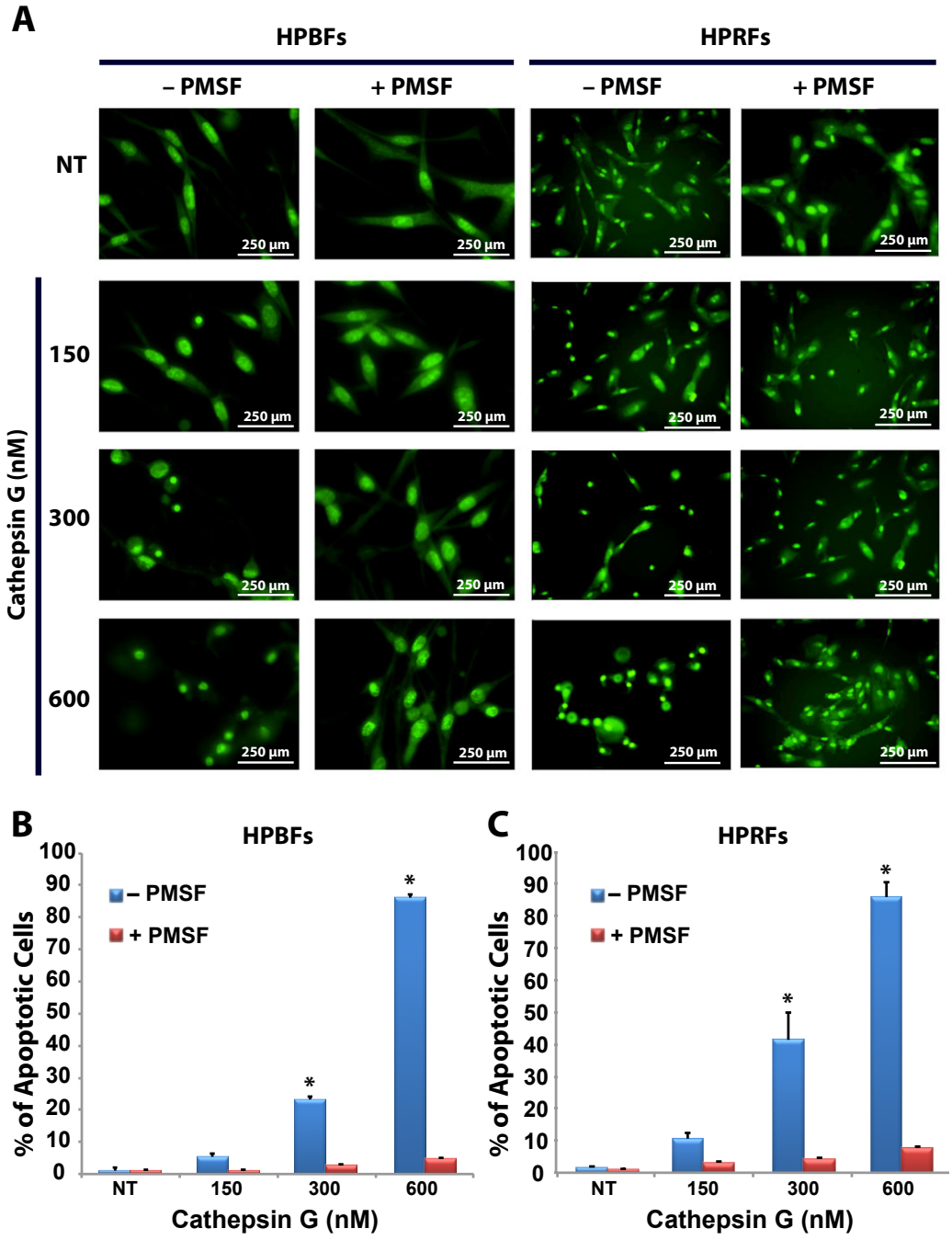
A
HPBFs
HPRFs
– PMSF
+ PMSF
– PMSF
+ PMSF
NT
150
300
600
Cathepsin G (nM)
250 µm
B
HPBFs
– PMSF
+ PMSF
% of Apoptotic Cells
Cathepsin G (nM)
NT
150
300
600
C
HPRFs
– PMSF
+ PMSF
% of Apoptotic Cells
Cathepsin G (nM)
NT
150
300
600

Figure 5.9: CG Induced Apoptosis in HPBFs and HPRFs in a Concentration Dependent Fashion. Cells at 70-85% confluence in 24-well plates were quiesced. Quiescent cells were then treated with different apoptosis inducers for 24 h. Then, acridine orange was added to the cells before visualising with fluorescent microscope. (A) HPBFs and HPRFs were treated with CG at various concentrations as indicated, either with or without pre-incubation with 1 mM PMSF. No CG was added in the untreated sample (NT). Pictures shown are representatives of six independent experiments. (B & C) Apoptotic cells were quantified. Error bars represent mean ± SEM of six independent experiments. * indicates $p < 0.05$ compared to NT in one way ANOVA with Dunnett's post hoc test.

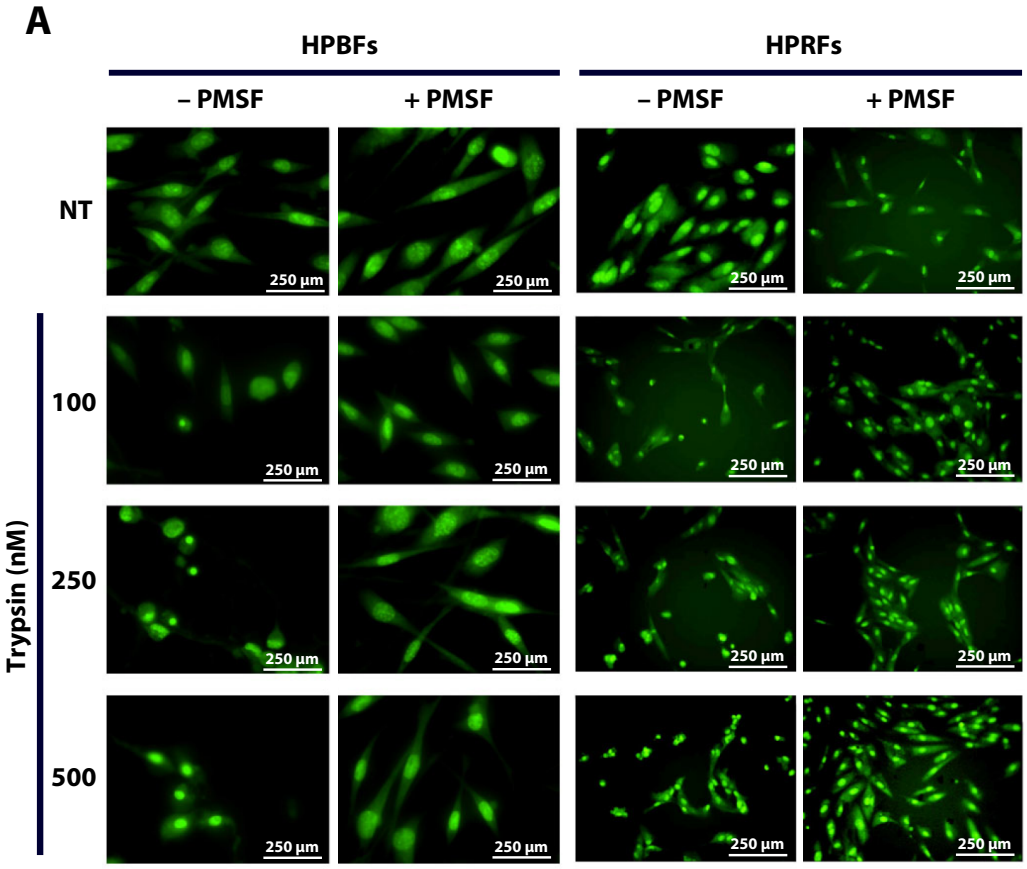
A
HPBFs
HPRFs
– PMSF
+ PMSF
– PMSF
+ PMSF
NT
100
250
500
Trypsin (nM)
250 µm

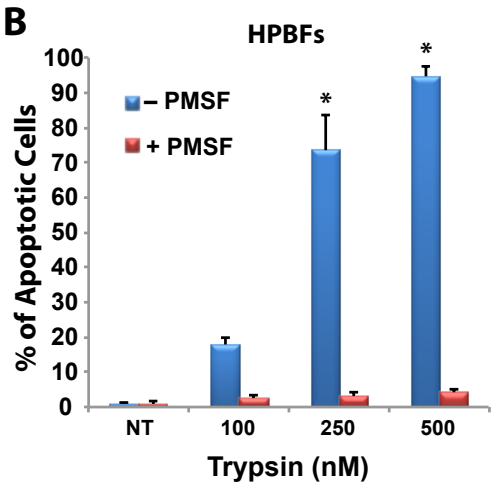
B
HPBFs
– PMSF
+ PMSF
% of Apoptotic Cells
0
10
20
30
40
50
60
70
80
90
100
NT
100
250
500
Trypsin (nM)
*

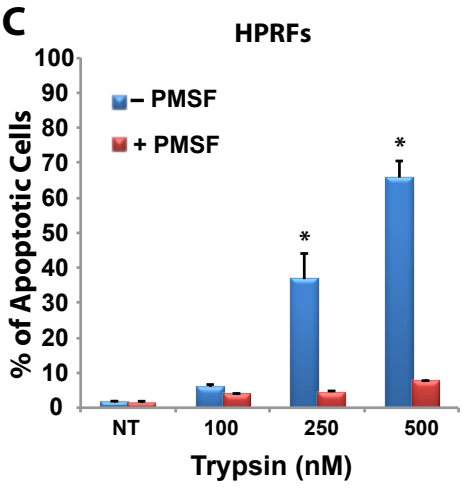
C
HPRFs
– PMSF
+ PMSF
% of Apoptotic Cells
0
10
20
30
40
50
60
70
80
90
100
NT
100
250
500
Trypsin (nM)
*

Figure 5.10: Trypsin Induced Apoptosis in HPBFs and HPRFs in a Concentration Dependent Fashion. Cells at 70-85% confluence in 24-well plates were quiesced. Quiescent cells were then treated with different apoptosis inducers for 24 h. Then, acridine orange was added to the cells before visualising with fluorescent microscope. (A) HPBFs and HPRFs were treated with trypsin at various concentrations as indicated, either with or without pre-incubation with 1 mM PMSF. No trypsin was added in the untreated sample (NT). Pictures shown are representatives of six independent experiments. (B & C) Apoptotic cells were quantified. Error bars represent mean ± SEM of six independent experiments. * indicates $p < 0.05$ compared to NT in one way ANOVA with Dunnett's post hoc test.

In order to confirm the induction of apoptosis, Western blot analysis was performed using antibodies specific to caspase-3 or cleaved caspase-3. During apoptosis, caspase-3 is cleaved into two active forms of caspase-3, the p17 and p19 forms ($\sim$17 or $\sim$19 kDa, respectively). The presence of these caspase-3 fragments in both HPBFs and HPRFs treated with H_2O_2, staurosporine, CG (**Figures 5.11 & 5.12**) or trypsin (**Figures 5.13, 5.14 & 5.15, 5.16**) indicates that apoptosis occurred in these samples. The intensities of cleaved caspase-3 bands increased when the concentrations of CG and trypsin increased. These cleaved caspase-3 fragments were not observed in the untreated sample and in the samples where CG and trypsin were pre-treated with PMSF (**Figures 5.11, 5.12, 5.13, 5.14 & 5.15, 5.16**).

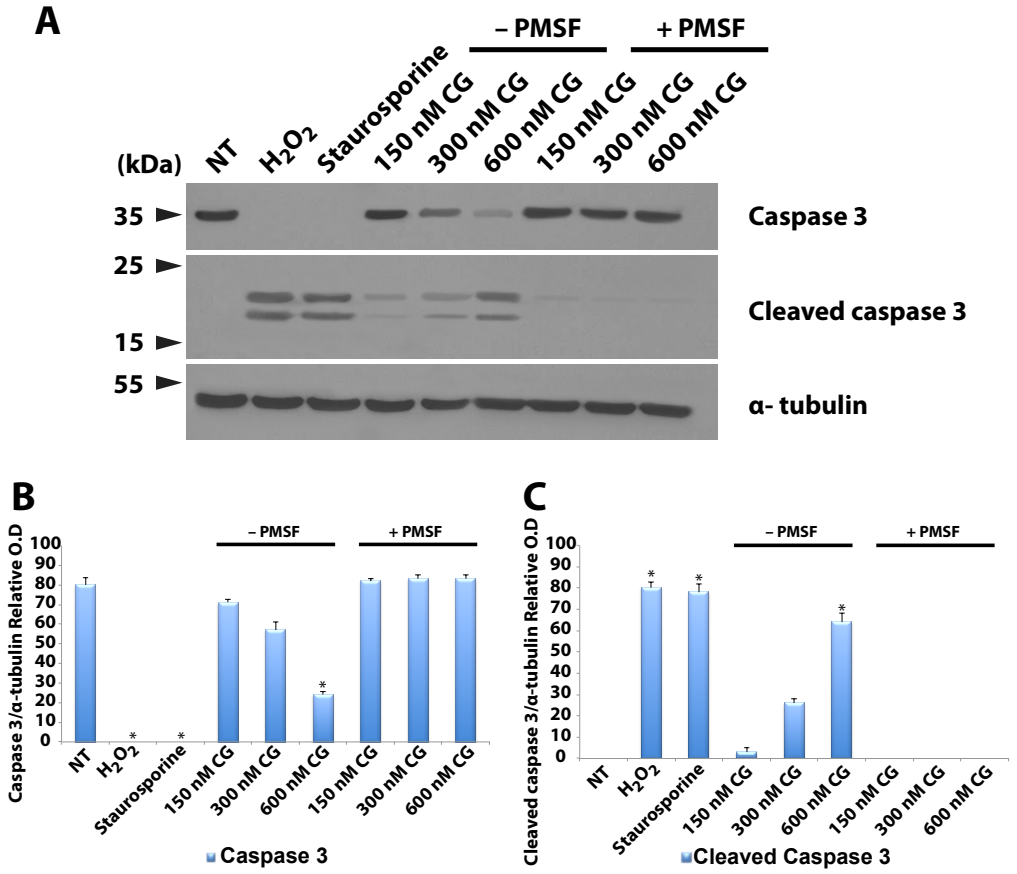

Figure 5.11: Cleaved Caspase-3 Fragments were Detected in Bronchial Fibroblasts Treated with CG. Quiescent cells were treated with different apoptosis inducers for 24 h. Cell lysates were obtained and then subjected to SDS-PAGE followed by immunoblotting with antibodies against caspase-3 and cleaved caspase-3. (A) HPBFs were treated with 1 mM H_2O_2, 1 μM staurosporine or various indicated concentrations of CG (with or without 1 mM PMSF pre-treatment). None of these agents were added in the untreated sample (NT). α-tubulin was used as a loading control. Expected band sizes: caspase-3 $\sim$35 kDa, cleaved caspase-3 $\sim$17 kDa and $\sim$19 kDa, and α-tubulin $\sim$52 kDa. (B) Results were quantitated and summarised in a bar chart, where optical densities were normalised to α-tubulin loading controls. Results are expressed as mean $\pm$ SEM of three independent experiments. * indicates $p < 0.05$ compared with NT in one way ANOVA with Dunnett's post hoc test.

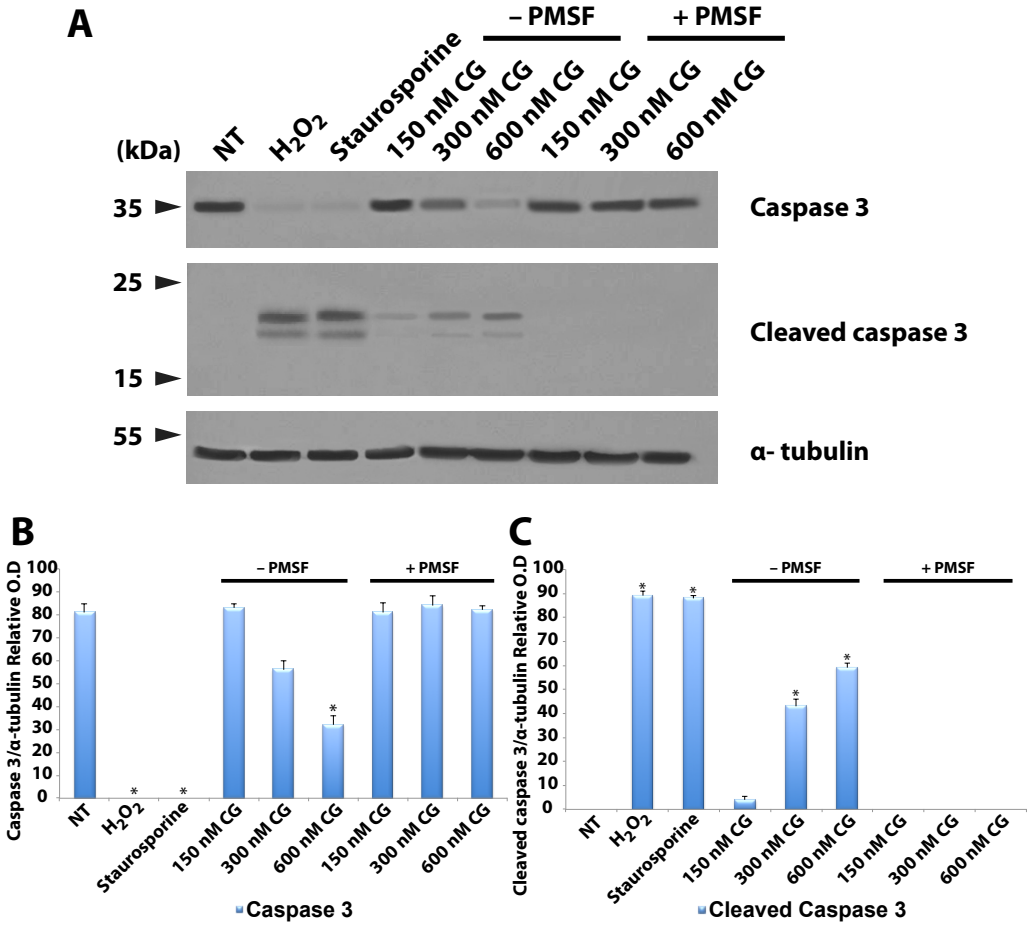

Figure 5.12: Cleaved Caspase-3 Fragments were Detected in Renal Fibroblasts Treated with CG. Quiescent cells were treated with different apoptosis inducers for 24 h. Cell lysates were obtained and then subjected to SDS-PAGE followed by immunoblotting with antibodies against caspase-3 and cleaved caspase-3. (A) HPRFs were treated with 1 mM H_2O_2, 1 μM staurosporine or various indicated concentrations of CG (with or without 1 mM PMSF pre-treatment). None of these agents were added in the untreated sample (NT). α-tubulin was used as a loading control. Expected band sizes: caspase-3 $\sim$35 kDa, cleaved caspase-3 $\sim$17 kDa and $\sim$19 kDa, and α-tubulin $\sim$52 kDa. (B) Results were quantitated and summarised in a bar chart, where optical densities were normalised to α-tubulin loading controls. Results are expressed as mean $\pm$ SEM of three independent experiments. * indicates $p < 0.05$ compared with NT in one-way ANOVA with Dunnett's post hoc test.

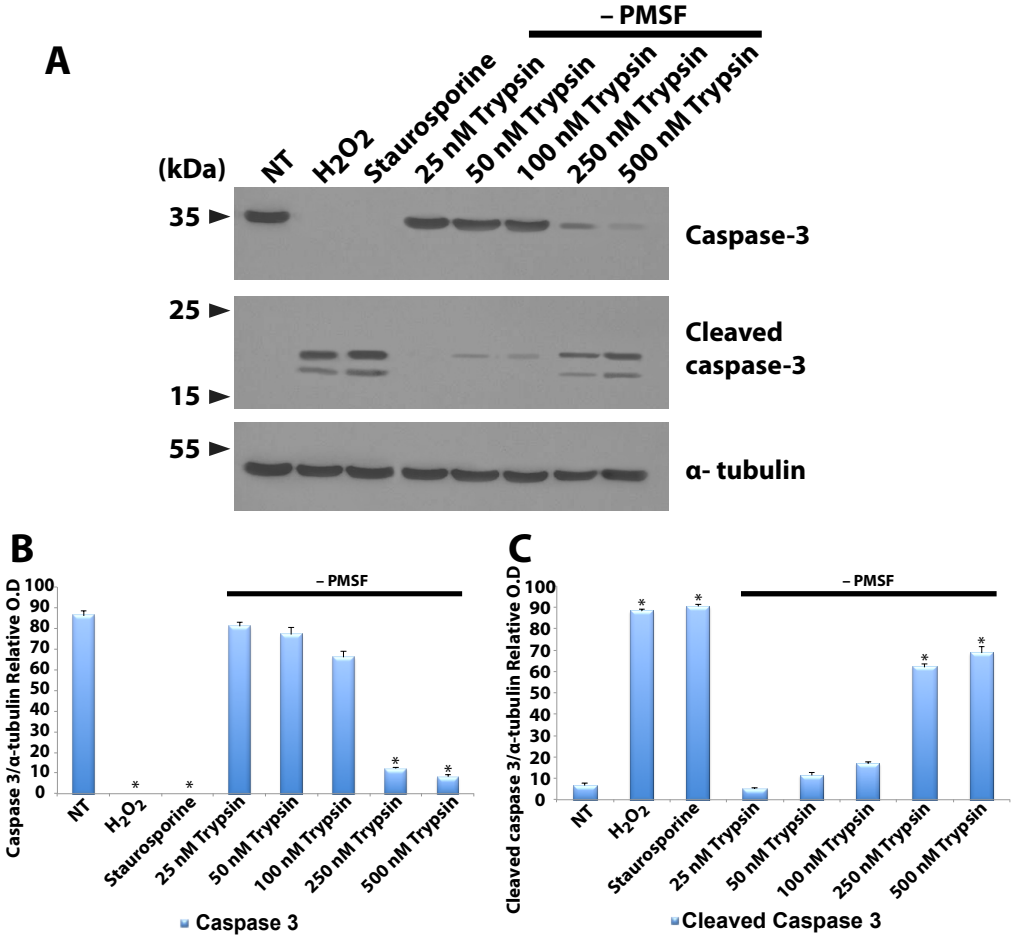

Figure 5.13: Cleaved Caspase-3 Fragments were Detected in Bronchial Fibroblasts Treated with Trypsin. Quiescent cells were treated with different apoptosis inducers for 24 h. Cell lysates were obtained and then subjected to SDS-PAGE followed by immunoblotting with antibodies against caspase-3 and cleaved caspase-3. (A) HPBFs were treated with 1 mM H_2O_2, 1 μM staurosporine or various indicated concentrations of trypsin. None of these agents were added in the untreated sample (NT). α-tubulin was used as a loading control. Expected band sizes: caspase-3 $\sim$35 kDa, cleaved caspase-3 $\sim$17 kDa and $\sim$19 kDa, and α-tubulin $\sim$52 kDa. (B & C) Results were quantitated and summarised in a bar chart, where optical densities were normalised to α-tubulin loading controls. Results are expressed as mean $\pm$ SEM of three independent experiments. * indicates $p < 0.05$ compared with NT in one-way ANOVA with Dunnett's post hoc test.

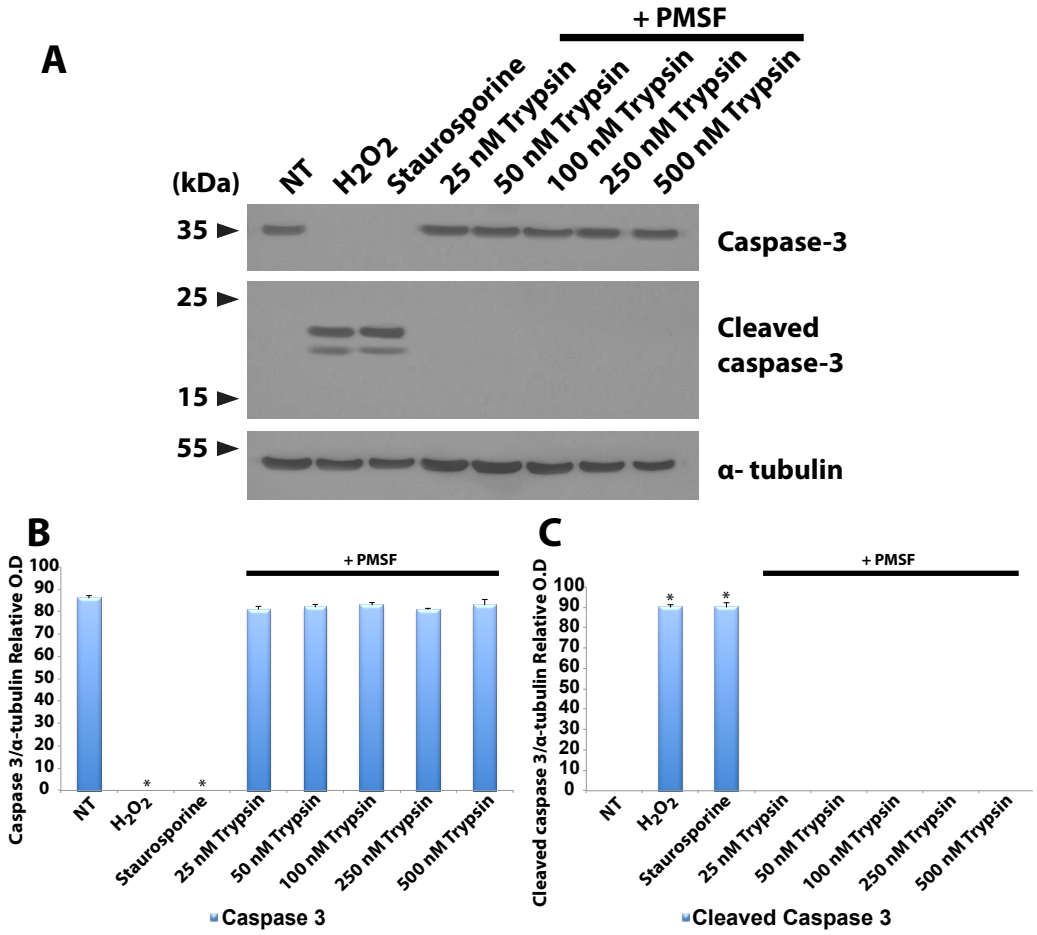

Figure 5.14: No Cleaved Caspase-3 Fragments were Detected in Bronchial Fibroblasts Treated with Trypsin Pretreated with PMSF. Quiescent cells were treated with different apoptosis inducers for 24 h. Cell lysates were obtained and then subjected to SDS-PAGE followed by immunoblotting with antibodies against caspase-3 and cleaved caspase-3. (A) HPBFs were treated with 1 mM H_2O_2, 1 μM staurosporine or various indicated concentrations of trypsin where trypsin was pre-treated with 1 mM PMSF. None of these agents were added in the untreated sample (NT). α-tubulin was used as a loading control. Expected band sizes: caspase-3 $\sim$35 kDa, cleaved caspase-3 $\sim$17 kDa and $\sim$19 kDa, and α-tubulin $\sim$52 kDa. (B & C) Results were quantitated and summarised in a bar chart, where optical densities were normalised to α-tubulin loading controls. Results are expressed as mean $\pm$ SEM of three independent experiments. * indicates $p < 0.05$ compared with NT in one-way ANOVA with Dunnett's post hoc test.

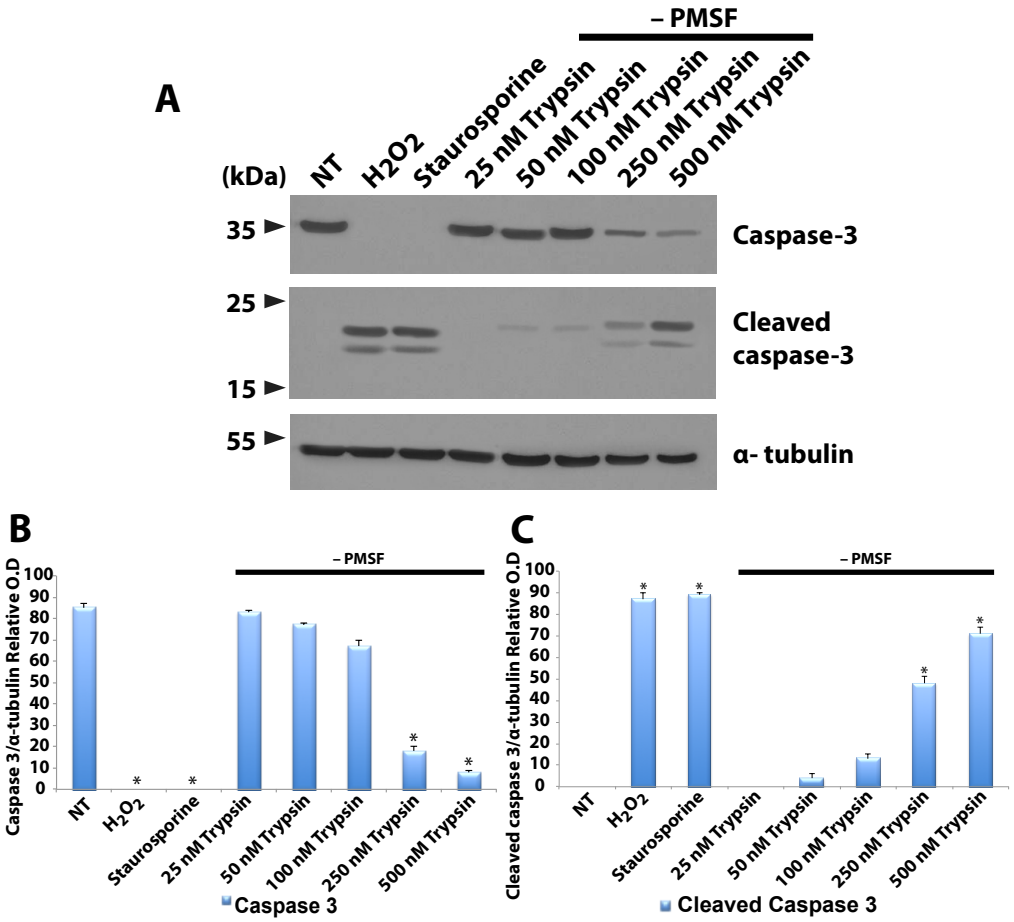

Figure 5.15: Cleaved Caspase-3 Fragments were Detected in Renal Fibroblasts Treated with Trypsin. Quiescent cells were treated with different apoptosis inducers for 24 h. Cell lysates were obtained and then subjected to SDS-PAGE followed by immunoblotting with antibodies against caspase-3 and cleaved caspase-3. (A) HPRFs were treated with 1 mM H_2O_2, 1 μM staurosporine or various indicated concentrations of trypsin. None of these agents were added in the untreated sample (NT). α-tubulin was used as a loading control. Expected band sizes: caspase-3 $\sim$35 kDa, cleaved caspase-3 $\sim$17 kDa and $\sim$19 kDa, and α-tubulin $\sim$52 kDa. (B & C) Results were quantitated and summarised in a bar chart, where optical densities were normalised to α-tubulin loading controls. Results are expressed as mean $\pm$ SEM of three independent experiments. * indicates $p < 0.05$ compared with NT in one-way ANOVA with Dunnett's post hoc test.

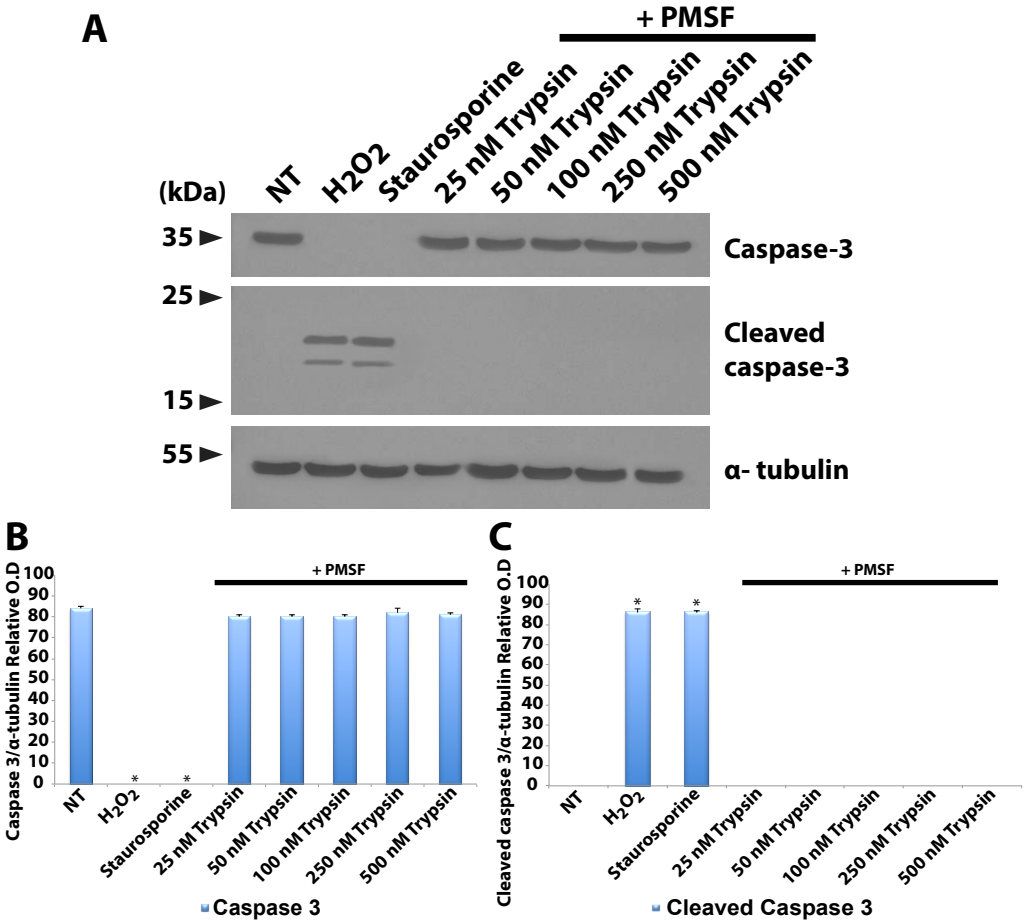

Figure 5.16: No Cleaved Caspase-3 Fragments were Detected in Renal Fibroblasts Treated with Trypsin Pretreated with PMSF. Quiescent cells were treated with different apoptosis inducers for 24 h. Cell lysates were obtained and then subjected to SDS-PAGE followed by immunoblotting with antibodies against caspase-3 and cleaved caspase-3. (A) HPRFs were treated with 1 mM H_2O_2, 1 μM staurosporine or various indicated concentrations of trypsin where trypsin was pre-incubated with 1 mM PMSF. None of these agents were added in the untreated sample (NT). α-tubulin was used as a loading control. Expected band sizes: caspase-3 $\sim$35 kDa, cleaved caspase-3 $\sim$17 kDa and $\sim$19 kDa, and α-tubulin $\sim$52 kDa. (B & C) Results were quantitated and summarised in a bar chart, where optical densities were normalised to α-tubulin loading controls. Results are expressed as mean $\pm$ SEM of three independent experiments. * indicates $p < 0.05$ compared with NT in one-way ANOVA with Dunnett's post hoc test.

5.4.3 Apoptosis Induction in HEK-PAR$_4$ Cells

Acridine orange staining is suboptimal for use with empty vector control and HEK-PAR$_4$ cells to detect apoptotic cells as some cells did not contain a recognisable nucleus and only the cytoplasm was stained by acridine orange (**Figure 5.17**). Therefore, FITC-Annexin-V staining using flow cytometry was used to detect apoptosis in empty vector control and HEK-PAR$_4$ cells. **Figure 5.18** shows representative flow cytometry dot-plots of FITC-Annexin V (FL1)/ propidium iodide (PI) (FL2) dual colour flow cytometry.

HEK-PAR$_4$ cells were used to investigate whether PAR$_4$ activation triggered apoptosis in the presence of PAR$_4$ AP and CG. First, as positive controls for determination of apoptotic index using this FITC-Annexin V flow cytometry assay, empty vector control and HEK-PAR$_4$ cells were treated with H_2O_2 and staurosporine. Results showed that >70% of apoptotic cells were detected in these samples (**Figure 5.19A**, $p<0.05$). After 24 h treatment with PAR$_4$ AP, the amounts of apoptotic cells in empty vector control and HEK-PAR$_4$ samples were 6 ± 0.35% and 41 ± 2%, respectively (**Figure 5.19B**). 20 nM CG induced 16% apoptotic cells in both empty vector control and HEK-PAR$_4$ cells. When treated with 300 nM CG, the numbers of apoptotic cells doubled to 30 ± 9.25% and 29 ± 4.7% in empty vector control and HEK-PAR$_4$ cells, respectively. It is statistically significant compared to the untreated sample. Blocking the CG activity with PMSF reduced apoptosis to less than 10% in both empty vector control and HEK-PAR$_4$ cells.

To further confirm these results, Western blot analysis was performed using caspase-3 and cleaved caspase-3 antibodies. The presence of the bands corresponding to cleaved caspase-3 fragments indicates that the cells underwent apoptosis (**Figures 5.20 & 5.21**).

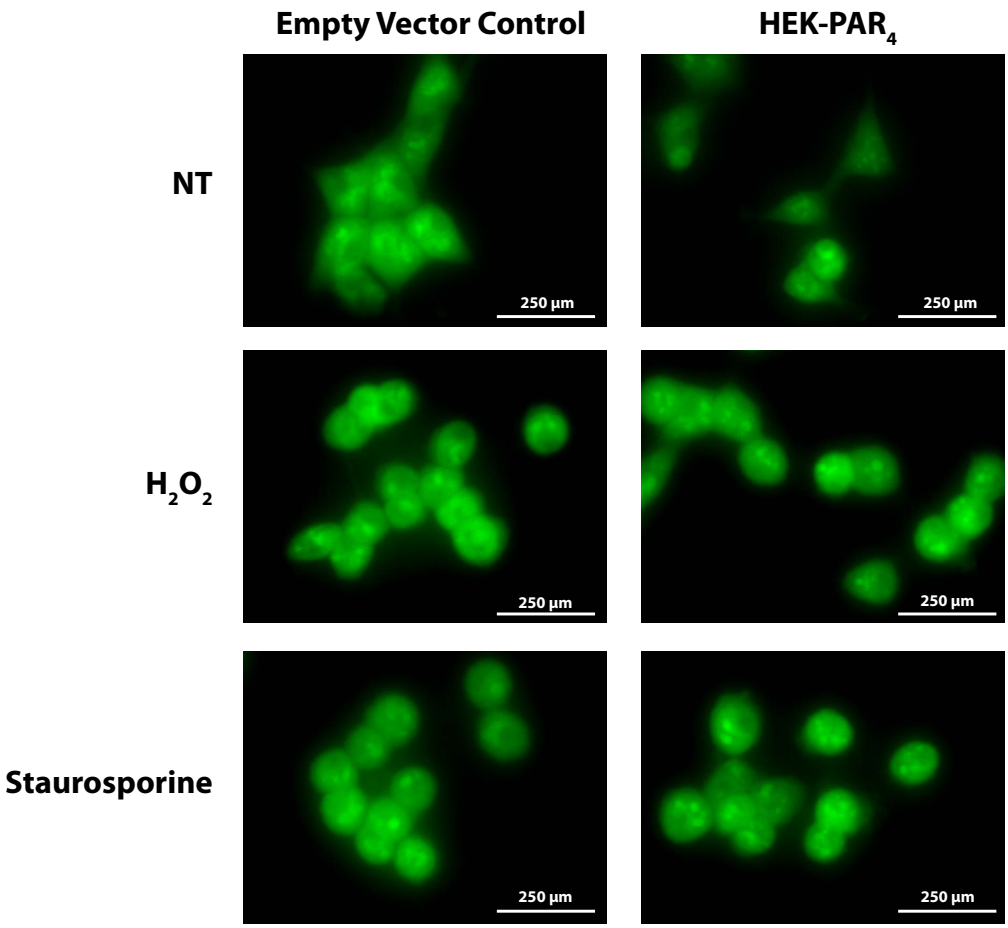

Figure 5.17: HEK-PAR$_4$ Cells Treated with H_2O_2 and Staurosporine in Acridine Orange Apoptosis Assay. Cells at 70-85% confluence in 24-well plates were quiesced. Quiescent cells were then treated with different apoptosis inducers for 24 h. Then, acridine orange was added to the cells before visualising with fluorescent microscope. Empty vector control or HEK-PAR$_4$ cells were treated with 1 mM H_2O_2 or 1 μM Staurosporine. No H_2O_2 or staurosporine was added in the untreated samples (NT). Results are representative of three independent experiments.

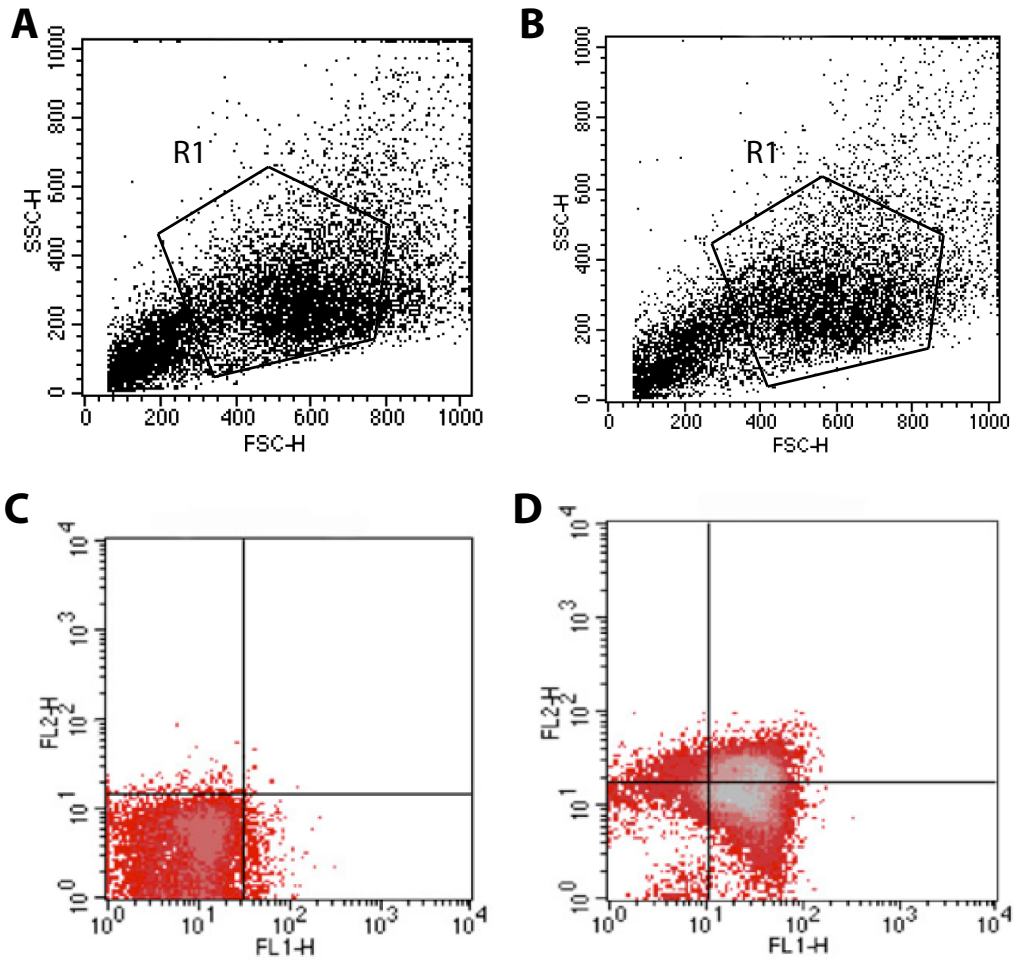

Figure 5.18: Representative Flow Cytometry Dot-plots of FITC-Annexin V (FL1)/ PI (FL2) Dual Colour Flow Cytometry. Cells at 70-85% confluence in 6-well plate were quiesced and treated with different apoptosis inducers for 24 h. The cells were then incubated with FITC-conjugated Annexin V and propidium iodide in the dark. Binding of Annexin V/PI to empty vector control and HEK-PAR_4 cells that were exposed to different apoptosis inducers were evaluated by flow cytometry. (A) Untreated empty vector control. (B) Empty vector control was treated with 1 mM H_2O_2 for 24 h. (C & D) Cells depicted in lower quadrants showed intact cytoplasmic membrane integrity (PI-negative), where the bottom left quadrant (Annexin V-negative) represents viable cells and the bottom right quadrant (Annexin V-positive) represents apoptotic cells. Cells depicted in the top left (Annexin V-negative/PI positive) and top right (Annexin V-positive/PI-positive) quadrants represent necrotic and late apoptotic cells, respectively.

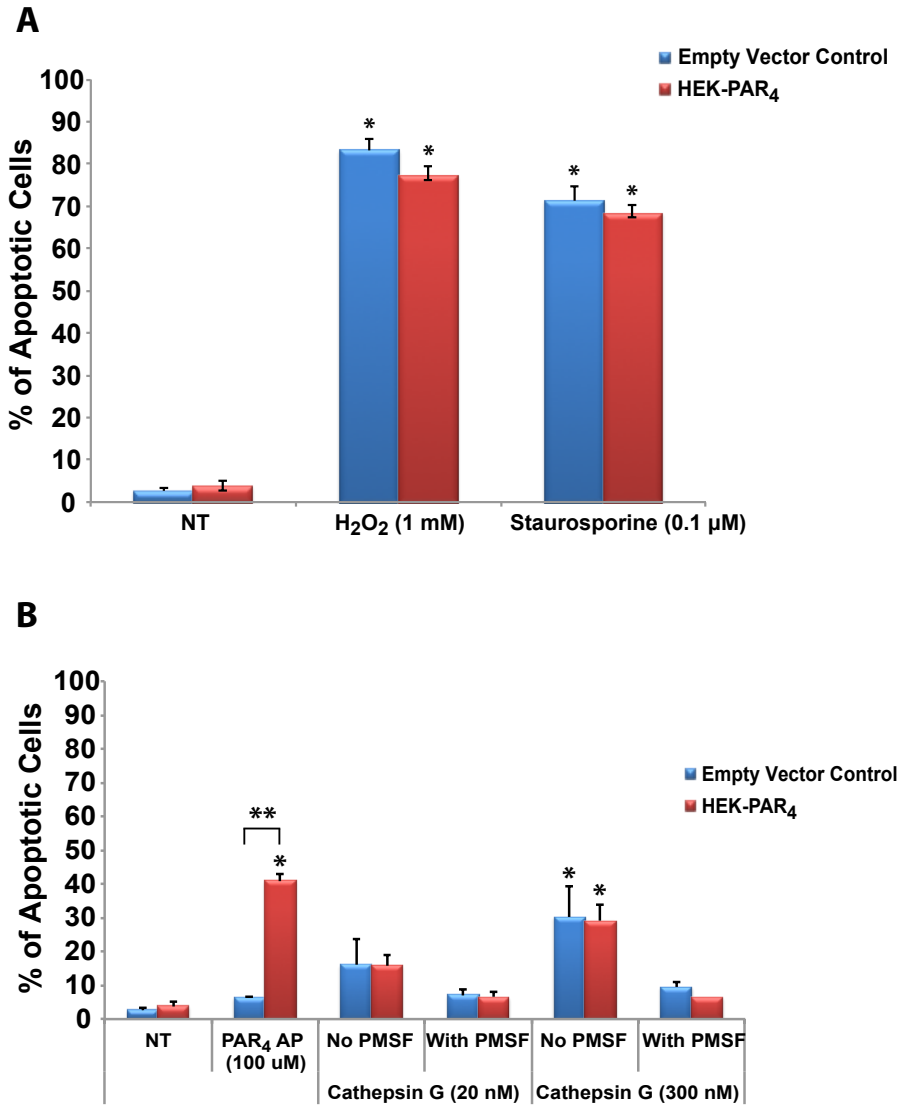

Figure 5.19: Summary of Annexin V Apoptosis Assay. (A) Empty vector control and (B) HEK-PAR_4 cells were treated with H_2O_2, Staurosporine, PAR_4-AP or CG. Results are expressed as percentage of apoptotic cells, presented as the mean ± SEM of five independent experiments. * indicates $p < 0.05$ compared with NT in one way ANOVA with Dunnett's post hoc test. ** indicates $p < 0.05$ between empty vector control and HEK-PAR_4 cells in one way ANOVA with Bonferroni post hoc test.

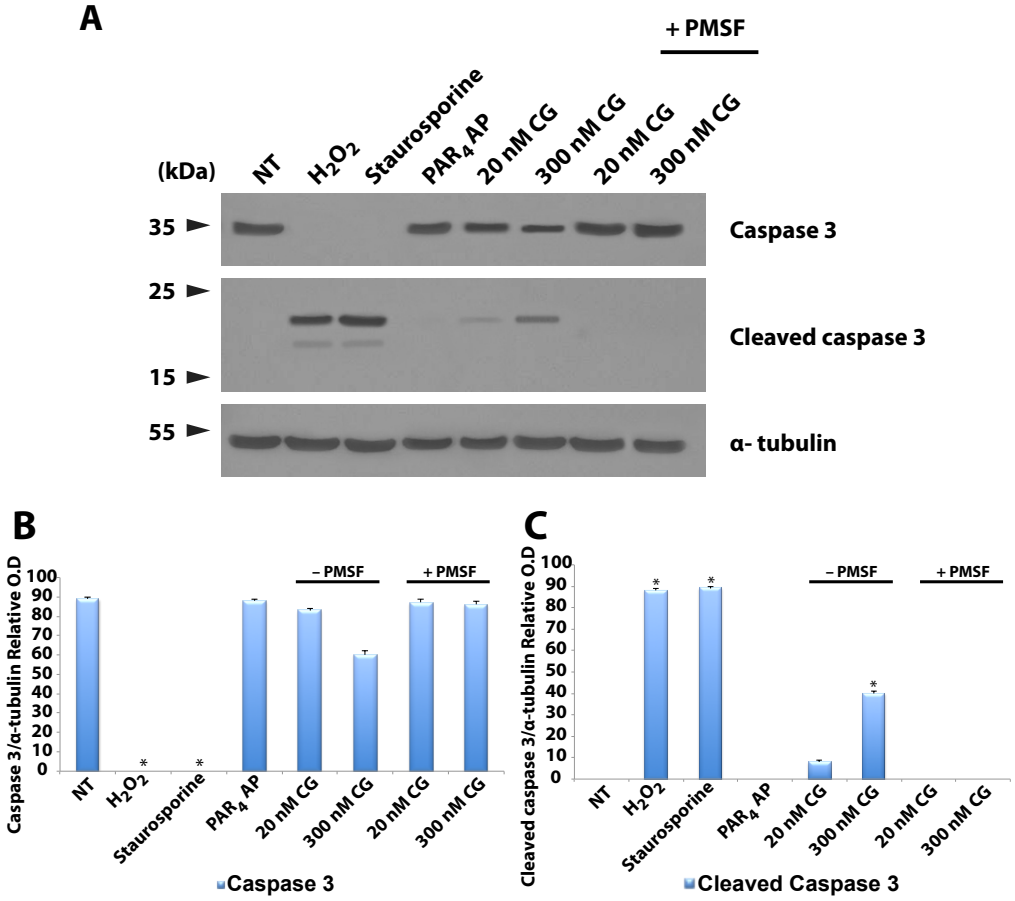

Figure 5.20: Cleaved Caspase-3 Fragments were Detected by Western Blotting in CG treated Empty Vector Control. Quiescent cells were treated with different apoptosis inducers for 24 h. Cell lysates were obtained and then subjected to SDS-PAGE followed by immunoblotting with antibodies against caspase-3 and cleaved caspase-3. Empty vector controls were treated with 1 mM H_2O_2, 1 μM staurosporine, 100 μM PAR_4 AP or 20 nM and 300 nM CG (with or without 1 mM PMSF pre-treatment). None of these agents were added in the untreated samples (NT). α-tubulin was used as a loading control. Expected band sizes: caspase-3 ($\sim$35 kDa), cleaved caspase-3 ($\sim$17 kDa and 19 kDa) and α-tubulin ($\sim$52 kDa). (B) Results were quantitated and summarised in a bar chart, where optical densities were normalised to α-tubulin loading controls. Results are expressed as mean $\pm$ SEM of two independent experiments. * indicates $p < 0.05$ compared with NT in one-way ANOVA with Dunnett's post hoc test.

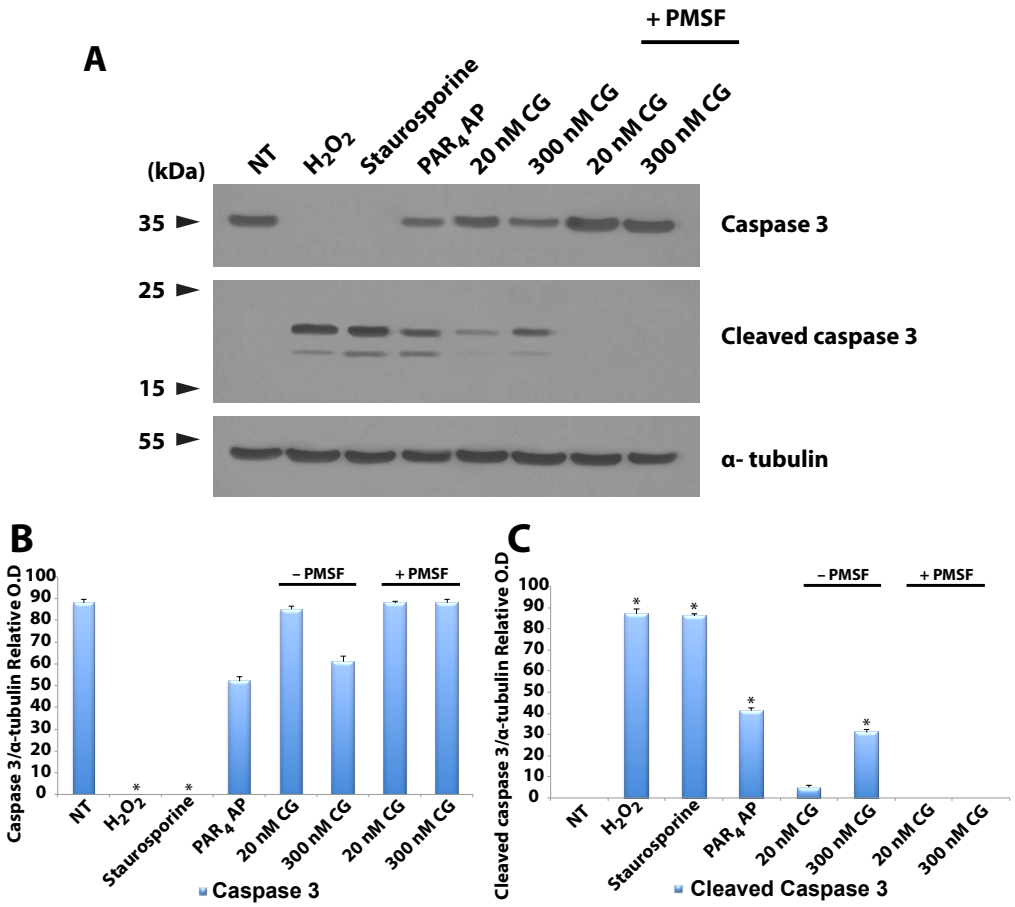

Figure 5.21: Cleaved Caspase-3 Fragments were Detected by Western Blotting in PAR_4 AP and CG treated HEK-PAR_4 Cells. Quiescent cells were treated with different apoptosis inducers for 24 h. Cell lysates were obtained and then subjected to SDS-PAGE followed by immunoblotting with antibodies against caspase-3 and cleaved caspase-3. (A) HEK-PAR_4 cells were treated with 1 mM H_2O_2, 1 μM staurosporine, 100 μM PAR_4 AP or 20 nM and 300 nM CG (with or without 1 mM PMSF pre-treatment). None of these agents were added in the untreated samples (NT). α-tubulin was used as a loading control. Expected band sizes: caspase-3 ($\sim$35 kDa), cleaved caspase-3 ($\sim$17 kDa and 19 kDa) and α-tubulin ($\sim$52 kDa). (B) Results were quantitated and summarised in a bar chart, where optical densities were normalised to α-tubulin loading controls. Results are expressed as mean $\pm$ SEM of two independent experiments. * indicates $p < 0.05$ compared with NT in one-way ANOVA with Dunnett's post hoc test.

5.5 Discussion

Apoptosis is a precisely regulated physiological form of cell death that leads to the elimination of intact cells by phagocytes without causing tissue injury (Savill, 1994). The pathogenesis of fibrosis might involve apoptotic defects. Wound healing and resolution of tissue injury are associated with apoptosis of activated fibroblasts and myofibroblasts, while tissue scarring and fibrosis are associated with an inappropriate decrease in apoptosis of these cells (Desmoulière *et al.*, 1995).

Serine proteases degrade proteins through their ability to catalyse the hydrolysis of covalent peptide bonds. The discovery of the PARs revealed a new intracellular signalling role for serine proteases that is in addition to their degradation function, provided new insight into the study of PARs (Russell *et al.*, 2010). Several experimental animal models demonstrated the importance of neutrophils in initiation and maintenance of the inflammatory response. Depletion of neutrophils abrogates inflammation in experimental arthritis (Wipke and Allen, 2001; Tanaka *et al.*, 2006), chronic inflammatory lung diseases (Park *et al.*, 2006; Chua *et al.*, 2007), and tissue damage following ischemia/reperfusion injury (Sisley *et al.*, 1994; Shimoda *et al.*, 2007). In patients with cystic fibrosis, the levels of CG and elastase are greatly increased (Sommerhoff *et al.*, 1990). These findings suggest a potential role for CG and trypsin in generating the pathologic manifestations of fibrosis. Trypsin is known to activate PAR_2 (Nystedt *et al.*, 1995) and PAR_4 (Xu *et al.*, 1998). Both HPBFs and HPRFs expressed PAR_2 while PAR_4 expression could be upregulated when HPBFs were stimulated with pro-inflammatory cytokines (see **Section 3.4.2**, Ramachandran *et al.*, 2007). PAR_4 is thought to be involved in pro-inflammatory responses (Vergnolle *et al.*, 2002; Ando *et al.*, 2007b). A greater understanding of PAR_4 activation and the ultimate downstream signalling pathways could reveal targets for the treatment of inflammatory diseases.

In PAR_4 functional studies using calcium mobilisation assay, PAR_4 activation by PAR_4 AP results in brisk rise in intracellular calcium, whereas CG stimulation does not affect intracellular calcium. In addition, CG does not activate PAR_4 in A549 cells which endogenously express PAR_4. These differences in the effect of PAR_4 AP versus CG suggest that CG might not contribute to the proteolytic cleavage of PAR_4. As the concentration, temperature and incubation time potentially affect the action of CG, various concentrations, temperatures and incubation times were tested. All results showed no calcium response (See **Appendix**). The experimental evidence implicating PAR_4 cleavage as the mechanism mediating CG actions is more tenuous and direct evidence that CG cleaves PAR_4 has never been reported. Furthermore, Cumashi *et al.* (2001) demonstrated that CG did not trigger aggregation in murine platelets and Sabri *et al.* (2003b) also demonstrated that human PAR_4 conferred responsiveness to thrombin and PAR_4 AP but not to CG. These studies and experimental data reported herein demonstrate that CG acts independently of PAR_4. Together this suggests that CG does not proteolytically activate PAR_4.

Interestingly, the results presented here indicate that CG might inhibit, rather than activate, PAR_4. When the cells pretreated with CG before the addition of PAR_4 AP, the amplitude of the calcium response to PAR_4 AP was reduced. Also, when CG was pretreated with 1 mM PMSF (as shown in **Figure 5.3**, CG (300 mM) action was completely blocked using 1 mM PMSF), the magnitude of the calcium responses were similar to those observed when PAR_4 AP alone was added. Furthermore, in order to investigate whether the reduced calcium response was due to the cleavage of PAR_4 AP by CG, PAR_4 AP and CG were mixed together before performing the calcium assay. Results obtained were similar to the observation when PAR_4 AP and CG were added sequentially, indicating that CG did not cleave PAR_4 AP. Hence, the inhibiting action of CG on HEK-PAR_4 and

A549 cells suggests that CG might cleave at a secondary site within the ECL2 domain of PAR_4, causing PAR_4 to be unresponsive to the PAR_4 AP.

In contrast, Sambrano *et al.* (2000) demonstrated that CG could activate PAR_4 in human platelets and lead to platelet aggregation. The differences in CG responses between the findings presented in this chapter and Sambrano *et al.* (2000) might be due to the cell specific differences in post-translational processing of PAR_4, such as phosphorylation and glycosylation. Although it is currently unclear if glycosylation happens to and affects PAR_4. It is known that the N-linked glycosylation of a receptor may regulate conformation, folding or stability, as well as protect the receptor from proteolytic degradation (Xiao *et al.*, 2011). N-linked glycosylation in ECL2 is important for optimal receptor cell surface expression, receptor stability and function (Xiao *et al.*, 2011). The extent of glycosylation of a receptor could influence the receptor activation. Nakayama *et al.* (2003) demonstrated that trypsin was able to cleave PAR_1 but did not activate PAR_1 in the endothelial cells, whereas Xiao *et al.* (2011) demonstrated that trypsin could activate PAR_1 in epithelial cells. This difference could be explained by the different extent of glycosylation of PAR_1 in different cell types. PAR_1 expressed in platelets and endothelial cells is not heavily glycosylated (Brass *et al.*, 1992), whereas PAR_1 expressed in epithelial cells is highly glycosylated (Xiao *et al.*, 2011).

Data obtained here suggest that CG does not activate PAR_4 in this HEK-PAR_4 cell line. Instead, the observation that CG-treated cells elicit a reduced signalling response to the stimulatory action of PAR_4 AP suggests that CG might inhibit PAR_4, at least in these HEK-PAR_4 cells. Thus, further studies are required to investigate if CG cleaves PAR_4 at another site to cause the inhibition. This could be done by first identify the other possible CG cleavage sites and then test the effects of mutations to these

sites. As discussed above, PAR activation can also be regulated by glycosylation, thus it would be interesting to study the effect of glycosylation in PAR_4 function.

This chapter also attempts to examine whether CG and trypsin could induce fibroblast cell death. After 24 h treatment with CG and trypsin, fibroblasts showed a reduction in size, progressive loss of cell-cell contacts and detachment from the plates. The addition of progressively higher concentrations of CG and trypsin to fibroblasts produced an increase in the percentage of apoptotic cells, suggesting that both CG and trypsin can induce apoptosis in HPBFs and HPRFs. The serine protease inhibitor PMSF partly interferes with the interaction of CG and trypsin with the receptor by specifically binds to their serine residues (Yamazaki and Aoki, 1997). When CG and trypsin were pre-treated with PMSF, the number of apoptotic cells dramatically reduced. The inhibitory effect of PMSF on fibroblast apoptosis in the presence of CG and trypsin suggests that the active catalytic site of the proteases is required for triggering apoptosis. These results were further supported by the observation of caspase-3 cleavage (an indication of apoptotic event) using Western blotting. This study is comparable to the study demonstrated by Sabri *et al.* (2003b). They demonstrated that CG can trigger detachment-induced apoptosis (anoikis) and activate caspase-3 in cardiomyctes. In addition, Ramachandran *et al.* (2007) demonstrated CG reduced cell number in TNF-α-treated HPBF where PAR_4 was induced.

Some proteases from the circulation, exocrine glands and inflammatory cells can cleave PARs and thereby regulate inflammation, healing, pain and homeostasis (Cottrell *et al.*, 2004). During inflammation, both CG and PAR_4 can be up-regulated by pro-inflammatory mediators (Sommerhoff *et al.*, 1990; Owen *et al.*, 1995; Ramachandran *et al.*, 2007). Hence, the second aim of this chapter was to examine if CG and PAR_4 AP could

induce apoptosis in HEK-PAR_4 cells when PAR_4 is activated. The acridine orange assay did not reliably identify apoptosis in empty vector control and HEK-PAR_4 cells (see **Figure 5.17**). Therefore, FITC-Annexin V flow cytometry was performed. The apoptotic cells were assessed by the binding of Annexin V to the phosphatidylserine (PS) exposed on the cell membrane. Annexin V is a calcium ion dependent phospholipid binding protein that has a high affinity for PS and binds to cells with exposed PS. It is conjugated to FITC and thus serves as a sensitive probe for flow cytometric analysis of cells that are undergoing apoptosis. The loss of cell membrane phospholipid asymmetry during early phases of apoptosis is accompanied by exposure of PS to the outer membrane. The movement of PS to the extracellular membrane surface is a characteristic event of cells undergoing apoptosis. As the externalisation of PS occurs in the earlier stages of apoptosis, FITC-Annexin V staining can identify apoptosis at an earlier stage than the other assays based on the nuclear changes such as DNA fragmentation (Rieger *et al.*, 2011). FITC-Annexin V staining is typically used in conjunction with PI to allow identification of early apoptotic cells (Annexin V positive, PI negative). Cells negative for both PI and Annexin V staining are viable cells; PI-negative and Annexin V-positive cells are early apoptotic cells; PI-positive and Annexin V-negative cells are necrotic cells; whereas PI-positive and Annexin V-positive cells are primarily cells in late stages of apoptosis (Rieger *et al.*, 2011).

An apoptosis assay was performed to test if CG triggers apoptosis via PAR_4 signalling. The percentage of apoptotic cells induced by CG is concentration dependent (see **Appendix, Figure A.6**), where the numbers of apoptotic cells increased as the concentrations of CG were increased from 20 nM to 600 nM. However, there is no significant difference in the numbers of apoptotic cells between empty vector control and HEK-PAR_4 cells following treatment with 20 or 300 nM CG (**Figure 5.19**). This effect of CG is dependant on CG activity, as pre-treatment of

CG with PMSF reduced the numbers of apoptotic cells. However, activation of PAR_4 with PAR_4 AP induced higher level of apoptosis in HEK-PAR_4 cells (41%), whereas only 6% apoptotic cells were observed in the PAR_4 AP-treated empty vector control cells. Together, these results suggest that CG induces apoptosis independently of PAR_4.

It was hypothesised that in fibrosis, enhancement of fibroblast apoptosis is beneficial to the host. The results presented above suggest that CG, trypsin and PAR_4 AP have the potential to induce cell death. Importantly, this study provides the first evidence that CG can act as a potent apoptosis inducer in human cultured lung and renal fibroblasts. Results obtained here also suggest that CG induces apoptosis independently of PAR_4. As HPBFs, HPRFs, and HEK-PAR_4 cells all express PAR_1 and PAR_2, CG might act on the other PARs or via another mechanism to induce fibroblast apoptosis. Thus, this suggests that CG and trypsin might help in tissue repair by triggering fibroblast cell death during inflammatory without PAR_4 expression. In contrast, PAR_4 AP induced a pronounced apoptosis in HEK-PAR_4 cells compared to the empty vector control, indicating a PAR_4-dependent apoptosis signalling pathway exists.

In conclusion, the results presented here suggest that CG and trypsin can induce fibroblasts apoptosis independently of PAR_4 and PAR_4 AP can trigger apoptosis in HEK-PAR_4 cells via PAR_4 signalling pathway. The local release of CG and trypsin in areas of inflammation may help tissue remodelling by triggering fibroblast cell death without PAR_4 expression. Although LPS failed to consistently induce PAR_4 expression in bronchial fibroblasts as demonstrated in chapter 3, it is still possible that bronchial fibroblasts express PAR_4 when expose to the pro-inflammatory mediators. In this case, fibroblast cell death can be triggered by PAR_4 activation. These PAR_4-dependent and independent mechanisms of cell death could reveal potential therapeutic targets for the treatment of fibrosis. A

potential problem for therapeutic manipulation is cell type specificity. Ideally, CG and trypsin should specifically induce apoptosis in fibroblasts while not affect the other cell types. Hence, further careful investigations to elucidate the regulation mechanisms of apoptosis in fibroblasts would contribute to the development of more specific therapies for IPF and renal fibrosis.

Chapter 6

Epithelial Cell-Derived Medium and PAR_4 Can Regulate Fibroblast Proliferation

6.1 Introduction

Epithelial cells attach to the basement membranes to provide context and architectural stability for the cell-cell contact. When the basement membrane is damaged by protease or disrupted by alteration in assembly, epithelial cells become activated, detach from damaged basement membranes and start secreting cytokines (Zeisberg and Kalluri, 2004). Fibroblasts are the major ECM producer in the wound healing and excessive fibroblast proliferation is associated with excessive collagen deposition and fibrosis (Ramos *et al.*, 2006). Damage of epithelial cells and disruption of a normal epithelial-fibroblast interaction are sufficient to promote fibroblast growth and excessive collagen deposition (Adamson *et al.*, 1988). Conversely, normal levels of fibroblast growth and collagen are seen in the cultured explants where little or no disruption of epithelial-fibroblast interaction takes place (Adamson *et al.*, 1988).

Several studies have implicated excessive apoptosis in epithelial cells as a potential mechanism of acute tissue injury and fibrosis (Hagimoto *et al.*, 1997c; Nomoto *et al.*, 1997; Kuwano *et al.*, 1999b). Apoptosis of damaged epithelium can be caused by death receptor-mediated pathway (Fas-FasL), loss of contact to the basement membrane or intrinsic organelle-dependent pathway which involves lysosomal permeabilisation or mitochondria damage (Kuwano *et al.*, 2004). In a mouse model of bleomycin-induced pulmonary fibrosis, FasL mRNA was upregulated in infiltrating lymphocytes, and Fas was upregulated in bronchiolar and AECs in which excessive apoptosis was detected. Fas is a type I membrane receptor protein that belongs to the TNF receptor family which can induce apoptosis after binding to FasL (Kuwano *et al.*, 1999a). Blockade of either the Fas-FasL pathway or caspase inactivation by caspase inhibitors has been shown to prevent epithelial cell apoptosis and fibrosis. Hence, loss of epithelial cells through the Fas-mediated pathway has a critical role in tissue injury and organ dysfunction (Kuwano *et al.*, 1999a). In addition, Hagimoto *et al.* (2002) demonstrated that upregulation of Fas and FasL expression was observed in bronchiolar and AECs in lung tissue from IPF patients. Thus, apoptosis of lung epithelial cells by Fas ligation may be involved in the pathogenesis of pulmonary fibrosis.

Damaged epithelial cells synthesis and release pro- and anti-inflammatory molecules that can recruit and activate inflammatory cells and thus modulate a variety of inflammatory responses (Knight *et al.*, 1994). Cytokines that are released by the epithelial cells include PGE_2, IL-1α, PDGF, bFGF and TGF-β, which are involved in the regulation of fibroblast proliferation (Holgate *et al.*, 2000; Knight and Holgate, 2003; Sacco *et al.*, 2004).

PGE_2 is a lipid mediator derived from cell membrane phospholipid and is a potent inhibitor of fibroblast functions, including migration (Kohyama *et al.*, 2001), proliferation (Bitterman *et al.*, 1986) and collagen synthesis (Goldstein and Polgar, 1982). It is the key mediator of the suppressive effects of epithelial cells on fibroblasts (Lama *et al.*, 2002; Moore *et al.*, 2003). IL-1α is an important inducer of PGE_2 and it suppresses fibroblast proliferation (Portnoy *et al.*, 2006). Hence, loss of epithelial cells may cause a deficit of anti-proliferative factors, promoting the fibroblast proliferation and the development of fibrosis. Fibrosis may also result from either an inadequate generation of these suppressive factors by the epithelial cells or from an inadequate response of fibroblasts to these factors (Hostettler *et al.*, 2008). PDGF is one of the most potent mitogens and chemoattractants for mesenchymal cells and it induces the proliferation of fibroblasts and synthesis of ECM (Rom *et al.*, 1988). bFGF is a potent stimulator of both fibroblast and endothelial cell proliferation and is associated with the fibroproliferative response (Kuwano *et al.*, 2004).

TGF-β is a potent cytokine associated with tissue fibrosis and structural remodelling (Anscher *et al.*, 1993; Westergren-Thorsson *et al.*, 1993; Sime *et al.*, 1997; Sagara *et al.*, 2002; Balzar *et al.*, 2005). TGF-β expression is upregulated in AECs and macrophages in fibroproliferative lesions (Madtes *et al.*, 1994). The production of active TGF-β by epithelial cells at the sites of injury may be a critical event in healing processes. It is involved in the regulation of fundamental cell functions, including proliferation, differentiation, apoptosis and migration. Conversely, it also inhibits the proliferation of many cell types, emphasising the complexity of this cytokine (McAnulty *et al.*, 1997). It has been shown to function as a potent mitogen on fibroblasts (Moses *et al.*, 1994), inhibiting the growth of epithelial cells and vascular endothelial cells (Tucker *et al.*, 1984; Takehara *et al.*, 1987).

There are studies which demonstrated that PAR activation mediates the release of inflammatory cytokines during inflammation. Human respiratory epithelial cells produce IL-6, IL-8 and PGE_2 in response to PAR_4 agonist peptides (Asokananthan *et al.*, 2002). It has also been demonstrated that PAR_4 is involved in the induction of actin fibre formation in lung vascular endothelial cells (Fujiwara *et al.*, 2005). Furthermore, PAR_4 stimulation induces EMT in primary cultured alveolar epithelial cells (Ando *et al.*, 2007c). These findings suggest that PAR_4 appear to play a role in mediating cytokines release from different cell types during injury and inflammation.

6.2 Aims

Severe injury with dysfunctional epithelial repair processes results in prolonged disruption of the normal intercellular relationships, particularly between the epithelial cells and the fibroblasts (Adamson *et al.*, 1988). Hence, the hypothesis of this chapter is that accumulation of fibroblasts during fibrosis is regulated by a number of mediators that can direct their recruitment and proliferation, which are possibly released by the injured epithelial cells or the activation of PAR_4.

The aims of this chapter are to examine:

1. The effect of media collected from confluent epithelial cell cultures, which are thought to contain a number of cytokines released by the epithelial cells, on the proliferation of HPBFs and HPRFs.

2. The effect of PAR_4 activation on fibroblast proliferation.

6.3 Methods

6.3.1 Preparation of Conditioned Media

A549, normal rat kidney epithelial cells (NRK52E) and HEK-PAR_4 cells were used in this chapter.

To obtain conditioned medium, cells were passaged into 75 cm^2 flasks and allowed to reach 100% confluence. In experiments designed to study PAR_4-induced mediator secretion, human PAR_4-AP (100 μM) was added to the flasks cultured with A549 or HEK-PAR_4 cells whereas rat PAR_4 AP (100 μM) was added to the flasks cultured with NRK52E cells for 24 h. The cultured medium was collected, centrifuged at 400 $\times$ g for 5 min to remove any cell debris, split into aliquots and stored at -80℃.

6.3.2 Proliferation Assay

HPBFs or HPRFs were cultured in 96-well plates with 200 μl fibroblast growth medium and allowed to grow to 40-50% confluence. The cells were then quiesced in serum free media for 24 h (see **Section 2.3**). Next, the conditioned medium collected in **Section 6.3.1** was added to each well at different volumes and incubated for 24 h. Wells with fibroblast complete growth medium only were used as a negative control. After 24 h, the microplate was gently inverted and blotted onto paper towels to remove the medium from the wells. The microplate with cells was then frozen at -80℃ for 24 h. Subsequently, the mircroplate was thawed at room temperature and the proliferation assay was performed using CyQUANT cell proliferation assay kit according to the manufacturer's instructions. This kit uses a proprietary green fluorescent dye (CyQUANT GR dye) which exhibits strong fluorescent enhancement when bound to cellular nucleic acids. The fluorescence of the samples in the microplate was measured

using a fluorescence microplate reader (Infinite 200) with excitation at 480 nm and emission at 520 nm.

6.3.3 Immunofluorescent Staining of α-SMA

HPBFs or HPRFs were seeded on the cover slips and grown in 6-well plates. Once the desired confluence (80%) was obtained, the cells were treated with fibroblast medium and conditioned medium at 1:1 ratio or solely the conditioned medium for 24 h before proceeding for staining as described in **Section 2.8**.

6.3.4 Generation of Whole Cell Lysates

HPBFs or HPRFs were passaged into 25 cm^2 culture flasks and allowed to reach over 80% confluence before treating with different conditioned media at different ratios for 24 h. The fibroblasts were then harvested by centrifugation at 500 $\times$ g for 5 min and lysed by adding 500 μl Laemilli's sample buffer as described in **Section 2.10**.

6.3.5 SDS-PAGE and Western Blotting

Protein samples were separated on a 12.5% SDS-PAGE gel before transferring to a nitrocellulose membrane using i-blot (Invitrogen, UK) as described in **Sections 2.11** and **2.12**.

The membrane was then blocked with 5% milk solution, incubated with primary and secondary antibodies as described in **Section 2.12**. Primary antibodies: rabbit polyclonal anti-α-SMA (1:100) and rabbit polyclonal anti-collagen type I (1:5000); secondary antibody: donkey anti-rabbit HRP. For loading control, mouse monoclonal IgG1 anti-α-tubulin (1:1000) was

used as primary antibody and goat anti-mouse IgG HRP (1:2000) was used as secondary antibody. The blot was visualised using the ECL detection system.

6.4 Results

6.4.1 Proliferation Assay

It is believed that during wound healing, the loss of epithelial cells will release mediators such as PDGF, TNF-α and FGF that can induce the proliferation of fibroblasts (Hostettler et al. 2008). Hence, the effect of epithelial cell-conditioned media (see **Section 6.3.1**) on fibroblast proliferation was evaluated using the CyQUANT cell proliferation assay kit. As TGF-β1 has important roles in the pathogenesis of fibrosis and the potential in regulation of cell proliferation. Thus, the effect of TGF-β1 on proliferation of HPBFs and HPRFs was tested. When grown in the presence of 1 ng/ml or 5 ng/ml TGF-β1, the numbers of HPBFs and HPRFs were higher compared to the controls without TGF-β1, particularly when they were treated with TGF-β1 (5 ng/ml) (**Figure 6.1**). This indicates that TGF-β1 induces proliferation of these fibroblasts. Hence, for the following proliferation experiments, TGF-β1 was used as a positive control. However, the number of cells is slightly increased when treated with 10 ng/ml of TGF-β1 (**Figure 6.1**).

To determine whether epithelial cell-conditioned media promotes fibroblast proliferation, HPBFs and HPRFs were cultured with A549 and NRK52E cell-derived conditioned media, respectively, for 24 h (see **6.3.1**). This led to a significant increase in the number of fibroblasts in a concentration dependent manner (**Figures 6.2 & 6.3**). The greatest proliferative activity was observed when 140 μl conditioned medium was added to HPBFs (p= 0.004) and HPRFs (p= 0.001) (**Figures 6.2 & 6.3**,

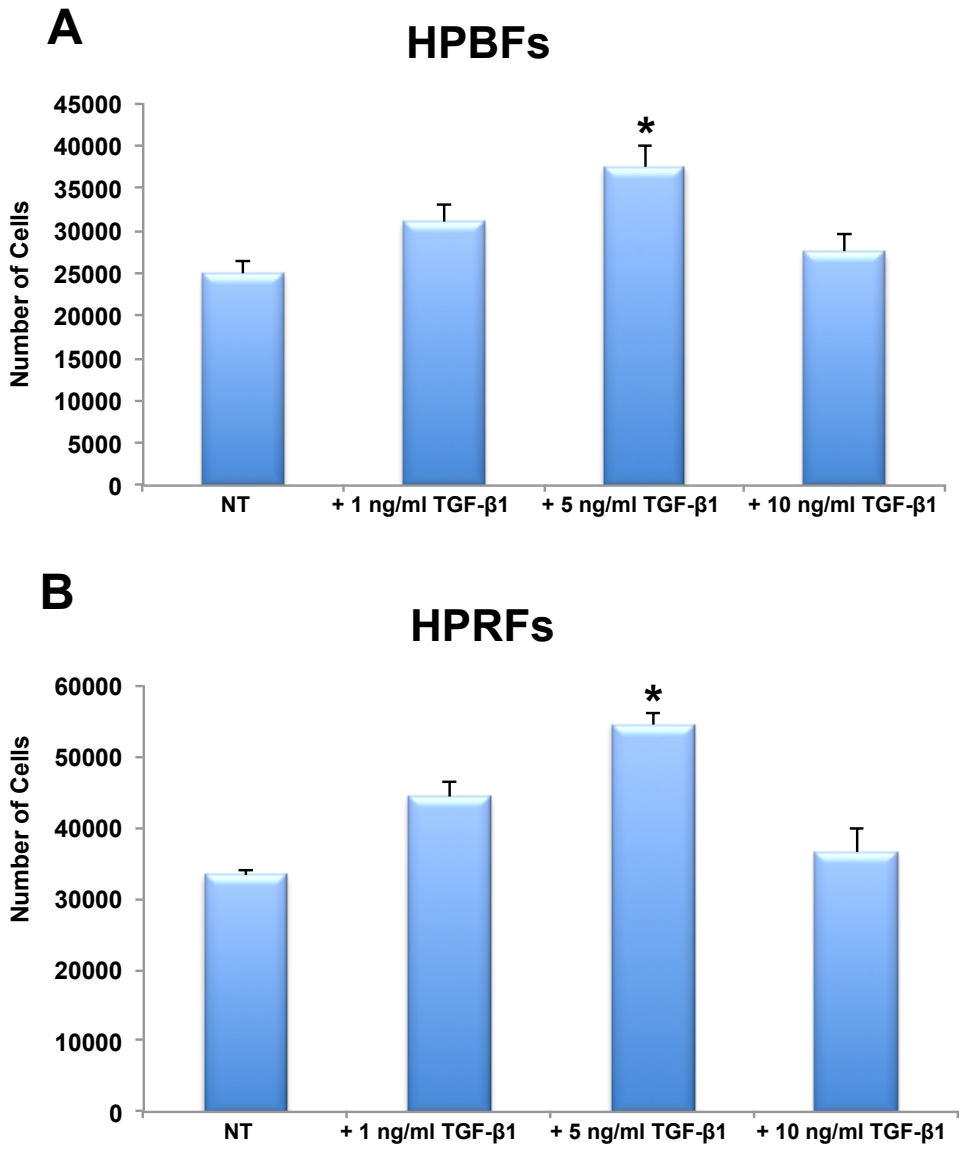

Figure 6.1: TGF-β1 Induced Proliferation of HPBFs and HPRFs. (A) HPBFs and (B) HPRFs at 40-50% confluence in 96-well plate were quiesced and treated with different concentrations of TGF-β1 as indicated. No TGF- β1 was added to the untreated sample (NT). Numbers of cells were scored using CyQUANT cell proliferation assay kit. Results were presented as mean ± SEM of six independent experiments. * indicates $p < 0.05$ *vs.* NT in one-way ANOVA with Dunnett's post hoc test.

blue bars). Proliferative activity decreased slowly after the peak but was still higher than the untreated samples (solely fibroblast growth medium, without any epithelial cell-derived conditioned media).

To examine the effect of epithelial cell-conditioned media on the fibroblast proliferation when PAR_4 is activated, A549 and NRK52E cells were stimulated with 100 μM PAR_4 AP for 24 h before collecting the medium. The epithelial cell-conditioned media with activated PAR_4 induced the proliferation of both HPBFs and HPRFs in a dose dependent manner (**Figures 6.2 & 6.3**, red bars). In the presence of PAR_4 AP, the peak of proliferative activity was observed when 180 μl of conditioned medium was added (p= 0.041) and 160 μl in HPRFs (p= 0.015), respectively.

The effect of culture medium from HEK-PAR_4 cells on fibroblasts was then investigated to test if activation of PAR_4 leads to secretion of cytokines that induce fibroblast proliferation during inflammation (**Figure 6.4**). When lower amounts of HEK-PAR_4-derived conditioned medium (up to 10 μl; with/without PAR_4 activation by PAR_4 AP) were used to treat the fibroblasts, the cell numbers for both HBPFs and HRPFs increased, indicating proliferation of the fibroblasts. When greater than 10 l of HEK-PAR_4-derived conditioned medium was added, the proliferative activity decreased. However, these proliferation activities are not statistically significant when compared to the controls where no HEK-PAR_4-derived conditioned medium was used. In addition, again, no statistical significance was observed when comparing the proliferation activities of cells treated in medium derived from PAR_4-activated culture to those treated in medium derived from culture without PAR_4 activation.

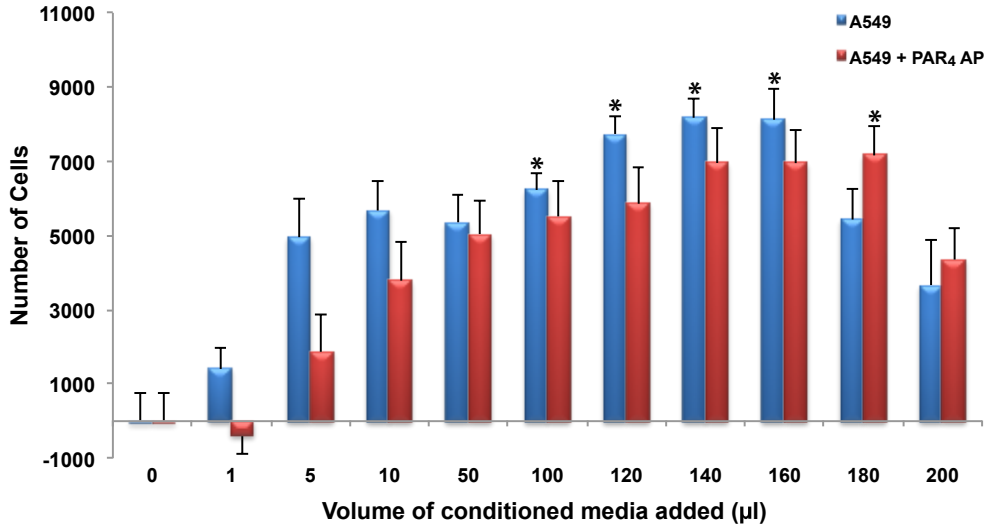

Figure 6.2: A549 Cell-derived Conditioned Medium Promotes Bronchial Fibroblasts Proliferation. A549 cells were cultured in the absence (blue) or presence (red) of 100 μM PAR_4 AP for 24 h. The culture medium was collected and added to the fibroblast culture medium of HPBFs at the indicated volumes, such that each sample was grown in a total volume of 200 μl, for a further 24 h period. Numbers of cells was scored using CyQUANT cell proliferation assay kit. Results are expressed as mean ± SEM of six independent experiments. * indicates $p < 0.05$ *vs.* 0 μl conditioned medium in one-way ANOVA with Dunnett's post hoc test.

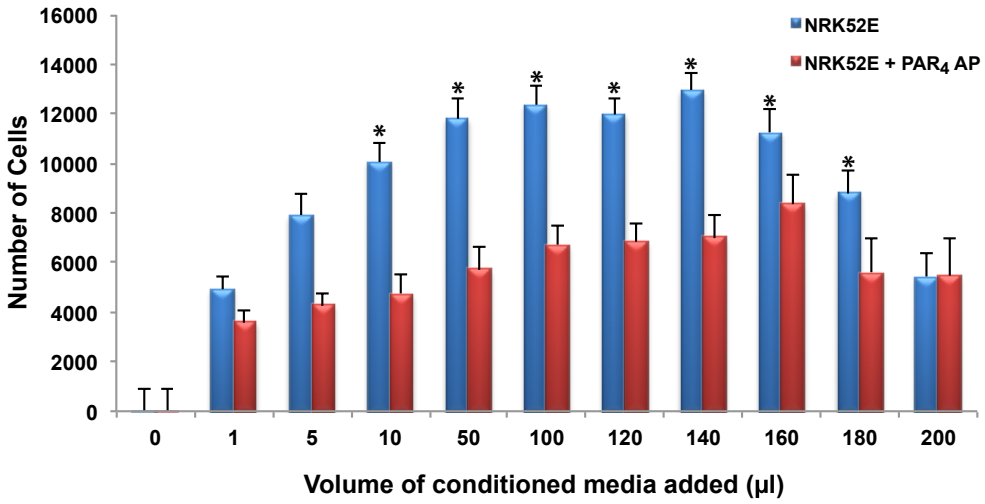

Figure 6.3: NRK52E Cell-derived Conditioned Medium Promotes Renal Fibroblasts Proliferation. NRK52E cells were cultured in the absence (blue) or presence (red) of 100 μM PAR_4 AP for 24 h. The culture medium was collected and added to the fibroblast culture medium of HPRFs at the indicated volumes, such that each sample was grown in a total volume of 200 μl, for a further 24 h period. Numbers of cells was scored using CyQUANT cell proliferation assay kit. Results are expressed as mean ± SEM of six independent experiments. * indicates $p < 0.05$ *vs.* 0 μl conditioned medium in one-way ANOVA with Dunnett's post hoc test.

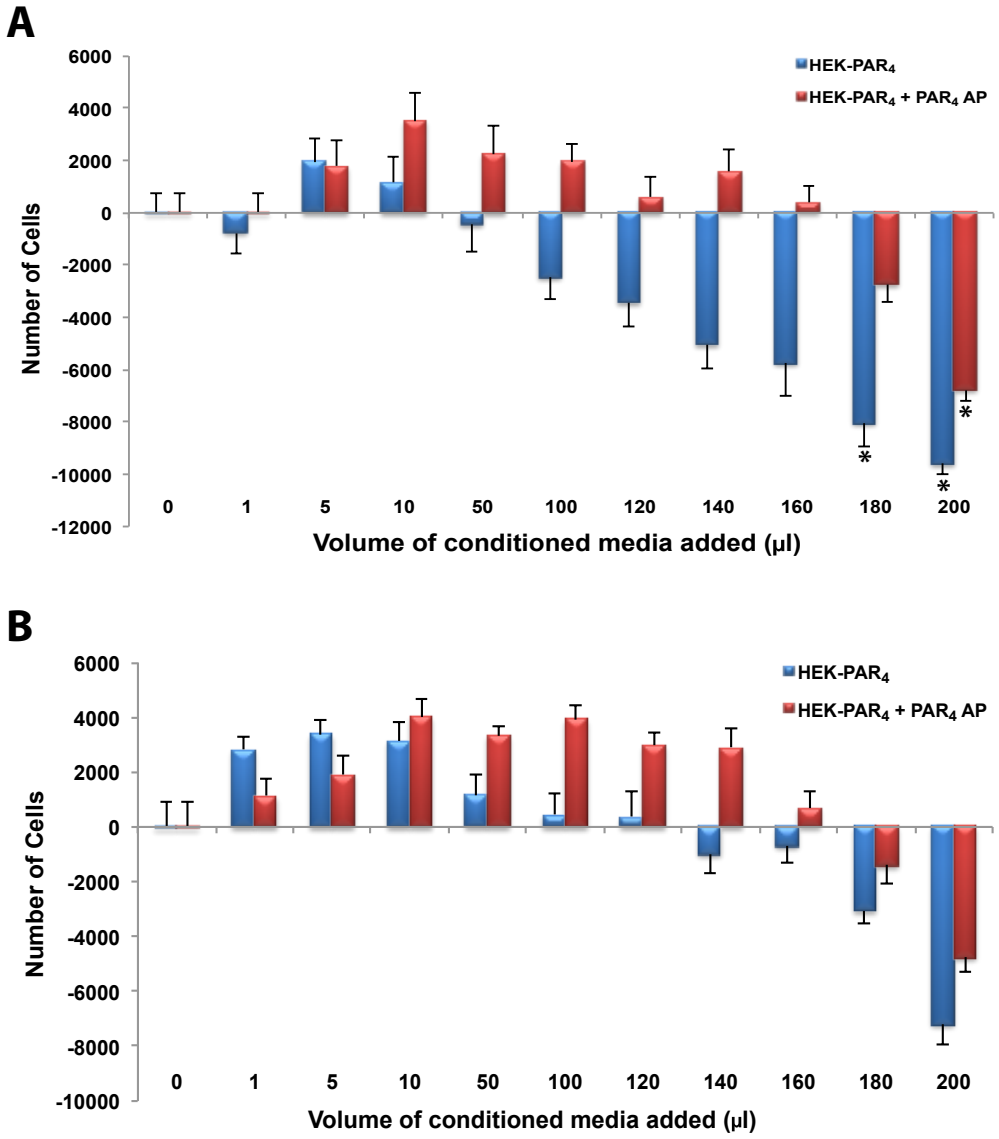

Figure 6.4: HEK-PAR$_4$ Cell-derived Conditioned Medium does not Promote Proliferation in Bronchial and Renal Fibroblasts. HEK-PAR$_4$ cells were cultured in the absence (blue) or presence (red) of 100 μM PAR$_4$ AP for 24 h. The culture medium was collected and added to the culture medium of (A) HPBFs or (B) HPRFs at the indicated volumes, such that each sample was grown in a total volume of 200 μl, for a further 24 h period. Numbers of cells were scored using CyQUANT cell proliferation assay kit. Results are expressed as mean $\pm$ SEM of six independent experiments. * indicates $p < 0.05$ *vs.* 0 μl conditioned medium in one-way ANOVA with Dunnett's post hoc test.

6.4.2 Immunofluorescent Staining for α-SMA

Immunofluorescent staining of α-SMA was used to investigate whether fibroblasts can differentiate into myofibroblasts in response to the epithelial cell-derived conditioned media. Both HPBFs and HPRFs did not differentiate into myofibroblasts in the absence of TGF-β1 as no actin stress fibres were observed (**Figures 6.5A & 6.5E**, respectively). When treated with 1 ng/ml or 5 ng/ml of TGF-β1, actin stress fibres appeared in neither HPBFs (**Figures 6.5B & 6.5C**) nor HPRFs (**Figures 6.5F & 6.5G**). However, at 10 ng/ml, TGF-β1 could induce the differentiation of HPBFs and HPRFs into myofibroblasts, as shown by the appearance of actin stress fibres in the cells (**Figures 6.5D & 6.5H**).

To investigate whether conditioned media derived from epithelial cells could differentiate fibroblasts into myofibroblasts, immunofluorescent staining of α-SMA was performed. Only fibroblasts cultured with solely epithelial cell-conditioned medium or equal ratio of fibroblast growth medium and epithelial cell-conditioned medium were used for staining. As shown in **Figure 6.6 & 6.7**, none of the conditioned media could differentiate fibroblasts into myofibroblasts as no actin stress fibres were observed.

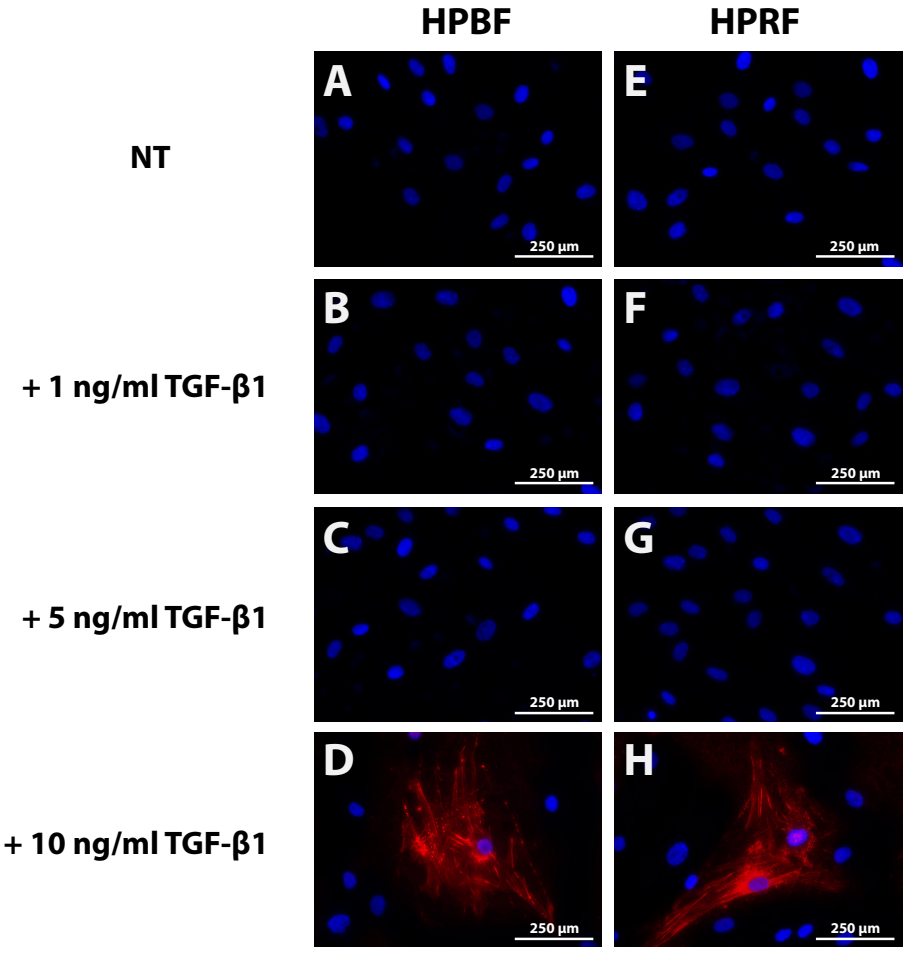

Figure 6.5: α-SMA Expression Observed in Bronchial and Renal Fibroblasts when Treated with 10 ng/ml TGF-β1. Cells were seeded on cover slips and grown in 6-well plates. Cells at 70-85% confluence were quiesced and treated with different concentrations of TGF-β1 as indicated. Cells were then fixed, permeabilised and blocked with 1% BSA/PBS. Finally, cells were stained with anti-α-SMA. All samples were also stained for nuclei (blue) using DAPI. These images represent results from three independent experiments.

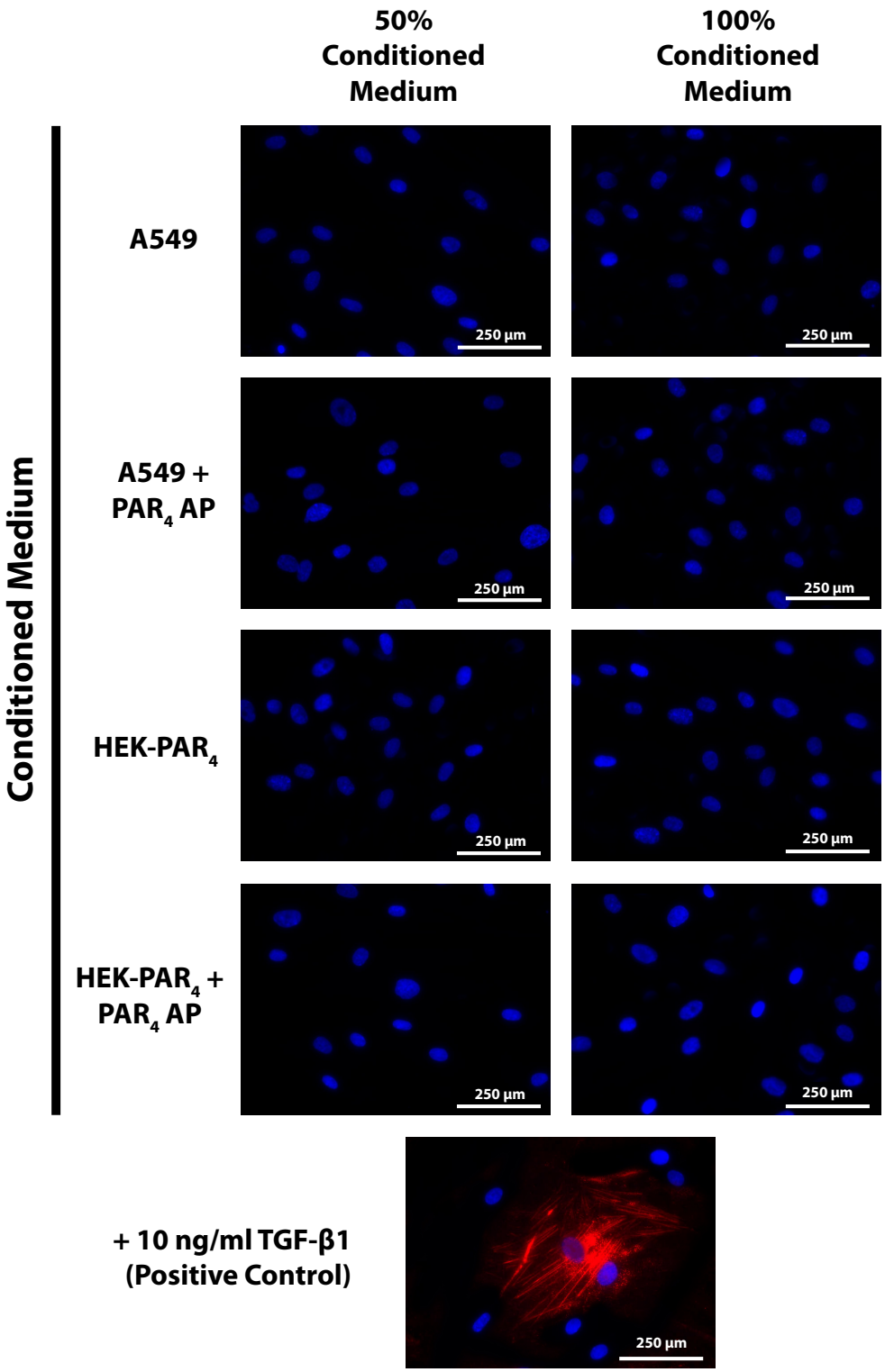
50% Conditioned Medium
100% Conditioned Medium
Conditioned Medium
A549
A549 + PAR4 AP
HEK-PAR4
HEK-PAR4 + PAR4 AP
250 µm
+ 10 ng/ml TGF-β1 (Positive Control)

Figure 6.6: No α-SMA Expression Observed in Bronchial Fibroblasts after Cultured with Different Conditioned Media. The conditioned media used were collected from A549 culture, A549 culture with PAR_4 AP, HEK-PAR_4 culture, and HEK-PAR_4 culture with PAR_4 AP. HPBFs were seeded on cover slips and grown in 6-well plates. HPBFs at 70-85% confluence were quiesced. Quiescent HPBFs were cultured with fibroblast growth medium and epithelial cell-derived conditioned media at 50% or 100% epithelial cell-derived conditioned media. HPBFs treated with 10 ng/ml TGF-β1 were used as a positive control. HPBFs were then fixed, permeabilised and blocked with 1% BSA/PBS. Finally, HPBFs were stained with anti-α-SMA. All samples were also stained for nuclei (blue) using DAPI. These pictures are representatives from three independent experiments.

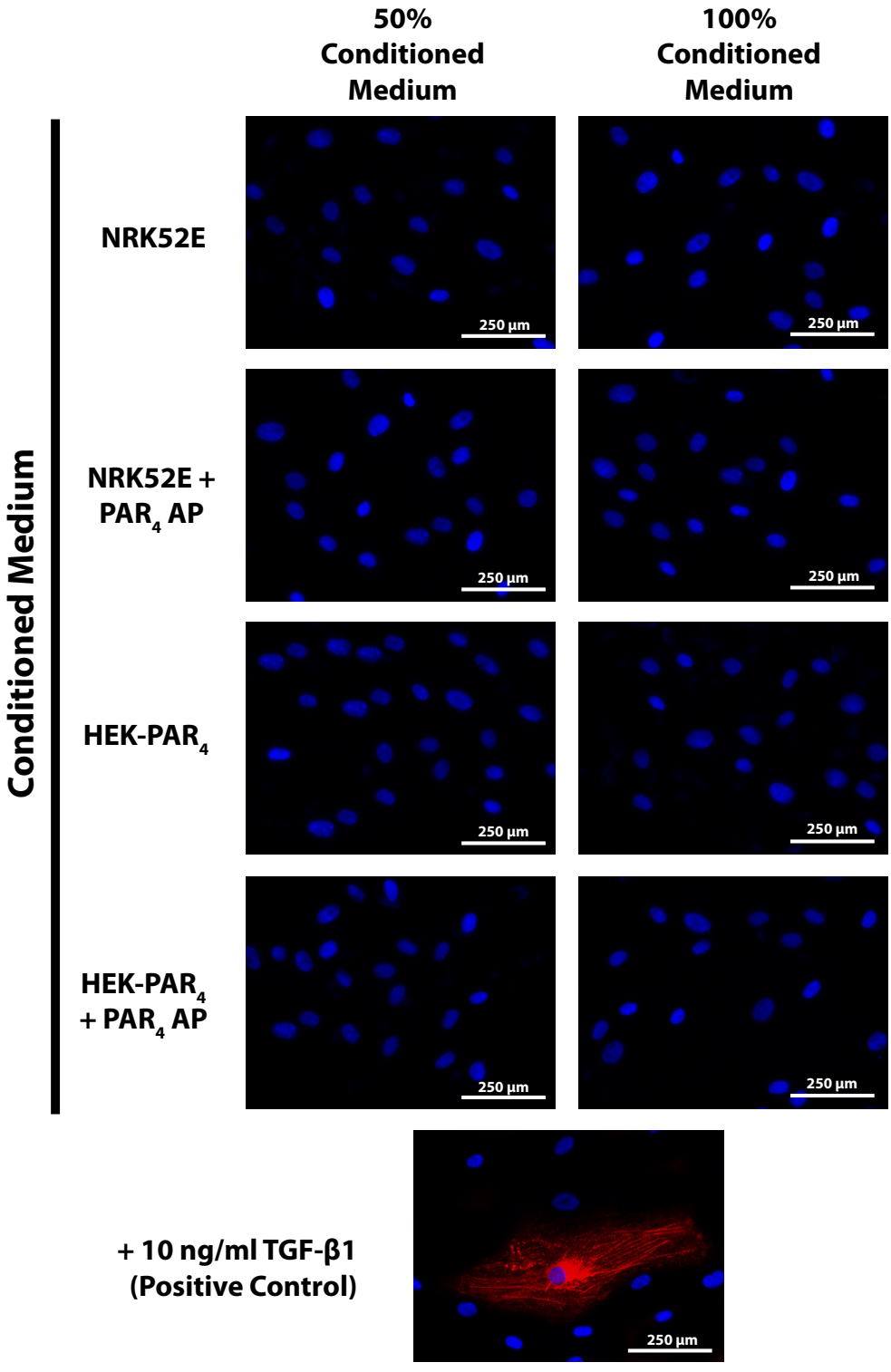
50% Conditioned Medium
100% Conditioned Medium
Conditioned Medium
NRK52E
NRK52E + PAR4 AP
HEK-PAR4
HEK-PAR4 + PAR4 AP
250 µm
+ 10 ng/ml TGF-β1 (Positive Control)

Figure 6.7: No α-SMA Expression Observed in Renal Fibroblasts after Cultured with Different Conditioned Media. The conditioned media used were collected from A549 culture, A549 culture with PAR_4 AP, HEK-PAR_4 culture, and HEK-PAR_4 culture with PAR_4 AP. HPRFs were seeded on cover slips and grown in 6-well plates. HPRFs at 70-85% confluence were quiesced. Quiescent HPRFs were cultured with fibroblast growth medium and epithelial cell-derived conditioned media at 50% or 100% epithelial cell-derived conditioned media. HPRFs treated with 10 ng/ml TGF-β1 were used as a positive control. HPRFs were then fixed, permeabilised and blocked with 1% BSA/PBS. Finally, HPRFs were stained with anti-α-SMA. All samples were also stained for nuclei (blue) using DAPI. These pictures are representatives from three independent experiments.

6.4.3 Western Blotting

To further validate the results from immunofluorescent staining described in **Section 6.4.2**, Western blotting was performed. α-SMA and collagen type I were not detected in either HPBFs or HPRFs when cultured with epithelial cell-conditioned media (**Figures 6.8 & 6.9**), further indicating that they did not differentiate into myofibroblasts in these experiments.

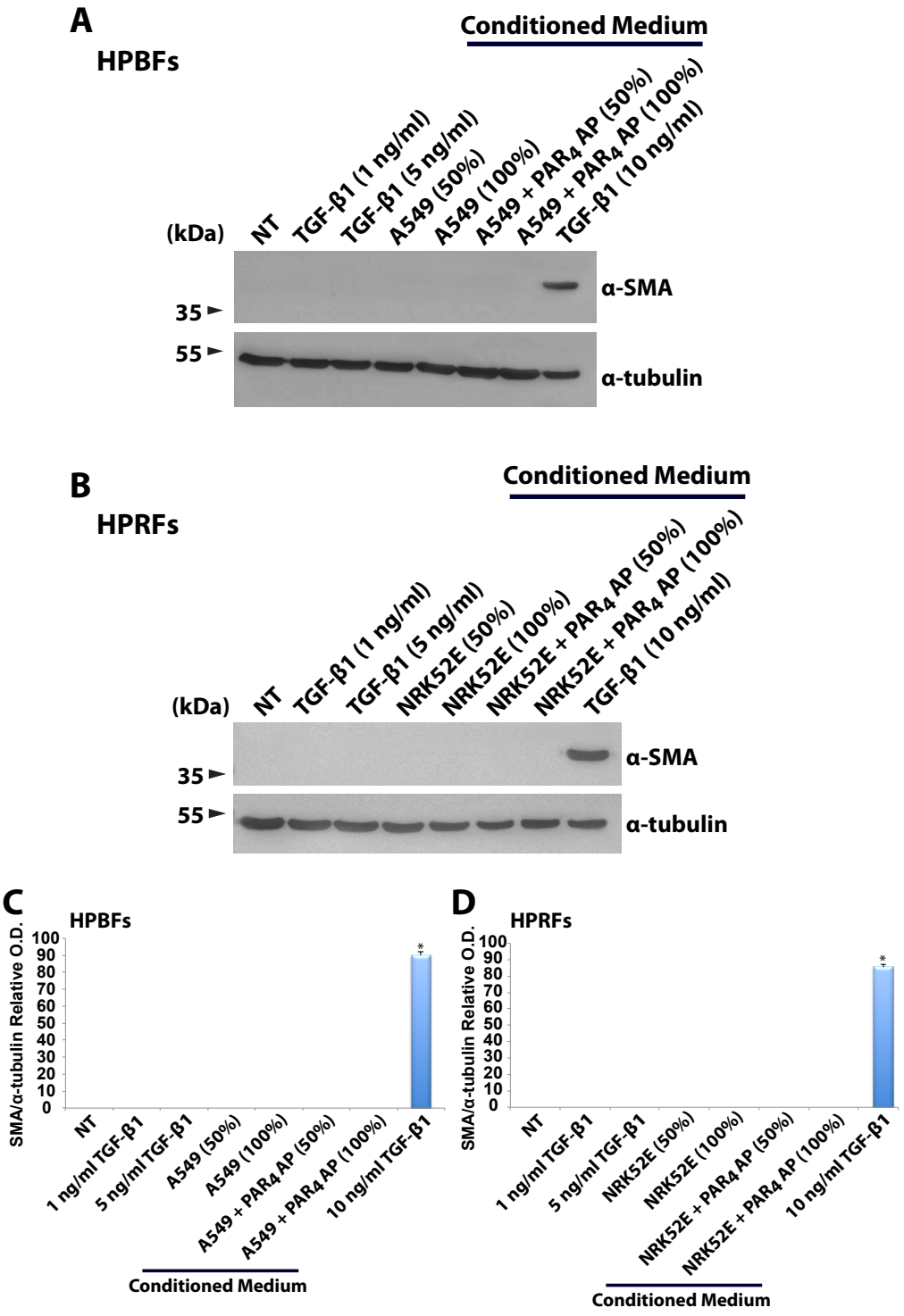
A
HPBFs
Conditioned Medium
(kDa)
NT
TGF-β1 (1 ng/ml)
TGF-β1 (5 ng/ml)
A549 (50%)
A549 (100%)
A549 + PAR4 AP (50%)
A549 + PAR4 AP (100%)
TGF-β1 (10 ng/ml)
35
55
α-SMA
α-tubulin
B
HPRFs
Conditioned Medium
(kDa)
NT
TGF-β1 (1 ng/ml)
TGF-β1 (5 ng/ml)
NRK52E (50%)
NRK52E (100%)
NRK52E + PAR4 AP (50%)
NRK52E + PAR4 AP (100%)
TGF-β1 (10 ng/ml)
35
55
α-SMA
α-tubulin
C
HPBFs
SMA/α-tubulin Relative O.D.
100
90
80
70
60
50
40
30
20
10
0
*
NT
1 ng/ml TGF-β1
5 ng/ml TGF-β1
A549 (50%)
A549 (100%)
A549 + PAR4 AP (50%)
A549 + PAR4 AP (100%)
10 ng/ml TGF-β1
Conditioned Medium
D
HPRFs
SMA/α-tubulin Relative O.D.
100
90
80
70
60
50
40
30
20
10
0
*
NT
1 ng/ml TGF-β1
5 ng/ml TGF-β1
NRK52E (50%)
NRK52E (100%)
NRK52E + PAR4 AP (50%)
NRK52E + PAR4 AP (100%)
10 ng/ml TGF-β1
Conditioned Medium

Figure 6.8: No α-SMA are detected by Western Blotting after Cultured with Different Conditioned Media. Quiescent (A) HPBFs or (B) HPRFs were cultured in the media as indicated for 24 h. Cell lysates were obtained and then subjected to SDS-PAGE followed by immunoblotting with antibodies against α-SMA and α-tubulin. α-tubulin was used as a loading control. Expected band sizes: collagen type I ($\sim$90 kDa), α-SMA ($\sim$42 kDa) and α-tubulin ($\sim$52 kDa). (C & D) Results were quantitated and summarised in a bar chart, where optical densities were normalised to α-tubulin loading controls. Results are expressed as mean $\pm$ SEM of three independent experiments. * indicates $p < 0.05$ compared with untreated samples (NT) in one-way ANOVA with Dunnett's post hoc test.

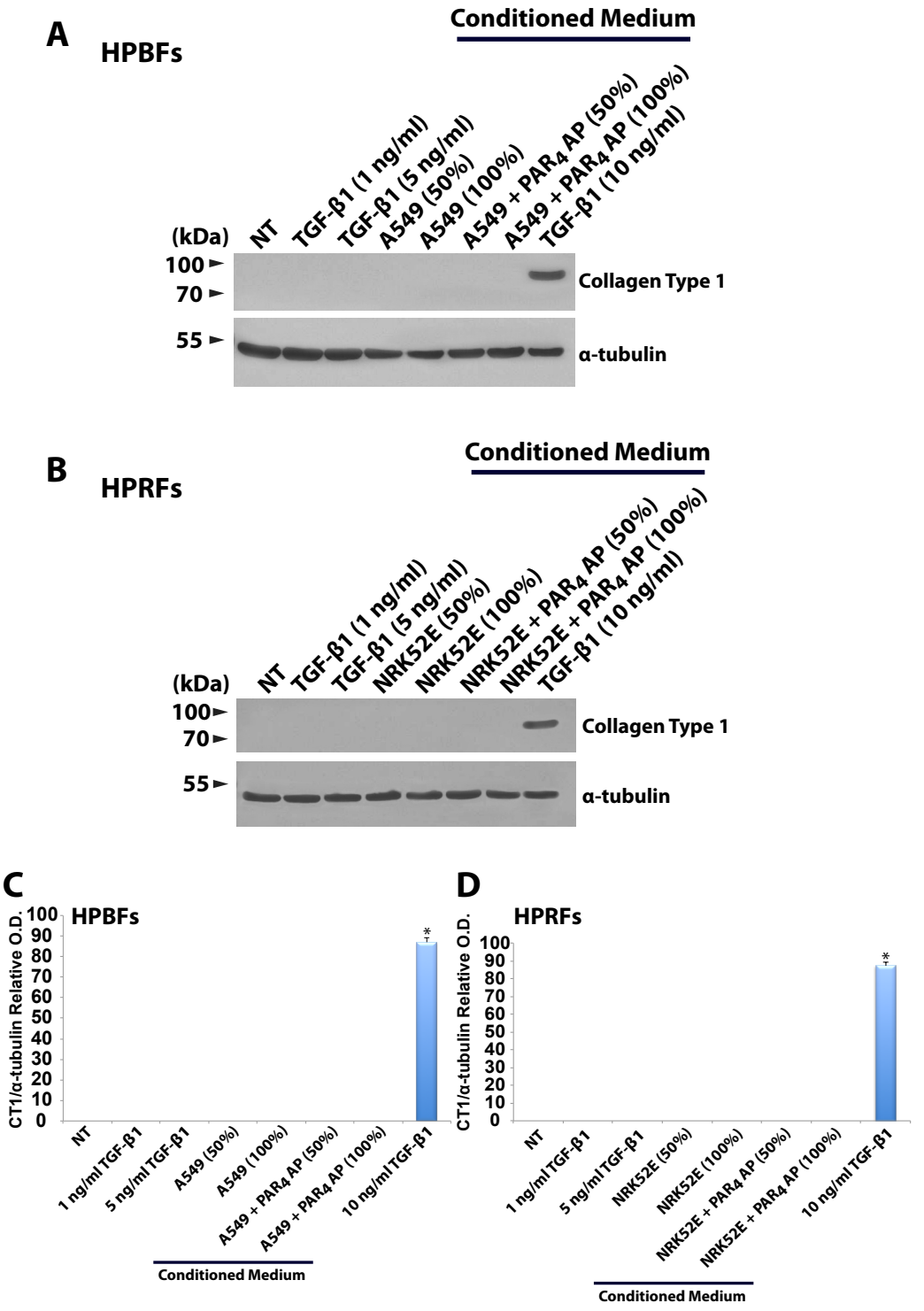
A
HPBFs
Conditioned Medium
NT
TGF-β1 (1 ng/ml)
TGF-β1 (5 ng/ml)
A549 (50%)
A549 (100%)
A549 + PAR4 AP (50%)
A549 + PAR4 AP (100%)
TGF-β1 (10 ng/ml)
(kDa)
100
70
55
Collagen Type 1
α-tubulin
B
HPRFs
Conditioned Medium
NT
TGF-β1 (1 ng/ml)
TGF-β1 (5 ng/ml)
NRK52E (50%)
NRK52E (100%)
NRK52E + PAR4 AP (50%)
NRK52E + PAR4 AP (100%)
TGF-β1 (10 ng/ml)
(kDa)
100
70
55
Collagen Type 1
α-tubulin
C
HPBFs
CT1/α-tubulin Relative O.D.
100
90
80
70
60
50
40
30
20
10
0
*
NT
1 ng/ml TGF-β1
5 ng/ml TGF-β1
A549 (50%)
A549 (100%)
A549 + PAR4 AP (50%)
A549 + PAR4 AP (100%)
10 ng/ml TGF-β1
Conditioned Medium
D
HPRFs
CT1/α-tubulin Relative O.D.
100
90
80
70
60
50
40
30
20
10
0
*
NT
1 ng/ml TGF-β1
5 ng/ml TGF-β1
NRK52E (50%)
NRK52E (100%)
NRK52E + PAR4 AP (50%)
NRK52E + PAR4 AP (100%)
10 ng/ml TGF-β1
Conditioned Medium

Figure 6.9: No Collagen Type 1 are detected by Western Blotting after Cultured with Different Conditioned Media. Quiescent (A) HPBFs or (B) HPRFs were cultured in the media as indicated for 24 h. Cell lysates were obtained and then subjected to SDS-PAGE followed by immunoblotting with antibodies against collagen type 1 and α-tubulin. α-tubulin was used as a loading control. Expected band sizes: collagen type I ($\sim$90 kDa) and α-tubulin ($\sim$52 kDa). (C & D) Results were quantitated and summarised in a bar chart, where optical densities were normalised to α-tubulin loading controls. Results are expressed as mean $\pm$ SEM of three independent experiments. * indicates $p < 0.05$ compared with untreated samples (NT) in one-way ANOVA with Dunnett's post hoc test.

6.5 Discussion

The goal of this chapter was to examine the effects of different conditioned media on HPBF and HPRF proliferation. Under normal conditions, the damaged epithelium is able to repair itself rapidly. It has been demonstrated that immediately after injury, the epithelial cells at the edge of the damaged area de-differentiate, flatten and rapidly migrate on a provisional matrix to provide a covering layer over the denuded basement membrane, followed by the proliferation of new epithelial cells. The new epithelial layer is formed within 24 h after the injury (Erjefält and Persson, 1997a). Damage of epithelial cells release a number of pro-fibrotic mediators including TGF-β, TNF-α, PDGF, FGF and PGE_2 that influence fibroblast proliferation and migration, matrix production and remodelling (Erjefält and Persson, 1997b).

The lung epithelium is the primary site of lung inflammation and damage as well as the release of inflammatory mediators. Alterations in the structure and function of lung epithelial cells may affect the production of these mediators. Extensive lesion and changes in the airway wall architecture are commonly found in patients with respiratory infections, asthma, cystic fibrosis and chronic obstructive pulmonary disease (Knight, 2001).

The normal airway is lined with a layer of pseudocolumnar epithelial cells (Breeze and Wheeldon, 1977). During inflammatory respiratory disorders, extensive injury of airway epithelium occurs, with shedding of the epithelial cells in the bronchial and alveolar lumen. Inflammatory cells then release cytokines that damage the surface epithelium and underlying tissues as well as stimulate fibroblast proliferation (Raeburn and Webber, 1994). Disruption of the integrity of the alveolar epithelium and slow re-epithelialisation of the denuded area are distinct pathologies in IPF and asthma (Selman *et al.*, 2001; Holgate *et al.*, 2006).

AEC in IPF secrete a number of cytokines, growth factors, proteases, surfactant proteins, adhesion molecules and matrix components, which may regulate the inflammatory and fibrotic response within the lung (Kuwano *et al.*, 2004). DNA damage or apoptosis of AEC has been reported in acute lung injury (Bardales *et al.*, 1996) and IPF (Kuwano *et al.*, 1996; Barbas-Filho *et al.*, 2001). Epithelial cell damage and cell death during alveolitis induce the formation of gaps in the epithelial basement membranes. When the degree of lung injury is mild, damaged tissue will normally be repaired, whereas excess cell death may lead to irreparable lung damage and pulmonary fibrosis (Kuwano *et al.*, 2004). The migration of fibroblasts through these gaps into the alveolar space leads to intra-alveolar fibrosis (Fukuda *et al.*, 1987). Hence, severe injury and impaired repair of AECs disturb normal epithelial-fibroblast interaction, causing proliferation of fibroblasts and eventually leading to pulmonary fibrosis (Kuwano *et al.*, 2004).

In the kidney, tubular damage and monocyte infiltration are two of the histopathological hallmarks of acute and chronic tubulointerstitial injury (Goor *et al.*, 1994; Wolf, 1995). Extensive injury of tubules and excessive deposition of ECM in the tubular insterstitium have been commonly described in patients with chronic kidney diseases (Kuncio *et al.*, 1991). There is increasing evidence that tubular epithelial cell damage is involved in the events that promote interstitial fibrosis as approximately 80% of renal volume is occupied by tubules (Eddy, 1994).

A recent study has suggested that injured tubular epithelium plays a crucial role in renal fibrosis by responding to the injuries and amplifying the pro-fibrotic cytokines (Wu *et al.*, 2013). The potential involvement of tubular epithelial cells in renal fibrosis is elucidated by the activation of inflammatory and fibrogenic signalling in renal tubules after injury (Liu,

2011). NFkB signalling is activated in renal tubular epithelium in response to injuries, causing the release and production of inflammatory cytokines that initiate peritubular inflammation (Molitoris, 1999). Therefore, damage and death of proximal tubular cells are responsible for the pathophysiological and clinical aspects of kidney injury, and ultimately converge on common pathways that lead to progressive renal scarring.

Collectively, these findings show that epithelial cells might play an important role in the pathogenesis of organ injury and fibrosis by releasing cytokines that promote fibroblast proliferation. Thus, the effect of epithelial cell derived conditioned media on HPBFs and HPRFs were examined. TGF-β1 promoted fibroblast proliferation in a dose dependent manner, showing a reliable positive control for fibroblast proliferation (**Figures 6.1A & 6.1B**). Although all three concentrations of TGF-β1 induced fibroblast proliferation, 5 ng/ml TGF-β1 had the most robust effect. The number of cells is slightly increased when treated with 10 ng/ml of TGF-β1, indicating they have differentiated into myofibroblasts (supported by the α-SMA staining and Western blotting). Similar to the results in this study, Strutz *et al.* (2001) reported that TGF-β1 caused a dose- and time- dependent induction of proliferation in human renal fibroblasts. They also demonstrated that TGF-β1 induces fibroblast proliferation is largely mediated by FGF-2.

The results demonstrate that epithelial cell derived conditioned medium promotes fibroblast proliferation *in vitro* in a concentration dependent manner. Conditioned media derived from A549 and NRK52E cultures showed similar concentration dependent activities in both HPBFs and HPRFs (**Figures 6.2 & 6.3**). The number of fibroblasts decreased after the peak proliferative activity, suggesting that apoptosis of fibroblasts might occur. When the volume of epithelial cell derived conditioned medium increased, the volume of fibroblast growth medium in the culture

medium decreased, suggesting that there may be a lack of nutrients that is essential for the growth of fibroblasts. In contrast, the proliferative activity of both HPBFs and HPRFs did not significantly increase when cultured with HEK-PAR_4 cell-derived conditioned media when PAR_4 is not activated (**Figures 6.4**).

A few studies demonstrated that PARs are involved in cell proliferation (Berger *et al.*, 2001a; Tanaka *et al.*, 2005; Furuhashi *et al.*, 2008). However, the potential effects of PAR_4 activation on fibroblast proliferation have not been examined. Here, A549 and NRK52E cell-derived conditioned media when PAR_4 activated promoted a lower proliferative activity in HPBFs and HPRFs compared to the media when PAR_4 is not activated (**Figures 6.2 & 6.3**). In contrast, HEK-PAR_4 cell-derived conditioned media promoted higher proliferative activity in both HPBFs and HPRFs in cultures when PAR_4 is activated compared to those cultured in medium when PAR_4 is not activated.

Together, these results show that the conditioned media derived from A549 and NRK52E cultures promote higher proliferative activities when PAR_4 is not activated, whereas those derived from HEK-PAR_4 cultures promote higher proliferative activities when PAR_4 is activated. The reason behind this is not clear. While PAR_4 is expressed in all three cell lines, it is overexpressed in HEK-PAR_4 cells. It is possible that different mediators are being produced and released in different cell types. Different pro-fibrotic mediators have different actions on fibroblasts, for example, PDGF is a strong inducer of fibroblast proliferation (Rom *et al.*, 1988) whereas PGE_2 is a potent inhibitor for fibroblast proliferation (Bitterman *et al.*, 1986). Also, the amount of mediators produced and released could also be one of the factors that cause different proliferative activities in different cell types.

TGF-β1 promotes the differentiation of fibroblasts into myofibroblasts

by increasing the expression of α-SMA and the formation of stress fibres (Desmoulière *et al.*, 1993; see **Chapter 3**). The addition of 10 ng/ml TGF-β1 to the fibroblast cultures promoted the differentiation of HPBFs and HPRFs into myofibroblasts but not in the lower concentrations. These results were confirmed by immunofluorescent staining using anti-α-SMA antibody (**Figures 6.5**) and Western blotting using α-SMA and collagen type I antibodies (**Figures 6.8 & 6.9**). Also, none of the epithelial cell-conditioned media could differentiate the fibroblasts into myofibroblasts in these experiments (**Figures 6.6 & 6.7 & 6.8 & 6.9**) . These findings suggest that fibroblasts that are proliferating (but not differentiating) do not express α-SMA and do not exhibit elevated levels of collagen synthesis. This is supported by the study demonstrated by Grotendorst *et al.* (2004). They demonstrated that fibroblast proliferation, differentiation and collagen synthesis are induced by TGF-β via the connective tissue growth factor (CTGF)-dependent pathways. TGF-β and CTGF are coordinately expressed at sites of tissue repair and fibrosis (Frazier *et al.*, 1996; Shinozaki *et al.*, 1997). TGF-β-stimulated fibroblast proliferation and differentiation can be blocked with anti-CTGF antibodies, indicating that CTGF plays an important role in fibrotic disease (Grotendorst *et al.*, 2004). However, CTGF alone is not responsible for determining whether cells respond to TGF-β by proliferation or differentiation. Rather, CTGF acts in conjunction with other growth factors such as epidermal growth factor (EGF) and insulin-like growth factor-2 (IGF-2) to control the events. In the presence of TGF-β, CTGF and EGF, cells undergo proliferation, whereas in the presence of TGF-β, CTGF and IGF-2, cells undergo differentiation (Grotendorst *et al.*, 2004). Thus, when cells are stimulated with TGF-β, the factor controlling TGF-β to induce cell proliferation or myofibroblast formation is dependent on the presence of the other growth factors. Different concentration of TGF-β1 present in the conditioned media will cause different concentration of pro-fibrotic mediators released and thus, causing different cellular responses.

In conclusion, this study provides preliminary results which support the idea that epithelial cell injury promotes proliferation of fibroblasts, an event that is thought to be involved in the pathogenesis of fibrosis. These experiments indicate that conditioned media derived from confluent epithelial cell cultures (when cell death starts to occur) contain factors which can stimulate fibroblast proliferation but not differentiation. However, due to time constraints, the mediators present in the conditioned media that promote the fibroblast proliferation were not identified in this chapter. Hence, additional studies are needed to address this, which could be done by using the commercially available enzyme-linked immunosorbent assay (ELISA) kits.

Chapter 7

General Discussion and Future Work

7.1 General Discussion

The interactions of fibroblasts, ECM production and the role of cytokines released in the fibrogenesis have been thought to contribute to the pathogenesis of fibrotic diseases. Incorporating the findings presented in this thesis and the published literature within the field, **Figure 7.1** demonstrates the possible events that might occur as a consequence of tissue injury (See below).

The hypothesis of this thesis is that 'PAR_4 is expressed in both lung and renal fibroblasts and PAR_4 activating peptide and cathepsin G can induce apoptosis in fibroblasts via PAR_4-dependent and independent mechanism'.

The data presented in this thesis indicate that: first, both HPBFs and HPRFs do not endogenously express PAR_4; second, CG and trypsin induce apoptosis in HPBFs and HPRFs PAR_4 independently and PAR_4 AP induces apoptosis in HEK- PAR_4 cells via PAR_4 signalling pathway. Hence, the above hypothesis has to be rejected.

The findings in this research are outlined below.

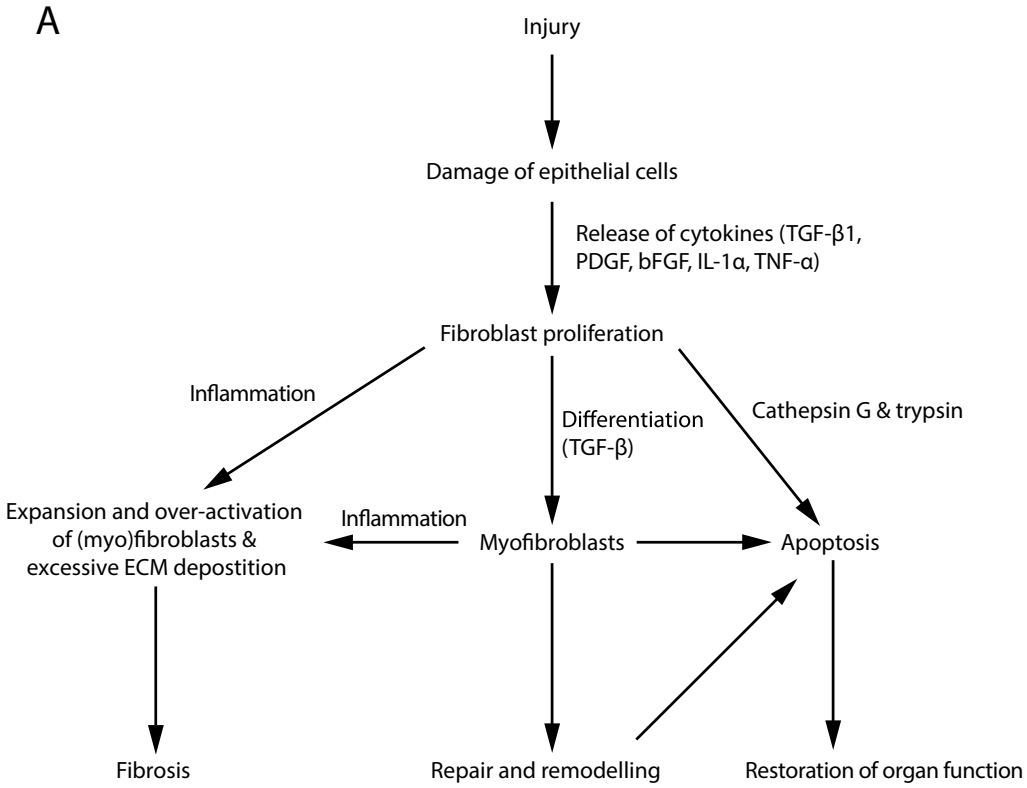
A
Injury
Damage of epithelial cells
Release of cytokines (TGF-β1, PDGF, bFGF, IL-1α, TNF-α)
Fibroblast proliferation
Inflammation
Differentiation (TGF-β)
Cathepsin G & trypsin
Expansion and over-activation of (myo)fibroblasts & excessive ECM depostition
Inflammation
Myofibroblasts
Apoptosis
Fibrosis
Repair and remodelling
Restoration of organ function
B
PAR4 AP
PAR4 activation
PAR4-expressing cells (HEK-PAR4 cells)
Apoptosis
C
Medium from confluent epithelial cell culture
unidentified factors
Fibroblast Proliferation

Figure 7.1: A Schematic Illustration Summarising the Main Findings in this Thesis (A) Damaged epithelial cells release a number of pro-fibrotic mediators that regulate fibroblast proliferation, matrix production and remodelling. Cathepsin G and trypsin were found to induce apoptosis in two types of fibroblasts, HPBFs and HPRFs, where endogenous PAR_4 expression was not detected. (B) When treated with PAR_4 AP, apoptosis was induced in PAR_4-expressing HEK293 cells. (C) Conditioned medium derived from confluent epithelial cell culture could induce the proliferation of HPBFs and HPRFs. The cellular and molecular factors contained in the conditioned medium which contributed to this proliferation effect remain to be identified. See text for details.

7.1.1 PAR Expression Characterised in HPBFs and HPRFs and transformation of fibroblasts into myofibroblasts

In this thesis, the use of human primary fibroblasts has provided a realistic understanding of cellular responses, compared to results obtained from immortalised cell lines. However, the major limitations when using human primary fibroblasts is the variabilities from donor to donor and the potential changes in phenotype with each passage. Here, both HPBFs and HPRFs were characterised by the positive expression of two fibroblast makers prolyl 4-hydroxylase and vimentin, confirming their fibroblastic nature. In addition, cells were only used between passage 2 and 5 in order to keep characteristics as consistent as possible. Without LPS stimulation, PAR_1, PAR_2 and PAR_3 are present in the HPBFs and only PAR_1 and PAR_2 are present in the HPRFs. The difference of PAR family expression in HPBFs and HPRFs may be due to the different origins of the fibroblasts used. There was no significant difference in PAR expression between different cultures of HPBFs or HPRFs. Contradictory to the findings of

this study, earlier reports showed LPS reproducibly induced expression of functional PAR_4 in HPBFs (Ramachandran *et al.*, 2007). In this study, experimental data inconsistently showed that LPS induced PAR_4 expression in HPBFs. PAR_4 expression was induced in some cases but in most cases, no PAR_4 was detected (presented in **Chapter 3**). These different observation may be to the differences in the anatomical location of the tissues. Even within a single tissue, fibroblasts are not a homogenous population and exist as sub-sets of cells (Fries *et al.*, 1994). Also, there are a number of factors that could influence the PAR expressions on fibroblast include age, sex, smoking habit or pathological changes *in situ* prior to isolation for the experiments, all of which could have affected the fibroblast phenotype. Since most experiments were repeated at least five times, it is likely that the results are robust.

The differentiation of fibroblasts to myofibroblasts is the key event in wound healing and remodelling processes. TGF-β1 is one of the most investigated profibrotic cytokines. Its critical role in tissue remodelling has been well recognised and *in vitro* studies have shown that it enhances myofibroblast differentiation of fibroblasts (Thannickal *et al.*, 2003; Serpero *et al.*, 2006). In this study, the protein levels of collagen type I and α-SMA for TGF-β1-treated fibroblasts were significantly higher than that for untreated fibroblasts, demonstrating the transformation of fibroblasts to myofibroblasts (presented in **Chapter 3**).

7.1.2 CG inhibit PAR_4 Activation

In **Chapter 4 and 5**, HEK293 cells with functional PAR_4 expression were successfully established (termed HEK-PAR_4). The effects of PAR_4 AP (AYPGQV) and CG on HEK-PAR_4 cells in intracellular calcium mobilisation were different. HEK-PAR_4 cells activated by PAR_4 AP resulted in a brisk rise in intracellular calcium whereas intracellular calcium

mobilisation did not change when stimulated with CG. These differences in the effect of PAR_4 AP and CG imply that CG does not activate PAR_4. Indeed, A549 cells, the human alveolar epithelial cells that endogenously expressed PAR_4, also failed to be activated by CG. The experimental evidence implicating PAR_4 cleavage as the mechanism mediating CG in fibroblasts is more questionable. Data obtained in **Chapter 5** demonstrated that expression of human PAR_4 confers responsiveness to PAR_4 AP but not to CG. The further observation that CG-treated HEK-PAR_4 cells elicit a reduced response to the stimulatory actions of PAR_4 AP suggests that CG might cleave PAR_4 at the ECL2 domain and cause PAR_4 to be unresponsive to the PAR_4 AP. In addition, Cumashi *et al.* (2001) demonstrated that CG did not trigger aggregation in murine platelets and Sabri *et al.* (2003b) also demonstrated that human PAR_4 conferred responsiveness to thrombin and PAR_4 AP but not to CG. These studies and experimental data reported herein demonstrate that CG acts independently of PAR_4. Together this suggests that CG does not proteolytically activate PAR_4 and raise doubts that CG contributes to the PAR_4 cleavage.

These results are in contrast to the experimental evidence by Sambrano *et al.* (2000) which demonstrated that CG is a strong agonist for PAR_4 in human platelets. This difference was likely due to the cell specific differences in post-translational processing of PAR_4. For example, a few studies demonstrated that the extent of glycosylation of receptor is important for receptor expression, stability and activation (see **Chapter 4 Discussion**) (Brass *et al.*, 1992; Nakayama *et al.*, 2003; Xiao *et al.*, 2011).

7.1.3 CG and Trypsin Induce Apoptosis Independently of PAR_4

The effect of CG on apoptosis of fibroblasts would be particularly vital in areas of interstitial inflammation, where neutrophil infiltration leads to fibroblast proliferation and ECM accumulation. In addition, the important regulatory role of PARs in both normal and inflammatory states emphasises the need to investigate further the relationship between PARs and the proteases that modulate their activities. Understanding the complicated network of extracellular proteases and PARs on lung and renal fibroblasts may reveal promising pharmaceutical targets for the treatment of fibrotic diseases in lung and kidney.

Targeting specific cell types with apoptotic agents represents a major challenge in therapeutic intervention for fibrotic diseases such as IPF and renal fibrosis. Apoptosis is one of several mechanisms involved in the development of fibrosis and the complexity of interactions between these different mechanisms remains far from being solved. This study provides evidence that CG and trypsin can induce apoptosis in lung and renal fibroblasts in concentration dependent fashion (see **Chapter 5**). CG and trypsin induced pronounced morphologic changes in lung and renal fibroblasts without PAR_4 expression. In addition, there was no significant difference in the percentage of apoptotic cells between empty vector control and HEK-PAR_4 cells when treated with CG, suggesting PAR_4 expression is not required for CG to trigger apoptosis. The mechanisms underlying the cellular actions of CG are still incompletely understood. Hence, further studies are required to investigate the downstream signalling pathway activated by CG.

7.1.4 PAR_4-dependent induction of apoptosis

As presented in **Chapter 5**, PAR_4 AP is able to trigger higher percentage of apoptosis in HEK-PAR_4 cells compared to empty vector control, suggesting that apoptosis can also be mediated by PAR_4 signalling. Although PAR_4 is not endogenously expressed in HPBFs and HPRFs (**Chapter 3**), it might be present in other types of fibroblasts. Thus, it would be worth determining the expression of PAR_4 in other fibroblasts and if PAR_4 activation by PAR_4 AP or other agonists could induce apoptosis.

Interestingly, coagulation Factor Xa and PAR_1 AP have been reported to induce apoptosis in some cancer cell lines (Borensztajn *et al.*, 2007; Borensztajn and Spek, 2008). Importantly, PAR_4 was detected in about 55% of malignant samples (see Review by Elste and Petersen (2010)). It is currently unclear whether the effect of PAR_4 activation on apoptosis is specific to the PAR_4-expressing HEK293 cells. This question could be answered by testing the effect of the same PAR_4 AP in another PAR_4-expressing cell line. Hence, if it is true that activation of PAR_4 would contribute to apoptosis in different cell lines, and given that PAR_4 is present in several cancer cells, careful evaluation of the molecular mechanism underlying apoptosis induction via PAR_4 activation might also benefit the drug development to treat certain cancers.

7.1.5 Conditioned Medium Derived from Epithelial Cell Culture Promotes Fibroblast Proliferation

Apoptosis can be detrimental or beneficial, depending on the cell type, the circumstances and the timing. For example, the stimulation of apoptosis in fibroblasts and myofibroblasts in the fibrotic disease can be beneficial because they are the key effector cells in fibrosis that produce excessive ECM. However, excessive epithelial cell apoptosis could lead to barrier

collapse and a deficit of anti-fibrotic mediators. The major function of the epithelium was thought to act as a physical barrier, but recent studies indicate that it has the capacity to modulate a variety of inflammatory processes through the production and release of inflammatory cytokines including TGF-β, TNF-α, and IL-1, -6, and -8. Some of these cytokines play important roles in fibroblast proliferation, myofibroblast differentiation and collagen production. Thus, in order to manipulate apoptosis therapeutically, the cell-type specificity and location of apoptosis must be considered.

This thesis demonstrates that conditioned media derived from confluent epithelial cell cultures (when cell death started to occur) contained factors sufficient to stimulate fibroblast proliferation but not differentiation. The conditioned media derived from A549 and NRK52E cultures promoted higher proliferative activities when there is no PAR_4 activated whereas HEK- PAR_4 cells promoted higher proliferative activities with PAR_4 activated (**Chapter6**). This study supports the concept that epithelial cell injury promotes the proliferation of fibroblasts. This finding is consistent with the previous findings demonstrated by Nakamura *et al.* (1995). They demonstrated that the bronchial epithelial cell-conditioned medium increased the number of fibroblasts in a serum-free culture system in a concentration dependent manner. However, due to time constraints, this chapter did not directly assess the mediators present in the conditioned media that promote the fibroblast proliferation, thus the contribution of mediators to the fibroblast growth stimulatory activity in the conditioned media could not be confirmed in this study.

7.2 Future Work

Under normal wound healing, myofibroblasts disappear from the repaired wound site via programmed cell death. Persistence of myofibroblasts likely depends on a variety of mediators released from the resident or infiltrating cells and causes hypertrophic scarring and fibrosis (Ramos *et al.*, 2006). Furthermore, myofibroblasts are resistant to apoptosis under pathological conditions. Therefore, strategies that promote myofibroblast apoptosis may highlight effective therapies for the treatment of fibrotic disease.

Future work will be aimed at elucidating the mechanisms of cell apoptosis mediated by CG, trypsin and PAR_4 AP. Hence, the molecular mechanism upstream of caspase-3 should be investigated to identify whether the cell death is derived from the TNF/death receptor pathway (i.e. probe for caspase-8) or the mitochondrial pathway (i.e. probe for caspase-9 or cytochrome) .

Findings in this study also lead to the prediction that CG and trypsin induce anoikis (cell detachment dependent apoptosis) of lung and renal fibroblasts. CG-induced cell death of rat cardiomyocytes has been reported (Sabri *et al.*, 2003b). Mechanisms of anoikis have not been fully characterised but an ECM/integrin-focal adhesion kinase (FAK) pathway is known to play a central role, with loss of constitutive adhesion signalling by FAK being one of the early events (Schaller, 2001). Western blot analysis using lysates from agonist treated cells could be performed to study whether CG and trypsin could affect the phosphorylation activity of FAK. If FAK activity is affected, this would suggest that CG- and trypsin-induced cell death is cell detachment dependent.

Furthermore, the ability of CG and trypsin to stimulate the activities of MAP kinases ERK1/2, JNK and p38-MAP kinase over a series of concentrations and time points could be assessed by Western blotting using

antibodies against phosphorylated (activated) signalling proteins. In addition, the P13K/Akt signalling pathway is also known as a major pathway for cell survival (Datta *et al.*, 1999) and cleavage of Akt by activated caspases disables this cell survival signalling pathway (Rokudai *et al.*, 2000). Therefore, degradation of Akt following CG or trypsin treatment could be assessed using Western blotting. All these experiments should be performed alongside the apoptosis experiments.

For PAR_4 driven apoptosis responses, it is plausible that the mechanism of cell death might mimic that reported for PAR_1 in bronchial epithelial cells (i.e. mitochondrial pathway) (Suzuki *et al.*, 2005). Similar to those experiments proposed for CG and trypsin above, activation of one or more of the three major MAP kinases (ERK1/2, JNK and p38-MAP kinases) induced by PAR_4 should be investigated. MAP kinase inhibitors could be used to assess which of these MAP kinases plays a role in the PAR_4 induced cell death.

Finally, it would be interesting to determine the cytokines or mediators that are present in the conditioned media. This could be done by using the commercially available enzyme-linked immunosorbent assay (ELISA) kits. The developments made in these areas have important clinical implications. However, several questions need to be considered before cytokine or antibody therapy can be effectively applied clinically. These include safety issues, dosage, treatment regimens and effective delivery systems. Furthermore, the majority of research has focused on targeting single mediator. It is likely that the combinations of cytokines and antibodies, or other agents such as protease inhibitors, will be more beneficial.

7.3 Conclusion

In conclusion, fibroblast activation, proliferation and apoptosis represent a useful experimental system for understanding the general biological processes of repair and remodelling after tissue injury. Continued exploration along the line of this thesis may ultimately shed lights on new therapies for fibrotic diseases based on pharmacological of apoptosis.

Appendix

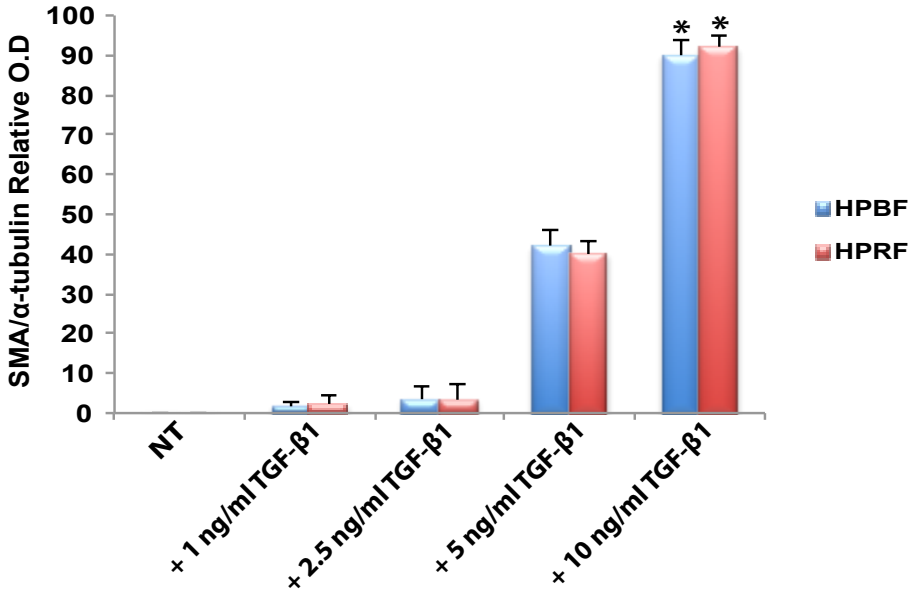

Figure A.1: Optimisation of the TGF-β concentration in the Induction of α-SMA. Quiescent HPBFs and HPRFs were stimulated with different concentration of TGF-β1 under serum free conditions for 24 h. Cell lysates were obtained and then subjected to SDS-PAGE followed by immunoblotting with antibodies against α-SMA and α-tubulin. Results were quantitated and summarised in a bar chart, where optical density was normalised against the α-tubulin. Results are expressed as mean $\pm$ SEM of three independent experiments. * indicates $p < 0.05$ compared with no treatment control (no TGF-β1 added) in one-way ANOVA with Dunnett's post hoc test.

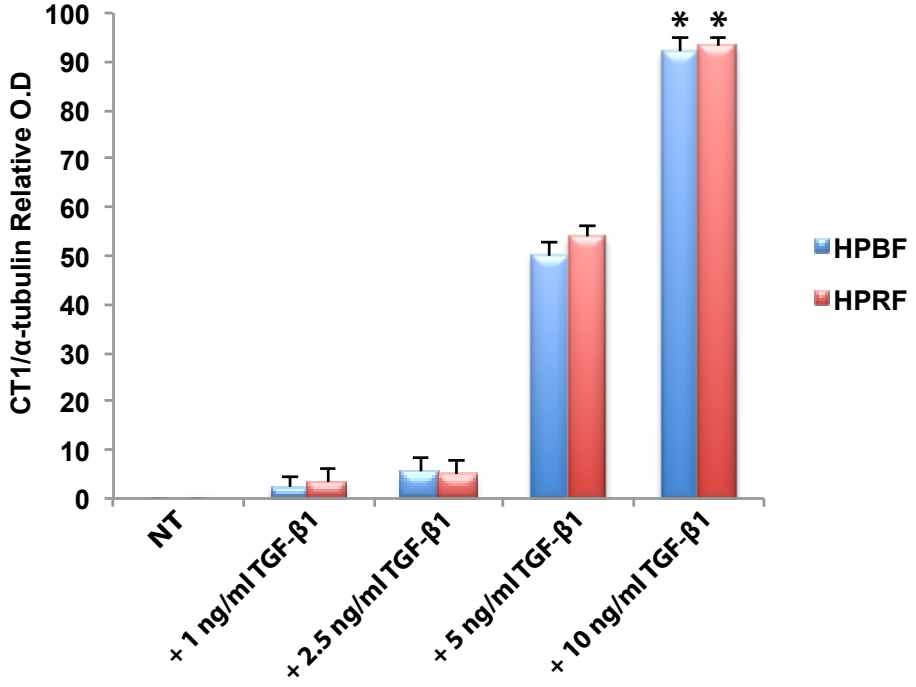

Figure A.2: Optimisation of the TGF-β concentration in the Induction of Collagen Type 1 expression. Quiescent HPBFs and HPRFs were stimulated with different concentration of TGF-β1 under serum free conditions for 24 h. Cell lysates were obtained and then subjected to SDS-PAGE followed by immunoblotting with antibodies against collagen type 1 and α-tubulin. Results were quantitated and summarised in a bar chart, where optical density was normalised against the α-tubulin. Results are expressed as mean $\pm$ SEM of three independent experiments. * indicates $p < 0.05$ compared with no treatment control (no TGF-β1 added) in one-way ANOVA with Dunnett's post hoc test.

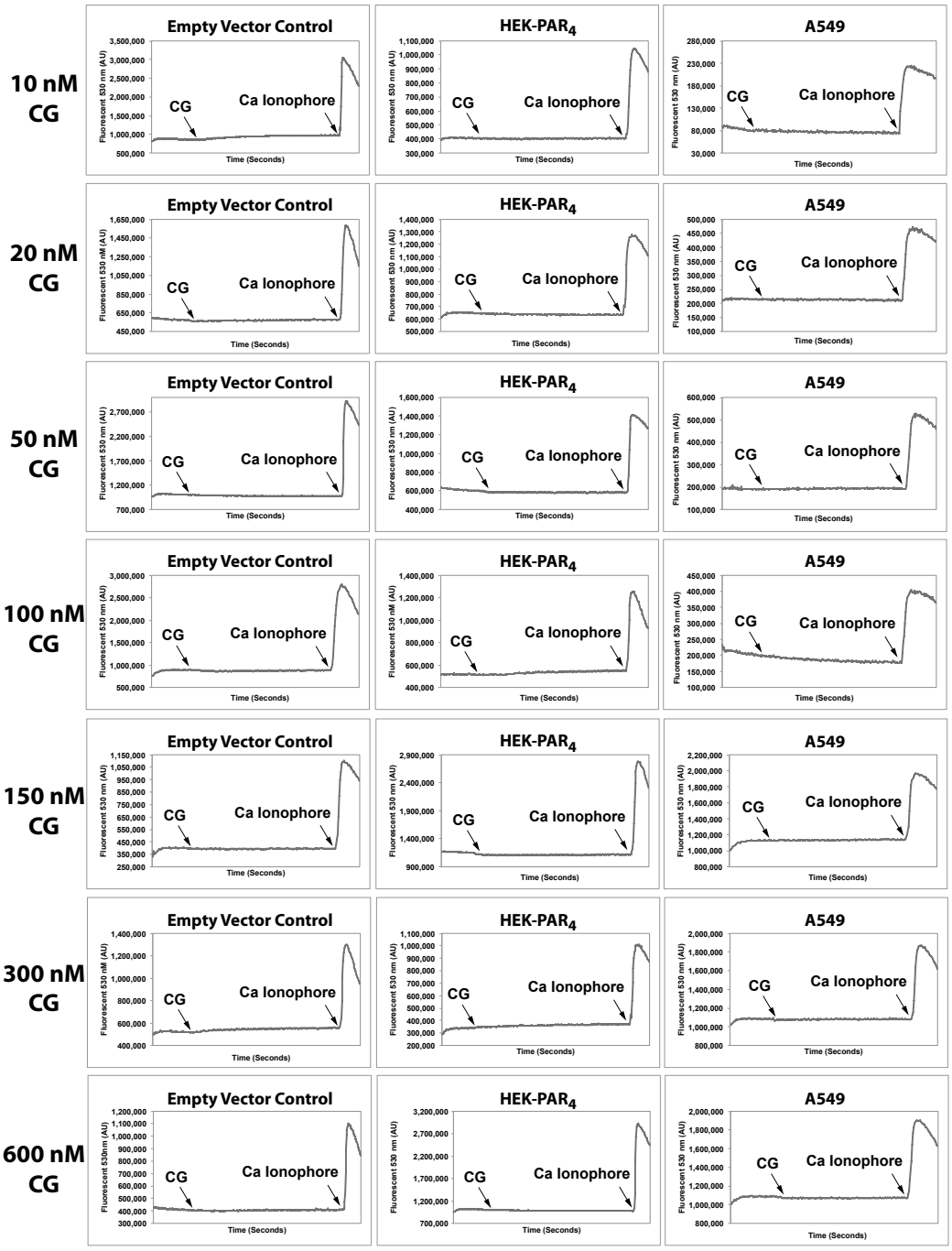
10 nM CG
20 nM CG
50 nM CG
100 nM CG
150 nM CG
300 nM CG
600 nM CG
Empty Vector Control
HEK-PAR4
A549
CG
Ca Ionophore
Time (Seconds)

Figure A.3: Optimisation of the Concentrations of CG in Calcium Mobilisation Assay. Cells at 70-85% confluence in 75 cm^2 flasks were harvested and incubated with Fluo-3 AM at room temperature for 25 min. Cells were then washed and resuspended in calcium assay buffer. Functional PAR_4 activities were assessed by treating the cells with different concentrations of CG as indicated. An increase in fluorescence (E530) monitored by fluorescence spectrophotometer is indicative of calcium mobilisation. Arrows indicate the time when test agonists were added. These results represent data from three independent experiments.

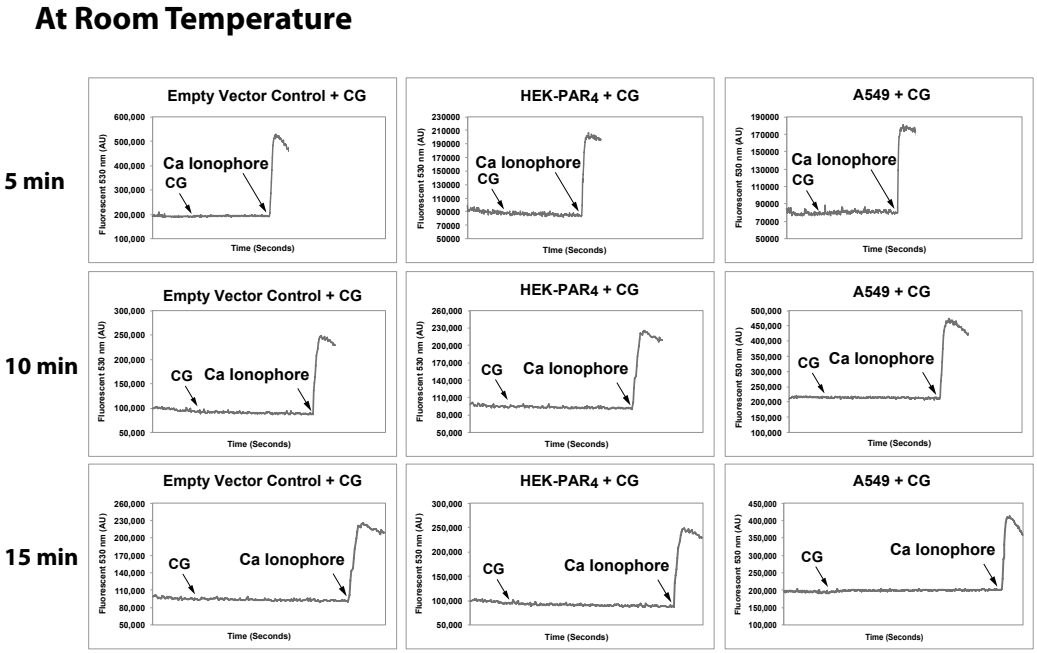

Figure A.4: Optimisation of the action of CG in Various Incubation Time at Room Temperature. Cells at 70-85% confluence in 75 cm^2 flasks were harvested and incubated with Fluo-3 AM at room temperature for 25 min. Cells were then washed and resuspended in calcium assay buffer. Functional PAR_4 activities were assessed by treating the cells with CG for 5, 10 and 15 min at room temperature. An increase in fluorescence (E530) monitored by fluorescence spectrophotometer is indicative of calcium mobilisation. Arrows indicate the time when test agonists were added. These results represent data from three independent experiments.

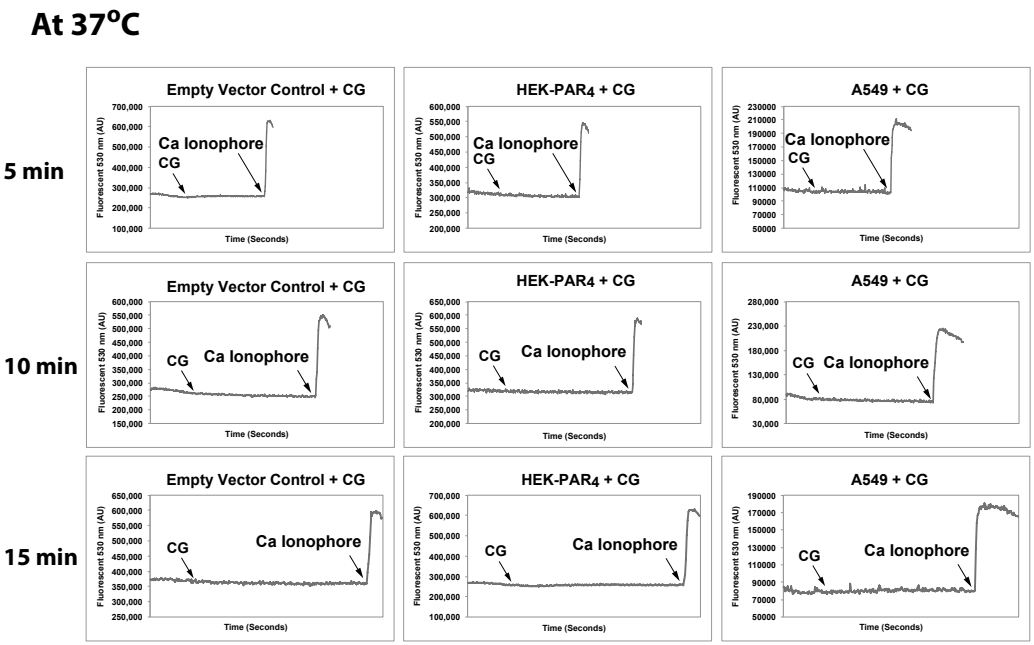

Figure A.5: Optimisation of the action of CG in Various Incubation Time at 37°C. Cells at 70-85% confluence in 75 cm^2 flasks were harvested and incubated with Fluo-3 AM at room temperature for 25 min. Cells were then washed and resuspended in calcium assay buffer. Functional PAR_4 activities were assessed by treating the cells with CG for 5, 10 and 15 min at 37°C. An increase in fluorescence (E530) monitored by fluorescence spectrophotometer is indicative of calcium mobilisation. Arrows indicate the time when test agonists were added. These results represent data from three independent experiments.

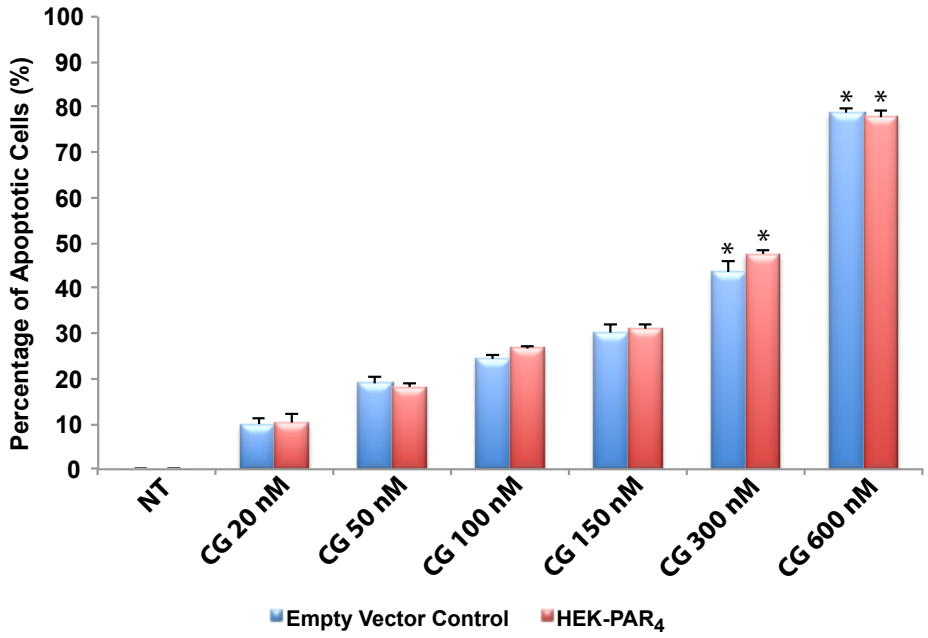

Figure A.6: Optimisation of the concentrations of CG in the Induction of Cell Apoptosis. Cells at 70-85% confluence in 6-well plate were quiesced and treated with different concentrations of the CG for 24 h. The cells were then incubated with FITC-conjugated Annexin V and propidium iodide in the dark. Binding of Annexin V/PI to empty vector control and HEK-PAR_4 cells that were exposed to different concentrations of CG was evaluated by flow cytometry. Results are expressed as percentage of apoptotic cells, presented as the mean ± SEM of three independent experiments. * indicates $p < 0.05$ compared with NT in one way ANOVA with Dunnett's post hoc test. ** indicates $p < 0.05$ between empty vector control and HEK-PAR_4 Cells in one way ANOVA with Bonferroni post hoc test.

Abbreviations

A549	Adenocarcinomic human alveolar basal epithelial cell
ACT	α1-antichymotrypsin
AEC	Alveolar epithelial cell
AKI	Acute kidney injury
AP	Activating peptide
Apaf-1	Apoptotic protease-activating factor 1
APS	Ammonium persulphate
ATP	Adenosine-5'-triphosphate
Bcl-2	B cell lymphoma-2
BICD1	Bicaudal D homolog 1
bFGF	Basic fibroblast growth factor
BMP	Bone morphogenic protein
bp	Base pair
BSA	Bovine serum albumin
CAB	Calcium assay buffer
CAM	Cell adhesion molecule
cAMP	Cyclic adenosine monophosphate
CBB	Coomassie brilliant blue
cDNA	Complementary DNA
CG	Cathepsin G
CKD	Chronic kidney disease
CTFG	Connective tissue growth factor
DAB	3,3'-diaminobenzinetetrahydrochloride

DAG	Diacylglycerol
DEPC	Diethylpyrocarbonate
DMEM	Dulbecco's modified Eagle's medium
DMSO	Dimethyl sulfoxide
DNA	Deoxyribonucleic acid
dNTP	Deoxynucleptide tri-phosphate
ECL2	Extracellular loop 2
ECL	Enhanced chemiluminescence
ECM	Extracellular matrix
ED-A	Ectodysplasin-A
EDTA	Ethylene diamine tetraacetic acid
EGF	Epidermal growth factor
EGFP	Enhanced green fluorescent protein
EGTA	Ethylene glycol tetraacetic acid
ELISA	Enzyme-linked immunosorbent assay
EMT	Epithelial-mesenchymal transition
EndoMT	Endothelial-mesenchymal transition
ERK	Extracellular signal-regulated kinase
FACS	Fluorescence-activated cell sorting
FAK	Focal adhesion kinase
FasL	Fas ligand
FBS	Foetal bovine serum
FGF	Fibroblast growth factor
FITC	Fluorescien isothiocyanate
Fluo-3 AM	Fluo-3 acetoxymethyl ester
GM-CSF	Granulocyte-macrophage colony-stimulating factor
GPCR	G protein-coupled receptor
GRK	G protein-couped receptor kinase
GTP	Guanosine triphosphate
H_2O_2	Hydrogen peroxide
HEK293	Human embryonic kidney 293 cell

HEPES	4-(2-hydroxyethyl)piperazine-1-ethanesulfonic acid
$hPAR_4$	Human PAR_4
HPBF	Human primary bronchial fibroblast
HPRF	Human primary renal fibroblast
HRP	Horseradish peroxidase
IFN	Interferon
IGF-2	Insulin-like growth factor
IL	Interleukin
InsP3	Inositol 1,4,5-triphosphate
IPF	Idiopathic pulmonary brosis
JNK	Jun amino-terminal kinase
kb	kilobase
kDa	kilo Dalton
LAP	Latency-associated peptide
LN-CAP cells	Androgen-sensitive human prostate adenocarcinoma cells
LPS	Lipopolysaccharide
MAPK	Mitogen-activated protein kinase
mRNA	Messenger RNA
NC	Negative control
NFkB	Nuclear Factor-KappaB
NRK52E	Normal rat kidney epithelial cell
nt	Nucleotide
PAGE	Polyacrylamide gel electrophoresis
PAR	Proteinase-activated receptor
PAK	p21 activated kinase
PBS	Phosphate buffered saline
PBS-T	Phosphate buffered saline with Tween-20
PCR	Polymerase chain reaction
PDGF	Platelet-derived growth factor
PGE_2	Prostaglandin E_2
PI	Propidium iodide

PIPES	1,4-Piperazinediethanesulfonic acid
PI3	Phosphatidylinositol 3
PKC	Protein kinase C
PLC	Phospholipase C
PMSF	Phenylmethylsulfonyl fluoride
PMN	Polymorphonuclear leukocytes neutrophil
POMC	Pro-opiomelanocortin
PS	Phosphatidylserine
RA	Rheumatoid arthritis
rDNase	Recombinant DNase
ROS	Reactive oxygen species
RNA	Ribonucleic acid
RNases	Ribonucleases
RPMI	Roswell Park Memorial Institute
RT-PCR	Reverse transcription PCR
SDS-PAGE	Sodium dodecyl sulfate polyacrylamide gel electrophoresis
SEM	Standard error of the mean
SMA	Smooth muscle actin
SNX1	Sorting nexin 1
TAE	Tris-acetate-EDTA
TBS	Tris-buffered saline
TBS-T	Tris-buffered saline with Tween-20
TBS-Tx	Tris-buffered saline with Triton X-100
TEMED	N,N,N′,N′-tetramethylethylenediamine
TGF	Transforming growth factor
TNF	Tumour necrosis factor
UV	Ultra violet

Bibliography

Abbate, M., C. Zoja, D. Rottoli, D. Corna, S. Tomasoni, *et al.*, 2002 Proximal tubular cells promote fibrogenesis by tgf-beta1-mediated induction of peritubular myofibroblasts. Kidney Int **61**: 2066–77.

Abboud, H. E., 1993 Growth factors in glomerulonephritis. Kidney International **43**: 252–67.

Abe, R., S. C. Donnelly, T. Peng, R. Bucala, and C. N. Metz, 2001 Peripheral blood fibrocytes: differentiation pathway and migration to wound sites. J Immunol **166**: 7556–62.

Adamczak, M., M.-L. Gross, J. Krtil, A. Koch, K. Tyralla, *et al.*, 2003 Reversal of glomerulosclerosis after high-dose enalapril treatment in subtotally nephrectomized rats. J Am Soc Nephrol **14**: 2833–42.

Adamson, I. Y., L. Young, and D. H. Bowden, 1988 Relationship of alveolar epithelial injury and repair to the induction of pulmonary fibrosis. Am J Pathol **130**: 377–83.

Akers, I. A., M. Parsons, M. R. Hill, M. D. Hollenberg, S. Sanjar, *et al.*, 2000 Mast cell tryptase stimulates human lung fibroblast proliferation via protease-activated receptor-2. Am J Physiol Lung Cell Mol Physiol **278**: L193–201.

Alikhani, M., Z. Alikhani, M. Raptis, and D. T. Graves, 2004 Tnf-alpha in vivo stimulates apoptosis in fibroblasts through caspase-8

activation and modulates the expression of pro-apoptotic genes. J Cell Physiol **201**: 341–8.

Allt, G., and J. G. Lawrenson, 2001 Pericytes: cell biology and pathology. Cells Tissues Organs (Print) **169**: 1–11.

Ando, S., H. Otani, Y. Yagi, K. Kawai, H. Araki, *et al.*, 2007a Protease-activated receptor 4-mediated ca2+ signaling in mouse lung alveolar epithelial cells. Life sciences **81**: 794–802.

Ando, S., H. Otani, Y. Yagi, K. Kawai, H. Araki, *et al.*, 2007b Proteinase-activated receptor 4 stimulation-induced epithelial-mesenchymal transition in alveolar epithelial cells. Respir Res **8**: 31.

Ando, S., H. Otani, Y. Yagi, K. Kawai, H. Araki, *et al.*, 2007c Proteinase-activated receptor 4 stimulation-induced epithelial-mesenchymal transition in alveolar epithelial cells. Respiratory Research **8**: 31–31.

Anscher, M. S., W. P. Peters, H. Reisenbichler, W. P. Petros, and R. L. Jirtle, 1993 Transforming growth factor beta as a predictor of liver and lung fibrosis after autologous bone marrow transplantation for advanced breast cancer. N Engl J Med **328**: 1592–8.

Aragay, A. M., L. R. Collins, G. R. Post, A. J. Watson, J. R. Feramisco, *et al.*, 1995 G12 requirement for thrombin-stimulated gene expression and dna synthesis in 1321n1 astrocytoma cells. J Biol Chem **270**: 20073–7.

Arora, P., T. K. Ricks, and J. Trejo, 2007 Protease-activated receptor signalling, endocytic sorting and dysregulation in cancer. J Cell Sci **120**: 921–8.

Asokananthan, N., P. T. Graham, J. Fink, D. A. Knight, A. J. Bakker, *et al.*, 2002 Activation of protease-activated receptor (par)-1,

par-2, and par-4 stimulates il-6, il-8, and prostaglandin e2 release from human respiratory epithelial cells. J Immunol **168**: 3577–85.

Azuma, A., T. Nukiwa, E. Tsuboi, M. Suga, S. Abe, *et al.*, 2005 Double-blind, placebo-controlled trial of pirfenidone in patients with idiopathic pulmonary fibrosis. American Journal of Respiratory and Critical Care Medicine **171**: 1040–7.

Babich, M., K. L. King, and R. A. Nissenson, 1990 Thrombin stimulates inositol phosphate production and intracellular free calcium by a pertussis toxin-insensitive mechanism in osteosarcoma cells. Endocrinology **126**: 948–54.

Bae, J.-S., and A. R. Rezaie, 2008 Protease activated receptor 1 (par-1) activation by thrombin is protective in human pulmonary artery endothelial cells if endothelial protein c receptor is occupied by its natural ligand. Thromb Haemost : 1–17.

Baffy, G., L. Yang, S. Raj, D. R. Manning, and J. R. Williamson, 1994 G protein coupling to the thrombin receptor in chinese hamster lung fibroblasts. J Biol Chem **269**: 8483–7.

Balzar, S., H. W. Chu, P. Silkoff, M. Cundall, J. B. Trudeau, *et al.*, 2005 Increased tgf-beta2 in severe asthma with eosinophilia. J Allergy Clin Immunol **115**: 110–7.

Banfi, C., M. Brioschi, S. Lento, A. Pirillo, S. Galli, *et al.*, 2011 Statins prevent tissue factor induction by protease-activated receptors 1 and 2 in human umbilical vein endothelial cells in vitro. J Thromb Haemost **9**: 1608–19.

Bar-Shavit, R., A. Kahn, J. W. Fenton, and G. D. Wilner, 1983a Chemotactic response of monocytes to thrombin. The Journal of cell biology **96**: 282–5.

Bar-Shavit, R., A. Kahn, G. D. Wilner, and J. W. Fenton, 1983b Monocyte chemotaxis: stimulation by specific exosite region in thrombin. Science **220**: 728–31.

Bar-Shavit, R., M. Maoz, Y. Yongjun, M. Groysman, I. Dekel, *et al.*, 2002 Signalling pathways induced by protease-activated receptors and integrins in t cells. Immunology **105**: 35–46.

Barbas-Filho, J. V., M. A. Ferreira, A. Sesso, R. A. Kairalla, C. R. Carvalho, *et al.*, 2001 Evidence of type ii pneumocyte apoptosis in the pathogenesis of idiopathic pulmonary fibrosis (ifp)/usual interstitial pneumonia (uip). J Clin Pathol **54**: 132–8.

Bardales, R. H., S. S. Xie, R. F. Schaefer, and S. M. Hsu, 1996 Apoptosis is a major pathway responsible for the resolution of type ii pneumocytes in acute lung injury. Am J Pathol **149**: 845–52.

Barnes, J. L., and Y. Gorin, 2011 Myofibroblast differentiation during fibrosis: role of nad(p)h oxidases. Kidney International : 1–13.

Bataller, R., and D. A. Brenner, 2005 Liver fibrosis. J Clin Invest **115**: 209–18.

Baumgartner, K. B., J. M. Samet, D. B. Coultas, C. A. Stidley, W. C. Hunt, *et al.*, 2000 Occupational and environmental risk factors for idiopathic pulmonary fibrosis: a multicenter case-control study. collaborating centers. Am J Epidemiol **152**: 307–15.

Baumgartner, K. B., J. M. Samet, C. A. Stidley, T. V. Colby, and J. A. Waldron, 1997 Cigarette smoking: a risk factor for idiopathic pulmonary fibrosis. Am J Respir Crit Care Med **155**: 242–8.

Belham, C. M., R. J. Tate, P. H. Scott, A. D. Pemberton, H. R. Miller, *et al.*, 1996 Trypsin stimulates proteinase-activated receptor-2-dependent and -independent activation of mitogen-activated protein kinases. Biochem J **320 (Pt 3)**: 939–46.

Berger, P., D. W. Perng, H. Thabrew, S. J. Compton, J. A. Cairns, *et al.*, 2001a Tryptase and agonists of par-2 induce the proliferation of human airway smooth muscle cells. J Appl Physiol **91**: 1372–9.

Berger, P., J. M. Tunon-De-Lara, J. P. Savineau, and R. Marthan, 2001b Selected contribution: tryptase-induced par-2-mediated ca(2+) signaling in human airway smooth muscle cells. J Appl Physiol **91**: 995–1003.

Bertog, M., B. Letz, W. Kong, M. Steinhoff, M. A. Higgins, *et al.*, 1999 Basolateral proteinase-activated receptor (par-2) induces chloride secretion in m-1 mouse renal cortical collecting duct cells. J Physiol (Lond) **521 Pt 1**: 3–17.

Bitterman, P. B., M. D. Wewers, S. I. Rennard, S. Adelberg, and R. G. Crystal, 1986 Modulation of alveolar macrophage-driven fibroblast proliferation by alternative macrophage mediators. The Journal of clinical investigation **77**: 700–8.

Blanc-Brude, O. P., F. Archer, P. Leoni, C. Derian, S. Bolsover, *et al.*, 2005 Factor xa stimulates fibroblast procollagen production, proliferation, and calcium signaling via par1 activation. Exp Cell Res **304**: 16–27.

Bogatkevich, G. S., E. Gustilo, J. C. Oates, C. Feghali-Bostwick, R. A. Harley, *et al.*, 2005 Distinct pkc isoforms mediate cell survival and dna synthesis in thrombin-induced myofibroblasts. Am J Physiol Lung Cell Mol Physiol **288**: L190–201.

Böhm, S. K., L. M. Khitin, E. F. Grady, G. Aponte, D. G. Payan, *et al.*, 1996 Mechanisms of desensitization and resensitization of proteinase-activated receptor-2. J Biol Chem **271**: 22003–16.

Bonniaud, P., M. Kolb, T. Galt, J. Robertson, C. Robbins, *et al.*, 2004 Smad3 null mice develop airspace enlargement and are resistant to tgf-beta-mediated pulmonary fibrosis. J Immunol **173**: 2099–108.

Boor, P., K. Šebeková, T. Ostendorf, and J. Floege, 2007 Treatment targets in renal fibrosis. Nephrology Dialysis Transplantation **22**: 3391.

Borensztajn, K. S., M. F. Bijlsma, A. P. Groot, L. W. Brüggemann, H. H. Versteeg, *et al.*, 2007 Coagulation factor xa drives tumor cells into apoptosis through bh3-only protein bim up-regulation. Exp Cell Res **313**: 2622–33.

Borensztajn, K. S., and C. A. Spek, 2008 Protease-activated receptors, apoptosis and tumor growth. Pathophysiol Haemos Thromb **36**: 137–47.

Bouton, M. C., M. Jandrot-Perrus, S. Moog, J. P. Cazenave, M. C. Guillin, *et al.*, 1995 Thrombin interaction with a recombinant n-terminal extracellular domain of the thrombin receptor in an acellular system. Biochem J **305 (Pt 2)**: 635–41.

Brady, H. R., 1994 Leukocyte adhesion molecules and kidney diseases. Kidney Int **45**: 1285–300.

Brass, L. F., R. R. Vassallo, E. Belmonte, M. Ahuja, K. Cichowski, *et al.*, 1992 Structure and function of the human platelet thrombin receptor. studies using monoclonal antibodies directed against a defined domain within the receptor n terminus. J Biol Chem **267**: 13795–8.

Breeze, R. G., and E. B. Wheeldon, 1977 The cells of the pulmonary airways. Am Rev Respir Dis **116**: 705–77.

Brenmoehl, J., S. Miller, and C. Hofmann. . . , 2009 Transforming growth factor-1 induces intestinal myofibroblast differentiation and modulates their migration. World Journal of . . . .

Bretschneider, E., R. Kaufmann, M. Braun, G. Nowak, E. Glusa, *et al.*, 2001 Evidence for functionally active protease-activated receptor-4 (par-4) in human vascular smooth muscle cells. Br J Pharmacol **132**: 1441–6.

Bucala, R., L. A. Spiegel, J. Chesney, M. Hogan, and A. Cerami, 1994 Circulating fibrocytes define a new leukocyte subpopulation that mediates tissue repair. Mol Med **1**: 71–81.

Budihardjo, I., H. Oliver, M. Lutter, X. Luo, and X. Wang, 1999 Biochemical pathways of caspase activation during apoptosis. Annu Rev Cell Dev Biol **15**: 269–90.

Budinger, G. R. S., G. M. Mutlu, J. Eisenbart, A. C. Fuller, A. A. Bellmeyer, *et al.*, 2006 Proapoptotic bid is required for pulmonary fibrosis. Proc Natl Acad Sci USA **103**: 4604–9.

Cabrera-Vera, T. M., J. Vanhauwe, T. O. Thomas, M. Medkova, A. Preininger, *et al.*, 2003 Insights into g protein structure, function, and regulation. Endocr Rev **24**: 765–81.

Camelliti, P., T. K. Borg, and P. Kohl, 2005 Structural and functional characterisation of cardiac fibroblasts. Cardiovasc Res **65**: 40–51.

Chambers, L. S., J. L. Black, Q. Ge, S. M. Carlin, W. W. Au, *et al.*, 2003 Par-2 activation, pge2, and cox-2 in human asthmatic and nonasthmatic airway smooth muscle cells. Am J Physiol Lung Cell Mol Physiol **285**: L619–27.

Chambers, R., P. Leoni, O. Blanc-Brude, D. Wembridge, and G. Laurent, 2000 Thrombin is a potent inducer of connective tissue growth factor production via proteolytic activation of protease-activated receptor-1. Journal of Biological Chemistry **275**: 35584.

Chambers, R. C., K. Dabbagh, R. J. McAnulty, A. J. Gray, O. P. Blanc-Brude, *et al.*, 1998 Thrombin stimulates fibroblast procollagen

production via proteolytic activation of protease-activated receptor 1. Biochem J **333 (Pt 1)**: 121–7.

Chang, F.-C., Y.-H. Chou, Y.-T. Chen, and S.-L. Lin, 2012 Novel insights into pericyte-myofibroblast transition and therapeutic targets in renal fibrosis. J Formos Med Assoc **111**: 589–98.

Chapman, H. A., 1999 A fas pathway to pulmonary fibrosis. J Clin Invest **104**: 1–2.

Chaqour, B., R. Yang, and Q. Sha, 2006 Mechanical stretch modulates the promoter activity of the profibrotic factor ccn2 through increased actin polymerization and nf-kappab activation. J Biol Chem **281**: 20608–22.

Chen, B., M. R. Dores, N. Grimsey, I. Canto, B. L. Barker, *et al.*, 2011a Adaptor protein complex-2 (ap-2) and epsin-1 mediate protease-activated receptor-1 internalization via phosphorylation- and ubiquitination-dependent sorting signals. J Biol Chem **286**: 40760–70.

Chen, Y.-T., F.-C. Chang, C.-F. Wu, Y.-H. Chou, H.-L. Hsu, *et al.*, 2011b Platelet-derived growth factor receptor signaling activates pericyte-myofibroblast transition in obstructive and post-ischemic kidney fibrosis. Kidney Int **80**: 1170–81.

Chignard, M., and D. Pidard, 2006 Neutrophil and pathogen proteinases versus proteinase-activated receptor-2 lung epithelial cells: more terminators than activators. American Journal of Respiratory Cell and Molecular Biology **34**: 394–8.

Choudhury, G. G., F. Marra, and H. E. Abboud, 1996 Thrombin stimulates association of src homology domain containing adaptor protein nck with pp125fak. Am J Physiol **270**: F295–300.

Chua, F., S. E. Dunsmore, P. H. Clingen, S. E. Mutsaers, S. D. Shapiro, *et al.*, 2007 Mice lacking neutrophil elastase are resistant to bleomycin-induced pulmonary fibrosis. Am J Pathol **170**: 65–74.

Clark, R. A., 1989 Wound repair. Curr Opin Cell Biol **1**: 1000–8.

Clarke, E. J., and V. Allan, 2002 Intermediate filaments: vimentin moves in. Curr Biol **12**: R596–8.

Cocks, T. M., and J. D. Moffatt, 2000 Protease-activated receptors: sentries for inflammation? Trends in pharmacological sciences **21**: 103–8.

Compton, S., B. Renaux, S. Wijesuriya, and M. Hollenberg, 2001 Glycosylation and the activation of proteinaseactivated receptor 2 (par2) by human mast cell tryptase. British journal of pharmacology **134**: 705–718.

Conant, K., N. Haughey, A. Nath, C. S. Hillaire, D. S. Gary, *et al.*, 2002 Matrix metalloproteinase-1 activates a pertussis toxin-sensitive signaling pathway that stimulates the release of matrix metalloproteinase-9. J Neurochem **82**: 885–93.

Connolly, A. J., H. Ishihara, M. L. Kahn, R. V. Farese, and S. R. Coughlin, 1996 Role of the thrombin receptor in development and evidence for a second receptor. Nature **381**: 516–9.

Considine, T., S. Geary, A. Kelly, and P. McSweeney, 2002 Proteolytic specificity of cathepsin g on bovine ¡ sub¿ s1¡/sub¿-and -caseins. Food chemistry .

Cottrell, G. S., S. Amadesi, E. F. Grady, and N. W. Bunnett, 2004 Trypsin iv, a novel agonist of protease-activated receptors 2 and 4. J Biol Chem **279**: 13532–9.

Cumashi, A., H. Ansuini, N. Celli, A. D. Blasi, P. J. O'Brien, *et al.*, 2001 Neutrophil proteases can inactivate human par3 and abolish the co-receptor function of par3 on murine platelets. Thromb Haemost **85**: 533–8.

Cunningham, M. A., E. Rondeau, X. Chen, S. R. Coughlin, S. R. Holdsworth, *et al.*, 2000 Protease-activated receptor 1 mediates

thrombin-dependent, cell-mediated renal inflammation in crescentic glomerulonephritis. J Exp Med **191**: 455–62.

D'Andrea, M. R., C. K. Derian, D. Leturcq, S. M. Baker, A. Brunmark, *et al.*, 1998 Characterization of protease-activated receptor-2 immunoreactivity in normal human tissues. J Histochem Cytochem **46**: 157–64.

D'Andrea, M. R., C. K. Derian, R. J. Santulli, and P. Andrade-Gordon, 2001 Differential expression of protease-activated receptors-1 and -2 in stromal fibroblasts of normal, benign, and malignant human tissues. Am J Pathol **158**: 2031–41.

Darrow, A. L., W. P. Fung-Leung, R. D. Ye, R. J. Santulli, W. M. Cheung, *et al.*, 1996 Biological consequences of thrombin receptor deficiency in mice. Thromb Haemost **76**: 860–6.

Datta, S. R., A. Brunet, and M. E. Greenberg, 1999 Cellular survival: a play in three akts. Genes Dev **13**: 2905–27.

Dean, D. C., R. F. Newby, and S. Bourgeois, 1988 Regulation of fibronectin biosynthesis by dexamethasone, transforming growth factor beta, and camp in human cell lines. The Journal of cell biology **106**: 2159–70.

DeFea, K. A., J. Zalevsky, M. S. Thoma, O. Déry, R. D. Mullins, *et al.*, 2000 beta-arrestin-dependent endocytosis of proteinase-activated receptor 2 is required for intracellular targeting of activated erk1/2. The Journal of cell biology **148**: 1267–81.

Déry, O., C. U. Corvera, M. Steinhoff, and N. W. Bunnett, 1998 Proteinase-activated receptors: novel mechanisms of signaling by serine proteases. Am J Physiol **274**: C1429–52.

Déry, O., M. S. Thoma, H. Wong, E. F. Grady, and N. W. Bunnett, 1999 Trafficking of proteinase-activated receptor-2 and beta-arrestin-1

tagged with green fluorescent protein. beta-arrestin-dependent endocytosis of a proteinase receptor. J Biol Chem **274**: 18524–35.

Desmoulière, A., C. Chaponnier, and G. Gabbiani, 2005 Tissue repair, contraction, and the myofibroblast. Wound Repair Regen **13**: 7–12.

Desmoulière, A., I. A. Darby, and G. Gabbiani, 2003 Normal and pathologic soft tissue remodeling: role of the myofibroblast, with special emphasis on liver and kidney fibrosis. Lab Invest **83**: 1689–707.

Desmoulière, A., A. Geinoz, F. Gabbiani, and G. Gabbiani, 1993 Transforming growth factor-beta 1 induces alpha-smooth muscle actin expression in granulation tissue myofibroblasts and in quiescent and growing cultured fibroblasts. The Journal of cell biology **122**: 103–11.

Desmoulière, A., M. Redard, I. Darby, and G. Gabbiani, 1995 Apoptosis mediates the decrease in cellularity during the transition between granulation tissue and scar. Am J Pathol **146**: 56–66.

Direkze, N. C., S. J. Forbes, M. Brittan, T. Hunt, R. Jeffery, *et al.*, 2003 Multiple organ engraftment by bone-marrow-derived myofibroblasts and fibroblasts in bone-marrow-transplanted mice. Stem Cells **21**: 514–20.

Dowdy, S. C., A. Mariani, M. M. Reinholz, G. L. Keeney, T. C. Spelsberg, *et al.*, 2005 Overexpression of the tgf-beta antagonist smad7 in endometrial cancer. Gynecol Oncol **96**: 368–73.

Drakopanagiotakis, F., A. Xifteri, V. Polychronopoulos, and D. Bouros, 2008 Apoptosis in lung injury and fibrosis. Eur Respir J **32**: 1631–8.

du Bois, R., 2012 An earlier and more confident diagnosis of idiopathic pulmonary fibrosis. European Respiratory Review .

Dulon, S., C. Candé, N. W. Bunnett, M. D. Hollenberg, M. Chignard, *et al.*, 2003 Proteinase-activated receptor-2 and human lung epithelial cells: disarming by neutrophil serine proteinases. Am J Respir Cell Mol Biol **28**: 339–46.

Earnshaw, W. C., L. M. Martins, and S. H. Kaufmann, 1999 Mammalian caspases: structure, activation, substrates, and functions during apoptosis. Annu Rev Biochem **68**: 383–424.

Eddy, A., 1996 Molecular insights into renal interstitial fibrosis. Journal of the American Society of Nephrology **7**: 2495.

Eddy, A. A., 1994 Experimental insights into the tubulointerstitial disease accompanying primary glomerular lesions. J Am Soc Nephrol **5**: 1273–87.

Eddy, A. A., 2000 Molecular basis of renal fibrosis. Pediatr Nephrol **15**: 290–301.

el Nahas, A. M., E. C. Muchaneta-Kubara, M. Essawy, and O. Soylemezoglu, 1997 Renal fibrosis: insights into pathogenesis and treatment. Int J Biochem Cell Biol **29**: 55–62.

Elger, M., D. Drenckhahn, R. Nobiling, P. Mundel, and W. Kriz, 1993 Cultured rat mesangial cells contain smooth muscle alpha-actin not found in vivo. Am J Pathol **142**: 497–509.

Elovic, A. E., H. Ohyama, A. Sauty, J. McBride, T. Tsuji, *et al.*, 1998 Il-4-dependent regulation of tgf-alpha and tgf-beta1 expression in human eosinophils. J Immunol **160**: 6121–7.

Elste, A. P., and I. Petersen, 2010 Expression of proteinase-activated receptor 1-4 (par 1-4) in human cancer. J Mol Histol **41**: 89–99.

Epperly, M. W., H. Guo, J. E. Gretton, and J. S. Greenberger, 2003 Bone marrow origin of myofibroblasts in irradiation pulmonary

fibrosis. American Journal of Respiratory Cell and Molecular Biology **29**: 213–24.

Erjefält, J. S., and C. G. Persson, 1997a Airway epithelial repair: breathtakingly quick and multipotentially pathogenic. Thorax **52**: 1010–2.

Erjefält, J. S., and C. G. Persson, 1997b Airway epithelial repair: breathtakingly quick and multipotentially pathogenic. Thorax **52**: 1010–2.

Erjefält, J. S., F. Sundler, and C. G. Persson, 1996 Eosinophils, neutrophils, and venular gaps in the airway mucosa at epithelial removal-restitution. Am J Respir Crit Care Med **153**: 1666–74.

Farahani, R. M., and L. C. Kloth, 2008 The hypothesis of 'biophysical matrix contraction': wound contraction revisited. Int Wound J **5**: 477–82.

Faruqi, T. R., E. J. Weiss, M. J. Shapiro, W. Huang, and S. R. Coughlin, 2000 Structure-function analysis of protease-activated receptor 4 tethered ligand peptides. determinants of specificity and utility in assays of receptor function. J Biol Chem **275**: 19728–34.

Fattman, C. L., 2008 Apoptosis in pulmonary fibrosis: too much or not enough? Antioxid Redox Signal **10**: 379–85.

Fee, J. A., J. D. Monsey, R. J. Handler, M. A. Leonis, S. R. Mullaney, *et al.*, 1994 A chinese hamster fibroblast mutant defective in thrombin-induced signaling has a low level of phospholipase c-beta 1. J Biol Chem **269**: 21699–708.

Fioretto, P., D. E. R. Sutherland, B. Najafian, and M. Mauer, 2006 Remodeling of renal interstitial and tubular lesions in pancreas transplant recipients. Kidney Int **69**: 907–12.

Floege, J., M. Burns, C. Alpers, and A. Yoshimura..., 1992 Glomerular cell proliferation and pdgf expression precede glomerulosclerosis in the remnant kidney model. Kidney Int .

Forbes, S. J., F. P. Russo, V. Rey, P. Burra, M. Rugge, *et al.*, 2004 A significant proportion of myofibroblasts are of bone marrow origin in human liver fibrosis. Gastroenterology **126**: 955–63.

Frazier, K., S. Williams, D. Kothapalli, H. Klapper, and G. R. Grotendorst, 1996 Stimulation of fibroblast cell growth, matrix production, and granulation tissue formation by connective tissue growth factor. J Invest Dermatol **107**: 404–11.

Fries, K. M., T. Blieden, R. J. Looney, G. D. Sempowski, M. R. Silvera, *et al.*, 1994 Evidence of fibroblast heterogeneity and the role of fibroblast subpopulations in fibrosis. Clin Immunol Immunopathol **72**: 283–92.

Fujiwara, M., E. Jin, M. Ghazizadeh, and O. Kawanami, 2005 Activation of par4 induces a distinct actin fiber formation via p38 mapk in human lung endothelial cells. J Histochem Cytochem **53**: 1121–9.

Fukuda, Y., M. Ishizaki, Y. Masuda, G. Kimura, O. Kawanami, *et al.*, 1987 The role of intraalveolar fibrosis in the process of pulmonary structural remodeling in patients with diffuse alveolar damage. Am J Pathol **126**: 171–82.

Furuhashi, I., K. Abe, T. Sato, and H. Inoue, 2008 Thrombin-stimulated proliferation of cultured human synovial fibroblasts through proteolytic activation of proteinase-activated receptor-1. J Pharmacol Sci **108**: 104–11.

Gabbiani, G., 2003 The myofibroblast in wound healing and fibrocontractive diseases. The Journal of pathology **200**: 500–503.

Gabbiani, G., G. B. Ryan, and G. Majne, 1971 Presence of modified fibroblasts in granulation tissue and their possible role in wound contraction. Experientia **27**: 549–50.

Gadek, J. E., G. A. Fells, R. L. Zimmerman, and R. G. Crystal, 1984 Role of connective tissue proteases in the pathogenesis of chronic inflammatory lung disease. Environ Health Perspect **55**: 297–306.

Gauldie, J., 2002 Pro: Inflammatory mechanisms are a minor component of the pathogenesis of idiopathic pulmonary fibrosis. Am J Respir Crit Care Med **165**: 1205–6.

Gerszten, R. E., J. Chen, M. Ishii, K. Ishii, L. Wang, *et al.*, 1994 Specificity of the thrombin receptor for agonist peptide is defined by its extracellular surface. Nature **368**: 648–51.

Gill, P. S., and C. S. Wilcox, 2006 Nadph oxidases in the kidney. Antioxid Redox Signal **8**: 1597–607.

Goldstein, R. H., and P. Polgar, 1982 The effect and interaction of bradykinin and prostaglandins on protein and collagen production by lung fibroblasts. J Biol Chem **257**: 8630–3.

Goltsev, Y. V., A. V. Kovalenko, E. Arnold, E. E. Varfolomeev, V. M. Brodianskii, *et al.*, 1997 Cash, a novel caspase homologue with death effector domains. J Biol Chem **272**: 19641–4.

Goor, H. V., G. Ding, D. Kees-Folts, J. Grond, G. F. Schreiner, *et al.*, 1994 Macrophages and renal disease. Lab Invest **71**: 456–64.

Grandaliano, G., P. Pontrelli, G. Cerullo, R. Monno, E. Ranieri, *et al.*, 2003 Protease-activated receptor-2 expression in iga nephropathy: a potential role in the pathogenesis of interstitial fibrosis. J Am Soc Nephrol **14**: 2072–83.

Green, D. R., 2000 Apoptotic pathways: paper wraps stone blunts scissors. Cell **102**: 1–4.

Grishina, Z., E. Ostrowska, W. Halangk, M. Sahin-Tóth, and G. Reiser, 2005 Activity of recombinant trypsin isoforms on human proteinase-activated receptors (par): mesotrypsin cannot activate epithelial par-1, -2, but weakly activates brain par-1. Br J Pharmacol **146**: 990–9.

Grotendorst, G. R., H. Rahmanie, and M. R. Duncan, 2004 Combinatorial signaling pathways determine fibroblast proliferation and myofibroblast differentiation. FASEB J **18**: 469–79.

Gui, Y., R. Loutzenhiser, and M. D. Hollenberg, 2003 Bidirectional regulation of renal hemodynamics by activation of par1 and par2 in isolated perfused rat kidney. Am J Physiol Renal Physiol **285**: F95–104.

Guzik, K., M. Bzowska, J. Smagur, O. Krupa, M. Sieprawska, *et al.*, 2007 A new insight into phagocytosis of apoptotic cells: proteolytic enzymes divert the recognition and clearance of polymorphonuclear leukocytes by macrophages. Cell Death Differ **14**: 171–82.

Hagimoto, N., K. Kuwano, I. Inoshima, M. Yoshimi, N. Nakamura, *et al.*, 2002 Tgf-beta 1 as an enhancer of fas-mediated apoptosis of lung epithelial cells. J Immunol **168**: 6470–8.

Hagimoto, N., K. Kuwano, H. Miyazaki, R. Kunitake, M. Fujita, *et al.*, 1997a Induction of apoptosis and pulmonary fibrosis in mice in response to ligation of fas antigen. Am J Respir Cell Mol Biol **17**: 272–8.

Hagimoto, N., K. Kuwano, H. Miyazaki, R. Kunitake, M. Fujita, *et al.*, 1997b Induction of apoptosis and pulmonary fibrosis in mice in response to ligation of fas antigen. Am J Respir Cell Mol Biol **17**: 272–8.

Hagimoto, N., K. Kuwano, Y. Nomoto, R. Kunitake, and N. Hara, 1997c Apoptosis and expression of fas/fas ligand mrna in bleomycin-induced pulmonary fibrosis in mice. American Journal of Respiratory Cell and Molecular Biology **16**: 91–101.

Hamilton, J., A. Frauman, and T. Cocks, 2001 Increased expression of protease-activated receptor-2 (par2) and par4 in human coronary artery by inflammatory stimuli unveils endothelium-dependent relaxations to par2 and par4 agonists. Circulation Research : 130109266.

Hansen, K. K., M. Saifeddine, and M. D. Hollenberg, 2004 Tethered ligand-derived peptides of proteinase-activated receptor 3 (par3) activate par1 and par2 in jurkat t cells. Immunology **112**: 183–90.

Hao, H., G. Gabbiani, E. Camenzind, M. Bacchetta, R. Virmani, *et al.*, 2006 Phenotypic modulation of intima and media smooth muscle cells in fatal cases of coronary artery lesion. Arterioscler Thromb Vasc Biol **26**: 326–32.

Harris, J., M. Wherlock, R. Rattihalli, R. Lennon, P. Mathieson, *et al.*, 2009 Fsgs plasma initiates specific signalling pathways in podocytes – evidence for an imbalance of circulating proteases in the pathogenesis of nephrotic syndromes. Renal Association meeting.

Hasdemir, B., J. E. Murphy, G. S. Cottrell, and N. W. Bunnett, 2009 Endosomal deubiquitinating enzymes control ubiquitination and down-regulation of protease-activated receptor 2. J Biol Chem **284**: 28453–66.

Hashimoto, N., H. Jin, T. Liu, S. W. Chensue, and S. H. Phan, 2004 Bone marrow-derived progenitor cells in pulmonary fibrosis. The Journal of clinical investigation **113**: 243–52.

Havasi, A., and S. C. Borkan, 2011 Apoptosis and acute kidney injury. Kidney International **80**: 29–40.

he Li, F., S. jie Xin, S. yang Zhang, Z. shi Cui, J. Gao, *et al.*, 2009 [the sonic hedgehog induce vascular adventitial fibroblasts phenotypic modulation, proliferation and migration]. Zhonghua Yi Xue Za Zhi **89**: 3079–82.

Hernández-Rodríguez, N. A., A. D. Cambrey, N. K. Harrison, R. C. Chambers, A. J. Gray, *et al.*, 1995 Role of thrombin in pulmonary fibrosis. Lancet **346**: 1071–3.

Hinz, B., 2006 Masters and servants of the force: the role of matrix adhesions in myofibroblast force perception and transmission. Eur J Cell Biol **85**: 175–81.

Hinz, B., 2007 Formation and function of the myofibroblast during tissue repair. J Investig Dermatol **127**: 526–37.

Hinz, B., S. H. Phan, V. J. Thannickal, A. Galli, M.-L. Bochaton-Piallat, *et al.*, 2007 The myofibroblast: one function, multiple origins. Am J Pathol **170**: 1807–16.

Hinz, B., S. H. Phan, V. J. Thannickal, M. Prunotto, A. Desmoulière, *et al.*, 2012 Recent developments in myofibroblast biology: paradigms for connective tissue remodeling. Am J Pathol **180**: 1340–55.

Hirano, F., A. Kobayashi, Y. Hirano, Y. Nomura, E. Fukawa, *et al.*, 2002 Thrombin-induced expression of rantes mrna through protease activated receptor-1 in human synovial fibroblasts. Ann Rheum Dis **61**: 834–7.

Holgate, S. T., D. E. Davies, P. M. Lackie, S. J. Wilson, S. M. Puddicombe, *et al.*, 2000 Epithelial-mesenchymal interactions in the pathogenesis of asthma. J Allergy Clin Immunol **105**: 193–204.

Holgate, S. T., J. Holloway, S. Wilson, P. H. Howarth, H. M. Haitchi, *et al.*, 2006 Understanding the pathophysiology of severe asthma to generate new therapeutic opportunities. J Allergy Clin Immunol **117**: 496–506; quiz 507.

Hollenberg, M., 2003 Proteinaseactivated receptors: Tethered ligands and receptoractivating peptides. Drug development research **59**: 336–343.

Hollenberg, M. D., and S. J. Compton, 2002 International union of pharmacology. xxviii. proteinase-activated receptors. Pharmacol Rev **54**: 203–17.

Hollenberg, M. D., M. Saifeddine, S. Sandhu, S. Houle, and N. Vergnolle, 2004 Proteinase-activated receptor-4: evaluation of tethered ligand-derived peptides as probes for receptor function and as inflammatory agonists in vivo. Br J Pharmacol **143**: 443–54.

Hollenberg, M. D., S. J. Wijesuriya, Y. Gui, and R. Loutzenhiser, 2003 Proteinase-activated receptors (pars) and the kidney. Drug development research **60**: 36–42.

Hostettler, K. E., M. Roth, J. K. Burgess, M. M. Gencay, F. Gambazzi, *et al.*, 2008 Airway epithelium-derived transforming growth factor-beta is a regulator of fibroblast proliferation in both fibrotic and normal subjects. Clin Exp Allergy **38**: 1309–17.

Hou, L., S. Ravenall, M. G. Macey, P. Harriott, S. Kapas, *et al.*, 1998 Protease-activated receptors and their role in il-6 and nf-il-6 expression in human gingival fibroblasts. J Periodont Res **33**: 205–11.

Houle, S., M. D. Papez, M. Ferazzini, M. D. Hollenberg, and N. Vergnolle, 2005 Neutrophils and the kallikrein-kinin system in proteinase-activated receptor 4-mediated inflammation in rodents. Br J Pharmacol **146**: 670–8.

Howell, D. C. J., R. H. Johns, J. A. Lasky, B. Shan, C. J. Scotton, *et al.*, 2005 Absence of proteinase-activated receptor-1 signaling affords protection from bleomycin-induced lung inflammation and fibrosis. Am J Pathol **166**: 1353–65.

Hoxie, J. A., M. Ahuja, E. Belmonte, S. Pizarro, R. Parton, *et al.*, 1993 Internalization and recycling of activated thrombin receptors. J Biol Chem **268**: 13756–63.

Humphreys, B. D., S.-L. Lin, A. Kobayashi, T. E. Hudson, B. T. Nowlin, *et al.*, 2010 Fate tracing reveals the pericyte and not epithelial origin of myofibroblasts in kidney fibrosis. Am J Pathol **176**: 85–97.

Hung, D. T., Y. H. Wong, T. K. Vu, and S. R. Coughlin, 1992 The cloned platelet thrombin receptor couples to at least two distinct effectors to stimulate phosphoinositide hydrolysis and inhibit adenylyl cyclase. J Biol Chem **267**: 20831–4.

Irmler, M., M. Thome, M. Hahne, P. Schneider, K. Hofmann, *et al.*, 1997 Inhibition of death receptor signals by cellular flip. Nature **388**: 190–5.

Ishihara, H., A. J. Connolly, D. Zeng, M. L. Kahn, Y. W. Zheng, *et al.*, 1997 Protease-activated receptor 3 is a second thrombin receptor in humans. Nature **386**: 502–6.

Ishihara, H., D. Zeng, A. J. Connolly, C. Tam, and S. R. Coughlin, 1998 Antibodies to protease-activated receptor 3 inhibit activation of mouse platelets by thrombin. Blood **91**: 4152–7.

Ishii, K., J. Chen, M. Ishii, W. J. Koch, N. J. Freedman, *et al.*, 1994 Inhibition of thrombin receptor signaling by a g-protein coupled receptor kinase. functional specificity among g-protein coupled receptor kinases. J Biol Chem **269**: 1125–30.

Iwano, M., D. Plieth, T. M. Danoff, C. Xue, H. Okada, *et al.*, 2002 Evidence that fibroblasts derive from epithelium during tissue fibrosis. J Clin Invest **110**: 341–50.

Jakab, G. J., 1990 Sequential virus infections, bacterial superinfections, and fibrogenesis. Am Rev Respir Dis **142**: 374–9.

Jarnagin, W. R., D. C. Rockey, V. E. Koteliansky, S. S. Wang, and D. M. Bissell, 1994 Expression of variant fibronectins in wound healing: cellular source and biological activity of the eiiia segment in rat hepatic fibrogenesis. The Journal of cell biology **127**: 2037–48.

Jimenez, S. A., B. Freundlich, and J. Rosenbloom, 1984 Selective inhibition of human diploid fibroblast collagen synthesis by interferons. J Clin Invest **74**: 1112–6.

Johnson, R. J., 1991 Platelets in inflammatory glomerular injury. Semin Nephrol **11**: 276–84.

Kahn, M. L., Y. W. Zheng, W. Huang, V. Bigornia, D. Zeng, *et al.*, 1998 A dual thrombin receptor system for platelet activation. Nature **394**: 690–4.

Kanke, T., S. R. Macfarlane, M. J. Seatter, E. Davenport, A. Paul, *et al.*, 2001 Proteinase-activated receptor-2-mediated activation of stress-activated protein kinases and inhibitory kappa b kinases in nctc 2544 keratinocytes. J Biol Chem **276**: 31657–66.

Kapetanaki, M. G., A. L. Mora, and M. Rojas, 2013 Influence of age on wound healing and fibrosis. J. Pathol. **229**: 310–22.

Kataoka, H., J. R. Hamilton, D. D. McKemy, E. Camerer, Y.-W. Zheng, *et al.*, 2003 Protease-activated receptors 1 and 4 mediate thrombin signaling in endothelial cells. Blood **102**: 3224–31.

Kaufmann, R., B. Schulze, G. Krause, L. M. Mayr, U. Settmacher, *et al.*, 2005 Proteinase-activated receptors (pars)–the par3 neo-n-terminal peptide tfrgap interacts with par1. Regul Pept **125**: 61–6.

Kawabata, A., and N. Kawao, 2005 Physiology and pathophysiology of proteinase-activated receptors (pars): Pars in the respiratory system: cellular signaling and physiological/pathological roles. J Pharmacol Sci **97**: 20–4.

Kawabata, A., S. Kubo, T. Ishiki, N. Kawao, F. Sekiguchi, *et al.*, 2004 Proteinase-activated receptor-2-mediated relaxation in mouse tracheal and bronchial smooth muscle: signal transduction mechanisms and distinct agonist sensitivity. J Pharmacol Exp Ther **311**: 402–10.

Kessenbrock, K., T. Dau, and D. E. Jenne, 2011 Tailor-made inflammation: how neutrophil serine proteases modulate the inflammatory response. J Mol Med **89**: 23–8.

Kim, K. K., M. C. Kugler, P. J. Wolters, L. Robillard, M. G. Galvez, *et al.*, 2006 Alveolar epithelial cell mesenchymal transition develops in vivo during pulmonary fibrosis and is regulated by the extracellular matrix. Proc Natl Acad Sci USA **103**: 13180–5.

Kimura, M., K. Tani, J. Miyata, K. Sato, A. Hayashi, *et al.*, 2005 The significance of cathepsins, thrombin and aminopeptidase in diffuse interstitial lung diseases. J Med Invest **52**: 93–100.

Kisseleva, T., and D. A. Brenner, 2006 Hepatic stellate cells and the reversal of fibrosis. J Gastroenterol Hepatol **21 Suppl 3**: S84–7.

Kisseleva, T., and D. A. Brenner, 2008 Mechanisms of fibrogenesis. Exp Biol Med (Maywood) **233**: 109–22.

Kluth, D. C., 2007 Pro-resolution properties of macrophages in renal injury. Kidney Int **72**: 234–6.

Knight, D., 2001 Epithelium-fibroblast interactions in response to airway inflammation. Immunol Cell Biol **79**: 160–4.

Knight, D. A., and S. T. Holgate, 2003 The airway epithelium: structural and functional properties in health and disease. Respirology **8**: 432–46.

Knight, D. A., S. Lim, A. K. Scaffidi, N. Roche, K. F. Chung, *et al.*, 2001 Protease-activated receptors in human airways: upregulation of par-2 in respiratory epithelium from patients with asthma. J Allergy Clin Immunol **108**: 797–803.

Knight, D. A., G. A. Stewart, and P. J. Thompson, 1994 The respiratory epithelium and airway smooth muscle homeostasis: its relevance to asthma. Clin Exp Allergy **24**: 698–706.

Koesters, R., B. Kaissling, M. Lehir, N. Picard, F. Theilig, *et al.*, 2010 Tubular overexpression of transforming growth factor-beta1 induces autophagy and fibrosis but not mesenchymal transition of renal epithelial cells. Am J Pathol **177**: 632–43.

Kohyama, T., R. F. Ertl, V. Valenti, J. Spurzem, M. Kawamoto, *et al.*, 2001 Prostaglandin e(2) inhibits fibroblast chemotaxis. Am J Physiol Lung Cell Mol Physiol **281**: L1257–63.

Komatsu, H., S. Enjouji, A. Ito, T. Ohama, and K. Sato, 2012 Prostaglandin e(2) inhibits proteinase-activated receptor 2-signal transduction through regulation of receptor internalization. J Vet Med Sci .

Kondo, S., S. Kagami, H. Kido, F. Strutz, G. A. Müller, *et al.*, 2001 Role of mast cell tryptase in renal interstitial fibrosis. J Am Soc Nephrol **12**: 1668–76.

Kong, W., K. McConalogue, L. M. Khitin, M. D. Hollenberg, D. G. Payan, *et al.*, 1997 Luminal trypsin may regulate enterocytes

through proteinase-activated receptor 2. Proc Natl Acad Sci USA **94**: 8884–9.

Koo, B. H., K. H. Chung, K. C. Hwang, and D. S. Kim, 2002 Factor xa induces mitogenesis of coronary artery smooth muscle cell via activation of par-2. FEBS Lett **523**: 85–9.

Kuncio, G., E. Neilson, and T. Haverty, 1991 Mechanisms of tubulointerstitial fibrosis. Kidney Int **39**: 550–556.

Kuwano, K., N. Hagimoto, M. Kawasaki, T. Yatomi, N. Nakamura, *et al.*, 1999a Essential roles of the fas-fas ligand pathway in the development of pulmonary fibrosis. The Journal of clinical investigation **104**: 13–9.

Kuwano, K., N. Hagimoto, and Y. Nakanishi, 2004 The role of apoptosis in pulmonary fibrosis. Histol Histopathol **19**: 867–81.

Kuwano, K., R. Kunitake, M. Kawasaki, Y. Nomoto, N. Hagimoto, *et al.*, 1996 P21waf1/cip1/sdi1 and p53 expression in association with dna strand breaks in idiopathic pulmonary fibrosis. Am J Respir Crit Care Med **154**: 477–83.

Kuwano, K., H. Miyazaki, N. Hagimoto, M. Kawasaki, M. Fujita, *et al.*, 1999b The involvement of fas-fas ligand pathway in fibrosing lung diseases. Am J Respir Cell Mol Biol **20**: 53–60.

Lama, V., B. B. Moore, P. Christensen, G. B. Toews, and M. Peters-Golden, 2002 Prostaglandin e2 synthesis and suppression of fibroblast proliferation by alveolar epithelial cells is cyclooxygenase-2-dependent. Am J Respir Cell Mol Biol **27**: 752–8.

Lan, R. S., G. A. Stewart, and P. J. Henry, 2000 Modulation of airway smooth muscle tone by protease activated receptor-1,-2,-3 and -4 in trachea isolated from influenza a virus-infected mice. Br J Pharmacol **129**: 63–70.

Laping, N. J., B. A. Olson, B. Short, and C. R. Albrightson, 1997 Thrombin increases clusterin mrna in glomerular epithelial and mesangial cells. J Am Soc Nephrol **8**: 906–14.

Leask, A., and D. J. Abraham, 2004 Tgf-beta signaling and the fibrotic response. FASEB J **18**: 816–27.

Lee, C. G., S. J. Cho, M. J. Kang, S. P. Chapoval, P. J. Lee, *et al.*, 2004 Early growth response gene 1-mediated apoptosis is essential for transforming growth factor beta1-induced pulmonary fibrosis. J Exp Med **200**: 377–89.

Lee, J. S., J. H. Ryu, B. M. Elicker, C. P. Lydell, K. D. Jones, *et al.*, 2011 Gastroesophageal reflux therapy is associated with longer survival in patients with idiopathic pulmonary fibrosis. American Journal of Respiratory and Critical Care Medicine **184**: 1390–4.

Leivonen, S.-K., A. Chantry, L. Hakkinen, J. Han, and V.-M. Kahari, 2002 Smad3 mediates transforming growth factor-beta-induced collagenase-3 (matrix metalloproteinase-13) expression in human gingival fibroblasts. evidence for cross-talk between smad3 and p38 signaling pathways. J Biol Chem **277**: 46338–46.

Lemley, K. V., and W. Kriz, 1991 Anatomy of the renal interstitium. Kidney Int **39**: 370–81.

Lerner, D. J., M. Chen, T. Tram, and S. R. Coughlin, 1996 Agonist recognition by proteinase-activated receptor 2 and thrombin receptor. importance of extracellular loop interactions for receptor function. J Biol Chem **271**: 13943–7.

Lim, A. I., S. C. W. Tang, K. N. Lai, and J. C. K. Leung, 2012 Kidney injury molecule-1: More than just an injury marker of tubular epithelial cells? J. Cell. Physiol. .

Lin, S.-L., T. Kisseleva, D. A. Brenner, and J. S. Duffield, 2008 Pericytes and perivascular fibroblasts are the primary source of collagen-producing cells in obstructive fibrosis of the kidney. Am J Pathol **173**: 1617–27.

Lindner, J. R., M. L. Kahn, S. R. Coughlin, G. R. Sambrano, E. Schauble, *et al.*, 2000 Delayed onset of inflammation in protease-activated receptor-2-deficient mice. J Immunol **165**: 6504–10.

Liu, L.-D., C.-H. Dong, H.-J. Shi, H.-L. Zhao, L.-C. Wang, *et al.*, 2006 A novel type ii membrane receptor up-regulated by ifn-alpha in fibroblasts functions in cell proliferation through the jak-stat signalling pathway. Cell Prolif **39**: 93–103.

Liu, T., Y. Nozaki, and S. H. Phan, 2002 Regulation of telomerase activity in rat lung fibroblasts. Am J Respir Cell Mol Biol **26**: 534–40.

Liu, Y., 2011 Cellular and molecular mechanisms of renal fibrosis. Nat Rev Nephrol **7**: 684–96.

Lourbakos, A., Y. Yuan, A. Jenkins, J. Travis, P. Andrade-Gordon, *et al.*, 2001 Activation of protease-activated receptors by gingipains fromporphyromonas gingivalis leads to platelet aggregation: a new trait in microbial pathogenicity. Blood **97**: 3790.

Ma, L.-J., H. Yang, A. Gaspert, G. Carlesso, M. M. Barty, *et al.*, 2003 Transforming growth factor-beta-dependent and -independent pathways of induction of tubulointerstitial fibrosis in beta6(-/-) mice. Am J Pathol **163**: 1261–73.

Macfarlane, S. R., M. J. Seatter, T. Kanke, G. D. Hunter, and R. Plevin, 2001 Proteinase-activated receptors. Pharmacol Rev **53**: 245–82.

Macfarlane, S. R., C. M. Sloss, P. Cameron, T. Kanke, R. C. McKenzie, *et al.*, 2005 The role of intracellular ca2+ in the regulation of

proteinase-activated receptor-2 mediated nuclear factor kappa b signalling in keratinocytes. British journal of pharmacology **145**: 535–44.

Madtes, D. K., H. K. Busby, T. P. Strandjord, and J. G. Clark, 1994 Expression of transforming growth factor-alpha and epidermal growth factor receptor is increased following bleomycin-induced lung injury in rats. Am J Respir Cell Mol Biol **11**: 540–51.

Major, C. D., R. J. Santulli, C. K. Derian, and P. Andrade-Gordon, 2003 Extracellular mediators in atherosclerosis and thrombosis: lessons from thrombin receptor knockout mice. Arteriosclerosis, Thrombosis, and Vascular Biology **23**: 931–9.

Malarkey, K., C. M. Belham, A. Paul, A. Graham, A. McLees, *et al.*, 1995 The regulation of tyrosine kinase signalling pathways by growth factor and g-protein-coupled receptors. Biochem J **309 (Pt 2)**: 361–75.

Manoury, B., S. Nenan, O. Leclerc, I. Guenon, E. Boichot, *et al.*, 2005 The absence of reactive oxygen species production protects mice against bleomycin-induced pulmonary fibrosis. Respir Res **6**: 11.

Marković-Lipkovski, J., 2002 Tubuloepithelial-myofibroblast transdifferentiation–possible pathogenic mechanism of interstitial fibrosis in balkan endemic nephropathy. Facta universitatis-series: Medicine and Biology **9**: 79–81.

Matsushima, R., A. Takahashi, Y. Nakaya, H. Maezawa, M. Miki, *et al.*, 2006 Human airway trypsin-like protease stimulates human bronchial fibroblast proliferation in a protease-activated receptor-2-dependent pathway. Am J Physiol Lung Cell Mol Physiol **290**: L385–95.

Matute-Bello, G., R. K. Winn, M. Jonas, E. Y. Chi, T. R. Martin, *et al.*, 2001 Fas (cd95) induces alveolar epithelial cell apoptosis in vivo: implications for acute pulmonary inflammation. Am J Pathol **158**: 153–61.

McAnulty, R. J., N. A. Hernández-Rodriguez, S. E. Mutsaers, R. K. Coker, and G. J. Laurent, 1997 Indomethacin suppresses the anti-proliferative effects of transforming growth factor-beta isoforms on fibroblast cell cultures. Biochem J **321 (Pt 3)**: 639–43.

Meliconi, R., P. Andreone, L. Fasano, S. Galli, A. Pacilli, *et al.*, 1996 Incidence of hepatitis c virus infection in italian patients with idiopathic pulmonary fibrosis. Thorax **51**: 315–7.

Meltzer, E. B., and P. W. Noble, 2008 Idiopathic pulmonary fibrosis. Orphanet J Rare Dis **3**: 8.

Meng, X., A. Chung, and H. Lan, 2013 Role of the tgf-beta/bmp-7/smad pathways in renal diseases. Clin. Sci. .

Mirastschijski, U., C. J. Haaksma, J. J. Tomasek, and M. S. Agren, 2004 Matrix metalloproteinase inhibitor gm 6001 attenuates keratinocyte migration, contraction and myofibroblast formation in skin wounds. Exp Cell Res **299**: 465–75.

Miyajima, A., J. Chen, C. Lawrence, S. Ledbetter, R. A. Soslow, *et al.*, 2000 Antibody to transforming growth factor-beta ameliorates tubular apoptosis in unilateral ureteral obstruction. Kidney Int **58**: 2301–13.

Miyata, J., K. Tani, K. Sato, S. Otsuka, T. Urata, *et al.*, 2007 Cathepsin g: the significance in rheumatoid arthritis as a monocyte chemoattractant. Rheumatol Int **27**: 375–382.

Molino, M., E. S. Barnathan, R. Numerof, J. Clark, M. Dreyer, *et al.*, 1997 Interactions of mast cell tryptase with thrombin receptors and par-2. J Biol Chem **272**: 4043–9.

Molino, M., N. Blanchard, E. Belmonte, A. P. Tarver, C. Abrams, *et al.*, 1995 Proteolysis of the human platelet and endothelial

cell thrombin receptor by neutrophil-derived cathepsin g. J Biol Chem **270**: 11168–75.

Molitoris, B. A., 1999 Acute renal failure. Drugs Today **35**: 659–66.

Moore, B. B., M. Peters-Golden, P. J. Christensen, V. Lama, W. A. Kuziel, *et al.*, 2003 Alveolar epithelial cell inhibition of fibroblast proliferation is regulated by mcp-1/ccr2 and mediated by pge2. Am J Physiol Lung Cell Mol Physiol **284**: L342–9.

Morrisey, E. E., 2003 Wnt signaling and pulmonary fibrosis. Am J Pathol **162**: 1393–7.

Morrissey, J., K. Hruska, G. Guo, S. Wang, Q. Chen, *et al.*, 2002 Bone morphogenetic protein-7 improves renal fibrosis and accelerates the return of renal function. J Am Soc Nephrol **13 Suppl 1**: S14–21.

Moses, H. L., C. L. Arteaga, M. G. Alexandrow, L. Dagnino, M. Kawabata, *et al.*, 1994 Tgf beta regulation of cell proliferation. Int Symp Princess Takamatsu Cancer Res Fund **24**: 250–63.

Munson, J. C., M. Kreider, Z. Chen, J. D. Christie, and S. E. Kimmel, 2010 Effect of treatment guidelines on the initial management of idiopathic pulmonary fibrosis. Br J Clin Pharmacol **70**: 118–25.

Muramatsu, I., A. Laniyonu, G. J. Moore, and M. D. Hollenberg, 1992 Vascular actions of thrombin receptor peptide. Can J Physiol Pharmacol **70**: 996–1003.

Mutsaers, S. E., J. E. Bishop, G. McGrouther, and G. J. Laurent, 1997 Mechanisms of tissue repair: from wound healing to fibrosis. Int J Biochem Cell Biol **29**: 5–17.

Nakamura, Y., L. Tate, R. F. Ertl, M. Kawamoto, T. Mio, *et al.*, 1995 Bronchial epithelial cells regulate fibroblast proliferation. Am J Physiol **269**: L377–87.

Nakanishi-Matsui, M., Y. Zheng, D. Sulciner, E. Weiss, M. Ludeman, *et al.*, 2000 Par3 is a cofactor for par4 activation by thrombin. Nature **404**: 609–613.

Nakayama, T., K. Hirano, Y. Shintani, J. Nishimura, A. Nakatsuka, *et al.*, 2003 Unproductive cleavage and the inactivation of protease-activated receptor-1 by trypsin in vascular endothelial cells. Br J Pharmacol **138**: 121–30.

Nangaku, M., 2004 Mechanisms of tubulointerstitial injury in the kidney: final common pathways to end-stage renal failure. Intern Med **43**: 9–17.

Navaratnam, V., K. Fleming, J. West, and C. Smith. . . , 2011 The rising incidence of idiopathic pulmonary fibrosis in the uk. Thorax .

Noble, P. W., C. Albera, W. Z. Bradford, U. Costabel, M. K. Glassberg, *et al.*, 2011 Pirfenidone in patients with idiopathic pulmonary fibrosis (capacity): two randomised trials. Lancet **377**: 1760–9.

Nomoto, Y., K. Kuwano, N. Hagimoto, R. Kunitake, M. Kawasaki, *et al.*, 1997 Apoptosis and fas/fas ligand mrna expression in acute immune complex alveolitis in mice. Eur Respir J **10**: 2351–9.

Noorbakhsh, F., S. Tsutsui, N. Vergnolle, L. A. Boven, N. Shariat, *et al.*, 2006 Proteinase-activated receptor 2 modulates neuroinflammation in experimental autoimmune encephalomyelitis and multiple sclerosis. J Exp Med **203**: 425–35.

Nystedt, S., K. Emilsson, A. K. Larsson, B. Strömbeck, and J. Sundelin, 1995 Molecular cloning and functional expression of the gene encoding the human proteinase-activated receptor 2. Eur J Biochem **232**: 84–9.

Nystedt, S., K. Emilsson, C. Wahlestedt, and J. Sundelin, 1994 Molecular cloning of a potential proteinase activated receptor. Proc Natl Acad Sci USA **91**: 9208–12.

Offermanns, S., K. L. Laugwitz, K. Spicher, and G. Schultz, 1994 G proteins of the g12 family are activated via thromboxane a2 and thrombin receptors in human platelets. Proc Natl Acad Sci USA **91**: 504–8.

Okada, H., T. M. Danoff, R. Kalluri, and E. G. Neilson, 1997 Early role of fsp1 in epithelial-mesenchymal transformation. Am J Physiol **273**: F563–74.

Okada, H., F. Strutz, T. M. Danoff, R. Kalluri, and E. G. Neilson, 1996 Possible mechanisms of renal fibrosis. Contrib Nephrol **118**: 147–54.

Okamoto, T., M. Nishibori, K. Sawada, H. Iwagaki, N. Nakaya, *et al.*, 2001a The effects of stimulating protease-activated receptor-1 and -2 in a172 human glioblastoma. J Neural Transm **108**: 125–40.

Okamoto, T., M. Nishibori, K. Sawada, H. Iwagaki, N. Nakaya, *et al.*, 2001b The effects of stimulating protease-activated receptor-1 and-2 in a172 human glioblastoma. Journal of neural transmission **108**: 125–140.

Okon, K., A. Szumera, and M. Kuzniewski, 2003 Are cd34+ cells found in renal interstitial fibrosis? Am J Nephrol **23**: 409–14.

Onuigbo, M. A. C., 2011 Can ace inhibitors and angiotensin receptor blockers be detrimental in ckd patients? Nephron Clin Pract **118**: c407–19.

Ortiz-Stern, A., X. Deng, N. Smoktunowicz, P. F. Mercer, and R. C. Chambers, 2012 Par-1-dependent and par-independent pro-inflammatory signaling in human lung fibroblasts exposed to thrombin. J. Cell. Physiol. **227**: 3575–84.

Ossovskaya, V. S., and N. W. Bunnett, 2004 Protease-activated receptors: contribution to physiology and disease. Physiol Rev **84**: 579–621.

Ostrowska, E., E. Sokolova, and G. Reiser, 2007 Par-2 activation and lps synergistically enhance inflammatory signaling in airway epithelial cells by raising par expression level and interleukin-8 release. Am J Physiol Lung Cell Mol Physiol **293**: L1208–18.

Owen, C. A., M. A. Campbell, P. L. Sannes, S. S. Boukedes, and E. J. Campbell, 1995 Cell surface-bound elastase and cathepsin g on human neutrophils: a novel, non-oxidative mechanism by which neutrophils focus and preserve catalytic activity of serine proteinases. The Journal of cell biology **131**: 775–89.

Owens, G. K., 1995 Regulation of differentiation of vascular smooth muscle cells. Physiol Rev **75**: 487–517.

Paing, M. M., C. A. Johnston, D. P. Siderovski, and J. Trejo, 2006 Clathrin adaptor ap2 regulates thrombin receptor constitutive internalization and endothelial cell resensitization. Mol Cell Biol **26**: 3231–42.

Pardo, A., K. Gibson, J. Cisneros, T. J. Richards, Y. Yang, *et al.*, 2005 Up-regulation and profibrotic role of osteopontin in human idiopathic pulmonary fibrosis. PLoS Med **2**: e251.

Park, M. A., V. Pejovic, K. G. Kerisit, S. Junius, and J. G. Thoene, 2006 Increased apoptosis in cystinotic fibroblasts and renal proximal tubule epithelial cells results from cysteinylation of protein kinase cdelta. J Am Soc Nephrol **17**: 3167–75.

Perbal, B., 2004 Ccn proteins: multifunctional signalling regulators. Lancet **363**: 62–4.

Pham, C. T. N., 2008 Neutrophil serine proteases fine-tune the inflammatory response. Int J Biochem Cell Biol **40**: 1317–33.

Phan, S. H., 2002 The myofibroblast in pulmonary fibrosis. Chest **122**: 286S–289S.

Phan, S. H., 2008 Biology of fibroblasts and myofibroblasts. Proc Am Thorac Soc **5**: 334–7.

Phillips, R. J., M. D. Burdick, K. Hong, M. A. Lutz, L. A. Murray, *et al.*, 2004 Circulating fibrocytes traffic to the lungs in response to cxcl12 and mediate fibrosis. J Clin Invest **114**: 438–46.

Piguet, P. F., 2003 Inflammation in idiopathic pulmonary fibrosis. Am J Respir Crit Care Med **167**: 1037; author reply 1037.

Pilz, B., E. Shagdarsuren, M. Wellner, A. Fiebeler, R. Dechend, *et al.*, 2005 Aliskiren, a human renin inhibitor, ameliorates cardiac and renal damage in double-transgenic rats. Hypertension **46**: 569–76.

Piotrowski, W. J., and J. Marczak, 2000 Cellular sources of oxidants in the lung. Int J Occup Med Environ Health **13**: 369–85.

Plataki, M., A. V. Koutsopoulos, K. Darivianaki, G. Delides, N. M. Siafakas, *et al.*, 2005 Expression of apoptotic and antiapoptotic markers in epithelial cells in idiopathic pulmonary fibrosis. Chest **127**: 266–74.

Polunovsky, V. A., B. Chen, C. Henke, D. Snover, C. Wendt, *et al.*, 1993 Role of mesenchymal cell death in lung remodeling after injury. The Journal of clinical investigation **92**: 388–97.

Portnoy, J., T. Pan, C. A. Dinarello, J. M. Shannon, J. Y. Westcott, *et al.*, 2006 Alveolar type ii cells inhibit fibroblast proliferation: role of il-1alpha. Am J Physiol Lung Cell Mol Physiol **290**: L307–16.

Postlethwaite, A. E., J. Keski-Oja, H. L. Moses, and A. H. Kang, 1987 Stimulation of the chemotactic migration of human fibroblasts by transforming growth factor beta. J Exp Med **165**: 251–6.

Powell, D., R. Mifflin, J. Valentich, S. Crowe, J. Saada, *et al.*, 1999 Myofibroblasts. i. paracrine cells important in health and disease. American Journal of Physiology-Cell Physiology **277**: C1.

Powell, D. W., 2000 Myofibroblasts: paracrine cells important in health and disease. Trans Am Clin Climatol Assoc **111**: 271–92; discussion 292–3.

Prunotto, M., D. C. Budd, G. Gabbiani, M. Meier, I. Formentini, *et al.*, 2012 Epithelial-mesenchymal crosstalk alteration in kidney fibrosis. J. Pathol. **228**: 131–47.

Qi, W., X. Chen, P. Poronnik, and C. A. Pollock, 2006 The renal cortical fibroblast in renal tubulointerstitial fibrosis. Int J Biochem Cell Biol **38**: 1–5.

Quan, T. E., S. E. Cowper, and R. Bucala, 2006 The role of circulating fibrocytes in fibrosis. Curr Rheumatol Rep **8**: 145–50.

Qunn, L., T. Takemura, S. Ikushima, T. Ando, T. Yanagawa, *et al.*, 2002 Hyperplastic epithelial foci in honeycomb lesions in idiopathic pulmonary fibrosis. Virchows Arch **441**: 271–8.

Raeburn, D., and S. E. Webber, 1994 Proinflammatory potential of the airway epithelium in bronchial asthma. Eur Respir J **7**: 2226–33.

Ramachandran, R., A. H. Morice, and S. J. Compton, 2006 Proteinase-activated receptor2 agonists upregulate granulocyte colony-stimulating factor, il-8, and vcam-1 expression in human bronchial fibroblasts. Am J Respir Cell Mol Biol **35**: 133–41.

Ramachandran, R., F. Noorbakhsh, K. Defea, and M. D. Hollenberg, 2012 Targeting proteinase-activated receptors: therapeutic potential and challenges. Nat Rev Drug Discov **11**: 69–86.

Ramachandran, R., L. R. Sadofsky, Y. Xiao, A. Botham, M. Cowen, *et al.*, 2007 Inflammatory mediators modulate thrombin and

cathepsin-g signaling in human bronchial fibroblasts by inducing expression of proteinase-activated receptor-4. Am J Physiol Lung Cell Mol Physiol **292**: L788–98.

Ramos, C., M. Montaño, C. Becerril, J. Cisneros-Lira, L. Barrera, *et al.*, 2006 Acidic fibroblast growth factor decreases alpha-smooth muscle actin expression and induces apoptosis in human normal lung fibroblasts. Am J Physiol Lung Cell Mol Physiol **291**: L871–9.

Ramos, C., M. Montaño, J. García-Alvarez, V. Ruiz, B. D. Uhal, *et al.*, 2001 Fibroblasts from idiopathic pulmonary fibrosis and normal lungs differ in growth rate, apoptosis, and tissue inhibitor of metalloproteinases expression. Am J Respir Cell Mol Biol **24**: 591–8.

Rasmussen, U. B., V. Vouret-Craviari, S. Jallat, Y. Schlesinger, G. Pagès, *et al.*, 1991 cdna cloning and expression of a hamster alpha-thrombin receptor coupled to ca2+ mobilization. FEBS Lett **288**: 123–8.

Renesto, P., M. Si-Tahar, M. Moniatte, V. Balloy, A. van Dorsselaer, *et al.*, 1997 Specific inhibition of thrombin-induced cell activation by the neutrophil proteinases elastase, cathepsin g, and proteinase 3: evidence for distinct cleavage sites within the aminoterminal domain of the thrombin receptor. Blood **89**: 1944–53.

Ricardo, S. D., H. van Goor, and A. A. Eddy, 2008 Macrophage diversity in renal injury and repair. J Clin Invest **118**: 3522–30.

Ricciardolo, F. L., M. Steinhoff, S. Amadesi, R. Guerrini, M. Tognetto, *et al.*, 2000 Presence and bronchomotor activity of protease-activated receptor-2 in guinea pig airways. Am J Respir Crit Care Med **161**: 1672–80.

Rieger, A. M., K. L. Nelson, J. D. Konowalchuk, and D. R. Barreda, 2011 Modified annexin v/propidium iodide apoptosis assay for accurate assessment of cell death. JoVE .

Roche, N., R. Stirling, S. Lim, B. Oliver, T. Oates, *et al.*, 2003 Effect of acute and chronic inflammatory stimuli on expression of protease-activated receptors 1 and 2 in alveolar macrophages. Journal of Allergy and Clinical Immunology **111**: 367–373.

Rokudai, S., N. Fujita, Y. Hashimoto, and T. Tsuruo, 2000 Cleavage and inactivation of antiapoptotic akt/pkb by caspases during apoptosis. J Cell Physiol **182**: 290–6.

Rom, W. N., P. Basset, G. A. Fells, T. Nukiwa, B. C. Trapnell, *et al.*, 1988 Alveolar macrophages release an insulin-like growth factor i-type molecule. J Clin Invest **82**: 1685–93.

Rondeau, E., C. Vigneau, and J. Berrou, 2001 Role of thrombin receptors in the kidney: lessons from par1 knock-out mice. Nephrol Dial Transplant **16**: 1529–31.

Ruiz-Ortega, M., M. Rupérez, V. Esteban, J. Rodríguez-Vita, E. Sánchez-López, *et al.*, 2006 Angiotensin ii: a key factor in the inflammatory and fibrotic response in kidney diseases. Nephrol Dial Transplant **21**: 16–20.

Russell, F. A., V. E. Veldhoen, D. Tchitchkan, and J. J. McDougall, 2010 Proteinase-activated receptor-4 (par4) activation leads to sensitization of rat joint primary afferents via a bradykinin b2 receptor-dependent mechanism. J Neurophysiol **103**: 155–63.

Sabri, A., S. Alcott, H. Elouardighi, E. Pak, C. Derian, *et al.*, 2003a Neutrophil cathepsin g promotes detachment-induced cardiomyocyte apoptosis via a protease-activated receptor-independent mechanism. Journal of Biological Chemistry **278**: 23944.

Sabri, A., J. Guo, H. Elouardighi, A. L. Darrow, P. Andrade-Gordon, *et al.*, 2003b Mechanisms of protease-activated receptor-4

actions in cardiomyocytes. role of src tyrosine kinase. J Biol Chem **278**: 11714–20.

Sabri, A., G. Muske, H. Zhang, E. Pak, A. Darrow, *et al.*, 2000 Signaling properties and functions of two distinct cardiomyocyte protease-activated receptors. Circulation Research **86**: 1054–61.

Sabri, A., J. Short, J. Guo, and S. Steinberg, 2002 Protease-activated receptor-1-mediated dna synthesis in cardiac fibroblast is via epidermal growth factor receptor transactivation: distinct par-1 signaling pathways in cardiac fibroblasts and cardiomyocytes. Circulation Research **91**: 532.

Sacco, O., M. Silvestri, F. Sabatini, R. Sale, A.-C. Defilippi, *et al.*, 2004 Epithelial cells and fibroblasts: structural repair and remodelling in the airways. Paediatr Respir Rev **5 Suppl A**: S35–40.

Sagara, H., T. Okada, K. Okumura, H. Ogawa, C. Ra, *et al.*, 2002 Activation of tgf-beta/smad2 signaling is associated with airway remodeling in asthma. J Allergy Clin Immunol **110**: 249–54.

Saifeddine, M., B. Al-Ani, S. Sandhu, S. J. Wijesuriya, and M. D. Hollenberg, 2001 Contractile actions of proteinase-activated receptor-derived polypeptides in guinea-pig gastric and lung parenchymal strips: evidence for distinct receptor systems. British journal of pharmacology **132**: 556–66.

Sakai, T., T. Nambu, M. Katoh, S. Uehara, T. Fukuroda, *et al.*, 2009 Up-regulation of protease-activated receptor-1 in diabetic glomerulosclerosis. Biochem Biophys Res Commun **384**: 173–9.

Sambrano, G. R., W. Huang, T. Faruqi, S. Mahrus, C. Craik, *et al.*, 2000 Cathepsin g activates protease-activated receptor-4 in human platelets. J Biol Chem **275**: 6819–23.

Sambrano, G. R., E. J. Weiss, Y. W. Zheng, W. Huang, and S. R. Coughlin, 2001 Role of thrombin signalling in platelets in haemostasis and thrombosis. Nature **413**: 74–8.

Saraste, A., and K. Pulkki, 2000 Morphologic and biochemical hallmarks of apoptosis. Cardiovasc Res **45**: 528–37.

Sato, M., Y. Muragaki, S. Saika, A. B. Roberts, and A. Ooshima, 2003 Targeted disruption of tgf-beta1/smad3 signaling protects against renal tubulointerstitial fibrosis induced by unilateral ureteral obstruction. J Clin Invest **112**: 1486–94.

Savage, C. O., 1994 The biology of the glomerulus: endothelial cells. Kidney International **45**: 314–9.

Savill, J., 1994 Apoptosis and the kidney. J Am Soc Nephrol **5**: 12–21.

Schaller, M. D., 2001 Biochemical signals and biological responses elicited by the focal adhesion kinase. Biochim Biophys Acta **1540**: 1–21.

Schechter, N. M., L. F. Brass, R. M. Lavker, and P. J. Jensen, 1998 Reaction of mast cell proteases tryptase and chymase with protease activated receptors (pars) on keratinocytes and fibroblasts. J Cell Physiol **176**: 365–73.

Schieppati, A., and G. Remuzzi, 2005 Chronic renal diseases as a public health problem: epidemiology, social, and economic implications. Kidney Int Suppl : S7–S10.

Schmidlin, F., S. Amadesi, K. Dabbagh, D. E. Lewis, P. Knott, *et al.*, 2002 Protease-activated receptor 2 mediates eosinophil infiltration and hyperreactivity in allergic inflammation of the airway. J Immunol **169**: 5315–21.

Schmidlin, F., S. Amadesi, R. Vidil, M. Trevisani, N. Martinet, *et al.*, 2001 Expression and function of proteinase-activated receptor 2 in

human bronchial smooth muscle. Am J Respir Crit Care Med **164**: 1276–81.

Schnaper, H. W., and J. B. Kopp, 2003 Renal fibrosis. Front Biosci **8**: e68–86.

Seatter, M. J., R. Drummond, T. Kanke, S. R. Macfarlane, M. D. Hollenberg, *et al.*, 2004 The role of the c-terminal tail in protease-activated receptor-2-mediated ca2+ signalling, proline-rich tyrosine kinase-2 activation, and mitogen-activated protein kinase activity. Cellular Signalling **16**: 21–9.

Selman, M., T. E. King, A. Pardo, A. T. Society, E. R. Society, *et al.*, 2001 Idiopathic pulmonary fibrosis: prevailing and evolving hypotheses about its pathogenesis and implications for therapy. Ann Intern Med **134**: 136–51.

Seppä, H., G. Grotendorst, S. Seppä, E. Schiffmann, and G. R. Martin, 1982 Platelet-derived growth factor in chemotactic for fibroblasts. The Journal of cell biology **92**: 584–8.

Serpero, L., L. Petecchia, F. Sabatini, M. Giuliani, M. Silvestri, *et al.*, 2006 The effect of transforming growth factor (tgf)-beta1 and (tgf)-beta2 on nasal polyp fibroblast activities involved upper airway remodeling: modulation by fluticasone propionate. Immunol Lett **105**: 61–7.

Serrano-Mollar, A., D. Closa, N. Prats, S. Blesa, M. Martinez-Losa, *et al.*, 2003 In vivo antioxidant treatment protects against bleomycin-induced lung damage in rats. British Journal of Pharmacology **138**: 1037–48.

Shapiro, M. J., E. J. Weiss, T. R. Faruqi, and S. R. Coughlin, 2000 Protease-activated receptors 1 and 4 are shut off with distinct kinetics after activation by thrombin. J Biol Chem **275**: 25216–21.

Shimizu, S., E. C. Gabazza, T. Hayashi, M. Ido, Y. Adachi, *et al.*, 2000 Thrombin stimulates the expression of pdgf in lung epithelial cells. Am J Physiol Lung Cell Mol Physiol **279**: L503–10.

Shimoda, N., N. Fukazawa, K. Nonomura, and R. L. Fairchild, 2007 Cathepsin g is required for sustained inflammation and tissue injury after reperfusion of ischemic kidneys. Am J Pathol **170**: 930–40.

Shinozaki, M., S. Kawara, N. Hayashi, T. Kakinuma, A. Igarashi, *et al.*, 1997 Induction of subcutaneous tissue fibrosis in newborn mice by transforming growth factor beta–simultaneous application with basic fibroblast growth factor causes persistent fibrosis. Biochem Biophys Res Commun **240**: 292–7.

Sime, P. J., Z. Xing, F. L. Graham, K. G. Csaky, and J. Gauldie, 1997 Adenovector-mediated gene transfer of active transforming growth factor-beta1 induces prolonged severe fibrosis in rat lung. The Journal of clinical investigation **100**: 768–76.

Singer, I. I., 1982 Fibronexus formation is an early event during fibronectin-induced restoration of more normal morphology and substrate adhesion patterns in transformed hamster fibroblasts. J Cell Sci **56**: 1–20.

Sisley, A. C., T. Desai, J. M. Harig, and B. L. Gewertz, 1994 Neutrophil depletion attenuates human intestinal reperfusion injury. J Surg Res **57**: 192–6.

Slofstra, S. H., M. F. Bijlsma, A. P. Groot, P. H. Reitsma, T. Lindhout, *et al.*, 2007 Protease-activated receptor-4 inhibition protects from multiorgan failure in a murine model of systemic inflammation. Blood **110**: 3176–82.

Smith, S. C., V. A. Folefac, D. K. Osei, and P. A. Revell, 1998 An immunocytochemical study of the distribution of proline-4-hydroxylase in

normal, osteoarthritic and rheumatoid arthritic synovium at both the light and electron microscopic level. Br J Rheumatol **37**: 287–91.

Smith, S. W., S. Chand, and C. O. S. Savage, 2012 Biology of the renal pericyte. Nephrol Dial Transplant **27**: 2149–55.

Sokolova, E., Z. Grishina, F. Bühling, T. Welte, and G. Reiser, 2005 Protease-activated receptor-1 in human lung fibroblasts mediates a negative feedback downregulation via prostaglandin e2. Am J Physiol Lung Cell Mol Physiol **288**: L793–802.

Sommerhoff, C. P., J. A. Nadel, C. B. Basbaum, and G. H. Caughey, 1990 Neutrophil elastase and cathepsin g stimulate secretion from cultured bovine airway gland serous cells. The Journal of clinical investigation **85**: 682–9.

Srinivasula, S. M., M. Ahmad, T. Fernandes-Alnemri, and E. S. Alnemri, 1998 Autoactivation of procaspase-9 by apaf-1-mediated oligomerization. Mol Cell **1**: 949–57.

Stahl, R. A., 1995 Chemoattractive cytokines (chemokines) and immune renal injury. Nephrol Dial Transplant **10**: 307–9.

Steinhoff, M., J. Buddenkotte, V. Shpacovitch, A. Rattenholl, C. Moormann, *et al.*, 2005 Proteinase-activated receptors: transducers of proteinase-mediated signaling in inflammation and immune response. Endocr Rev **26**: 1–43.

Storck, J., B. Kusters, M. Vahland, C. Morys-Wortmann, and E. Zimmermann, 1996 Trypsin induced von willebrand factor release from human endothelial cells is mediated by par-2 activation. Thrombosis research **84**: 463–473.

Strande, J. L., and S. A. Phillips, 2009 Thrombin increases inflammatory cytokine and angiogenic growth factor secretion in human adipose cells in vitro. J Inflamm (Lond) **6**: 4.

Strutz, F., 1995 Novel aspects of renal fibrogenesis. Nephrol Dial Transplant **10**: 1526–32.

Strutz, F., M. Zeisberg, A. Renziehausen, B. Raschke, V. Becker, *et al.*, 2001 Tgf-beta 1 induces proliferation in human renal fibroblasts via induction of basic fibroblast growth factor (fgf-2). Kidney International **59**: 579–92.

Su, X., E. Camerer, J. R. Hamilton, S. R. Coughlin, and M. A. Matthay, 2005 Protease-activated receptor-2 activation induces acute lung inflammation by neuropeptide-dependent mechanisms. J Immunol **175**: 2598–605.

Suda, T., T. Takahashi, P. Golstein, and S. Nagata, 1993 Molecular cloning and expression of the fas ligand, a novel member of the tumor necrosis factor family. Cell **75**: 1169–78.

Suzuki, T., T. Moraes, E. Vachon, H. Ginzberg, T. Huang, *et al.*, 2005 Proteinase-activated receptor-1 mediates elastase-induced apoptosis of human lung epithelial cells. Am J Respir Cell Mol Biol **33**: 231.

Takehara, K., E. C. LeRoy, and G. R. Grotendorst, 1987 Tgf-beta inhibition of endothelial cell proliferation: alteration of egf binding and egf-induced growth-regulatory (competence) gene expression. Cell **49**: 415–22.

Tanaka, D., T. Kagari, H. Doi, and T. Shimozato, 2006 Essential role of neutrophils in anti-type ii collagen antibody and lipopolysaccharide-induced arthritis. Immunology **119**: 195–202.

Tanaka, M., H. Arai, N. Liu, F. Nogaki, K. Nomura, *et al.*, 2005 Role of coagulation factor xa and protease-activated receptor 2 in human mesangial cell proliferation. Kidney International **67**: 2123–33.

Tang, P. S., M. Mura, R. Seth, and M. Liu, 2008 Acute lung injury and cell death: how many ways can cells die? Am J Physiol Lung Cell Mol Physiol **294**: L632–41.

Taniguchi, H., M. Ebina, Y. Kondoh, T. Ogura, A. Azuma, *et al.*, 2010 Pirfenidone in idiopathic pulmonary fibrosis. Eur Respir J **35**: 821–9.

Tanjore, H., X. C. Xu, V. V. Polosukhin, A. L. Degryse, B. Li, *et al.*, 2009 Contribution of epithelial-derived fibroblasts to bleomycin-induced lung fibrosis. American Journal of Respiratory and Critical Care Medicine **180**: 657–65.

Thannickal, V. J., and J. C. Horowitz, 2006 Evolving concepts of apoptosis in idiopathic pulmonary fibrosis. Proc Am Thorac Soc **3**: 350–6.

Thannickal, V. J., D. Y. Lee, E. S. White, Z. Cui, J. M. Larios, *et al.*, 2003 Myofibroblast differentiation by transforming growth factor-beta1 is dependent on cell adhesion and integrin signaling via focal adhesion kinase. J Biol Chem **278**: 12384–9.

Thannickal, V. J., G. B. Toews, E. S. White, J. P. Lynch, and F. J. Martinez, 2004 Mechanisms of pulmonary fibrosis. Annu Rev Med **55**: 395–417.

Thomas, P., and T. G. Smart, 2005 Hek293 cell line: a vehicle for the expression of recombinant proteins. J Pharmacol Toxicol Methods **51**: 187–200.

Thornberry, N. A., T. A. Rano, E. P. Peterson, D. M. Rasper, T. Timkey, *et al.*, 1997 A combinatorial approach defines specificities of members of the caspase family and granzyme b. functional relationships established for key mediators of apoptosis. J Biol Chem **272**: 17907–11.

Tomasek, J. J., G. Gabbiani, B. Hinz, C. Chaponnier, and R. A. Brown, 2002 Myofibroblasts and mechano-regulation of connective tissue remodelling. Nat Rev Mol Cell Biol **3**: 349–63.

Trejo, J., Y. Altschuler, H. W. Fu, K. E. Mostov, and S. R. Coughlin, 2000 Protease-activated receptor-1 down-regulation: a mutant

hela cell line suggests novel requirements for par1 phosphorylation and recruitment to clathrin-coated pits. J Biol Chem **275**: 31255–65.

Trejo, J., A. J. Connolly, and S. R. Coughlin, 1996 The cloned thrombin receptor is necessary and sufficient for activation of mitogen-activated protein kinase and mitogenesis in mouse lung fibroblasts. loss of responses in fibroblasts from receptor knockout mice. J Biol Chem **271**: 21536–41.

Trottier, G., M. Hollenberg, X. Wang, Y. Gui, K. Loutzenhiser, *et al.*, 2002 Par-2 elicits afferent arteriolar vasodilation by no-dependent and no-independent actions. Am J Physiol Renal Physiol **282**: F891–7.

Tucker, R. F., G. D. Shipley, H. L. Moses, and R. W. Holley, 1984 Growth inhibitor from bsc-1 cells closely related to platelet type beta transforming growth factor. Science **226**: 705–7.

Vancheri, C., C. Mastruzzo, M. A. Sortino, and N. Crimi, 2004 The lung as a privileged site for the beneficial actions of pge2. TRENDS in Immunology **25**: 40–6.

Vandivier, R., V. Fadok, C. Ogden, P. Hoffmann, J. Brain, *et al.*, 2002 Impaired clearance of apoptotic cells from cystic fibrosis airways*. Chest **121**: 89S.

Vergnolle, N., L. Cellars, A. Mencarelli, G. Rizzo, S. Swaminathan, *et al.*, 2004 A role for proteinase-activated receptor $# x02013; 1 in inflammatory bowel diseases. Journal of Clinical Investigation **114**: 1444.

Vergnolle, N., C. K. Derian, M. R. D'Andrea, M. Steinhoff, and P. Andrade-Gordon, 2002 Characterization of thrombin-induced leukocyte rolling and adherence: a potential proinflammatory role for proteinase-activated receptor-4. J Immunol **169**: 1467–73.

Vergnolle, N., J. L. Wallace, N. W. Bunnett, and M. D. Hollenberg, 2001 Protease-activated receptors in inflammation, neuronal signaling and pain. Trends Pharmacol Sci **22**: 146–52.

Vesey, D., J. Hooper, G. Gobe, and D. Johnson, 2007 Potential physiological and pathophysiological roles for proteaseactivated receptor2 in the kidney (review article). Nephrology **12**: 36–43.

Vouret-Craviari, V., D. Grall, and E. V. Obberghen-Schilling, 2003 Modulation of rho gtpase activity in endothelial cells by selective proteinase-activated receptor (par) agonists. J Thromb Haemost **1**: 1103–11.

Vouret-Craviari, V., E. V. Obberghen-Schilling, J. C. Scimeca, E. V. Obberghen, and J. Pouysségur, 1993 Differential activation of p44mapk (erk1) by alpha-thrombin and thrombin-receptor peptide agonist. Biochem J **289 (Pt 1)**: 209–14.

Vu, T. K., D. T. Hung, V. I. Wheaton, and S. R. Coughlin, 1991a Molecular cloning of a functional thrombin receptor reveals a novel proteolytic mechanism of receptor activation. Cell **64**: 1057–68.

Vu, T. K., V. I. Wheaton, D. T. Hung, I. Charo, and S. R. Coughlin, 1991b Domains specifying thrombin-receptor interaction. Nature **353**: 674–7.

Waghray, M., Z. Cui, J. C. Horowitz, I. M. Subramanian, F. J. Martinez, *et al.*, 2005 Hydrogen peroxide is a diffusible paracrine signal for the induction of epithelial cell death by activated myofibroblasts. FASEB J **19**: 854–6.

Walker, T. R., K. A. Cadwallader, A. MacKinnon, and E. R. Chilvers, 2005 Thrombin induces dna synthesis and phosphoinositide hydrolysis in airway smooth muscle by activation of distinct receptors. Biochem Pharmacol **70**: 959–67.

Wallach-Dayan, S. B., G. Izbicki, P. Y. Cohen, R. Gerstl-Golan, A. Fine, *et al.*, 2006 Bleomycin initiates apoptosis of lung epithelial cells by ros but not by fas/fasl pathway. Am J Physiol Lung Cell Mol Physiol **290**: L790–L796.

Wang, J., R. Zohar, and C. A. McCulloch, 2006 Multiple roles of alpha-smooth muscle actin in mechanotransduction. Experimental Cell Research **312**: 205–14.

Weksler, B. B., C. W. Ley, and E. A. Jaffe, 1978 Stimulation of endothelial cell prostacyclin production by thrombin, trypsin, and the ionophore a 23187. J Clin Invest **62**: 923–30.

Wenzel, U. O., and H. E. Abboud, 1995 Chemokines and renal disease. Am J Kidney Dis **26**: 982–94.

Westergren-Thorsson, G., J. Hernnäs, B. Särnstrand, A. Oldberg, D. Heinegård, *et al.*, 1993 Altered expression of small proteoglycans, collagen, and transforming growth factor-beta 1 in developing bleomycin-induced pulmonary fibrosis in rats. The Journal of clinical investigation **92**: 632–7.

Wettschureck, N., and S. Offermanns, 2005 Mammalian g proteins and their cell type specific functions. Physiol Rev **85**: 1159–204.

Willis, B. C., R. M. duBois, and Z. Borok, 2006 Epithelial origin of myofibroblasts during fibrosis in the lung. Proceedings of the American Thoracic Society **3**: 377–82.

Wilson, M. S., and T. A. Wynn, 2009 Pulmonary fibrosis: pathogenesis, etiology and regulation. Mucosal Immunol **2**: 103–21.

Wipke, B. T., and P. M. Allen, 2001 Essential role of neutrophils in the initiation and progression of a murine model of rheumatoid arthritis. J Immunol **167**: 1601–8.

Wolf, G., 1995 Cellular mechanisms of tubule hypertrophy and hyperplasia in renal injury. Miner Electrolyte Metab **21**: 303–16.

Wolf, G., and E. Ritz, 2005 Combination therapy with ace inhibitors and angiotensin ii receptor blockers to halt progression of chronic renal disease: pathophysiology and indications. Kidney Int **67**: 799–812.

Wolfe, B. L., A. Marchese, and J. Trejo, 2007 Ubiquitination differentially regulates clathrin-dependent internalization of protease-activated receptor-1. The Journal of cell biology **177**: 905–16.

Wu, C.-F., W.-C. Chiang, C.-F. Lai, F.-C. Chang, Y.-T. Chen, *et al.*, 2013 Transforming growth factor -1 stimulates profibrotic epithelial signaling to activate pericyte-myofibroblast transition in obstructive kidney fibrosis. Am J Pathol **182**: 118–31.

Wynn, T. A., 2008 Cellular and molecular mechanisms of fibrosis. J Pathol **214**: 199–210.

Wynn, T. A., and T. R. Ramalingam, 2012 Mechanisms of fibrosis: therapeutic translation for fibrotic disease. Nat Med **18**: 1028–40.

Xiao, Y. P., A. H. Morice, S. J. Compton, and L. Sadofsky, 2011 N-linked glycosylation regulates human proteinase-activated receptor-1 cell surface expression and disarming via neutrophil proteinases and thermolysin. J Biol Chem **286**: 22991–3002.

Xiong, J., Z. Zhu, J. Liu, Y. Wang, and Z. Li, 2005 Role of protease activated receptor-2 expression in renal interstitial fibrosis model in mice. J Huazhong Univ Sci Technol Med Sci **25**: 523–6.

Xu, W. F., H. Andersen, T. E. Whitmore, S. R. Presnell, D. P. Yee, *et al.*, 1998 Cloning and characterization of human protease-activated receptor 4. Proc Natl Acad Sci USA **95**: 6642–6.

Xu, Y. D., J. Hua, A. Mui, R. O'Connor, G. Grotendorst, *et al.*, 2003 Release of biologically active tgf-beta1 by alveolar epithelial cells results in pulmonary fibrosis. Am J Physiol Lung Cell Mol Physiol **285**: L527–39.

Yamazaki, T., and Y. Aoki, 1997 Cathepsin g binds to human lymphocytes. J Leukoc Biol **61**: 73–9.

Yano, T., R. R. Deterding, L. D. Nielsen, C. Jacoby, J. M. Shannon, *et al.*, 1997 Surfactant protein and cc-10 expression in acute lung injury and in response to keratinocyte growth factor. Chest **111**: 137S–138S.

Zeisberg, M., J. ichi Hanai, H. Sugimoto, T. Mammoto, D. Charytan, *et al.*, 2003 Bmp-7 counteracts tgf-beta1-induced epithelial-to-mesenchymal transition and reverses chronic renal injury. Nat Med **9**: 964–8.

Zeisberg, M., and R. Kalluri, 2004 The role of epithelial-to-mesenchymal transition in renal fibrosis. J Mol Med **82**: 175–81.

Zeisberg, M., F. Strutz, and G. A. Müller, 2000 Role of fibroblast activation in inducing interstitial fibrosis. J Nephrol **13 Suppl 3**: S111–20.

Zeisberg, M., F. Strutz, and G. A. Müller, 2001 Renal fibrosis: an update. Curr Opin Nephrol Hypertens **10**: 315–20.

Zhang, K., M. D. Rekhter, D. Gordon, and S. H. Phan, 1994 Myofibroblasts and their role in lung collagen gene expression during pulmonary fibrosis. a combined immunohistochemical and in situ hybridization study. Am J Pathol **145**: 114–25.

Zhang, Y., Y. Wang, Y. Xiang, W. Lee, and Y. Zhang, 2012 Prohibitins are involved in protease-activated receptor 1-mediated platelet aggregation. J Thromb Haemost **10**: 411–8.

Zhao, J., W. Shi, Y.-L. Wang, H. Chen, P. Bringas, *et al.*, 2002 Smad3 deficiency attenuates bleomycin-induced pulmonary fibrosis in mice. Am J Physiol Lung Cell Mol Physiol **282**: L585–93.

Zou, H., W. J. Henzel, X. Liu, A. Lutschg, and X. Wang, 1997 Apaf-1, a human protein homologous to c. elegans ced-4, participates in cytochrome c-dependent activation of caspase-3. Cell **90**: 405–13.